



University of Novi Sad
FACULTY OF TECHNICAL SCIENCES
DEPARTMENT OF PRODUCTION ENGINEERING
21000 NOVI SAD, Trg Dositeja Obradovica 6, SERBIA



UDK 621

ISSN 1821-4932

JOURNAL OF
PRODUCTION ENGINEERING

Volume 17

Number 1

Novi Sad, June 2014

Publisher: FACULTY OF TECHNICAL SCIENCES
DEPARTMENT OF PRODUCTION ENGINEERING
21000 NOVI SAD, Trg Dositeja Obradovica 6
SERBIA

Editor-in-chief: Dr. Pavel Kovač, *Professor, Serbia*

Reviewers: Dr. Janko HODOLIČ, *Professor, Serbia*
Dr. Marin GOSTIMIROVIĆ, *Professor, Serbia*
Dr. František HOLEŠOVSKY, *Professor, Czech Republic*
Dr. Janez KOPAČ, *Professor, Slovenia*
Dr. Pavel KOVAČ, *Professor, Serbia*
Dr. Mikolaj KUZINOVSKI, *Professor, Macedonia*
Dr. Ildiko MANKOVA, *Professor, Slovak Republic*
Dr. Snežana RADONJIĆ, *Professor, Serbia*
Dr. Branko ŠKORIĆ, *Professor, Serbia*
Dr. Ljubomir ŠOOŠ, *Professor., Slovak Republic*
Dr. Wojciech ZEBALA, *Professor, Poland*
Dr. Miodrag HADŽISTEVIĆ, *Assoc. Professor, Serbia*
Dr. Slobodan TABAKOVIĆ, *Assoc. Professor, Serbia*
Dr. Đorđe VUKELIĆ, *Assist. Professor, Serbia*

Technical treatment and design: M.Sc. Borislav Savković, *Assistant*

Manuscript submitted for publication: June 22, 2014.

Printing: 1st

Circulation: 300 copies

CIP classification:

*Printing by: FTN, Graphic Center
GRID, Novi Sad*

ISSN: 1821-4932

CIP – Каталогизacija u publikaciji
Библиотека Матице српске, Нови Сад

621

JOURNAL of Production Engineering / editor in chief
Pavel Kovač. – Vol. 12, No. 1 (2009)- . – Novi Sad :
Faculty of Technical Sciences, Department for Production
Engineering, 2009-. – 30 cm

Dva puta godišnje (2012-). Je nastavak: Časopis proizvodno
mašinstvo = ISSN
0354-6446
ISSN 1821-4932

INTERNATIONAL EDITORIAL BOARD

Dr. Joze BALIĆ, Professor, Slovenia
Dr. Marian BORZAN, Professor, Romania
Dr. Konstantin BOUZAKIS, Professor, Greece
Dr. Miran BREZOČNIK, Professor, Slovenia
Dr. Ilija ČOSIĆ, Professor, Serbia
Dr. Pantelija DAKIĆ, Professor, Bosnia and Herzegovina
Dr. Numan DURAKBASA, Professor, Austria
Dr. Katarina GERIĆ, Professor, Serbia
Dr. Marin GOSTIMIROVIĆ, Professor, Serbia
Dr. Janko HODOLIČ, Professor, Serbia
Dr. František HOLEŠOVSKY, Professor, Czech Republic
Dr. Juliana JAVOROVA, Professor, Bulgaria
Dr. Vid JOVIŠEVIĆ, Professor, Bosnia and Herzegovina
Dr. Janez KOPAČ, Professor, Slovenia
Dr. Borut KOSEC, Professor, Slovenia
Dr. Mikolaj KUZINOVSKI, Professor, Macedonia
Dr. Miodrag LAZIĆ, Professor, Serbia
Dr. Stanislaw LEGUTKO, Professor, Poland
Dr. Chusak LIMSAKUL, Professor, Thailand
Dr. Vidosav MAJSTOROVIC, Professor, Serbia
Dr. Ildiko MANKOVA, Professor, Slovak Republic
Dr. Mirko SOKOVIĆ, Professor, Slovenia
Dr. Antun STOIĆ, Professor, Croatia
Dr. Peter SUGAR, Professor, Slovak Republic
Dr. Katica ŠIMUNOVIĆ, Professor, Croatia
Dr. Branko ŠKORIĆ, Professor, Serbia
Dr. Ljubomir ŠOOŠ, Professor, Slovak Republic
Dr. Ljubodrag TANOVIĆ, Professor, Serbia
Dr. Wiktor TARANENKO, Professor, Ukraine
Dr. Marian TOLNAY, Professor, Slovak Republic
Dr. Gyula VARGA, Professor, Hungary
Dr. Milan ZELJKOVIĆ, Professor, Serbia
Dr. Miodrag HADŽISTEVIĆ, Assoc. Professor, Serbia
Dr. Milenko SEKULIĆ, Assoc. Professor, Serbia
Dr. Aco ANTIĆ, Assist. Professor, Serbia
Dr. Sebastian BALOŠ, Assist. Professor, Serbia
Dr. Igor BUDAK, Assist. Professor, Serbia
Dr. Arkadiusz GOLA, Assist. Professor, Poland
Dr. Ognjan LUŽANIN, Assist. Professor, Serbia
Dr. Mijodrag MILOŠEVIĆ, Assist. Professor, Serbia
Dr. Slobodan TABAKOVIĆ, Assist. Professor, Serbia
Dr. Đorđe VUKELIĆ, Assist. Professor, Serbia

Editorial

*The **Journal of Production Engineering** dates back to 1984, when the first issue of the **Proceedings of the Institute of Production Engineering** was published in order to present its accomplishments. In 1994, after a decade of successful publication, the Proceedings changed the name into **Production Engineering**, with a basic idea of becoming a Yugoslav journal which publishes original scientific papers in this area.*

*In 2009 year, our Journal finally acquires its present title - **Journal of Production Engineering**. To meet the Ministry requirements for becoming an international journal, a new international editorial board was formed of renowned domestic and foreign scientists, refereeing is now international, while the papers are published exclusively in English. From the year 2011 Journal is in the data base COBISS and KoBSON presented.*

The Journal is distributed to a large number of recipients home and abroad, and is also open to foreign authors. In this way we wanted to heighten the quality of papers and at the same time alleviate the lack of reputable international and domestic journals in this area.

In this journal are published, reviewed papers from International Conference "ETIKUM 2014" which was in Novi Sad, Serbia and certain number of new scientific papers as well.

Editor in Chief

Professor Pavel Kovač, PhD,



Contents

ORIGINAL SCIENTIFIC PAPER

Mangesh R. Phate, Dr. V.H.Tatwawadi ANN BASED MODEL FOR PREDICTION OF HUMAN ENERGY IN CONVENCTIONAL MACHINING OF NONFERROUS MATERIAL FROM INDIAN INDUSTRY PROSPECTIVE	1
Irgolic, T., Cus, F., Zuperl, U. THE USE OF PARTICLE SWARM OPTIMIZATION FOR TOOL WEAR PREDICTION	7
Trif, A., Borzan, M., Rus. A., Nedezki, C., Agarski, B. STUDIES AND RESEARCHES ON INSERT WEAR IN TURNING PROCESS	11
Kishore Debnath, Inderdeep Singh, Akshay Dvivedi EVALUATION OF SURFACE ROUGHNESS DURING ROTARY-MODE ULTRASONIC DRILLING OF GLASS/EPOXY COMPOSITE LAMINATES	16
Kishore Debnath, Vikas Dhawan, Inderdeep Singh, Akshay Dvivedi ADHESIVE WEAR AND FRICTIONAL BEHAVIOR OF RICE HUSK FILLED GLASS/EPOXY COMPOSITES	21
M. Venkata Ramana, G. Krishna Mohan Rao, D. Hanumantha Rao CHIP MORPHOLOGY IN TURNING OF Ti-6Al-4V ALLOY UNDER DIFFERENT MACHINING CONDITIONS	27
Kaplonek, W., Kukielka, K., Kukielka, L., Nadolny, K., Hloch, S. CLSM-BASED MEASUREMENTS OF THE SURFACES OF THE EXTERNAL ROUND THREADS ROLLED ON COLD	33
Cica, Dj., Sredanovic, B., Kramar, D. PREDICTION OF CUTTING ZONE TEMPERATURE IN HIGH-PRESSURE ASSISTED TURNING USING GA AND PSO BASED ANN	43
Župerl, U., Čuš, F., Irgolič, T., Vukelić, D. INDIRECT TOOL WEAR MEASURING TECHNIQUE COMBINED WITH OPTOELECTRONIC SYSTEM FOR AUTOMATED TOOL CONDITION CONTROL.....	47
Mladenović,C., Kalentić, N., Zeljković,M., Tabaković, S. THE INFLUENCE OF MILLING STRATEGIES ON ROUGHNESS OF COMPLEX SURFACES	51
Ješić, D., Pulić, J., Kovač, P., Savković, B., Kulundžić, N. APPLICATION OF NODULAR CASTINGS IN THE MODERN INDUSTRY OF TRIBO- MECHANICAL SYSTEMS TODAY AND TOMORROW	55

Živković, S. PROFILING OF MANDREL FOR ROTARY FORGING	59
Topčić, A., Cerjaković, E., Lovrić, S. ANALYSIS OF DIMENSIONAL DEVIATION OF PARTS BASED ON CERAMIC PRODUCED BY THREE DIMENSIONAL PRINTING PROCESS	63
Brajlih, T., Kostevšek, U., Zupančič, H. T., Paulič, M., Irgolič, T., Balič, J., Hadžistević, M., Drstvenšek, I. COMPARISON OF MANUFACTURING TECHNOLOGIES OF FIXED STRUCTURES IN PROSTHETIC DENTISTRY	67
Živanović, S., Glavonjić, M. METHODOLOGY FOR IMPLEMENTATION SCENARIOS FOR APPLYING PROTOCOL STEP-NC	71
Mishra Antaryami INVESTIGATIONS ON WEAR CHARACTERISTICS OF TEAK WOOD DUST FILLED EPOXY COMPOSITES	75
Križan, P., Svátek, M., Matúš, M., Beniak, J. IMPACT OF PRESSING TEMPERATURE ON THE PRESSING CONDITIONS IN BRIQUETTING MACHINE PRESSING CHAMBER.....	79
Senderská, K., Mareš, A., Kandra T. TIME ANALYSIS IN THE LEAN ASSEMBLY DESIGN EXCEL APPLICATION.....	83
Salokyová, Š., Gerková, J. SCANNING AND EVALUATING VIBRATIONS ON A LABORATORY MODEL.....	87
PRELIMINARY NOTE	
Klos, Z. A SIMPLE TOOL FOR QUALITY IMPROVEMENT OF TECHNICAL OBJECTS AND PROCESSES	92
Krčmar, D., Baloš, S., Dalmacija, B., Prica, M., Tričković, J., Rončević, S., Maletić, S. MECHANICAL PROPERTIES OF THERMALLY STABILIZED SEDIMENT-CLAY MIXTURES	97
Kuruc, M., Ncpal, M., Peterka, J. MACHINING OF POLY-CRYSTALLINE CUBIC BORON NITRIDE BY LASER BEAM MACHINING IN TERMS OF SURFACE ROUGHNESS	101
INSTRUCTION FOR CONTRIBUTORS	105



Mangesh R. Phate, Dr. V.H.Tatwawadi

ANN BASED MODEL FOR PREDICTION OF HUMAN ENERGY IN CONVENTIONAL MACHINING OF NONFERROUS MATERIAL FROM INDIAN INDUSTRY PROSPECTIVE

Received: 04 January 2014 / Accepted: 10 February 2014

Abstract: In this paper, human energy prediction model for the conventional dry turning (CTD) using artificial neural network (ANN) is developed to investigate the effect of various field parameters. The ANN model of human energy (HE) is developed with the field parameters such as machine operators, cutting tools, work piece (Al 6063 & Brass), cutting process parameters, lathe machine parameters and the machining environmental parameters. The experiments are planned as per the Indian geographical conditions and the random plan of field experimentation. An attempt was made to minimise the human energy and effective utilization of the existing man-machine system. To increase the accuracy and minimise the error in the modeling, an artificial neural network (ANN) was used to correlate the various dependent and the independent parameters. The study shows that the approach of field data coupled with the artificial neural network (ANN) is best suited for investigating the CDT in Indian perspective.

Key words: Field data based approach, Artificial neural network model, aluminium 6063, brass, human energy.

Model veštačke neuronske mreže za predviđanje ljudske energije pri konvencionalnoj obradi obojenih materijala sa Indijske industrijske perspektive. U ovom radu, razvijen je model za predviđanje ljudske energije pri konvencionalnoj suvoj obradi struganjem korišćenjem veštačkih neuronskih mreža (VNN) da bi se ispitalo uticaj različitih parametara. VNN model ljudske energije je razvijen sa parametrima kao što su operateri mašine, rezni alat, obradak (Al 6063 i mesing), parametri rezanja, parametri struga i ekološki parametri obrade. Eksperimenti su planirani po indijskim geografskim uslovima i slučajnom planu polja eksperimentisanja. Učinjen je pokušaj da se smanji ljudska energija i efikasno iskorišćenje postojećeg sistema čovek-mašina. Da bi se povećala tačnost i minimizirala greška modeliranja, veštačke neuronske mreže (VNM) koriste korelaciju različitih zavisnih i nezavisnih parametara. Studije pokazuju da izbor podataka sa veštačkim neuronskim mrežama najbolje odgovara istraživanju suve obrade sa pogleda Indijske perspektive.

Ključne reči: Pristup bazi podataka, veštačke neuronske mreže, aluminijum 6063, mesing, ljudska energija.

1. INTRODUCTION

Turning is a most commonly used machining process in manufacturing. Therefore, an most favorable selection of cutting parameters to satisfy an profitable objective within the constraints of turning operations is a very important task [1]. conventionally, the selection of cutting conditions for metal cutting is left to the machine operator. Surface roughness, power consumption, material removal rate and productivity has received serious attention for many years [2]. A significant number of studies have investigated the general effects of the speed, feed, and depth of cut on the turning process [3]. Some researchers studied on the machinability of aluminum-silicon alloys [4,5,6,7]. Kumar et. al compared the influence of several factors (cutting speed, feed rate and depth of cut) on cutting force and surface roughness by orthogonal tests in turning Si-Al alloy [8]. The results showed that the surface roughness could be improved by using diamond tool. Recently, in order to obtain practical cutting parameters in turning casting aluminum alloy ZL108. Vinayak et al analyzed main influential factors of cutting force using carbide tool YG8 [9]. The results indicated the depth of cut had great influence on

stability of whole cutting process in rough machining. Agapiou et. al (1992) investigated unconstrained machine-parameter optimization using differential calculus [10]. Brewer et.al (1963) carried out simplified optimum analysis for non-ferrous materials [11]. For cast iron (CI) and steels, they employed the criterion of reducing the machining cost to a minimum. A number of monograms were worked out to facilitate the practical determination of the most economic machining conditions. They pointed out that the more difficult-to-machine materials have a restricted range of parameters over which machining can be carried out and thus any attempt at optimizing their costs are artificial. Brewer suggested the use of Lagrangian multipliers for optimization of the constrained problem of unit cost, with cutting power as the main constraint. Walvekar et.al (1970) discussed the use of geometric programming to selection of machine they optimized cutting speed and feed rate to yield minimum production cost [12]. Petropoulos [13] (1973) described the design and development of an analytical tool for the selection of machine parameters in turning. Geometric programming [14] was used as the basic methodology to determine values for feed rate and cutting speed that minimize the total cost of machining SAE 1045 steel

with cemented carbide tools of ISO P-10 grade. Surface finish and machine power were taken as the constraints while optimizing cutting speed and feed rate for a given depth of cut. In Indian scenario where majority of total machining operation are still executed manually which needs to be focused. A traditional machining process involves many process parameters which is directly or indirectly affects the human energy [15]. The literature review shows that no attempt has been made to formulate the human energy model in the turning of nonferrous material in the convectional dry turning operation.

2. EXPERIMENTAL SETUP

2.1 List of Parameters under Investigation

The variables affecting the effectiveness of the phenomenon under consideration are operator data, single point cutting tool, lathe machine, work piece, process parameters and the environmental parameters [16,17]. The dependent or the response variables in this case of turning operation is human energy (HE). The list of various process variables which affects the machining phenomenon is as shown in table 1.

2.2 Dimensional Analysis to reduce the variables

According to the theories of engineering experimentation by H. Schenck Jr. [18] the choice of principal dimensions requires at least three primaries, but the analyst is free to choose any reasonable set he wishes, the only requirement being that his variables must be expressible in his system. There is really nothing base or fundamental about the principal dimensions. For this case, the variables are expressed in mass(M), length(L) and time(T). The final dimensionless pi terms are formed on the basis of dimensional analysis and grouped according to the functional similarity. The final dimensional pi terms are as shown in table 2.

2.3 Setup for Experimentation

The two different types of nonferrous materials are used for the experimentation. Al 6063 and Brass are considered for the traditional dry turning process. The geometry of the finish work piece is as shown in the following figure 1. The experimental setup for the work is as shown in figure 2.

2.4 Bicycle Ergometer test to measure the human Energy (HE).

The heart rate is measured to find out the human energy input of the lathe machine operator. Before the test is carried out i.e. at the start of work pulse rate was measured manually. Pulse rate was measured by a single person, for all the operators, to minimize the error. Heart rate or pulse was measured at the beginning of the operation and at the end of the operation. The pi terms related to the human energy is given by the following equation 1.

Sr. No	Description	Symbol
1	Anthropometric of the operator.	An
2	Weight of the operator.	W_p
3	Age of the operator.	AGP
4	Experience	EX
5	Skill rating	SK
6	Educational qualifications	EDU
7	Psychological Distress	PS
8	Systolic Blood pressure	SBP
9	Diastolic Blood pressure	DBP
10	Oxygen saturation in the blood	SPO2
11	Blood Sugar Level during Working	BSG
12	Cutting Tool angles ratio.	CTAR
13	Tool nose radius	R
14	Tool overhang length	Lo
15	Approach angle	α
16	Setting angle	β
17	Single point cutting Hardness	BHNT
18	Lip or Nose angle of tool	LP
19	Wedge angle	WG
20	Shank Length	LS
21	Total length of the tool	LT
22	Tool shank width	SB
23	Tool shank Height	SH
24	Work piece hardness	BHNW
25	Weight of the raw work piece.	W
26	Shear stress of the work piece	τ
27	Density of the workpiece Material	ρ
28	Length of the raw workpiece	LR
29	Diameter of the raw workpiece	DR
30	Cutting Speed	VC
31	Feed	f
32	Depth of cut	D
33	Cutting force	FC
34	Tangential Force.	FT
35	Spindle revolution	N
36	Tool – workpiece interface temp.	\square_{wp}
37	Machine vibration	$VB_{m/c}$
38	Tool vibration	VB_{tool}
39	Machine Specification ratio	MSP
40	Power of the Machine motor	P_{HP}
41	Weight of the machine	W_m
42	Age of the machine	AGM
43	Air flow	Vf
44	Light Intensity	LUX
45	Atmospheric Temperature	DTO
46	Sound Level	DB
47	Humidity	HUM
48	Human Energy	HE

Table 1. List of parameters under investigation

$$\Pi D_1 = HE / Fc * V \quad (1)$$

During the machining process, pulse rate of the

operator was measured. This was done for complete machining operation .The observation for the pulse rise during the bicycle test is as shown in table 2.

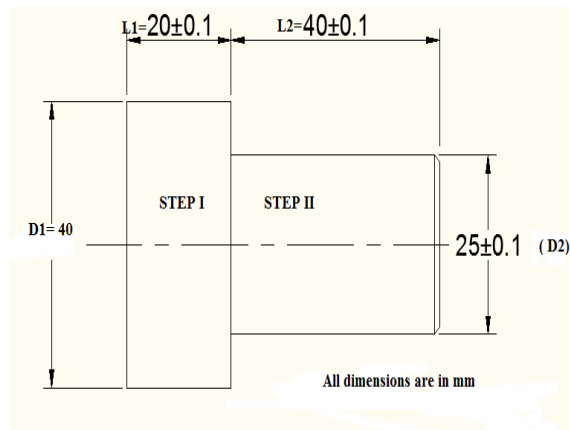


Fig. 1. Dimensions of the finished workpiece



Fig. 2. Schematic view of the Experimental setup

Sr. No	Description	Symbol
Π_1	$An * SBP * SK * Ag * Wp * SPO2 / DBP * PS * EDU * EX * BSG * D^3$	Operator
Π_2	$AR * r * \beta * BHNT * LT * LP * LS / \alpha * LO * SW * SH * WG$	Cutting Tool
Π_3	$BHNW * W_{raw} * LR * \tau / D * FC * \rho * DR$	Work Piece
Π_4	$f * FT * N * \theta_{wp} * VB_{Tool} / VB_{M/c} * FC * VC$	Cutting Process
Π_5	$SP * P_{HP} * W_{m/c} / AGM * FC^2$	Lathe Machine
Π_6	$HUM * DTO * Vf * DB * VC * FC / LUX * D^3$	Environment
ΠD_1	$HE / FC * D$	Human Energy

Table 2. List of dimensionless pi term.

The area under the above curve represents human energy input for the respective operation .This human energy input needs to be stated in engineering units of N-m, for this purpose normally bicycle ergo meter should be adopted. However, in view of the actual work as it is carried out in the industry and because of some reservations on the part of workers. An ergonomist may not agree to this method as an alternative to the bicycle ergo meter. However, it is not always possible to send the operator to the ergonomics

laboratory because:

- Operators are reluctant to go to new premises.
- Managements think that the work may suffer in the absence of the worker.
- Normally industrial areas are at large distance from the laboratories and thus arranging their transport to and for takes a lot of time and money.

In view of the reasons stated earlier of not using a bicycle ergo meter for this purpose in an ergonomic laboratory, a method fairly close to the same is thought of and executed.

A bicycle was arranged with a certain weight on its carrier. The same operator was asked to ride the bicycle over a certain distance .The pulse rate was recorded at the beginning of ride and at the end. The variation in the pulse rate is observed during the test is presented in above figure 3. During this ride, the work done in N-M in riding the bicycle can be estimated as under .The various forces acting during the bicycle ride are shown in the following figure 5.

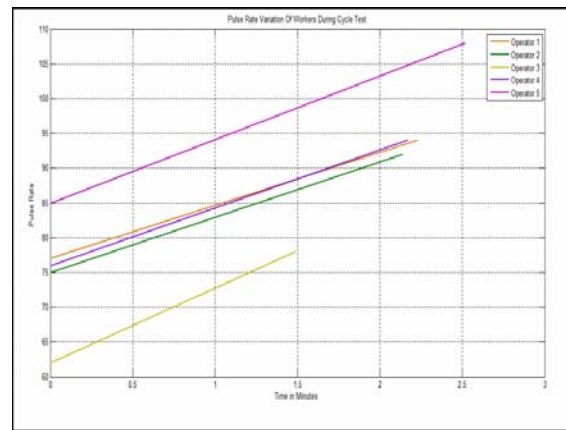


Fig. 3. Pulse rate variation of workers during bicycle test

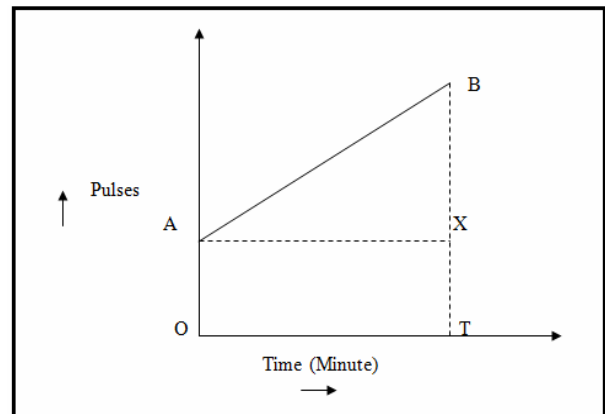


Fig. 4. General pulse rate vs. riding time curve for the workers during bicycle test

$$\text{Work Done} = \text{Area under Line AB} \\ = 1/2 * AX * BX + OT * AO$$

$$\text{Work done} = 1/2 * \text{Ride time in Minute} * \text{Change in Pulse Rate} + \text{Ride Time} * \text{Pulse at the start of the Ride.}$$

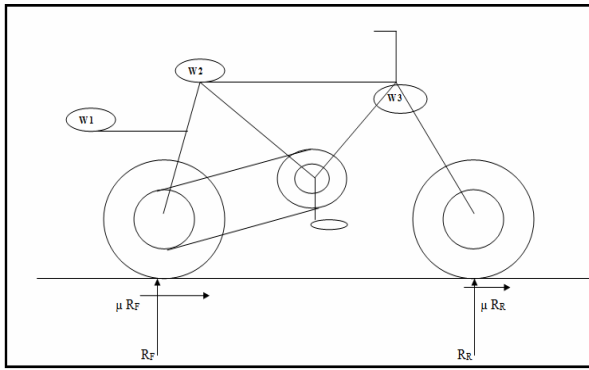


Fig. 5. Free body diagram for the bicycle showing the various forces acting on the bicycle

Let

- R_R - Rear wheel reaction.
- R_F - Front wheel reaction.
- L - Distance travelled by the rider.
- D - Diameter of the bicycle Wheel.
- Total moment of resisting force = $(\mu R_R \times D/2) + (\mu R_F \times D/2)$
- Number of revolutions $(N) = L / \pi D$
- W_1 - Weight Placed on the Carrier.
- W_2 - Weight of the operator.
- W_3 - Weight of the bicycle.

Hence

$$\star \text{ Total Work done} = 2 \pi N (R_R + R_F) \times \mu \times D/2$$

- $R_R + R_F = W_1 + W_2 + W_3$
 - Total work done = $2 \pi N (\mu R_R \times D/2) + 2 \pi N (\mu R_F \times D/2)$
 - Total work done = $2 \pi N (W_1 + W_2 + W_3) (\mu \times D/2)$
 - Total work done = (Total weight) μL
- The observation and deductions of some parameters are as shown in table 3.
- Thus unit pulse energy while cycling (X) = Work done during cycling / Area under pulse rate – time curve for the cycling
 - Work intensity while cycling (Y) in pulse /min/ min = Pulse rise during the cycling / duration of the bicycle ride
 - Work intensity while machining operation (Z) in pulse /min/ min = Pulse rise during the operation / duration of the operation.
 - The unit pulse energy while machining (U) = $Z * X / Y$
 - Area under the Pulse –time curve for the machining operation (A) = Operation time * Starting Pulse + $1/2 * \text{Operation time (Pulse at end – Start Pulse)}$
 - Human energy Input in (kgf-m) = $A * U$
 - Human energy input in (Kgf-m/ sec) = HE in kgf-m/ Total machining Time

Parameters	Operator 1	Operator 2	Operator 3	Operator 4	Operator 5
Weight of the Operator (W2)in Kg	62	52	49	56	52
Weight on the carrier(W1)in Kg	12	12	12	12	12
Distance covered(L)in meter	500	500	500	500	500
Pulse at Start of the Ride	77	75	62	76	85
Pulse at End of the Ride	94	92	78	94	108
Time taken for the Ride in minutes	2.23	2.14	1.49	2.17	2.52
Wheel Diameter (D)	0.65	0.65	0.65	0.65	0.65
Weight of the Bicycle(W3)in Kg	26.3	26.3	26.3	26.3	26.3
Coefficient of Friction	0.3	0.3	0.3	0.3	0.3
$R_R + R_F = W_1 + W_2 + W_3$	100.3	90.3	87.3	94.3	90.3
Number of Revolution (N)=L/πD	244.9	244.6	244.9	244.9779	244.9
Total Work done in Kgf-m	15045	13545	13095	14145	13545
Pulse Rate Rise while cycling	17	17	16	18	23
Area under the curve	190.6	178.6	104.3	184.45	243.18
Unit pulse energy = how much Kgf-m while cycling (X)	78.9080324	75.80166	125.55129	76.68744	55.699481
Work intensity while cycling in pulse/min/min (Y)	7.62331838	7.943925	10.73825	8.299308	9.1269841

Table 3. Operator data for the bicycle test

3.MODEL FORMULATION USING ARTIFICIAL NEURAL NETWORK (ANN)

6,5,1 Ann network is used to predict the human energy in the turning of nonferrous materials (Al 6060 & Brass). Following figure shows the network developed for the human energy data. Figure 6 shows the ANN network developed for the human energy in the turning of nonferrous material.

The following ANN model is develop using the above network. Majorities of the sigmoid function are observed to be of exponential nature. Any function with an infinite scope ($-\infty$ to $+\infty$) be suitable, provided that it is continuous. Typical preferences go to

hyperbolic tan and. Selection of such function is decided by experienced programmers. A define methodology about selection of sigmoid function ($1/1+e^{-X}$) is devoid of reasons.

Figure 6 shows the ANN model formulated for the turning of nonferrous material . The results between an experimental and the ANN model are as shown in the figure 8. The reliability, root mean square error and the correlation are as given below The developed ANN model for the HE is as follows:

$$X_{1,1} = (1 - e^{-1 * \text{sum}(\text{layer } 1 \text{ cell } 0)}) / (1 - e^{-1 * \text{sum}(\text{layer } 1 \text{ cell } 0)})$$

Where

$$\begin{aligned} \text{Sum}(\text{layer1cell0}) &= 1.15517X_{0,1} + 0.26357X_{0,2} + \\ & 0.73517X_{0,3} + 0.48153X_{0,4} - 0.06662X_{0,5} - \\ & 0.13787X_{0,6} - 0.2871 \end{aligned}$$

$$X_{1,2} = (1 - e^{-1 * \text{sum}(\text{layer1cell1})}) / (1 - e^{-1 * \text{sum}(\text{layer1cell1})})$$

Where

$$\begin{aligned} \text{Sum}(\text{layer1cell1}) &= 1.9449X_{0,1} + 0.29155X_{0,2} + \\ & 0.62438X_{0,3} - 0.29265X_{0,4} - 0.79713X_{0,5} + \\ & 0.83810X_{0,6} - 0.1951 \end{aligned}$$

$$X_{1,3} = (1 - e^{-1 * \text{sum}(\text{layer1cell2})}) / (1 - e^{-1 * \text{sum}(\text{layer1cell2})})$$

Where

$$\begin{aligned} \text{Sum}(\text{layer1cell2}) &= 1.25256X_{0,1} + 0.76898X_{0,2} + \\ & 0.25572X_{0,3} + 0.77218X_{0,4} + 0.35933X_{0,5} + \\ & 0.59912X_{0,6} - 0.2336 \end{aligned}$$

$$X_{1,4} = (1 - e^{-1 * \text{sum}(\text{layer1cell3})}) / (1 - e^{-1 * \text{sum}(\text{layer1cell3})})$$

Where

$$\begin{aligned} \text{Sum}(\text{layer1cell3}) &= 0.54847X_{0,1} + 0.41890X_{0,2} + \\ & 0.83719X_{0,3} - 0.13027X_{0,4} + 0.34085X_{0,5} - \\ & 0.71772X_{0,6} - 0.4377 \end{aligned}$$

$$X_{1,5} = (1 - e^{-1 * \text{sum}(\text{layer1cell4})}) / (1 - e^{-1 * \text{sum}(\text{layer1cell4})})$$

Where

$$\begin{aligned} \text{Sum}(\text{layer1cell4}) &= -0.84622X_{0,1} + 0.73966X_{0,2} - \\ & 0.16738X_{0,3} + 0.29844X_{0,4} + 0.54729X_{0,5} + \\ & 0.57091X_{0,6} - 0.1634 \end{aligned}$$

$$\text{Output} = (1 - e^{-1 * \text{sum}(\text{layer2cell0})}) / (1 - e^{-1 * \text{sum}(\text{layer2cell0})})$$

Where

$$\begin{aligned} \text{Sum}(\text{layer2cell0}) &= 0.48333X_{1,1} + 1.26329X_{1,2} + \\ & 0.07178X_{1,3} + 0.05818X_{1,4} - 0.51818X_{1,5} + 0.0000 \end{aligned}$$

Univariate analysis is used for the optimization and sensitivity results of the ANN developed model. The algorithm used for the univariate analysis is as given below.

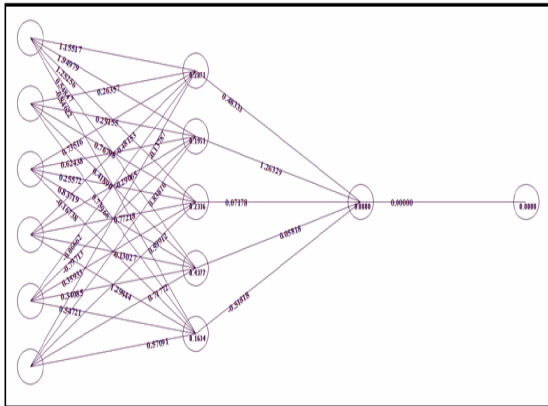


Fig. 6. ANN model for the HE required in the turning of nonferrous material.

Following algorithm is used for the univariate analysis.

Function NeuroOutput(w) as double, threshold) as double, age as integer, eno as integer, presentvalue() as double, tempr as double)
Maxlayers as integer and cells_in() as double are declared global

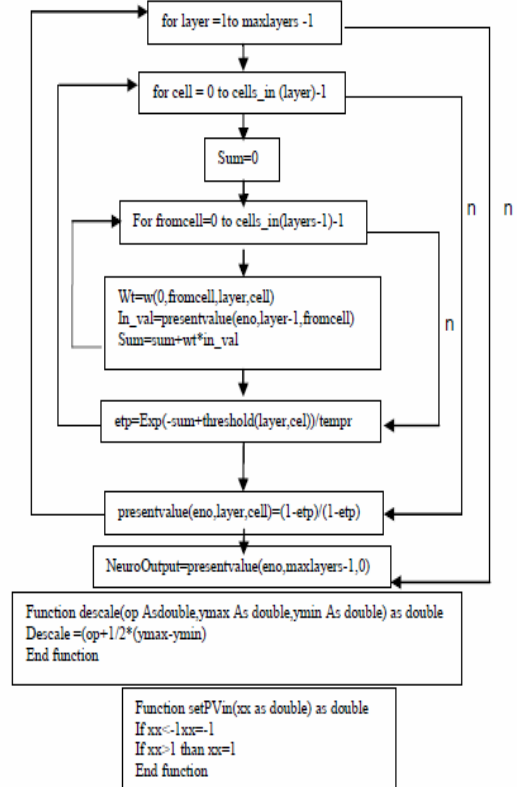


Fig. 7. Flow chart for univariate analysis.

- Correlation Coefficient = 0.9803538046
- Root Mean Square = 0.51517385441
- Reliability = 96.246045873%

4. OPTIMIZATION & SENSITIVITY ANALYSIS OF ANN MODEL

Univariate analysis is used to optimize and to find out the sensitivity of the response variable i.e. human energy w.r.t. the input parameters. The results obtain by using univariate analysis is as shown in the following table 4-5.

Input	Network	Optimum Value
Π_1 (M/C Operator)	6,5,1	0.551213
Π_2 (Cutting Tool)	6,5,1	8363.1482
Π_3 (Work Piece)	6,5,1	321393.67
Π_4 (Cutting Process)	6,5,1	0.619755
Π_5 (Lathe Machine)	6,5,1	0.639734
Π_6 (Environment)	6,5,1	6.22044
ΠD_1 (Power Consumption)	Minimum	0.0543729

Table 4. Optimization result for the minimum Human Energy model

RVN	Length of Influence Variables	Most Influence Variables
1	10	Operator
2	6	Cutting Process

Table 5. Sensitivity result for the minimum Human Energy model

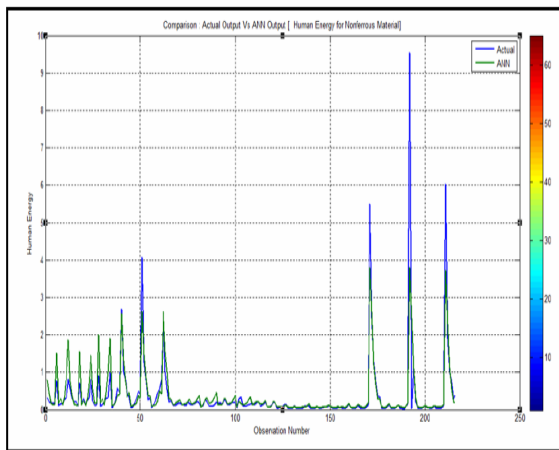


Fig. 8. Comparison between Experimental and the ANN human energy

5. RESULTS AND DISCUSSION

According to the present study and investigation in the convectional dry turning of non-ferrous material, the following conclusions can be drawn.

- (1) Feed forward Back propagation neural network is the most noteworthy and precious artificial neural network applied in the various researches to find out the complex behaviour of the system.
- (2) The ANN model obtained has showed the higher accuracy than any other traditional approaches of model formulation.
- (3) Univariant algorithms coupled with ANN are widely used for analyzing the sensitivity and optimization of the various process parameters.
- (4) No work has been reported on ANN modelling, optimization and sensitivity analysis of the model.
- (4) Results show that the human energy required for the machining of nonferrous materials (Al 6063 and Brass) depends on operator data and the various cutting process parameters under consideration.

6. REFERENCES

- [1] Klir G.J and, Yuan B. , Fuzzy system and fuzzy logic – theory and practice (*Englewood Cliffs, NJ: Prentice Hall*), (1998)
- [2] Phate M.R., Tatwawadi V.H., Modak J.P., Formulation of A Generalized Field Data Based Model For The Surface Roughness of Aluminum 6063 In Dry Turning Operation, *New York Science Journal*, 2012, PP. 38-46 .
- [3] Iwona Piotrowska, Christina Brandt, Hamid Reza Karimi, Peter Mass, Mathematical model of micro turning process, *International Journal of Advanced Manufacturing Technology*, 2009, PP.33–40.
- [4] Kahraman, The use of response surface methodology for the prediction and analysis of surface roughness of AISI 4140 steel, *Materials and technology*, 2009 , PP. 267–270.
- [5] Jeffrey B. Dahmus and Timothy G. Gutowski, An environmental analysis of machining, 2004 , *ASME International Mechanical Engineering Congress and RD&D Expo* November 13-19, 2004, Anaheim, California USA.
- [6] H. Soleimanimehr, M. J. Nategh , S. Amini, Modeling of Surface Roughness in Vibration Cutting by Artificial Neural Network, *World Academy of Science, Engineering and Technology* 52 2009, PP 386-391.
- [7] Petropoulos G., Ntziantzias I. and Anghel C., in: *International Conference on Experiments/ Process/ System Modelling/ Simulation/Optimization*, Athens, 2005, PP.25-34.
- [8] Atul Kumar, Dr. Sudhir Kumar and Dr. Rohit Garg, Statistical Modeling of surface roughness in turning process *International Journal of Engineering Science and Technology (IJEST) Vol. 3 No. 5 May 2011*, PP 4246-4252
- [9] Vinayak Neelakanth Gaitonde, S. R. Karnik, Luis Figueira, J. Paulo Davim, Performance comparison of conventional and wiper ceramic inserts in hard turning through artificial neural network modeling, *Int J Adv Manuf Technol (2011) 52*:101–114 DOI 10.1007/s00170-010-2714-3.
- [10] Agapiou J.S., The optimization of machining operations based on a combined criterion, Part 1 The use of combined objectives in single-pass operations, Part 2: Multi-pass operations. *J. Eng Ind., Trans. ASME, 1(14)*, 500–513 (1992).
- [11] Brewer R.C. and Rueda R., A simplified approach to the optimum selection of machining parameters, *Eng, Dig.*, 1963, PP.133–150.
- [12] Walvekar A.G. and Lambert B.K., An application of geometric programming to machining variable selection. *Int. J. Prod. Res.*, 1970, PP.38-45.
- [13] Petropoulos P.G., Optimal selection of machining rate Variable by geometric programming. *J Prod. Res.*, 1973, PP. 305–314.
- [14] Sundaram R.M., An application of goal programming technique in metal cutting, *Int. J. Prod. Res.*, 1978, PP. 375-382.
- [15] Tatwawadi V.H., Modak J.P. and Chibule S.G., Mathematical Modeling and simulation of working of enterprise manufacturing electric motor, *International Journal of Industrial Engineering*, 2010, PP.341-351.
- [16] Gilbert W.W., Economics of machining. In *Machining – Theory and practice. Am. Soc. M1950*, PP. 476–480.
- [17] Muwll K.F.H., Nature of Ergonomics, Ergonomics (Man In His Working Environment), *Chapman and Hall, London, New York*, 1956, PP.69-85
- [18] H. Schenck Jr., *Theories of Engineering a experimentation*, McGraw Hill Book Co , New York, 1954, PP.40-50.

Authors: Mr. Mangesh R. Phate, Assist. Professor, Mechanical Engineering Department, TSSM'S, Padmabhooshan Vasantdada Patil Institute of Technology, University of Pune, Maharashtra, Pune, India 411021.

Dr. V.H. Tatwawadi, Principal, Dr. Babasaheb Ambedkar Institute of Technology and research, Wanadongri, Nagpur, Maharashtra, India 441110.

Phone.: +91-9850330348.

E-mail: mangesh_phate@rediffmail.com

tatwawadi@yahoo.com



Irgolic, T., Cus, F., Zuperl, U.

THE USE OF PARTICLE SWARM OPTIMIZATION FOR TOOL WEAR PREDICTION

Received: 20 May 2014 / Accepted: 18 June 2014

Abstract: Nowadays a tool wear prediction in advanced manufacturing systems is becoming very important for optimizing cutting processes. In the present work, a particle swarm optimization algorithm for prediction of tool wear in end milling has been used. Helix angle (α), spindle speed (N), feed rate (Z), axial depth of cut (X) and radial depth of cut (Y) were taken as input parameters and tool wear (T) as an output parameter. In our application the particle swarm optimization algorithm has searched for the optimal solution of developed polynomial model. Predicted values of PSO model are compared with experimental results. The best solution of polynomial model was proposed as a model for predicting of tool wear.

Key words: particle swarm optimization, tool wear, end milling

Upotreba optimizacije metodom roja čestica za predviđanje postojanosti alata. U današnje vreme predviđanje habanja alata postaje veoma važno za optimizaciju procesa rezanja. U ovom radu, optimizacijom roja čestica koriste algoritam za predviđanje postojanosti kod glodanja u odnosu na veličinu habanja alata. Ugao zavojnice (α), broj obrtaja vretena (N), pomak (Z), aksijalna dubina rezanja (X) i radijalna dubina rezanja (Y) su uzeti kao ulazni parametri dok je kao izlazni parametar uzeta postojanost alata (T). U našoj aplikaciji su optimizacijom roja čestica optimalnog rešenja algoritmi su tražili pomoću razvijenog polinomskog modela. Predviđene vrednosti PSO modela su upoređene sa eksperimentalnim rezultatima. Najbolje rešenje polinomskog modela je predloženo kao model za predviđanje postojanosti alata.

Ključne reči: čestica roj optimizacije, habanje alata, postojanost kod glodanja

1. INTRODUCTION

Tool wear is one of the most influential factors in the process planning by cutting processes. This parameter tells us how sustainable is our cutting tool and when it has to be replaced with the new one or when its cutting edge has to be re-sharpen. However, the machined surface has to be properly finished and during this time cutting tool has to be in proper shape otherwise intermediate tool replacement leaves visible trace on a surface of a workpiece. By reducing the cutting speed and other cutting parameters the resistant time could usually be extended, but on the other hand the productivity decreases and the production time extends. Decisions about selection of the cutting parameters have significant impact on the level of production, production costs and product quality. Therefore, optimization of manufacturing processes has become a permanent job of today's industrial production. Nowadays, modern manufacturing process technologies are optimized with the help of artificial intelligence methods [1-5].

Many researchers are engaged in the research of tool wear. Zuperl et al. [6] developed mathematical model to predict the tool wear in terms of machining parameters such as helix angle of cutting tool, spindle speed, feed rate, axial and radial depth of cut. In his work the coefficients of the polynomials were calculated by multiple regression method. Sert et al. [7] established the tool wear progression by relating with dimensional deviation and surface roughness. Klancnik

et al. [8] focused on development of two different models for predicting tool wear. They presented regression mathematical and artificial neural network models. Dhar et al. [9] investigated the role of cryogenic cooling by liquid nitrogen jets on tool wear, dimensional deviation and surface finish in turning. Özel et al. [5] developed multiple linear regression models and neural network models for predicting surface roughness and tool flank wear. Other authors [8, 9, 10] also developed mathematical model which was used to relate the wear to the input parameters for a turning operation. The model was then used to predict the tool wear.

Carrying out experiments generally requires considerable time and material and hence it is relatively expensive procedure. Therefore, nowadays many researchers give focus on development of different models. In this paper prediction of tool wear by developed polynomial model and particle swarm optimization (PSO) algorithm in terms of selected machining parameters is shown. Section 2 describes experimental details, section 3 presents the functioning of PSO algorithm and section 4 describes results of PSO model. A short conclusion is given in section 5.

2. TOOL WEAR

Tool wear describes the gradual failure of cutting tools due to regular operation. It is a term often associated with tipped tools, tool bits, or drill bits that are used with machine tools.

Types of wear include:

- flank wear in which the portion of the tool in contact with the finished part erodes.
- crater wear in which contact with chips erodes the rake face. This is somewhat normal for tool wear, and does not seriously degrade the use of a tool until it becomes serious enough to cause a cutting edge failure.
- built-up edge in which material being machined builds up on the cutting edge. Some materials (notably aluminum and copper) have a tendency to anneal themselves to the cutting edge of a tool. It occurs most frequently on softer metals, with a lower melting point. It can be prevented by increasing cutting speeds and using lubricant. When drilling it can be noticed as alternating dark and shiny rings.
- glazing occurs on grinding wheels, and occurs when the exposed abrasive becomes dulled. It is noticeable as a sheen while the wheel is in motion.
- edge wear, in drills, refers to wear to the outer edge of a drill bit around the cutting face caused by excessive cutting speed. It extends down the drill flutes, and requires a large volume of material to be removed from the drill bit before it can be corrected.

Program for measuring tool wear was developed in Matlab. Section of the program window, which allows measurement of tool wear is shown in Fig. 1.

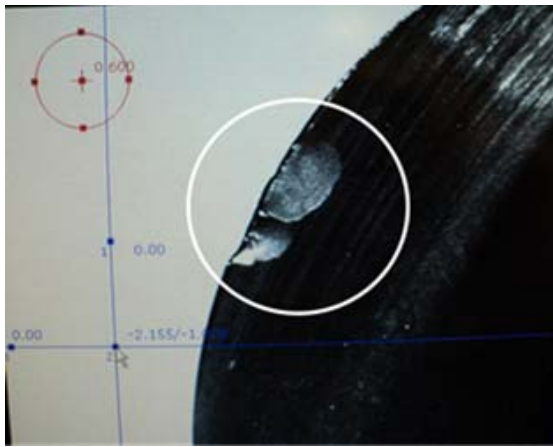


Fig. 1: Cutting edge breakage on the ball-end mill

3. EXPERIMENTAL DETAILS

The experimental work was carried out by Sivasakthivel et al. [6] on a HASS vertical machining center using high speed steel end mill cutter under dry conditions. Material used in experiments (end milling) was aluminium alloy (Al 6063). Dimensions of the workpiece specimen were 32 mm x 32 mm in cross section and 40 mm in length. After milling, the tool wear was measured using a microscope (Metzer) on the flank surface of the end mill cutter.

Experiments were conducted for various sets of machining conditions, i.e. helix angle (α), spindle speed (N), feed rate (Z), axial depth of cut (X) and radial depth of cut (Y). The parameters were set at five levels. Influential factors and their levels are shown in Table 1.

Parameter	Units	Factor levels				
		-2	-1	0	1	2
Helix angle (α)	degree ($^{\circ}$)	30	35	40	45	50
Spindle speed (N)	1/min	2500	3000	3500	4000	4500
Feed rate (Z)	mm/rev	0.03	0.04	0.05	0.06	0.07
Axial depth of cut (X)	mm	1.5	2	2.5	3	3.5
Axial depth of cut (Y)	mm	1.5	2	2.5	3	3.5

Table 1. Influential factors and their levels

4. PARTICLE SWARM OPTIMIZATION

In computer science, particle swarm optimization (PSO) is a computational method that optimizes a problem by iteratively trying to improve a candidate solution with regard to a given measure of quality. PSO optimizes a problem by having a population of candidate solutions, here dubbed particles, and moving these particles around in the search-space according to simple mathematical formulae over the particle's position and velocity. Each particle's movement is influenced by its local best known position but, is also guided toward the best known positions in the search-space, which are updated as better positions are found by other particles. This is expected to move the swarm toward the best solutions.

PSO is originally attributed to Eberhart, Kennedy and Shi in 1995, inspired by the social behaviour of a flock of birds [10]. PSO is initialized with a group of random particles (solutions) and then searches for optima by updating generations. PSO algorithm working procedure is presented on block scheme in Fig. 2. Within iteration each particle is updated by following the two best values. The first one is the best solution (fitness) achieved so far. This fitness value is also stored and is called *pbest*. Another "best" value tracked by the particle swarm optimizer is the best value obtained so far by any particle in the population. This best value is the global best and called *gbest*. After finding the two best values, the particle updates its velocity using the Eq. (1):

$$v_i = v_i + c_1 \text{rand}() (p_i - x_i) + c_2 \text{Rand}() (p_g - x_i) \quad (1)$$

and positions by Eq. (2):

$$x_i = x_i + v_i \quad (2)$$

In Eq. (1) and (2), the designations have the following meanings:

- c_1 and c_2 are learning factors;
- $\text{rand}()$ and $\text{Rand}()$ are random numbers between (0,1);
- $x_i = (x_{i1}, x_{i2}, \dots, x_{iD})$ is a i -th particle;
- p_i is the best position for the i -th particle in the history (*pbest*);
- p_g is globally the best position among all particles (*gbest*);
- v_i is the particle velocity.

For effective convergence of the system the adequate algorithm parameters must be selected, when using the PSO. For tool wear prediction of workpiece with assistance of PSO-algorithm the following parameters were used:

- Number of swarm particles: 750;
- Number of iterations: 500.000;
- Particle size: 21;
- Acceleration coefficient c_1 (cognitive parameter): 1.2;
- Acceleration coefficient c_2 (social parameter): 2.4.

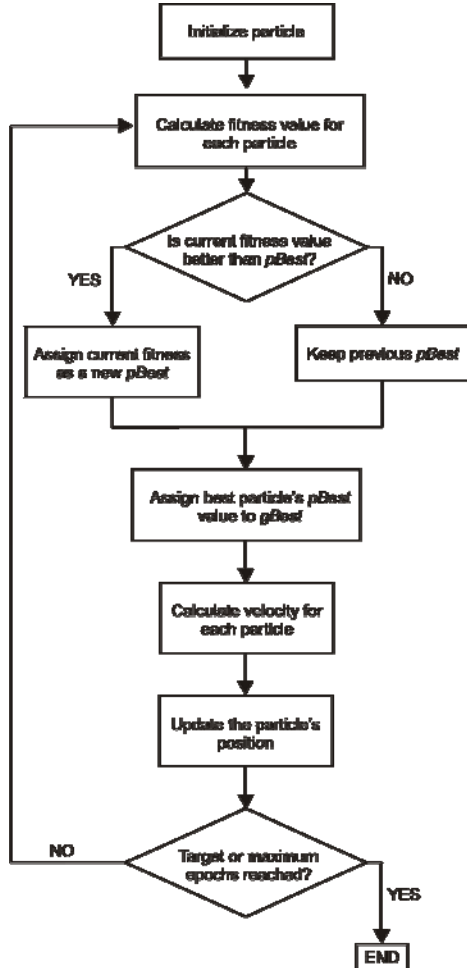


Fig. 2. PSO algorithm working scheme

5. PARTICLE SWARM OPTIMIZATION MODEL RESULTS

Through evolution a developed system has searched the optimal coefficient values of the selected polynomial model given by the Eq. (3). The polynomial model with 21 coefficients was selected on the basis of many trials and on the basis of experience.

$$\begin{aligned}
 T = & k_1 + k_2\alpha + k_3N + k_4Z + k_5X + k_6Y + k_7\alpha^2 \\
 & + k_8N^2 + k_9Z^2 + k_{10}X^2 + k_{11}Y^2 + k_{12}\alpha N + k_{13}\alpha Z \\
 & + k_{14}\alpha X + k_{15}\alpha Y + k_{16}NZ + k_{17}NX + k_{18}NY \\
 & + k_{19}ZX + k_{20}ZY + k_{21}XY
 \end{aligned} \quad (3)$$

The best solution proposed for calculation of tool wear T , by algorithm is the following:

$$\begin{aligned}
 T = & 6,2868 - 0,2228\alpha - 2,7661 \cdot 10^{-4} N - 22,6074Z \\
 & - 0,6518X + 0,3942Y + 0,0018\alpha^2 - 2,0209 \cdot 10^{-9} N^2 \\
 & - 42,5521Z^2 - 0,0045X^2 + 0,0380Y^2 \\
 & + 3,3742 \cdot 10^{-6} \alpha N + 0,4463\alpha Z + 0,0173\alpha X \\
 & - 0,0026\alpha Y + 0,0059NZ + 2,8741 \cdot 10^{-5} NX \\
 & - 8,0744 \cdot 10^{-5} NY - 1,5371ZX - 2,3129ZY \\
 & - 0,0362XY
 \end{aligned} \quad (4)$$

With the Eq. (4) we can predict the tool wear achieved in end milling by the proposed cutting parameters. Tab. 2 presents the prediction of tool wear results with a use of model that is presented by Eq. (3), also for the data which were used in testing (test base) by PSO-algorithm. Test base was composed of three samples (Exp. no. 10, 12 and 31). Deviation of PSO model prediction regarding the conducted tool wear measurements is also calculated.

It is evident from Tab. 2 and Fig. 3 that in most cases, the error in prediction is smaller than 5 %. The average error of PSO model prediction equals 1.62 % for a learning base and 15.94 % for a testing base. Only in two cases, the error was more than 17.0 %. In these cases these two samples were composing the test base. However, most of the samples have much smaller errors in prediction, which means that developed model is suitable for prediction of tool wear.

Exp. no.	Measured values T [mm]	Predicted values using PSO	% Error
1	0.620	0.6194	0.09
2	0.185	0.1795	2.97
3	0.375	0.3744	0.15
4	0.165	0.1582	4.09
5	0.405	0.4060	0.25
6	0.285	0.2798	1.81
7	0.450	0.4497	0.06
8	0.265	0.2598	1.95
9	0.350	0.3562	1.76
10	0.275	0.3240	17.82
11	0.315	0.3199	1.56
12	0.270	0.2040	24.46
13	0.320	0.3265	2.03
14	0.230	0.2316	0.69
15	0.305	0.3115	2.13
16	0.275	0.2753	0.12
17	0.615	0.6035	1.86
18	0.280	0.2907	3.82
19	0.315	0.3134	0.51
20	0.220	0.2209	0.40
21	0.250	0.2515	0.62
22	0.255	0.2527	0.90
23	0.300	0.3119	3.96
24	0.230	0.2174	5.49
25	0.255	0.2534	0.64
26	0.360	0.3609	0.24
27	0.275	0.2691	2.13
28	0.265	0.2691	1.57
29	0.275	0.2691	2.13
30	0.265	0.2691	1.57
31	0.255	0.2691	5.55
32	0.265	0.2691	1.57

Table 2. Results of PSO model prediction

Fig. 3 graphically presents comparison of % of error for each experiment. Selected polynomial model given by the Eq. (3) was successful because convergence chart shows that after 35000 iterations mean squared error of model was minimal.

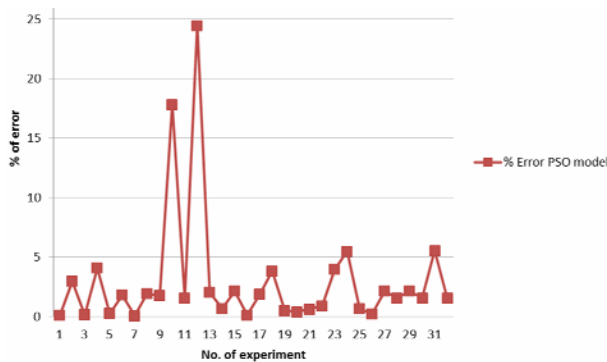


Fig. 3. % Error of PSO model

Fig. 4 shows graph of convergence.

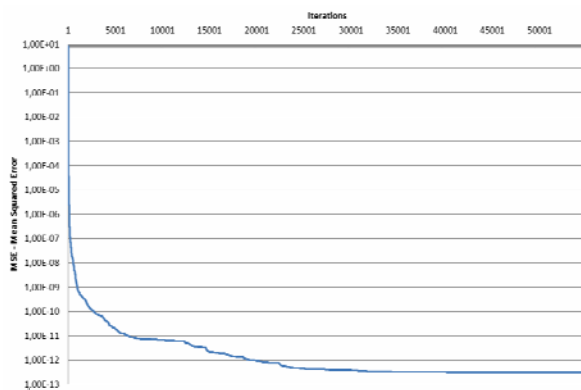


Fig. 4. % Error of PSO model

6. CONCLUSION

In this work the basic aim of tool wear prediction in end milling has been fulfilled. Through evolution and searching for the best solution, polynomial model has been proved to be very effective and robust. When we examined the learning base on which the system was searching for the optimal solution it was discovered that the prediction error is less than 5 % and the average error of the test base was 1.82 %. Only in two cases the error was bigger than 15 % but in these cases these two samples were from the test base. Results showed that developed model is reliable and could be used effectively for tool wear prediction.

Possibility to predict the tool wear helps the operator in selecting the appropriate machining parameters in order to maximize the tool life and product quality. In the future it is provided to develop a model for tool wear prediction based on a gravitational search algorithm (GSA) and to compare the results gained by various models.

7. REFERENCES

[1] Senveter, J., Klančnik, S., Balic, J., Cus, F.: *Prediction of surface roughness using a feed-*

forward neural network. Management and production engineering review, Vol. 1, no. 2, p.p. 47-55, 2010.

[2] Leo Dev Wins, K., Varadarajan, A.S.: *Simulation of surface milling of hardened AISi4340 steel with minimal fluid application using artificial neural network.* Advances in Production Engineering & Management, vol. 7, no. 1, p.p. 51-60, 2012.

[3] Ungureanu, N., Ungureanu, M., Hatala, M.: *Estimation of reliability of equipment.* Scientific Bulletin, Serie C. vol. 2012, no. 26, p.p.76-79, 2012.

[4] Sahoo, P.: *Optimization of turning para-meters for surface roughness using RSM and GA.* Advances in Production Engineering & Management, Vol. 6, no. 3, p.p. 197-208, 2011.

[5] Özel, T., Karpat, Y., Figueira, L., Davim, J.P.: *Modelling of surface finish and tool flank wear in turning of AISI D2 steel with ceramic wiper inserts.* Journal of Materials Processing Technology, Vol. 189, no. 1-3, p.p. 192-198, 2007.

[6] Zuperl, U., Kiker, E., Cus, F.: *Optimization in ball-end milling by using adaptive neural controller.* Industrial technology, Vol. 1, p.p. 393-398, 2003.

[7] Sert, H., Can, A., Habali, K., F., Okay, F.: *Wear behavior of PVD TiAlN, CVD TiN coated and cermet cutting tools.* Tribology in industry, Vol. 27, no. 3-4, p.p. 3-9, 2005.

[8] Klančnik, S., Balic, J., Cus, F.: *Intelligent prediction of milling strategy using neural networks.* Control and Cybernetics, Vol. 39, no. 1, p.p. 9-22, 2010.

[9] Dhar, N.R., Islam, S., Kamruzzaman, M., Paul, S.: *Wear behavior of uncoated carbide inserts under dry, wet and cryogenic cooling conditions in turning C-60 steel.* Journal of the Brazilian Society of Mechanical Sciences and Engineering, Vol. 28, no. 2, p.p. 146-152, 2006.

[10] Kennedy, J., Eberhart, R.: *Particle swarm optimization.* Proceeding of the IEEE International Conference on Neural Network, Vol. 4, p.p. 1942-1948, 1995.

Authors: B.Sc., researcher **Tomaz Irgolic**, Full Professor **Dr. Franc Cus**, Assist. Professor **Dr. Uros Zuperl.**, University of Maribor, Faculty of Mechanical Engineering, Institute for Production Engineering, Smetanova 17, 2000 Maribor, Slovenia, Phone.: +386 22 207-597, Fax: +386 22 207-996.
E-mail: tomaz.irgolic@um.si
franc.cus@um.si
uros.zuperl@um.si

Trif, A., Borzan, M., Rus, A., Nedezki, C., Agarski, B.

STUDIES AND RESEARCHES ON INSERT WEAR IN TURNING PROCESS

Received: 05 June 2014 / Accepted: 20 June 2014

Abstract: *The purpose of this paper is to analyze the wear of the cutting tools in terms of the parameters which influence the wear and make a comparative study of the various metallic materials with different inserts, in turning. Among the parameters that influence the degree of wear of the cutting tool, is shown in detail the impact of the temperature during cutting concerning the wear of the insert. The temperature achieved in cutting was compared with the temperature obtained after the simulation using DEFORM 2D program.*

Key words: wear, turning, DEFORM, cutting tools

Studije i istraživanja o habanju reznih pločica kod struganja. *Svrha ovog rada je da analizira habanje alata za sečenje sa stanovišta parametara koji utiču na habanje i napravi komparativnu studiju ponašanja različitih metalnih materijala sa različitim pločicama kod struganja. Među parametrima koji utiču na stepen pohabanosti reznog alata, detaljno je prikazan uticaj temperature tokom sečenja na habanje rezne pločice. Temperatura postignuta pri procesu sečenja je upoređena sa temperaturom dobijenom simulacijom pomoću DEFORM 2D softvera.*

Ključne reči: habanje, struganje, DEFORM, alati za sečenje

1. INTRODUCTION

The main objective of this study is to determine the cutting tool wear. Once determined the wear, an important step was measuring the temperature achieved in cutting, which was compared with the temperature obtained after the simulation using DEFORM 2D program.

As a result of the pressure on the contact surface, of the temperature and of relative movement chip-tool and workpiece-tool, surfaces of the cutting tool is subject to wear. Wear of cutting tools is the progressive removal of material from the operative surfaces of the tool having the effect of changing geometry and reduction of the cutting capacity of the cutting tool. Cutting tool wear preponderantly affects dimensional accuracy and the surface quality. Cutting tool wear influences cutting conditions, and it worsens by heating cutters, leading to increasing of energy consumption. In the cutting process of the various types of wear occurring rarely separated, usually simultaneously, one way or another of wear having preponderant role depending on the conditions of the cutting [1-6].

The main cutting conditions which influence the wear are:

- the material of the tool and the workpiece;
- cutting speed;
- the temperature in the cutting process.

In this study will be analyze the effect of temperature in the cutting process on the contact area chip-cutting tool, and comparison of the wear between two different inserts, for two different materials.

The obtained results have been then compared to those which are obtained by simulation by means of a software. The software used to simulate the cutting

process which allows to obtain some models of high accuracy necessary for reliable monitoring is DEORM 2D.

2. THE EXPERIMENTAL TURNING PROCESS

2.1 Workpiece material

The experiment was intended to measure temperature and tool wear forms appearing in cutting stainless steel and in cutting OLC 45 steel.

The first material to be processed is a stainless steel X5CrNi18-10, manufactured with a diameter of $D = 40$ mm, having the following composition: C - 0.05%; Cr - 18%; Ni - 10%



Fig.1. Workpiece material (stainless steel)

Another used material is OLC 45:

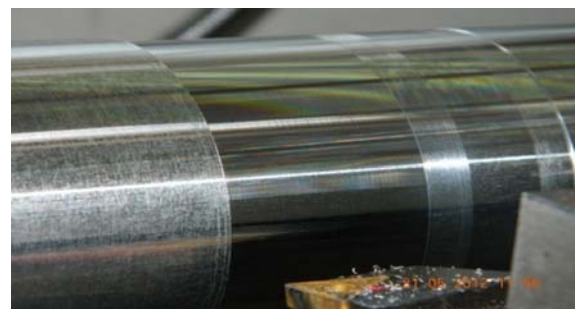


Fig. 2. OLC 45 workpiece material

The workpiece of OLC 45, with diameter $D = 77$ mm, is a quality steel (C45U according to EN ISO 4957:202). Mechanical characteristics and chemical composition of this steel are governed by STAS 880-88. Remembered standard for steel OLC45 (C45U) are imposed (chemical composition) : C: 0.43 0.48%; Mn: 0.5 0.80%; Si: 0.17 0.370%; Cr: max0.03% ; Ni: max0.030%.

2.2 Used cutting inserts

The 2 cutting tool inserts is represented by type Sumitomo CNMG 120408N-MU AC830P (1) and by type Sandvik TNMG 16 04 08:



Fig. 3. The first used cutting insert (Sumitomo)

In the turning process simulation was used CNMG 120408N-MU AC830P insertcoated with two layers: one titanium carbonitride (TiCN), and the second aluminum oxide (Al_2O_3).

AC830P inserts are used for a wide range of applications being recommended for both mass production as well as small series.

AC830P inserts are part of the super-heavyweight class for roughing, being used even in unstable conditions.

This type of inserts are characterized by a special coating and through a special control of the chip evacuation due to a special geometry:

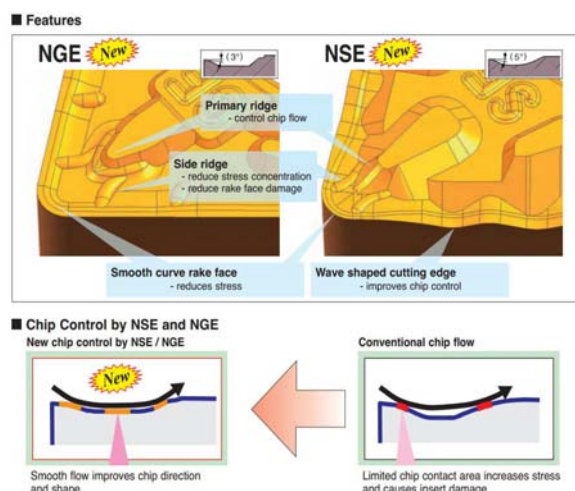


Fig. 4. Special control of the chip evacuation.

The layer super - FF consisting of titanium carbonitride over which is placed a layer of aluminum oxide layer is ultra-hard, allowing higher cutting speed, improves the surface quality, prolongs the life of the insert. Ceramic layers improves the thermal resistance required for the dry cutting speeds [7].

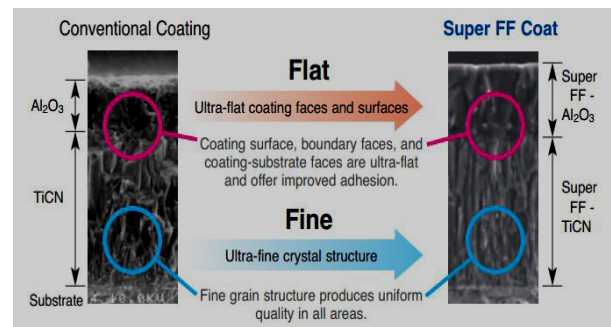


Fig. 5. The coating structure of AC830P inserts

Another used insert is Sandvik TNMG 16 04 08:



Fig. 6. TNMG 16 04 08 insert (Sandvik)

2.3 The measuring device

In the experiment has been used an infrared thermometer called TempLS. The infrared Thermometer as in the figure below is used in a wide range of temperature ($- 35^{\circ}C$ to $900^{\circ}C$) and enables the highly accurate non-contact measurements to determine exactly the right temperature of components. This thermometer includes a temperature sensor type K. Uses the four lasers for good focus. Presents the USB interface for PC software to display OPTRIS Connect with the possibility of 20 measurements per second.



Fig. 7. The temperature measuring device



Fig. 8. The turning process of stainless steel material

For temperature measurement of the inserts in different cutting conditions have been changed machining rotation and feed maintaining the constant cutting depth.

Depending on the cutting regime, by using device TempLS and the software Optris Connect were identified cutting tool temperature graphs.

No	Tool geometry	Feed [mm/rot]	Cutting depth [mm]	Cutting speed [m/min]
1	$\alpha = 6^\circ$ $\gamma = 6^\circ$ R=0,05 mm	0,2	1	370
2		0,3	1	370
3		0,4	1	370
4		0,2	1	560
5		0,3	1	560
6		0,4	1	560
7		0,2	1	830
8		0,3	1	830
9		0,4	1	830

Table 1. Cutting conditions

Is observed temperature increase with increasing the speed and feed (a variation of temperature between 244 and 331 degrees in the time interval studied).

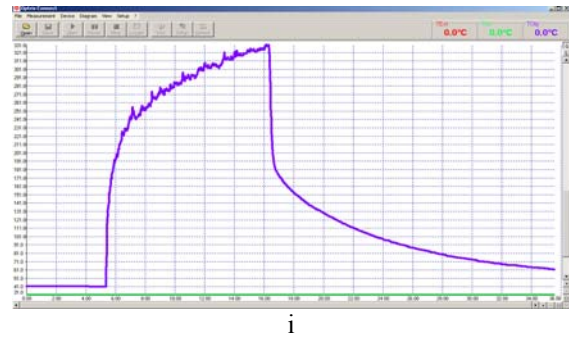
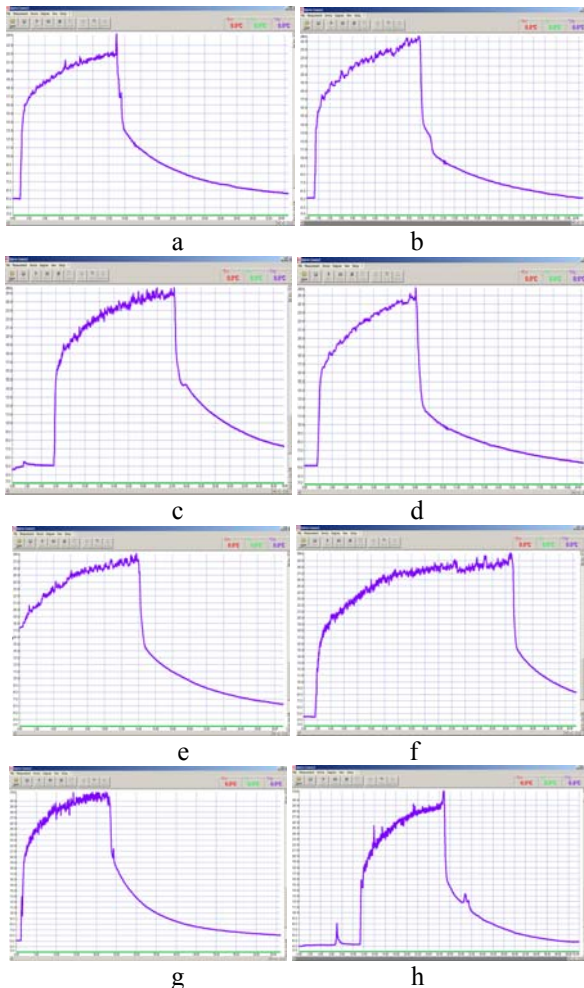


Fig. 9. The graphs of the nine cutting data in coordinates time-temperature (a,b,c,d,e,f,g,h,i)

Similarly, the measuring temperature values in turning process of OLC 45 material, ranges between 145 and 178 degrees.



Fig. 10. The turning process of OLC 45 material

3. THE TURNING PROCESS SIMULATION

The simulation turning process is assimilated to the planing operation, given the deployment of the propeller materialized by the chip for a distance of 50 mm. It is considered that the cutting process get to a relative stability in terms of finite element analysis for the distance considered in the simulation (fig.11)

3.1. The cutting conditions

For the beginning the cutting simulation was achieved for a stainless steel X5CrNi18-10 material.

Establishing the the cutting regime requires to specify the following processing machine parameters: cutting speed, diameter, cutting depth and feed (Table 1).

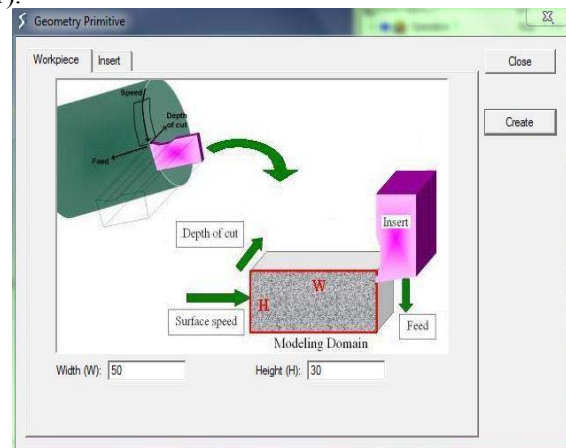


Fig. 11. Assimilation of turning process with the planing operation within the DEFORM 2D software [8], [9]

In defining of tool geometry must be inserted the values of its linear and angular parameters:

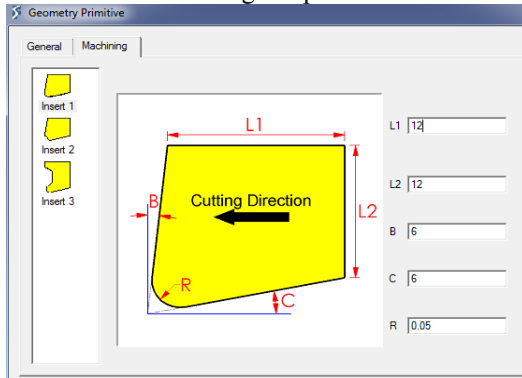


Fig. 12. Linear and angular parameters of the cutting tool

In the control region of the simulation were determined number of steps and the length of cutting simulation in order to generate the required database necessary to calculation:

- number of steps: 500
- cutting Length: 50 mm

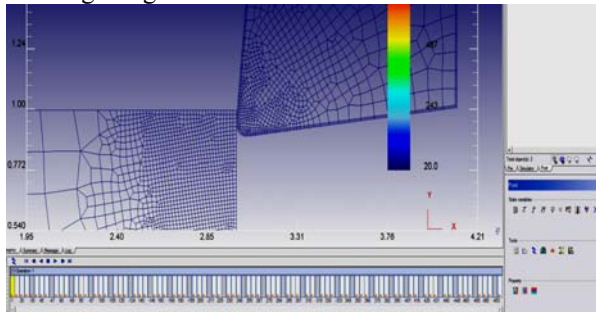


Fig. 13. The simulation of the turning process

3.2. The simulation results

After running the finite element program with which was simulated the cutting process for turning operation it shows the following values of cutting zone temperature, step by step:

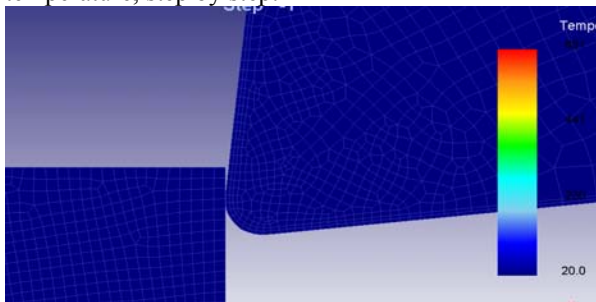


Fig. 14. Beginning of the simulation

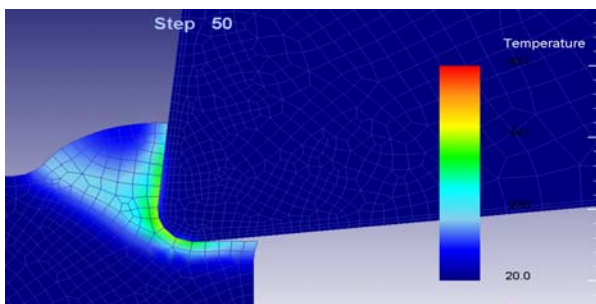


Fig. 15. The temperature in step 50

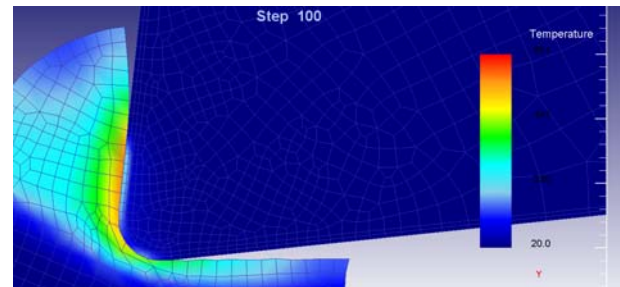


Fig. 16. The temperature in step 100

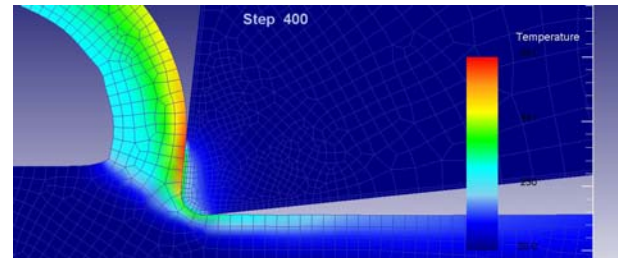


Fig. 17. The temperature in step 400

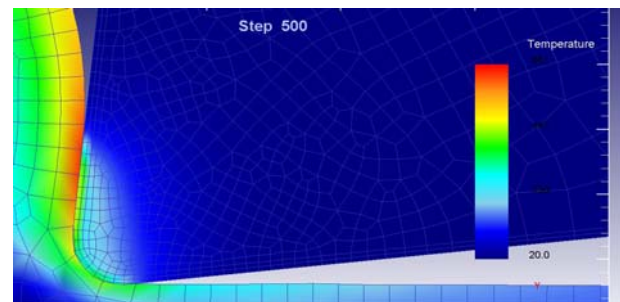


Fig. 18. The temperature in step 500



Fig. 19. Temperature evolution by isotherms

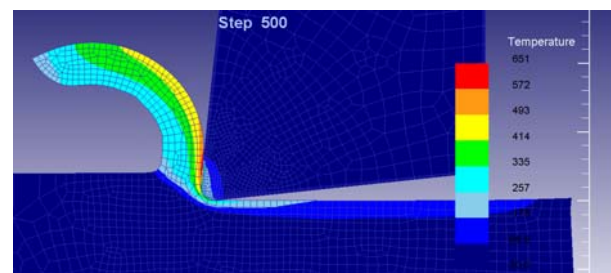


Fig. 20. Temperature evolution by solid contour

From the state of the temperature, it can be seen the position of the center of wear on the rake face which is located at a distance from the cutting edge and coincides with the maximum depth of crater's wear, more than, the representation of isotherms highlights precisely the form of the crater wear on the rake face and of wear on the face area. The temperatures of the tool will be used in determining of the theoretical model and of the experimental model of wear.

After cutting was measure a temperature of 244°C, up to a maximum of 331°C. With DEFORM 2D program using the same cutting data, we obtained a temperature of 280-320°C (the turning process of a stainless steel material).

Similarly, the cutting simulation was achieved for OLC 45. In this case DEFORM 2D simulation reveals a temperature variation of 130 to 180 degrees (145 to 178 degrees in experimental case).

4. CONCLUSIONS

- This paper has presented an experimental study and a modeling of the the cutting process respectively of a turnings, using the finite element method.
- A study was carried on temperature measurement in the cutting process.
- It then compared the results with those which are obtained by simulation using a software. The software used to simulate the cutting process which generates some models of high precision required for reliable monitoring process is DEFORM 2D Machining.
- Using this software the simulations have been performed for turning process of a stainless steel material and for a OLC 45 steel.
- The temperature values in turning process, experimentally obtained are similar to those obtained by the simulation with DEFORM 2D software.
- There is an increase of the temperature with increasing feed and cutting speed.
- In the experimental study, the difference between the measured temperature and that obtained by finite element simulation occurs because in the experiment were measured the average temperatures, and the finite element analysis reveals the cutting tool temperature at the contact with the workpiece.
- By comparison with the the situation in the start of the experiment is noted that under the same cutting conditions, the wear of a cutting insert TNMG 16 08 04 OLC 45 when cutting material is OLC 45 is much higher than of the insert Sumitomo CNMG 120408N-MU AC830P, when cutting material is stainless steel, although the stainless steel hardness is about 50% higher than the hardness of the steel OLC 45:



Fig. 21. The wear of cutting insert Sumitomo

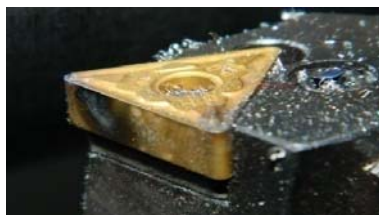


Fig. 22. The wear of cutting insert TNMG

5. REFERENCES

- [1] Antić ,A., Hodolič J., Soković M., *Development of an intelligent system for tool wear monitoring applying neural networks*, Journal of Achievements in Materials and Manufacturing Engineering, Poland, Volume 14, Issue 1-2, January-February 2006
- [2] Deacu L., Gurgiuman H., Oancea N., s.a., *Bazele așchierii și generării suprafețelor, vol. II*, Universitatea Tehnică Cluj-Napoca, Facultatea de Construcții de Mașini ; 1992
- [3] Gavrițaș I., Drăguț E., Vleru V., Bonoiu V., *Tehnologii de prelucrare cu scule din materiale dure și extradure*, Editura Tehnică, București, 1977.
- [4] Hollanda D., Mehedințeanu M., Oancea N., *Așchieria și scule așchietoare*, editura Didactică și Pedagogică, București; 1982
- [5] Lazărescu I., Abrudan Gl., Stețiu Gr., *Așchieria și scule așchietoare curs pentru subingineri*, editura Didactică și Pedagogică, București; 1978
- [6] Muntean A., *Bazele așchierii și generării suprafețelor*, editura Universității „Lucian Blaga”, Sibiu, 2002
- [7] http://www.sumicarbide.com/pdf/AC820P_AC830P%20Brochure.pdf
- [8] www.deform.com
- [9] Deform 2D Machining Manual V 9.0

Authors:

Senior Lecturer. Dr. Ing. Adrian TRIF, Technical University of Cluj-Napoca, Department of Manufacturing Engineering, Bd. Muncii, 103-105 , 400641, Cluj-Napoca, Romania, Phone: 004-0757-079796, e-mail: adrian.trif@tcm.utcluj.ro

Professor Dr. Ing. Marian BORZAN, Technical University of Cluj-Napoca, Department of Manufacturing Engineering, Bd. Muncii, 103-105 , 400641 Cluj Napoca, Romania, Phone:004-0747-033882, e-mail: marian.borzan@tcm.utcluj.ro

Prof. Ing. Adriana RUS, “Romulus Ladea Fine Arts Highschool, No 56, Dorobantilor Street, 400117 Cluj-Napoca, Phone on Fax: 0264-431449, 0264-593006 , Romania, e-mail: adi_adrianarus@yahoo.com

Senior Lecturer. Dr. Ing. Claudiu NEDEZKI, Technical University of Cluj-Napoca, Department of Engineering Design and Robotics, Bd. Muncii, 103-105, 400641 Cluj Napoca, Romania, Phone: 004-0264-401639, e-mail: Claudiu.Nedezki@muri.utcluj.ro

M.Sc. Boris Agarski, University of Novi Sad, Faculty of Technical Sciences, Department of Production Engineering, Trg Dositeja Obradovica 6, 21000 Novi Sad, Srbija, Tel: +381-21-485-23-50, Fax: +381-21-454-495. e-mail: agarski@uns.ac.rs



Kishore Debnath, Inderdeep Singh, Akshay Dvivedi

EVALUATION OF SURFACE ROUGHNESS DURING ROTARY-MODE ULTRASONIC DRILLING OF GLASS/EPOXY COMPOSITE LAMINATES

Received: 20 May 2014 / Accepted: 20 June 2014

Abstract: The application spectrum of fiber reinforced plastics (FRP's) has increased enormously in the last few years. The demand of FRP's has multiplied due to the fact that the properties of these materials are superior to the conventional metals and alloys. The increasing demand of FRP's expands the requirement of machining operation, especially when intricate parts are made up of FRP's. In a complex FRP product, components are mostly assembled through mechanical fastening. Mechanical fastening such as bolting demands the hole of desired size and good quality. The quality of the hole decides the ultimate load carrying capacity of the final assembly. The production of good quality hole in FRP's through traditional method is still a challenging task. The unwanted surface damage in and around the drilling zone is the major drilling problem. Therefore, continuous efforts have been put for the manufacturing of high precision good quality holes. In the present research investigation, an innovative method has been conceptualized and developed for the drilling of good quality holes in glass/epoxy laminates. Experimental investigation has been carried out to analyze the effect of several process parameters on the hole wall surface roughness. The major outcome of the study emphasize that the surface roughness near the hole entrance side is low as compared to the surface roughness at the hole exit side.

Key words: Composites, Polymer, Laminates, Ultrasonic Drilling, Surface Roughness.

Ocena hrapavost površine u toku rotacionog ultrazvučnog bušenja staklo/epoksi kompozitnih laminata. Upotrebni spektar vlaknima ojačanih plastika (FRP) se u poslednjih nekoliko godina znatno proširio. Potražnja FRP-a se povećala zbog činjenice da osobine ovih materijala su superiornije u poređenju sa konvencionalnim metalima i legurama. Povećana potražnja FRP-a proširuje zahteve operacija obrade, posebno kada su u pitanju složeni delovi od FRP-a. Kod kompleksnog FRP dela delovi su obično spojeni mehaničkim pričvršćivanjem. Mehaničko pričvršćivanje kao napr. spajanje vijcima zahteva otvor određene veličine i dobrog kvaliteta. Kvalitet rupe određuje nominalno opterećenje nošenja celog sklopa. Izrada kvalitetnog otvora kod FRP-a upotrebom klasičnih metoda je još uvek izazovni poduhvat. Neželjeno površinsko oštećenje u i oko zone bušenja je veliki problem. Stoga su ostvareni veliki napori u cilju poboljšanja izrade kvalitetnih otvora. U ovom radu je razvijena i opisana inovativna metoda bušenja kvalitetnih otvora u staklo/epoxy laminatima. Eksperimentalno istraživanje je sprovedeno da bi se analizirali efekti nekoliko parametara na hrapavost zidova otvora. Veliki rezultat istraživanja naglašava da je hrapavost blizu ulaza otvora mala u poređenju sa hrapavošću na strani izlaza otvora.

Ključne reči: Kompoziti, polimeri, laminate, ultrazvučno bušenje, površinska hrapavost.

1. INTRODUCTION

The superior strength and stiffness, light-weight and anti-corrosion characteristic are the few properties that make FRP's an excellent class of material system [1-4]. These materials have replaced many metallic components in aerospace and automobile industry. The use of FRP's in structural and non-structural applications necessitates joining through mechanical fastening of several components [5,6]. The efficiency of mechanical fastening is highly dependent on the precision and accuracy of the drilled hole. Mostly, drilling of FRP is performed in a conventional way by rotating and feeding the drill against the work material. The major drawback of the conventional drilling is the drilling induced damage that cannot be completely avoided [7,8]. The main reason of drilling induced damage is the generation of thrust force during drilling. The thrust force is generated because of the direct interaction between the tool and work material. The interaction between the tool and work material cannot

be avoided if the hole is made by means of conventional drilling process. This challenge leads to the development of new drilling methods where the direct contact between the tool and work material can be avoided. In order to achieve this, non-conventional machining methods can be useful for making of holes in FRP's.

Rotary ultrasonic machining (RUM) has been developed for drilling of FRP parts when there is a requirement of good quality holes. RUM is a hybrid machining process which is a combination of diamond grinding and ultrasonic machining process [9]. Cong et al. [10] has experimentally proved that RUM is much superior to the twist drilling of carbon fiber reinforced plastics (CFRP). The study shows that thrust force, torque, surface roughness, delamination and tool wear is less in RUM as compared to twist drilling. Liu et al. [11] has developed a new drilling method named rotary ultrasonic elliptical machining (RUEM) for drilling of CFRP. RUEM combines the advantages of both RUM and ultrasonic elliptical vibration cutting (UEVC). The

study reported that the precision of holes, and the surface quality around the hole edge has been substantially improved while delamination at the exit of the hole has been prevented during the drilling of CFRP. The fundamental reason of getting good quality hole in RUM and RUEM is that, in both processes the tool and work material interaction is pulse intermittent. The intermittent contact of the tool with the work material results in decrease in average cutting force and hence improves the quality of hole. The capability of ultrasonic machining for drilling of CFRP has been investigated by Hocheng and Hsu [12]. The study revealed that ultrasonic machining produce better surface finish and hole quality than the conventional drilling. The unconventional methods of drilling such as, RUM, RUEM and USM are of paramount importance for drilling of high precision good quality hole in fiber reinforced composites. The present study is concerned with the rotary-mode ultrasonic machining of glass fiber reinforced epoxy laminates. The viability of modified ultrasonic drilling process has been investigated in order to achieve good quality clean-cut holes. The evaluation of surface roughness at the various sections of drilled hole cylindrical wall has been investigated. The effect of various process parameters on the surface roughness of the hole cylindrical wall at the entry and exit side has been found out experimentally.

2. EXPERIMENTAL DETAILS

2.1 Materials And Experimental Setup

The glass/epoxy composite laminate of four millimeter thickness was prepared. A chrome plated mild steel mold was specifically designed to fabricate laminates with the thickness of 4 mm. The laminate consists of six layers of woven glass fiber mat. Hand lay-up method was used for the fabrication of composite laminate. Epoxy resin, Araldite LY 556 (density of 1.12 g/cm³) and hardener HY 951 (density of 1 g/cm³) were used as matrix material. The weight percentage of fiber varies in the range of 50-55% in the composite laminates.

The ultrasonic machining method was used for the drilling of glass-epoxy laminate. The method was substantially modified in order to expedite the drilling operation. A rotary setup has been developed on Stationary 500 W Sonic-Mill, AP-500 (Albuquerque, NM). The complete experimental set-up consisting of power supply unit, mill-module assembly, abrasive slurry flow system, rotary set-up and dedicated work piece holder is schematically shown in Figure 1. The rotation of work piece against the tool facilitates chip removal. The tool used for the study is hollow stainless steel (S304) rod of outer diameter of 8 mm. The range of frequency and amplitude of vibration during the experimentation were 20 kHz \pm 200 Hz and 0.0253-0.0258 mm. The rotational speed of the work piece was kept constant to 300 rpm throughout the experiments.

2.2 Experimental Planning and Measurements

The prime factors considered for the present experimental study are power rating, slurry

concentration and abrasive grit number. All the selected input parameters vary at three different levels. Power rating which has been recognized as a significant process parameter varies from 150 to 350 W. The level of slurry concentration varies from 25 to 35 % by the weight of the abrasives to the water. Three different types of slurry were prepared where particles grit number varies at three different levels, 220, 320 and 500. Full factorial experimental design, i.e., 3³ = 27 numbers of drilling experiments were carried out. All tests have been repeated three times and the average value of the output response was taken for analysis.

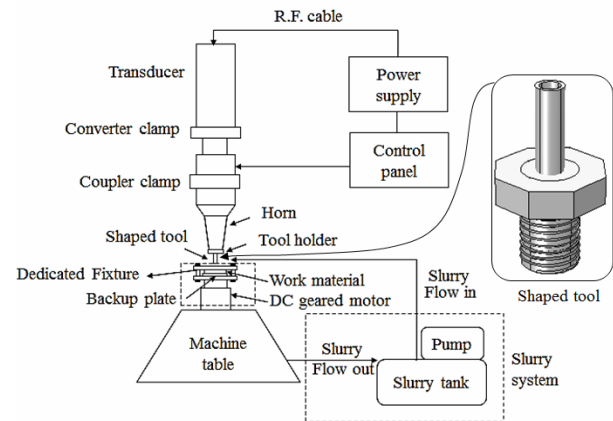


Fig. 1. Schematic of experimental setup.

Variable input parameters		Setting values
1.	Power rating	150, 250 and 350 W
2.	Slurry concentration	25, 30, and 35 %
3.	Abrasive grit number	220, 320, and 500
Constant parameters		
1.	Tool geometry	Hollow tool
2.	Outer diameter	8 mm
3.	Wall thickness	0.625 mm
4.	Work material	Glass/epoxy laminates
5.	Work piece thickness	4 mm
6.	Abrasive type	Silicon carbide
7.	Suspension medium	Water
8.	Flow rate	5 l-min ⁻¹
9.	Frequency of vibration	20 kHz \pm 200 Hz
10.	Rotational speed	300 rpm

Table 1 Process parameters and their values.

The average surface roughness, R_a of the hole cylindrical wall was measured by using Taylor Hobson, SURTRONIC S25. The cut-off length and evaluation length during measurement of R_a was set to 0.25 mm and 1.25 mm, respectively. The R_a value was obtained by moving the stylus parallel to the axis of the hole. Hole diameter of 8 mm was chosen because the stylus can move easily through the hole. Surface roughness of the drilled hole was measured at the entry and exit side of the hole. The value of R_a was taken as 90° interval around the hole periphery. The surface roughness value at the entrance and exit of each hole was taken as the mean of four circumferential readings. As each experimental run was replicated three times, that means a total number of 3 \times 4 = 12 data points were taken and their average value was calculated to get a single value

of R_a . The range of the values of the input parameters is listed in table 1.

3. RESULTS AND DISCUSSION

In order to determine the machining accuracy, a quantitative analysis has been performed on the surface feature generated during ultrasonic drilling. During ultrasonic drilling of glass/epoxy laminates, two different parts were formed, one is laminates with drilled hole and another is cut-out rod (Figure 2).

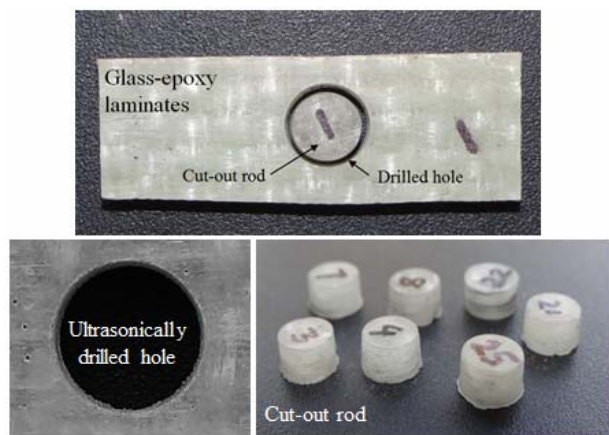


Fig. 2. Work piece with drilled hole and cut-out rod.

The surface roughness evaluation of machined features is a significant aspect because it often defines the performance characteristics of the machined parts. Moreover, surface roughness plays a significant role when factors, such as, fatigue loads, precision fits, fastener holes and aesthetic requirements are considered [13]. Contrary, it has been reported that evaluation of surface roughness in fiber reinforced composites is less dependable than metals [14]. It is attributed due to the fact that protruding fiber tips may cause incorrect results. Furthermore, the hooking of fibers to the stylus of the surface roughness tester may also results in an additional error in the measured surface roughness values.

The cutting mechanism of fiber and matrix during conventional drilling of glass/epoxy laminates is fundamentally different from non-conventional drilling of glass/epoxy laminates. It is well understood that, during the conventional drilling of glass/epoxy laminates, the cutting of fiber and matrix take places due to the combination of plastic deformation, shearing and bending rupture [15]. But, in case of ultrasonic drilling of glass/epoxy laminates, the material is removed because of the brittle fracture and plastic deformation [12]. The ultrasonic drilling shows lesser amount of exposed fibers in the machined surface as compared to the conventional drilling of glass/epoxy composite laminates (Figure 3 and Figure 4). Therefore, from the above discussion it can be said that the surface roughness evaluation is more reliable when holes are produced by means of ultrasonic drilling as compared to the conventional drilling.

In the present experimental investigation, the rotary-mode of ultrasonic machining has been performed on glass/epoxy laminates and the effect of various process

parameters has been evaluated on the surface roughness.

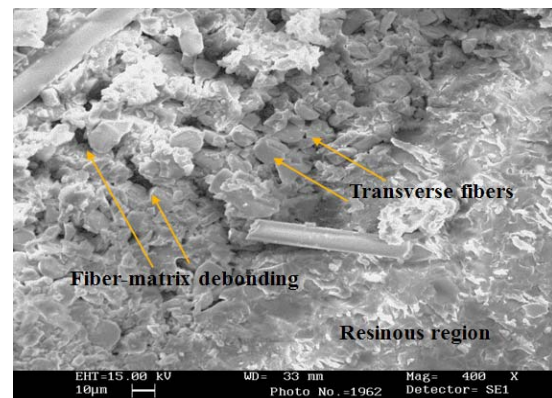


Fig. 3. Microscopic image of the drilled hole wall obtained through conventional drilling.

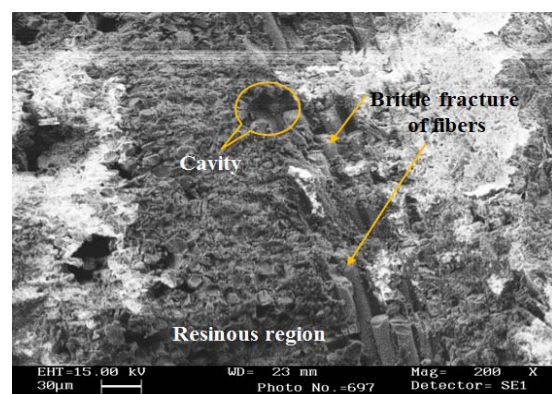


Fig. 4. Microscopic image of the drilled hole wall obtained through rotary mode ultrasonic drilling.

Figures 5-7 shows the effect of various process parameters on the average surface roughness at the entry and exit side of the hole. From the figures, it can be concluded that with increase in the power rating, slurry concentration and abrasive grain size, the R_a value increases linearly. When, the level of power rating and abrasive grain size increase, there is an increasing trend in the average surface roughness values. As both the power rating and the abrasive grain size increases, the kinetic energy of the abrasive particles increases. The increased kinetic energy of the abrasive particles strikes the glass/epoxy laminates with a greater impact force. The high impact force of the abrasive particles results in removal of large chunk or volume of material from the machined surface. This fact leads to the formation of larger craters in the machined surface. The size of the crater significantly affects the height of micro cavities formed in the machined surface which determine the average surface roughness value of the drilled hole surface [16]. It is also worth mentioning that with an increase in slurry concentration, the material removal rate increases. The presence of total number of abrasive particles increases with an increase in the slurry concentration which results in increase in material removal and in turn results in high surface roughness. It is also important to note that the average surface roughness is more at the hole exit side than the hole entry side for all combinations of the levels of the input process

parameters. During rotary-mode ultrasonic drilling of glass/epoxy laminates the material is removed due to the hammering and impact of the abrasive particles. Due to the presence of abrasive particles in the lateral gap (gap between the hole cylindrical surface and the tool periphery) and the rotation of the work piece, abrasion occurs in the lateral gap. Due to this abrasion action the surface roughness near the exit side is different from the surface roughness at the entry side of the drilled hole. This can be attributed due to the fact that as the drilling operation culminates the tool retreats to its starting position. During this period, the rotation of work piece still continues which may results in again abrasion of hole cylindrical surface near the entrance of the hole. But, this phenomenon is not repeated at the exit side of the hole. This means the abrasion duration experienced by the hole surface at the entrance location is more as compared to the exit location, which results in more surface roughness at the exit than the entrance surface of the drilled hole. Cong et al. [17] also reported that the surface roughness near the hole entrance is less as compared to the exit of the hole in rotary ultrasonic machining of stainless steel (15-5).

The authors presents three hypotheses and their testing via experiments and simulations and finally, concluded that the location near the entrance side was ground longer than the location near the exit side by the abrasive portion of the tool. This result in low surface roughness value near the entrance than the exit of the hole.

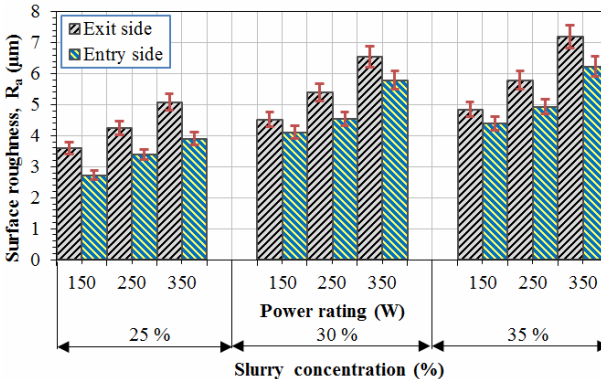


Fig. 5. Surface roughness variation with input parameters for abrasive grit number 220.

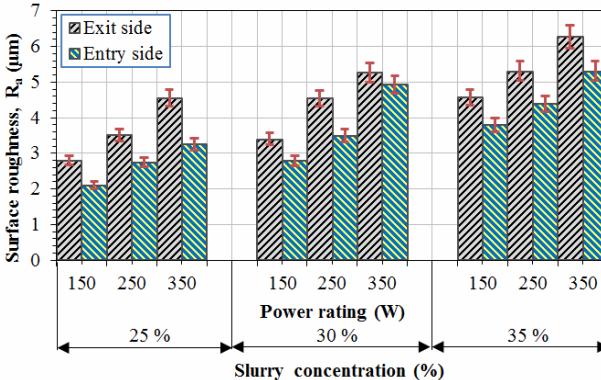


Fig. 6. Surface roughness variation with input parameters for abrasive grit number 320.

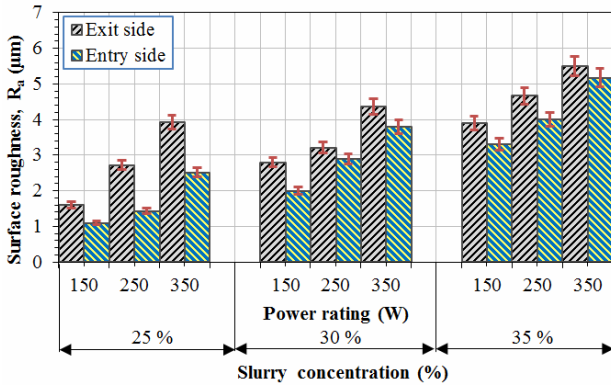


Fig. 7. Surface roughness variation with input parameters for abrasive grit number 500.

4. CONCLUSIONS

In the present research endeavor, an innovative technique has been conceptualized and developed for the drilling of glass/epoxy laminates. The work piece rotation during drilling establishes significant improvement in the process performance. The drilling behavior of glass/epoxy laminates has been experimentally investigated. The effect of various process parameters on the output response (surface roughness) has been discussed comprehensively. From the results and discussion, it has been found that the surface roughness of the drilled hole cylindrical wall increases with an increase in power rating, slurry concentration and abrasive grain size. The average surface roughness value ascribed as low at hole entry side when compared with the surface roughness value at hole exit side.

5. REFERENCES

- [1] Singh, I., Bhatnagar, N.: *Drilling of uni-directional glass fiber reinforced plastic (UD-GFRP) composite laminates*, International Journal of Advanced Manufacturing Technology, Vol. 27, p.p. 870-876, 2006.
- [2] Dhawan, V., Debnath, K., Singh, I., Singh, S.: *Drilling of glass fiber-reinforced epoxy laminates with natural fillers: Thrust force analysis*, Proceedings of the International Conference on Research and Innovations in Mechanical Engineering, p.p. 105-115, Guru Nanak Dev Engineering College, Springer India, Ludhiana, October 24-26, 2013.
- [3] Debnath, K.: *A study on mechanical behavior and damage assessment of short bamboo fiber based polymer composites*, M.Tech. Thesis, National Institute of Technology Rourkela, 2011.
- [4] Debnath, K., Dhawan, V., Singh, I., Dvivedi, A.: *Effect of natural fillers on wear behavior of glass-fiber-reinforced epoxy composites*, Proceedings of the International Conference on Research and Innovations in Mechanical Engineering, p.p. 441-450, Guru Nanak Dev Engineering College, Springer India, Ludhiana, October 24-26, 2013.
- [5] Singh, I., Bhatnagar, N.: *Drilling induced damage in uni-directional glass fiber reinforced plastic*

- (UD-GFRP) composite laminates, International Journal of Advanced Manufacturing Technology, Vol. 27, p.p. 877-882, 2006.
- [6] Debnath, K., Singh, I., Dvivedi, A.: *Rotary mode ultrasonic drilling of glass fiber-reinforced epoxy laminates*, Journal of Composite Materials, 2014. DOI: 10.1177/0021998314527857.
- [7] Singh, I., Bhatnagar, N., Viswanath, P., *Drilling of uni-directional glass fiber reinforced plastics: Experimental and finite element study*, Materials and Design, Vol. 29, p.p. 546-553, 2008.
- [8] Debnath, K., Singh, I., Dvivedi, A., Kumar, P.: *Recent advances in composite materials for wind turbine blades*, World Academic Publishing-Advances in Materials Science and Applications, Hong Kong, 2013.
- [9] Cong, W.L., Feng, Q, Pei, Z.J., Deines, T.W., Treadwell, C.: *Rotary ultrasonic machining of carbon fiber-reinforced plastic composites: Using cutting fluid vs. cold air as coolant*, Journal of Composite Materials, Vol. 47, p.p. 1745-1753, 2012.
- [10] Cong, W.L., Pei, Z.J., Feng, Q, Deines, T.W., Treadwell, C.: *Rotary ultrasonic machining of CFRP: A comparison with twist drilling*, Journal of Reinforced Plastics and Composites, Vol. 31, p.p. 313-321, 2012.
- [11] Liu, J., Zhang, D., Qin, L., Yan L.: *Feasibility study of the rotary ultrasonic elliptical machining of carbon fiber reinforced plastics (CFRP)*, International Journal of Machine Tools & Manufacture, Vol. 53, p.p. 141-150, 2012.
- [12] Hocheng, H., Hsu, C.C.: *Preliminary study of ultrasonic drilling of fiber reinforced plastics*, Journal of Materials Processing Technology, Vol. 48, p.p. 255-266, 1995.
- [13] Wang, X., Feng, C.X.: *Development of empirical models for surface roughness prediction in finish turning*, International Journal of Advanced Manufacturing Technology, Vol. 20, p.p. 348-356, 2002.
- [14] Konig, W., Grab, P.: *Quality definition and assessment in drilling of fiber reinforced thermosets*, CIRP Annals - Manufacturing Technology, Vol. 38, p.p. 119-124, 1989.
- [15] Santhanakrishnan, G.: *Investigations on machining of FRP composites and their tribological behavior*, Ph.D. Thesis, Indian Institute of Technology Madras, 1990.
- [16] Debnath, K., Singh, I., Dvivedi, A.: *Ultrasonic vibration assisted hole making in glass-epoxy laminates*, Proceedings of Twenty - First International Symposium on Processing and Fabrication of Advanced Materials, p.p. 969-974, Indian Institute of Technology Guwahati, Guwahati, December 10-13, 2012.
- [17] Cong, W.L., Pei, Z.J., Deines, T.W., Zhang, P.F., Treadwell, C.: *Surface roughness in rotary ultrasonic machining: hypotheses and their testing via experiments and simulations*, International Journal of Manufacturing Research, Vol. 8, p.p. 378-393, 2013.

Authors: Kishore Debnath, Research Scholar., Dr. Inderdeep Singh, Associate Professor., Dr. Akshay Dvivedi, Assistant Professor., Department of Mechanical and Industrial Engineering, Indian Institute of Technology Roorkee – 247 667, INDIA.

E-mail: debnath.iitr@gmail.com
dr.inderdeep@gmail.com
akshaydvivedi@gmail.com



ADHESIVE WEAR AND FRICTIONAL BEHAVIOR OF RICE HUSK FILLED GLASS/EPOXY COMPOSITES

Received: 20 May 2014 / Accepted: 20 June 2014

Abstract: Low density, high strength and modulus, high corrosion resistance, and self-lubricating properties are the few important properties which makes polymer composites a potential candidate for tribological applications. Development of new materials and their tribological study is still being explored to solve many industrial problems. The present research endeavor aims at development of new tribo-material in order to minimize the specific wear rate and coefficient of friction. The present study experimentally explores the wear and frictional performance of glass fiber reinforced polymer composites filled with rice husk. The dry sliding wear tests are carried out on pin-on-disc wear test machine at ambient conditions. Tests are conducted for sliding speeds of 1, 2 and 3 m/s by applying normal loads of 10, 20 and 30 N. The weight loss and friction force is measured by varying the sliding distance 1000 to 3000 m. Further, the worn surface morphology is examined by using scanning electron microscope (SEM) to analyze the wear mechanism.

Key words: Glass/epoxy laminates, Rice husk, Specific wear rate, Coefficient of friction, SEM.

Adhezivno habanje i frikciono ponašanje staklo/epoksi kompozita napunjenih pirinčanom ljuskom. Mala gustina, visoka čvrstoća i modul, visoka otpornost na koroziju i odlične samopodmazujuće osobine su nekoliko važnih osobina koje čine polimerne kompozite potencijalnim kandidatima za tribološke primene. Razvoj novih materijala i njihova tribološka ispitivanja su još uvek u fazi realizacije da bi se rešili mnogi industrijski problemi. Ovaj rad se bavi razvojem novih tribo materijala u cilju smanjenja specifičnog habanja i koeficijenta trenja. Ova studija eksperimentalno istražuje habanje i osobine trenja polimernih kompozita ojačanih staklenim vlaknima i ispunjenih pirinčanom ljuskom. Testovi suvog trenja su realizovani na pin-on-disk mašini u uslovima sobnog ambijenta. Testovi su realizovani za brzine klizanja 1, 2 and 3 m/s sa primenom normalnog opterećenja od 10, 20 i 30 N. Smanjenje težine i sila trenja su mereni promenom dužine trenja od 1000 do 3000 m. Morfologija pohabane površine je ispitana pomoću skening elektronskog mikroskopa (SEM) da bi se analizirao mehanizam trenja.

Ključne reči: Staklo/epoxy laminati, pirinčana ljuska, specifično habanje, koeficijent trenja, SEM.

1. INTRODUCTION

The tribological study of polymers is more vital than the metals and alloys because the energy spent during sliding is transformed into heat energy which results in rise in local temperature at the interface of the rubbing surfaces. This temperature rise has a significant effect on the tribological performance of polymer and polymer based composite materials [1-4]. The use of polymer composites cannot be avoided because these materials have superior physical and mechanical properties as compared to the conventional materials [5,6]. These materials can be used in making different mechanical components such as gears, cams, wheels, bearings, bushes and clutches. The study of tribological behavior of such sliding components is highly decisive as wear is a very common phenomenon that can be observed when they are subjected to high load and temperature [7-9]. The wear resistance and coefficient of friction of polymers can be significantly improved by reinforcing fibers. Further the tribological properties of the polymer composites can be notably enhanced by incorporating filler materials. Ahmed et al. [10] experimentally investigated the effect of various ceramic fillers on dry sliding wear behavior of jute-epoxy laminated composites. The results reveal that on

addition of small amount of filler materials, the wear resistance of jute fiber reinforced epoxy composite improved significantly. It was also observed that Al_2O_3 filled composite laminates has better wear resistance than SiC filled laminates. Chauhan et al. [11] conducted experiments to study the tribological performance of pure vinylester, glass fiber reinforced vinylester and glass fiber reinforced vinylester filled with SiC under dry and water lubricated sliding conditions. Their results show that on incorporation of glass fiber and SiC particles to the vinylester polymer, the wear characteristics enhanced considerably in both dry and water lubricated sliding conditions. Srivastava and Wahne [12] found that the particulate fillers significantly improve the mechanical properties and as well as wear resistance of the E-glass fiber epoxy composites. This is because fillers in particle form enrich the bonding strength between the fiber and the epoxy resin. Moreover, addition of filler materials in different weight fractions has a notably significant effect on reducing wear and frictional properties of the random E-glass fiber composites.

Due to the growing environmental awareness, the use of lignocellulosic materials such as rice husk, wood flour, jute, sisal, nettle and bagasse has grown tremendously [13-15]. Furthermore, these materials

introduce some advantages over conventional materials which include low density, low cost, non-abrasive properties, reasonable strength, biodegradation and renewable nature. Easy availability and high silica content are the two main factors which has attracted many researchers to study the tribological property of rice husk filled polymer composites [16]. The major constituents of rice husk are 32% cellulose, 21% hemicelluloses, 22% lignin and 15% mineral ash. The mineral ash comprises of 96.34% SiO₂, 2.11% K₂O, 0.45% MgO, 0.2% Fe₂O₃, 0.41% CaO and 0.08% MnO₂ [17]. Moreover, rice husk is a low-cost bio-based by-product which is one of the major agricultural wastes for the agro processing industry. The large amount of production of rice which is approximately 600 million tons per year is the only source of production of such waste material. The amount of production of rice husk waste depends upon the production of rice which is nearby 20 wt.% of the total amount of rice production [18]. The literature confirms many applications of rice husk such as electricity generation, particle boards, light weight concrete, rice husk fueled steam engines, building materials, as filler material in various polymers, but, its tribological investigation is on nascent stage [19]. The studies on rice husk filled glass-epoxy composites for improving the specific wear rate and coefficient of friction (COF) are scanty. Therefore, an attempt has been made in the present work to improve the tribological behavior of glass/epoxy composites by using rice husk as the filler material.

2. MATERIALS AND METHODS

2.1 Tribo Materials Used

Composite laminates were prepared by conventional hand lay-up technique in chrome plated mild steel mold (560 mm × 460 mm) at room temperature. The mold is specially designed to produce 4 mm thick laminate sheet. The laminates possess six layers of woven boron free EC-R glass fiber mats of 610 GSM manufactured by Owens Corning Fiber Glass, USA. Epoxy resin LY556 and hardener HY 951 were used as the matrix materials. The resin and hardener is mixed and stirred mechanically in a ratio of 10:1 by weight. The rice husk is used in a proportion of 5% of the weight of glass fibers, whereas, the weight percentage of glass fiber varies in the range of 50 - 55 %. The length of the rice husk filler varies from 4-5 mm. Specimens of suitable dimension are cut using a diamond cutter. The specimens of size 30 × 10 × 4 mm³ were prepared for the test.

2.2 Test Procedure

Dry sliding wear test is conducted on a pin-on-disc wear tribometer (Ducom India TR20LE) as per ASTM G 99. The counter body is a disc (140 mm × 8 mm) made up of ground hardened steel (EN-31, 64 HRC, average surface roughness, R_a = 0.361 μm). The contact surface of all specimens is polished with an emery paper of 800 grit size to ensure proper intimate contact between the specimens and counterface. Before the test, both the rotating disc and specimens are

cleaned with acetone. The average surface roughness value of sliding surface of the specimen was R_a = 1.1 μm. The surface roughness of the specimen is measured by using Mitutoyo SJ-401 surface roughness tester. The weight of the specimens is measured by using high precision electronic balance Shimdzu-AUW220D with an accuracy of 0.0001 g.

Wear tests are performed on pin-on-disc tribo-test machine (Figure 1). Tests are conducted at varying sliding speeds (1, 2 and 3 m/s) under applied normal loads of 10, 20 and 30 N and sliding distances of 1000, 2000 and 3000 m. The weight difference is measured before and after the test for all specimens. The weight difference gives the weight loss of the composite specimen during a particular sliding experimentation. The wear performance is expressed in terms of specific wear rate. The specific wear rate, W_r of the specimens can be calculated using equation (1). Each value reported is the average of three specimen tests.

$$W_r = \Delta w / (\rho D F_N) \quad (1)$$

Where, Δw = Mass loss during test duration (gm);
 ρ = Density of the specimen (gm/mm³);
 D = Sliding distance (m); and
 F_N = Applied normal load (N).

As the disc starts rotating, rubbing starts between the specimen and the disc, the control unit continuously monitors the friction force. The value of the friction force is recorded to compute coefficient of friction, by using equation (2).

$$\mu = F / F_N \quad (2)$$

Where, F = Measured frictional force (N); and
 F_N = Applied normal load (N).



Fig. 1. Pin-on-disc tribo test machine.

2.3 Worn Surface Analysis

The worn surface morphology of the specimens is examined by using scanning electron microscope (LEO 435VP). The electrical conductivity of the specimen is enhanced before the photomicrographs are taken. To enhance the conductivity, a thin film of gold is coated

using sputter coater (BALTEC SCD 005).

3. RESULTS AND DISCUSSION

3.1 Specific Wear Rate

The variation of specific wear rate with applied normal load, sliding distance and sliding speed is presented in Figures 2-4. Figures 2-4 reveals that specific wear rate decreases with an increase in applied normal load for all the specimens. However, specific wear rate initially increase with sliding speed and drops beyond sliding speed of 2 m/s. The results also depict that the highest specific wear rate is obtained at sliding speed of 2 m/s under the applied normal load of 10 N and sliding distance of 1000 m. The highest specific wear rate is measured with a value of $11.48 \times 10^{-8} \text{ mm}^3/\text{N}\cdot\text{mm}$. The lowest specific wear rate measured is $1.28 \times 10^{-8} \text{ mm}^3/\text{N}\cdot\text{mm}$ which is obtained at a sliding speed of 3 m/s and sliding distance of 3000 m on application of 30 N normal load. It has also been observed that the specific wear rate increases at the beginning of the experiment. This is probably due to the fact that initially only the specimen and rotating disc are in contact with each other which results in asperities physically interlocking into the crevices. Now, as the disc starts rotating, even on application of small amount of load, the asperities deform plastically due to shearing. As a result, weight loss is too high at the starting of the experiment. The specific wear rate gradually drop-down with an increase in applied normal load because as the normal load increases the pressure at the interface of specimen and counterface becomes high. Due to this high pressure the debris deposited on counterface transferred back onto the specimen rubbing surface which act as a shield and protect the specimen from severe wear. Moreover, at higher load the film generation is more frequent when compared with low load application. Apart from this, sometimes fillers decompose and produce some reaction products which improve the bonding between transfer film and counterface and hence enhance the wear resistance [20]. A similar finding is reported by Yousif [21] where the wear characteristic of the neat polyester is highly improved by reinforcing coir fibers under dry sliding condition. The identical specific wear rate behavior is observed when sliding distance vary from 1000 to 3000 m for all specimens under various loads and sliding speeds. The specific wear rate increased when the sliding speed is increased from 1 m/s to 2 m/s and then decreases in spite of increase in sliding speed for sliding distance of 1000 m and 2000 m. The wear rate increases with the sliding speed because at higher speed, disc rotational speed becomes high which results in high temperature generation at the interface. When the temperature reaches to the softening point of polymer, fiber-matrix and filler-matrix debonding starts which in turn results in easy shearing of fiber or filler. But the specific wear rate reduced when sliding speed is increased from 2 m/s to 3 m/s because at this speed range, the formation of film transfer layer is very fast which finally stick to the specimen mating surface. The highest wear loss for specimen was observed at sliding speed of 2 m/s,

applied normal load of 10 N and sliding distance of 1000 m, which is 9.8% and 7.9% higher when compared with sliding speed of 1 and 3 m/s under the same load application.

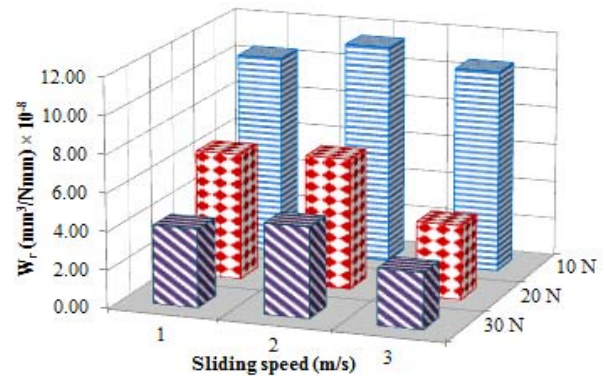


Fig. 2. Variation of specific wear rate with input parametrs for sliding distance of 1000 m.

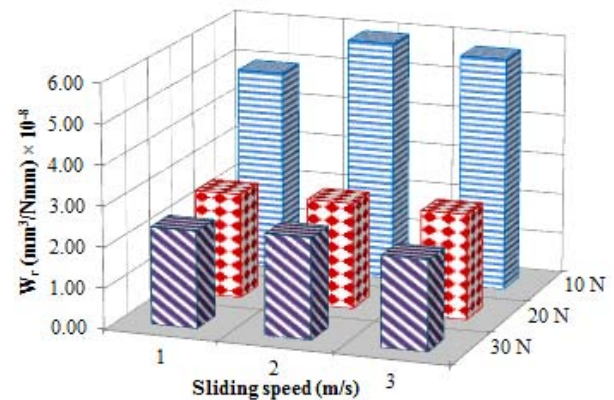


Fig. 3. Variation of specific wear rate with input parametrs for sliding distance of 2000 m.

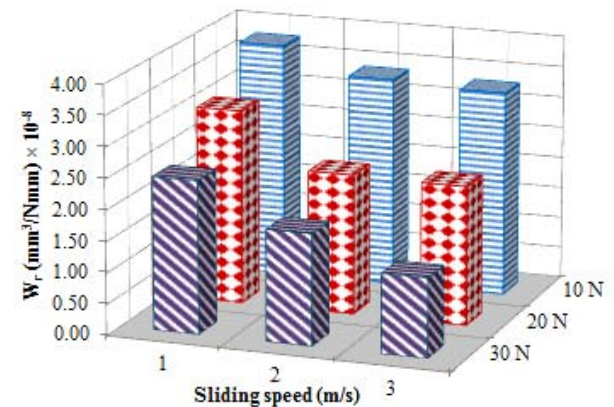


Fig. 4. Variation of specific wear rate with input parametrs for sliding distance of 3000 m.

3.2 Co-efficient of Friction

In order to study the frictional performance of the developed composites lainates, the average coefficient of friction (μ) is plotted against the applied normal load under different sliding velocities and distances. The friction force is measured by transducer mounted on the lever arm. Friction force data are recorded by using a microprocessor controlled data acquisition system. The friction force is recorded periodically after every 30 seconds during the sliding test. The average coefficient of friction for all specimens decreased with an increase

in applied normal load for sliding speed of 1 and 3 m/s as presented in Figure 5 to Figure 7, respectively. But, at sliding speed of 2 m/s specimen experienced an opposite trend in coefficient of friction with increase in applied normal load. The higher value of coefficient of friction with normal load is attributed to the formation of high amount of debris and exposure of fiber and filler materials. The other factors that may results in higher value of coefficient of friction are embedding of filler partile at the interface between the specimen and counterface, rubbing of third body particles, rupture due to irregular surfaces and delamination due to sticking of filler particles. To clarify the decreasing trend of coefficient of friction, it is observed that increase in normal load leads to rise in temperature at interface of the rubbing surfaces (specimen and counterface). Again, this increased temperature causes thermal degradation of polymer because polymers become soft with rise in temperature. This type behavior of polymer matrix results in weaker adhesive bonding between fibers/fillers and polymer, which in turn results in formation of back film transfer and smooth shearing of fiber or filler. These are the few common causes of decrease in coefficient of friction. The least value of coefficient of friction recorded is 0.17 which is obtained at sliding speed of 3 m/s, applied normal load of 30 N and sliding distance of 1000 m.

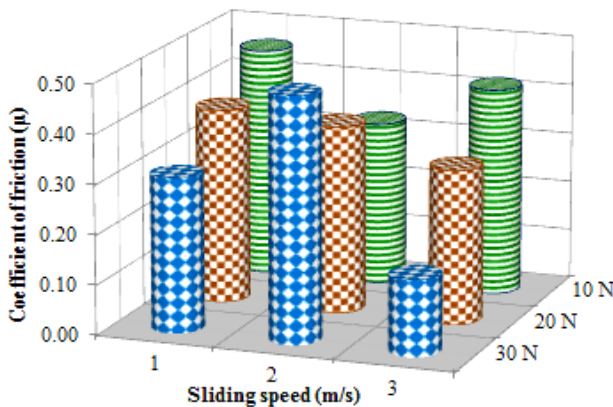


Fig. 5. Variation of coefficient of friction with input parametrs for sliding distance of 1000 m.

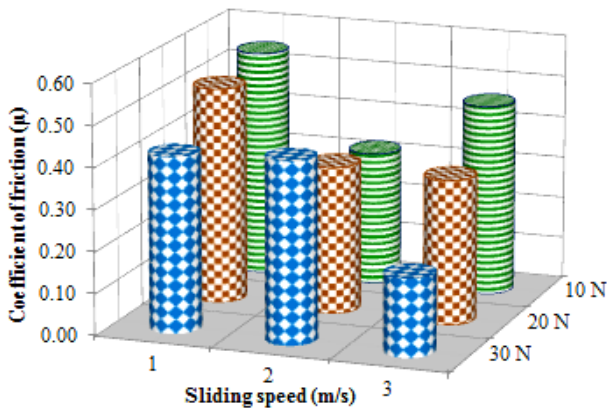


Fig. 6. Variation of coefficient of friction with input parametrs for sliding distance of 2000 m.

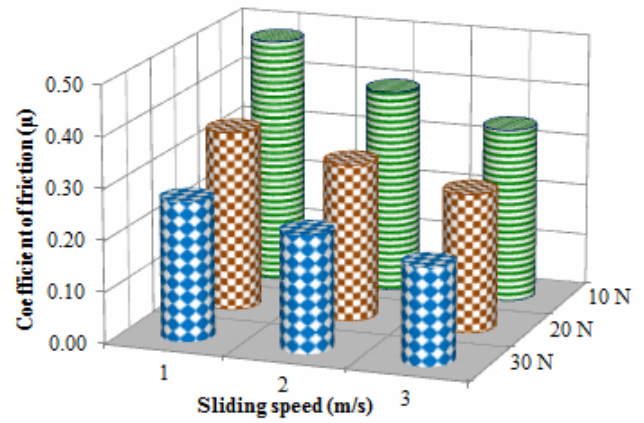


Fig. 7. Variation of coefficient of friction with input parametrs for sliding distance of 3000 m.

3.3 Scanning Electron Microscopy

Figures 8-10 represents the morphology of the worn surfaces at different normal loads for sliding speed of 1 m/s and sliding distance of 1000 m. Figure 8 manifest severe wear loss at applied normal load of 10 N, where fiber fracture, matrix breakage and debris formation are the common damage forms. Moreover, filler pull out is detected which appeared as deep grooves in the SEM image. Figure 9 indicates the surface morphology of the worn sample where less damage is observed in terms of debris formation and fiber fracture that is obtained at applied normal load of 20 N. Figure 10 shows surface damages of the specimen when specimen is subjected to 30 N load. A mild wear is observed at higher load application which includes back film transfer, microcracks and patches of thin polymer film that is formed over the fibers due to plastic deformation of polymers which shields the composite surface and contributes to higher wear resistance. Tayeb et al. [22] found that deposition of fiber fragments on soft polyester might be the one reason of lower mass loss of chopped glass fiber reinforced polyester while sliding in anti-parallel orientation.

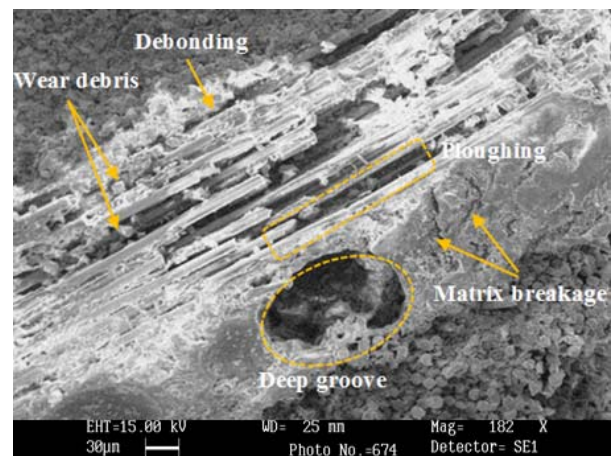


Fig. 8. SEM micrograph of the worn specimen under a constant applied normal load of 10 N, sliding speed of 1 m/s and sliding distance of 1000 m.

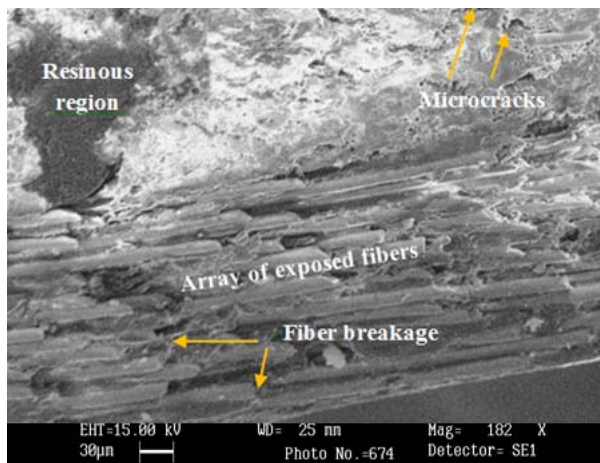


Fig. 9. SEM micrograph of the worn specimen under a constant applied normal load of 20 N, sliding speed of 1 m/s and sliding distance of 1000 m.

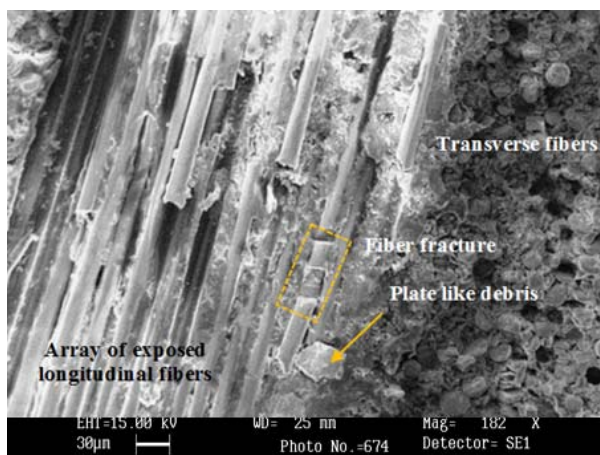


Fig. 10. SEM micrograph of the worn specimen under a constant applied normal load of 30 N, sliding speed of 1 m/s and sliding distance of 1000 m.

4. CONCLUSIONS

In the present study, friction and wear performance of glass fiber reinforced polymer composites filled with rice husk is experimentally investigated. From the results and discussion the following conclusions can be drawn:

1. The specific wear rate of the rice husk filled glass-epoxy composites decreased with increase in applied normal load. The lowest specific wear rate for rice husk filled laminate composite reported with a value of $1.28 \times 10^{-8} \text{ mm}^3/\text{N}\cdot\text{mm}$ which is obtained at applied normal load of 30 N, sliding speed of 3 m/s and sliding distance of 3000 m.
2. The coefficient of friction for all the specimens decreased with increase in applied normal load except at sliding speed of 2 m/s. The minimum coefficient of friction calculated is 0.17 that can be found at applied normal load of 30 N, sliding speed of 3 m/s and sliding distance of 1000 m.
3. The worn surface morphology of the specimens displayed that back film transfer and debris formation are the main reasons of low wear rate. The debonding of fibers, matrix cracking, fiber breakage and ploughing in the resinous region are

also observed.

4. Results show that the wear properties of the developed composites are much more profound to variation of applied normal load than the sliding speed.

5. REFERENCES

- [1] Unal, H., Kurt, M., Mimaroglu, A.: *Tribological performance of industrial polyamide-imide and its composite under different cooling conditions*, Journal of Polymer Engineering, Vol. 32, p.p. 201-206, 2012.
- [2] Debnath, K., Singh, I., Dvivedi, A.: *Dry sliding wear behaviour of glass fibre reinforced epoxy composites filled with natural fillers*, Reason - A Technical Journal, Vol. XII, p.p. 61-68, 2013.
- [3] Debnath, K., Dhawan, V., Singh, I., Dvivedi, A.: *Effect of natural fillers on wear behavior of glass-fiber-reinforced epoxy composites*, Proceedings of the International Conference on Research and Innovations in Mechanical Engineering, p.p. 441-450, Guru Nanak Dev Engineering College, Springer India, Ludhiana, October 24-26, 2013.
- [4] Debnath, K.: *A study on mechanical behavior and damage assessment of short bamboo fiber based polymer composites*, M.Tech. Thesis, National Institute of Technology Rourkela, 2011.
- [5] Dhawan, V., Debnath, K., Singh, I., Singh, S.: *Drilling of glass fiber-reinforced epoxy laminates with natural fillers: Thrust force analysis*, Proceedings of the International Conference on Research and Innovations in Mechanical Engineering, p.p. 105-115, Guru Nanak Dev Engineering College, Springer India, Ludhiana, October 24-26, 2013.
- [6] Debnath, K., Singh, I., Dvivedi, A.: *Rotary mode ultrasonic drilling of glass fiber-reinforced epoxy laminates*, Journal of Composite Materials, 2014. DOI: 10.1177/0021998314527857.
- [7] Lu, Z., Friedrich, K.: *Wear and friction of a unidirectional carbon fiber-glass matrix composite against various counterparts*, Wear, Vol. 162, p.p. 1103-1113, 1993.
- [8] Hegeler, H., Bruckner, R.: *Fiber reinforced glasses: Influence of thermal expansion of the glass matrix on strength and fracture toughness of the composite*, Journal of Materials Science, Vol. 25, p.p. 4836-4846, 1990.
- [9] Srivasstava, V.K., Pathak, J.P., Tahzibi, K.: *Wear and friction characteristics of mica filled fiber reinforced epoxy resin composites*, Wear, Vol. 152, p.p. 343-350, 1992.
- [10] Ahmed, K.S., Khalid, S.S., Mallinatha, V., Amith Kumar, S.J.: *Dry sliding wear behavior of SiC/Al₂O₃ filled jute/epoxy composites*, Materials and Design, Vol. 36, p.p. 306-315, 2012.
- [11] Chauhan, S.R., Kumar, A., Singh, I.: *Sliding friction and wear behavior of vinylester and its composites under dry and water lubricated sliding conditions*, Materials and Design, Vol. 31, p.p. 2745-2751, 2010.
- [12] Srivastava, V.K., Wahne, S.: *Wear and friction*

- behavior of soft particles filled random direction short GFRP composites*, Materials Science and Engineering A, Vol. 458, p.p. 25-33, 2007.
- [13] Bajpai, P.K., Singh, I., Madaan, J.: *Frictional and adhesive wear performance of natural fibre reinforced polypropylene composites*, Proceedings of the Institution of Mechanical Engineers, Part J: Journal of Engineering Tribology, Vol. 227, p.p. 385-392, 2013.
- [14] Bajpai, P.K., Singh, I., Madaan, J.: *Tribological behavior of natural fiber reinforced PLA composites*, Wear, Vol. 297, p.p. 829-840, 2013.
- [15] Debnath, K., Singh, I., Dvivedi, A., Kumar, P.: *Recent advances in composite materials for wind turbine blades*, World Academic Publishing-Advances in Materials Science and Applications, Hong Kong, 2013.
- [16] Kumar, V., Saini, M.S., Kanungo, B.K., Sinha, S.: *Effect of various additives on mechanical properties of rice husk polypropylene (RHPP) composites*, Journal of Polymer Engineering Vol. 32, p.p. 163-166, 2012.
- [17] Rahman, I.A., Ismail, J., Osman, H.: *Effect of nitric acid digestion on organic materials and silica in rice husk*. Journal of Materials Chemistry, Vol. 7, p.p. 1505-1509, 1997.
- [18] Kim, H.S., Yang, H.S., Kim, H.J., Park H.J.: *Thermogravimetric analysis of rice husk flour filled thermoplastic polymer composites*, Journal of Thermal Analysis and Calorimetry, Vol. 76, p.p. 395-404, 2004.
- [19] Rout, A.K., Satapathy, A.: *Study on mechanical and tribo-performance of rice husk filled glass-epoxy hybrid composites*, Materials and Design, Vol. 41, p.p. 131-141, 2012.
- [20] Briscoe, B.J.: *Advances in composite tribology*, Elsevier, Amsterdam, 1993.
- [21] Yousif, B.F.: *Frictional and wear performance of polyester composites based on coir fibres*, Proceedings of the Institution of Mechanical Engineers, Part J: Journal of Engineering Tribology, Vol. 223, p.p. 51-59, 2009.
- [22] El-Tayeb, N.S.M., Yousif, B.F., Yap, T.C.: *An investigation on worn surfaces of chopped glass fiber reinforced polyester through SEM observations*, Tribology International, Vol. 41, p.p. 331-340, 2008.

Authors: Kishore Debnath¹, Research Scholar., Dr. Vikas Dhawan², Director., Dr. Inderdeep Singh¹, Associate Professor., Dr. Akshay Dvivedi¹, Assistant Professor., ¹Department of Mechanical and Industrial Engineering, Indian Institute of Technology Roorkee – 247 667, INDIA. ²Jai Parkash Mukand Lal Innovative Engineering and Technology Institute, Radaur – 135 133, INDIA.

E-mail: debnath.iitr@gmail.com
vikas251999@gmail.com
dr.inderdeep@gmail.com
akshaydvivedi@gmail.com



CHIP MORPHOLOGY IN TURNING OF Ti-6Al-4V ALLOY UNDER DIFFERENT MACHINING CONDITIONS

Received: 02 May 2014 / Accepted: 30 May 2014

Abstract: Chip morphology is one of the important parameters to determine the machinability of any material. This paper deals with the effect of machining environment on chip morphology during turning of Ti-6Al-4V. The different types of chips are formed under different cutting conditions. It is found that, significant variation in the formation of chips under different conditions. The experimental results indicate that the chip formation becomes more favourable under Minimum Quantity Lubrication (MQL) machining compared to dry and flooded machining conditions. It also observed that the chip thickness and slip angles are less in MQL machining compared to dry and flooded machining conditions.

Key words: Chip morphology, Turning, Machining environment and Ti-6Al-4V alloy

Morfološki izgled korena strugotine pri struganju legure Ti-6Al-4V pod različitim uslovima obrade. Morfologija korena strugotine je jedan od važnih parametara za određivanje mašinske obrade bilo kog materijala. Ovaj rad predstavlja uticaj radnog okruženja na koren strugotine Ti-6Al-4V. Različiti tipovi korena strugotine su formirani pod različitim uslovima rezanja. Nađene su značajne varijacije u formiranju korena strugotine pod različitim uslovima. Eksperimentalni rezultati pokazuju da formiranje korena strugotine postaje povoljnije pod minimalnom količinom sredstva za podmazivanje (MQL) u odnosu na suhu obradu uz primenu sredstava za podmazivanje. Takođe je primećeno da je debljina korena strugotine i uglova klizanja manji kod obrade na suvo u odnosu na obradu uz primenu sredstava za podmazivanje (MQL).

Ključne reči: Morfologija korena strugotine, struganje, Mašinstvo u životnoj sredini i Ti-6Al-4V legure

1. INTRODUCTION

Titanium is a useful material but not commonly used until the late 1940s. It is most often alloyed with molybdenum, manganese, iron and aluminium. It is one of the strongest readily available materials, making it ideal for wide range of practical applications. It is 45% lighter than steel with comparable strength and twice as strong as aluminium, while being only 60% heavier. The most widely used Titanium alloy is Ti-6Al-4V alloy. It consists of a base metal Ti with 6%Al and 4%V. Ti-6Al-4V is α - β alloy. Alpha stabilizing materials such as Aluminium and Oxygen raise the transition temperature, while a beta-stabilizing material such as Vanadium and Tungsten (W) lowers the transition temperature. Titanium alloys are low thermal conductivity and high chemical reactivity with many cutting tool materials. Its low thermal conductivity increases the temperature at the cutting edge of tool [1].

Chip segmentation by shear localization is an important process which was observed in a certain range of cutting velocities. This phenomenon might be desirable in reducing the level of the cutting forces and by improving chip's evacuation [2]. The shear bond width and distance between bands were analyzed by micrographic observations; these results were compared and resembled with proposed model [3].

The chip formation behaviour was investigated using metallurgical analysis. It was found that, machining of Ti-6Al-4V alloy some non-diffusional phase transformation took place in the shear localized chips. The chip formation process with shear banding and its effects on shear banding frequency with cutting

conditions were observed [4].

The chip formation during dry turning of Ti-6Al-4V alloy with dynamic cutting force measurements was carried under different machining conditions. It was found both continuous and segmented chip formation processes were observed in one cut under conditions of low cutting speed and large feed rate. The slipping angle in the segmented chip was higher than that in the continuous chip [5]. The effects of different coolant supply strategies on cutting performance in continuous and interrupted turning process of Ti-6Al-4V was studied in terms of cutting forces and chip morphology. It was observed the chips obtained under MQL were long continuous chips and in dry and flooded conditions snarled continuous chips [6].

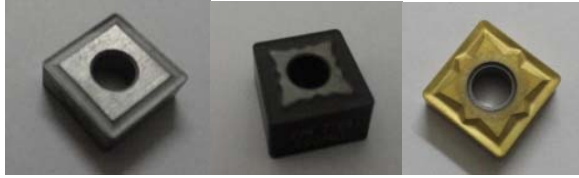
The influence of the cutting speed and feed rate during of Ti-6Al-4V on cutting forces and the chip morphology were analyzed in the range of cutting speeds from 50 m/min to 250 m/min. It was observed continuous chip at 50 m/min, flow chip for around 100 m/min and shear localized chip above 125 m/min cutting speeds [7].

The effect cutting conditions on tool wear and chip morphology was examined in the machining of Titanium alloy. It is observed that the saw tooth height increases with an increase in depth of cut and cutting speed at constant feed and nose radius [8].

In this paper, an experimental study on chip morphology is carried out under different machining conditions as shown in Table 1. The influence of the machining environment with cutting speed, feed rate, depth of cut and tool material on chip morphology is analyzed in turning of Ti-6Al-4V.

Cutting parameter	Level 1	Level 2	Level 3
Type of Machining Environment(TME)	Dry	Flooded	MQL
Cutting speed (m/min) –V	40	70	105
Feed rate (mm/rev) - F	0.18	0.2	0.25
Depth of cut (mm) – D	0.5	0.8	1.1
Type of Tool Material (TM)	Uncoated	CVD	PVD

Table 1: Cutting parameters and their levels



(a) Uncoated (b) CVD Coated (c) PVD Coated
Fig. 1. Carbide Tools

2. EXPERIMENTAL DETAILS

The turning operations are carried out on kirloskar made lathe TURNMASTER 35. The three different types of carbide tools are used in this work made by SECO. These are uncoated, CVD and PVD coated tools. The uncoated tungsten carbide tool made of micro grain abrasives is shown in Fig. 1(a). Generally, it is high hardness, good toughness and principally intended for rough turning of super alloys. It is specified as SNMG120408-MR4 883. CVD coated tool has excellent wear resistance and the superior edge toughness is shown in Fig. 1(b). It is coated with $Ti(C,N) + Al_2O_3$. The basic structure is Aluminium Oxide represents a very good starting point for machining, but the coatings enhance overall ductility significantly. This cumulative result improves mechanical and thermal properties. It is specified as SNMG120408-MR7 TM4000. PVD coated tool is made of tungsten carbide hard micro grain abrasives shown in Fig. 1(c). It is new grade of heat resistant alloys coated with $(Ti,Al)N + TiN$. It is intended for finishing of super alloys. It machines faster, works harder and last longer. It is specified as SNMG120408-MR3 TS2000. The sandvik coromant make PSBNR tool holder used for machining in this work.

In dry machining, no cutting fluid is used. In flooded machining smoothkut SO 7100 soluble oil made by molygraph is used. It is water soluble metal working fluid having high oil content, fully soluble in water with milky white emulsion, extended service life, good load carrying capacity of oil, offers excellent rust and corrosion protection on tools, components and machines, eco-friendly as it does not contain ozone depleting substances, free from coloring dyes, boron additives, low foaming characteristics. Typical application of this cutting fluid is diluted with water from 1:16 to 1:20 ratio for general machining and flushed in the cutting zone at rate of 5 liters / min. In MQL machining, same cutting fluid is supplied with compressed air stream in the form mist directed at the cutting tool edge with the flow rate of 50 ml/hr.

3. RESULTS AND DISCUSSIONS

Chip morphology plays a major role in determining machinability of Titanium alloys. In addition, chip morphology significantly influences the thermal behaviour at the work piece/tool interface, which in turn affects the tool life

In order to increase productivity and tool life in the machining of Titanium alloys, it is necessary to study the chip morphology and its effect on machinability. The experiments are conducted under different machining conditions as shown in Table. 2. The collected chips after machining are shown in Table. 2. These chips are compared and categorized with ISO 3685 standards as shown in Table 3 [9].

It is observed from Table.2 that the nature chips obtained are different forms of continuous chips. The chips formed in dry machining are snarled ribbon, snarled washer, snarled tubular and helical washer. These chips obtained at higher cutter speeds. Snarled tubular chips are obtained at moderate cutting speed, feed rate and high depth of cut. Under flooded machining most of the chips obtained are snarled tubular at low cutting speeds. Long tubular chips are obtained at high cutting speed, feed rate and moderate depth of cut. Under MQL condition the chips obtained are snarled ribbon, snarled tubular, snarled conical helical and helical washer. The different chips are formed due to different cutting conditions; different normal and frictional forces at tool and chip interface and also different coefficient of friction developed at chip and tool interface under different machining environmental conditions.

The burnt and black coloured chips are obtained in dry machining indicates the temperature developed in cutting zone is high. It also observed that the back surface of chip is rough; it resulted with high surface roughness on machined surface. Whereas back surface of chips obtained from the flooded and MQL machining conditions appeared much brighter and smoother, it indicates that the surface roughness on machined surface is less. This indicates, that the heat developed in flooded and MQL machining observed by cutting fluid, thereby less friction, hence smoother surface is obtained on back of the chip.

Chip thickness ratio is one of the important parameters to evaluate machinability of the material. This ratio indicates the degree of deformation, friction and heat developed in machining process. It is the ratio between undeformed chip thicknesses (t_c) to deformed chip thicknesses. In general undeformed chip thickness is assumed equal to feed rate in orthogonal cutting. The deformed chip thickness is calculated by $t = f * \sin\phi$. Where f is feed rate in mm/rev and ϕ is approach angle. The deformed chip thickness is measured by micrometer made by mitutoyo. The measured chip thickness values are shown in Table 4.

It observed from Fig.2 that, the chip thickness increases as the feed rate increases. Because at higher feed rates more heat is generates, this leads thermal softening and easier deformation of chips. From Fig. 2, it is also observed that, the chip thickness is less in MQL compared dry and flooded machining. Under the effect of high pressure of air and air - cutting fluid mixture in MQL, takes away chips with in less time. Hence, chip

does not have sufficient time to deform plastically. Under dry condition, chips are difficult to deform, this result in increase in chip thickness.

Fig. 3 shows comparison of chip thickness ratios among dry, flooded and MQL. Higher values of chip thickness ratios indicate high deformation process. In most of experimental results shown in Fig. 3, MQL

shows higher cutting ratios compared to dry and flooded machining. The main reason is in MQL, less friction and heat is developed at the cutting zone due to effective controlling of friction by both cooling and lubricating. This resulted in higher deformation process at the cutting zone in MQL, hence higher chip thickness ratios are obtained compared dry and flooded.







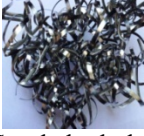

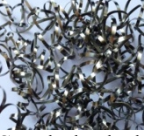








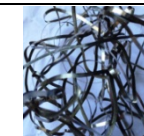









Factors		DRY	FLOODED	MQL
Uncoated tool	Vc=40 F=0.18 Dc=0.5	 Snarled washer	 Snarled tubular	 Snarled ribbon
	Vc=70 F=0.2 Dc=1.1	 Snarled tubular	 Conical helical	 Long helical washer
	Vc=105 F=0.25 Dc=0.8	 Snarled tubular	 Long tubular	 Snarled tubular
CVD Coated tool	Vc=40 F=0.2 Dc=0.8	 Snarled ribbon	 Snarled tubular	 Long tubular
	Vc=70 F=0.25 Dc=0.5	 Snarled ribbon	 Snarled tubular	 Long ribbon
	Vc=105 F=0.18 Dc=1.1	 Snarled ribbon	 Helical washer	 Snarled ribbon
PVD Coated tool	Vc=40 F=0.25 Dc=1.1	 Snarled ribbon	 Snarled tubular	 Snarled conical helical
	Vc=70 F=0.18 Dc=0.8	 Helical washer	 Snarled ribbon	 Snarled conical helical
	Vc=105 F=0.2 Dc=0.5	 Snarled ribbon	 Long tubular	 Snarled ribbon

Table 2: Chip morphology of Ti-6Al-4V with different machining environments







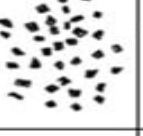
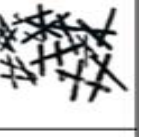










1 Ribbon chips	2 Tubular chips	3 Spiral chips	4 Washer-type helical chips	5 Conical helical chips	6 Arc chips	7 Elemental chips	8 Needle chips
1.1 Long 	2.1 Long 	3.1 Flat 	4.1 Long 	5.1 Long 	6.1 Connected 		
1.2 Short 	2.2 Short 	3.2 Conical 	4.2 Short 	5.2 Short 	6.2 Loose 		
1.3 Snarled 	2.3 Snarled 		4.3 Snarled 	5.3 Snarled 			

Table 3: ISO 3685 standard chip forms

Exp.no	TME	V	F	D	TM	tc	t	r = t/tc
1	Dry	40	0.18	0.5	Uncoated	0.19	0.1272	0.669
2	Dry	40	0.2	0.8	CVD	0.215	0.1414	0.6577
3	Dry	40	0.25	1.1	PVD	0.27	0.1767	0.6547
4	Dry	70	0.18	0.8	PVD	0.185	0.1272	0.687
5	Dry	70	0.2	1.1	Uncoated	0.20	0.1414	0.7071
6	Dry	70	0.25	0.5	CVD	0.255	0.1767	0.6932
7	Dry	105	0.18	1.1	CVD	0.185	0.1272	0.687
8	Dry	105	0.2	0.5	PVD	0.235	0.1414	0.657
9	Dry	105	0.25	0.8	Uncoated	0.25	0.1767	0.7071
10	Flooded	40	0.18	0.5	Uncoated	0.18	0.1272	0.7071
11	Flooded	40	0.2	0.8	CVD	0.19	0.1414	0.744
12	Flooded	40	0.25	1.1	PVD	0.26	0.1767	0.679
13	Flooded	70	0.18	0.8	PVD	0.18	0.1272	0.706
14	Flooded	70	0.2	1.1	Uncoated	0.21	0.1414	0.673
15	Flooded	70	0.25	0.5	CVD	0.24	0.1767	0.736
16	Flooded	105	0.18	1.1	CVD	0.18	0.1272	0.7071
17	Flooded	105	0.2	0.5	PVD	0.21	0.1414	0.673
18	Flooded	105	0.25	0.8	Uncoated	0.24	0.1767	0.736
19	MQL	40	0.18	0.5	Uncoated	0.18	0.1272	0.7071
20	MQL	40	0.2	0.8	CVD	0.21	0.1414	0.670
21	MQL	40	0.25	1.1	PVD	0.24	0.1767	0.736
22	MQL	70	0.18	0.8	PVD	0.17	0.1272	0.748
23	MQL	70	0.2	1.1	Uncoated	0.2	0.1414	0.707
24	MQL	70	0.25	0.5	CVD	0.24	0.1767	0.736
25	MQL	105	0.18	1.1	CVD	0.18	0.1272	0.706
26	MQL	105	0.2	0.5	PVD	0.21	0.1414	0.673
27	MQL	105	0.25	0.8	Uncoated	0.24	0.1767	0.736

Table 4: Experimental results for chip thickness and its cutting ratio

The typical segmented chips obtained under dry, flooded and MQL are shown in Fig. 4. The slipping angle is defined as an angle between the shear band and the tangent of the machine surface at the end of the shear band. The chip obtained in the form of saw tooth pattern as shown in Fig.4 and also shows the slip angle of the chips in dry, flooded and MQL machining conditions. Under dry condition, the deformation process is difficult due to high friction, hence high slip angle are obtained, where as in flooded and MQL machining conditions, the heat generated at the cutting

zone takes away by the cutting fluid, hence friction is less, this helps in easy to deform, therefore the less slip angles obtained in flooded and MQL machining. It is also observed that, in MQL the slip angle is much less than dry and flooded machining due to the heat transfer takes place very fast and quickly. This leads to less tool wear, high tool life, less cutting forces and high surface finish can be expected in MQL machining.

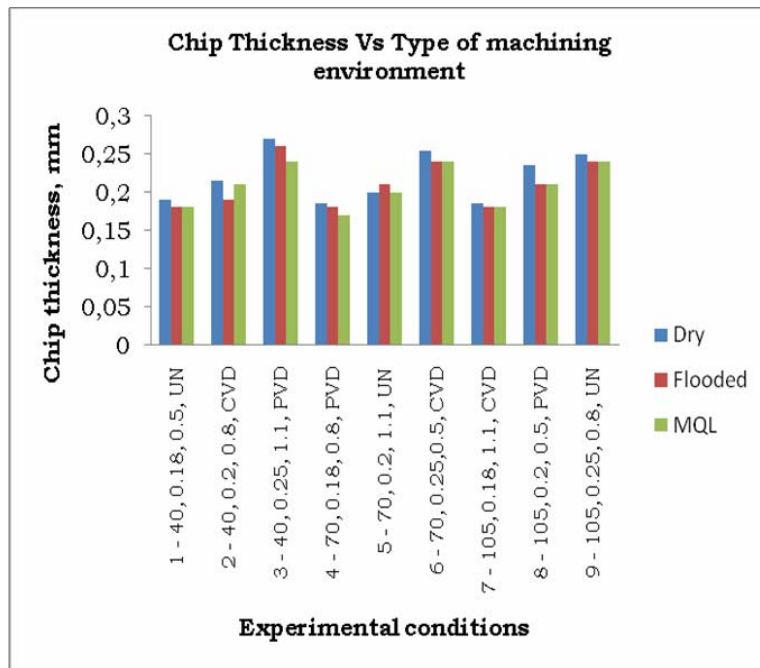


Fig.2: Comparison of chip thickness

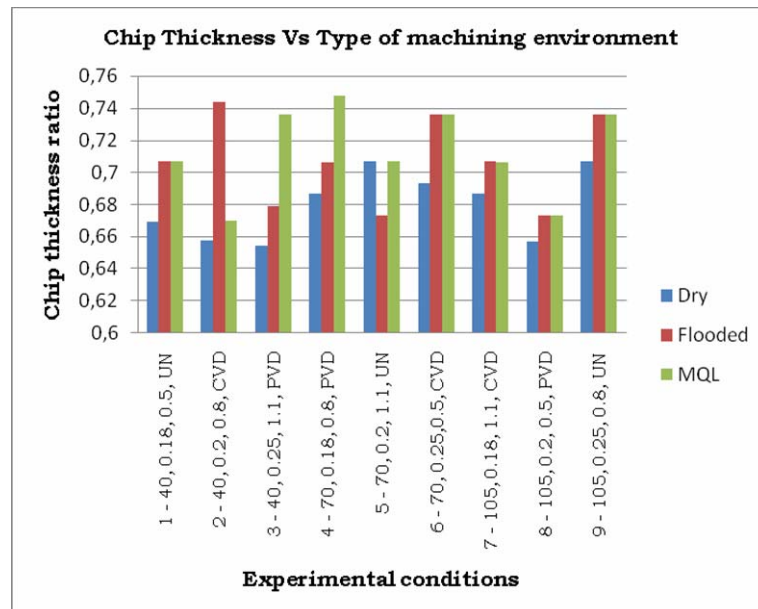


Fig. 3: Comparison of chip thickness ratios

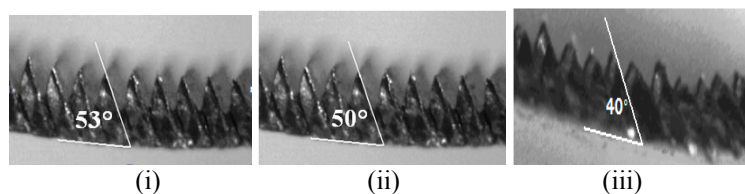


Fig.4: Slip angles in (i) Dry (ii) flooded and (iii) MQL conditions

4. CONCLUSIONS

Based on the results of this research the following conclusions can be drawn:

- The cutting performance of MQL machining shows favourable and better results compared to dry and flooded conditions.
- The chips obtained in all the experimental conditions are continuous chips only.
- The chips obtained are carried away very quickly in MQL compared to dry and flooded machining, this reduces the friction between rake and chip interface, this leads to decrease the tool wear, thereby increases the tool life.
- The chip thickness is less in MQL machining as compared to dry and flooded machining and chip thickness ratios are high in MQL

machining compared to dry and flooded machining.

- In the MQL condition, the back surface of the chip appeared as bright and smooth; this indicates that friction and heat developed is less compared to dry and flooded machining.

The low slip angles are observed in MQL machining compared to dry and flooded machining condition at moderate cutting speeds, it leads to less tool wear and high surface finish.

5. REFERENCES

- [1] Ezugwu E.O. and Wang Z.M., *Titanium alloys and their machinability- a review*, Journal of Materials Processing Technology, Vol. 68, pp: 262-274, 1997.
- [2] R. Komanduri, R.H. Brown, *The mechanics of chip segmentation in machining*, Journal of Engineering for Industry, Vol. 103, pp: 33-51, 1981.
- [3] A. Molinari, C. Musquar and G. Sutter, *Adiabatic shear banding in high speed machining of Ti-6Al-4V: experiments and modeling*, International Journal of Plasticity”, Vol. 18, pp. 443–459, 2002.
- [4] Bayoumi, A.E., Xie, J.Q., “*Some metallurgical aspects of chip formation in cutting Ti-6Al-4V alloy*”, Materials Science and Engineering, A190, 173, 1995.
- [5] Sun S., Brandt M., Dargusch M.S., “*Characteristics of cutting forces and chip formation in machining of titanium alloys*”, International Journal of Machine Tools & Manufacture, Vol. 49, pp. 561–568, 2009.
- [6] Wang Z. G., Rahman M., Wong Y. S., Neo K. S., Sun J., Tan C. H., Onozuka H., “*Study on orthogonal turning of titanium alloys with different coolant supply strategies*”, International Journal of Advanced Manufacturing Technology, Vol. 42, pp. 621–632, 2009.
- [7] A. Daymi, M. Boujelbene, S. Ben Salem and B. Hadj Sassi, “*Effect of the cutting speed on the chip morphology and the cutting forces*”, Computational Materials Science and Surface Engineering, Vol. 1, pp. 77- 83, 2009.
- [8] Srajan Kumar Goyal, R. Vinayagamoorthy and M. Anthony Xavier, “*Investigation of chip morphology and tool wear in precision turning process*”. International Journal of Current Research, volume 4, pp.001-004, 2012.
- [9] ISO (1977) Tool-life testing with single-point turning tools, ISO: 3685:1977.

Authors: M. Venkata Ramana, Department of Automobile Engineering, VNR Vignana Jyothi Institute of Engineering & Technology, Hyderabad, India.

G. Krishna Mohan Rao, Department of Mechanical Engineering, JNTUH College of Engineering, Hyderabad, India

D. Hanumantha Rao, Principal, Mathrusri Engineering College, Hyderabad, India

E – Mail: mandalavenki@gmail.com



Kaplonek, W., Kukielka, K., Kukielka, L., Nadolny, K., Hloch, S.

CLSM-BASED MEASUREMENTS OF THE SURFACES OF THE EXTERNAL ROUND THREADS ROLLED ON COLD

Received: 16 March 2014 / Accepted: 14 April 2014

Abstract: In recent years, a rapid development in optical metrology has been observed. In many applications, optical measurement systems are very broadly utilized due to their unique properties. In this work the Authors analysed the possibility of using a new advanced measurement technique based on confocal laser scanning microscopy, for the purposes of garnering precise measurements of the surface of external cold rolled round threads. During experimental tests The 3D laser microscope LEXT OLS4000, produced by Olympus, and equipped with OLS4000 2.1 dedicated software, was used. The test results obtained enabled a proper analysis of the important features of the assessed surface, particularly in terms of determining the correctness of the performed thread rolling process.

Key words: Confocal laser scanning microscopy, 3D measurements, image analysis, cold rolling thread process

CLSM- na bazi merenja spoljašnje površine hladno valjanih navoja. U poslednjih nekoliko godina primećen je brz razvoj u optičkoj metrologiji. U mnogim primerima, optički sistemi merenja se veoma široko koriste zbog svoje jedinstvenosti. U ovom radu autori analiziraju mogućnosti korišćenja nove napredne tehnike merenja na osnovu konfokalne lasersko skenirane mikroskopije, za potrebe preciznog merenja spoljne površine kod hladno valjanih navoja. Tokom eksperimentalnih testova korišćen je 3D laserski mikroskop LEKST OLS4000, proizvođača Olympus, podržan sa namenskim softverom OLS4000 2.1. Rezultati testa dobijeni omogućuju pravilnu analizu značajnih karakteristika procesirane površine, naročito u pogledu utvrđivanja ispravnosti navoja nakon procesa valjanja.

Ključne reči: Konfokalno lasersko skenirana mikroskopija, 3D merenje, analiza slika proces hladnog valjanja navoja

1. INTRODUCTION

In the last few years there has been a large increase of interest in the capabilities offered by modern optical metrology [1] within the scientific and engineering community. It's hard to imagine scientific research in areas such as mechanics [2], materials science [3], microelectronics [4] or the broader activities related to quality control [5] carried out in the automotive, aerospace and machine industries, without the use of modern measurement systems based on optical techniques. The rapid and dynamic progress in developing the next generation of these systems has also made it possible to extend the scope of the areas in which such systems may potentially be applied, with a particular focus on those areas in which no solutions had yet been found [6]. Optical metrology utilizes a variety of such measurement techniques. Some of the most important that have rapidly developed in recent years are:

- interference microscopy, using monochromatic laser radiation (from visible range and IR) or white light for very precise 3D surface measurements (WLI-White-Light Interferometry) [7],
- confocal laser scanning microscopy, using laser radiation for imaging and precise 3D surface measurements [8],
- optical profilometry, using a chromatic aberration phenomenon for precise 3D surface measurements and analysis [9],
- digital/opto-digital microscopy, using LED (Light-Emitting Diode) or halogen light for the rapid

imaging and 2D/3D surface measurements required within many laboratory/industrial applications [10].

Among the above mentioned optical techniques, a special role especially in the measurement and analysis of technical surfaces, is played by the new advanced variety of confocal microscopy, called confocal laser scanning microscopy (CLSM) [11]. This method, characterized by a high accuracy and repeatability of measurements, was adapted from the biological/ medical sciences to the field of technical sciences and industry.

In this work, the use of CLSM for precise measurement of the surface of cold rolled round threads was proposed. Brief characteristics of this method, taking into account the genesis of its development as well as the principles of operation of instruments based on it (Section 2), were also described. In the following part of the work (Section 3), was presented an example of the use of just such an instrument - the 3D laser microscope LEXT OLS4000 produced by Olympus - used in the recording of precision surface measurements of round threads. A description of the methodology and a review of selected results obtained during the tests are given in the final part of the work (Section 4).

2. CHARACTERISTICS OF THE CLSM TECHNIQUE

2.1. The genesis of the CLSM technique

Confocal microscopy is a technique originally developed in the mid 1950's in the United States by

M. Minsky (Harvard University). In addition to the description of the theoretical basis of a new method Minsky also developed a technical solution in the form of a double-focusing stage scanning microscope [12]. This instrument was patented at the end of 1961 [13].

Over the years, Minsky's idea, mainly due to large technical limitations, has not found wide interest, nonetheless a similar work has also led other scientists. M. D. Egger (Yale University) and M. Petráň (Charles University School of Medicine) fabricated in the late 1960's a multiple-beam confocal microscope using a rotating scanning disk (Nipkow wheel). This instrument was used for examining unstained brain sections and *Ganglion* cells [14]. A few years later, M. D. Egger developed the first mechanically scanned confocal laser microscope [15].

Further development of confocal techniques occurred in the 1970's and 1980's. In 1979 G. F. Brakenhoff (University of Amsterdam) with his team developed the construction of a confocal microscope. Construction of a new instrument was presented in the work [16] and this is where the term "*confocal*" is defined for the first time. At that time similar research works were also carried out by K. Carlsson (Royal Institute of Technology, Linköping University) [17], R. W. Wijnaendts Van Resandt (EMBL, Heidelberg) [18], C. Sheppard (University of Oxford) [19].

The first commercial confocal microscopes appeared in 1987, but only at the beginning of the 1990's did the interest in confocal microscopy increase considerably, mostly due to significant progress in the area of optoelectronics, microelectronics and computer science. These instruments He-Ne lasers as a light source, and enabled a simple 2D linear scan process to be carried out. Over the years, this has been improved and modified with an emphasis on:

- replacing gas lasers with more stable semiconductor lasers (at present mainly lasers with a wavelength $\lambda = 405\text{-}408\text{ nm}$ are being used),
- development of the optical elements, which enable a reduction in deformation of the image obtained due to the occurrence of aberrations in the short-wave range, as well as a maximizing of the transmission of light having a wavelength of $\lambda = 405\text{-}408\text{ nm}$,
- development of the scanning systems enabling precise 3D measurements of the surface of the examined objects,
- developing new, more effective, measurement data processing algorithms,
- developing software for the implementation of procedures related to the processing, analysis and visualization of measurement data.

The above mentioned technical possibilities enabled the development of microscopes with more advanced designs. This is how the new class of advanced microscopes were developed – thus stimulating developments in CLSM [20].

2.2 The principle of confocal measurements

The principle of confocal measurement requires that the source of light (laser diode) and detector (photomultiplier, CCD detector) have a common focus. The

word "*confocal*" literally means "*in a common focus*". Technically his is realized by dividing the optical path using a beam splitter. It uses the well-known relationship of the inverse proportionality between spatial resolution and field of view. The field of view is limited on one side by using a light source, which is focused on a small surface to be measured, whilst the objective lens focuses light reflected from a measured surface on the detector, which has the same focal length as the illuminator. With such a configuration of focus centers the light scattered from the surface situated in front and outside of the focal plane is effectively eliminated, which results in the increasing resolution and contrast of the image. The increase in the above mentioned parameters significantly affects the limitation of the field of view. In order to increase the field of view the scanned transverse method is deployed. The measurements are carried out by moving a measuring beam or examined object simultaneously with the detector. This technique allows the measurement of points uniformly distributed within the examined field.

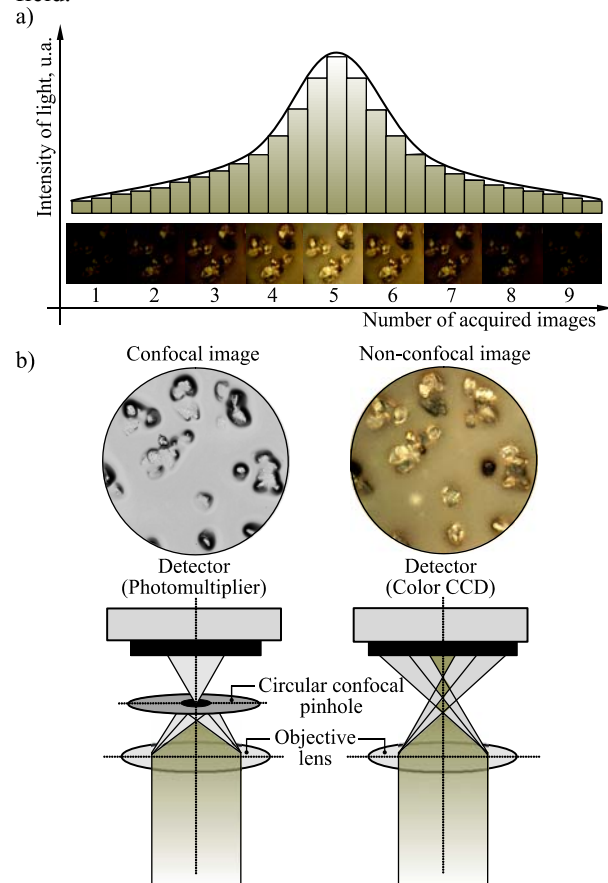


Fig. 1. The principle of confocal measurements: a) change in intensity of light reflected from the surface of microfinished film (IDLF type produced by 3M[®]), acquired by the confocal detection system dependent upon the position relative to the scanning beam focus, b) forming of image (a fragment of the surface of the microfinished film IDLF type produced by 3M[®]) in confocal and non-confocal (microscopic) sections of the 3D laser microscope

As a result an array of points corresponding to the numerical values characterizing the optical properties used in the process for digital analysis for reconstruction of the image of the examined surface are obtained [21].

In order to obtain the high-resolution image output, a method of optical scanning is used, which is characterized by a relatively high number of individual 2D images (sections) acquired when axially moving the focal plane. In the system of confocal detection the area is illuminated by the beam scanning, which increases increases when the distance from the center of focus is increased. Because the image is projected onto the circular confocal pinhole the brightness of the individual scan points changes depending on the position of the focal plane; reaching the maximum value when the examined element will be in the focal point of the beam. This situation is presented in the Fig. 1a.

As a result of analysis of the corresponding points on the scans acquired from the successive layers, data can be obtained which helps to determine the positional coordinates of the individual elements related to the direction of the beam axis, whereby the value of the maximum intensity enables the characterization of optical properties on the examined surface. The confocal method allows for simultaneous acquisition of real images and the generation of spatial images of the examined surface [21], which is presented in Fig. 1b.

3. EXPERIMENTAL TESTS

3.1 Main goals of the experiment

The main goal of experiment was carrying out a measurements and analysis of the important features, which can characterize the surfaces of round threads after the external cold rolling thread process. During the experiments, attempts were made to also test the 3D laser microscope, as well as its dedicated software.

Experiments were carried out in the correct order corresponding to the following steps:

- Step 1: Selecting material for the samples.
- Step 2: Preparing a set of the samples.
- Step 3: Acquiring images of selected areas of the samples.
- Step 4: Carrying out the processing, analysis and visualization of the measurement data.
- Step 5: Carrying out the proper interpretation of the obtained results.

3.2 Characteristics of the sample

6 samples were selected for the purposes of experimentation. These were in the form of a rectangular plate made from steel S235JR with dimensions $40 \times 20 \times 8$ mm, presented in Fig. 2.

The samples were cut from two tubes with a length $l = 1000$ mm and a diameter $\square = 31$ mm. The external surfaces were turned, whereas the inner surfaces were precisely bored on the TUD-35 lathe produced by WAFUM (Poland). Processing was carried out with a liquid coolant 5% water solution of Castrol Syntilo RHS oil). The surfaces of the tubes after the turning process were characterized by the following roughness

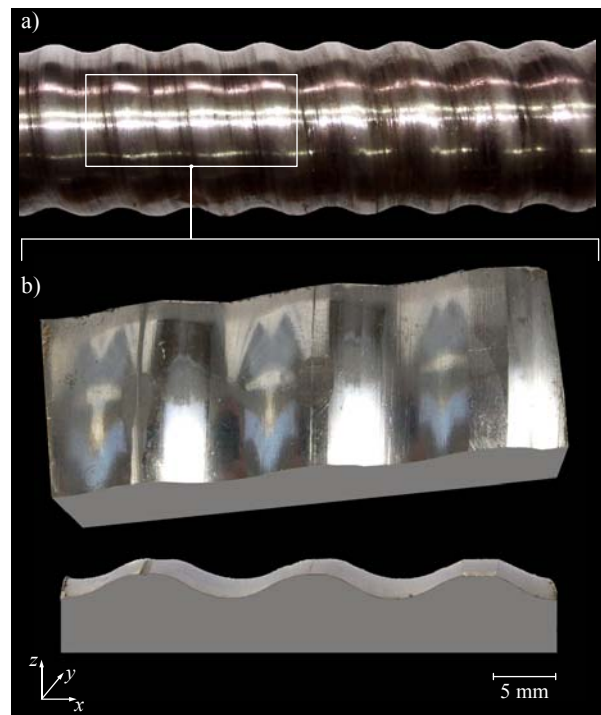


Fig. 2. Sample used in the experimental tests: a) a fragment of the pipe $\square 31 \times 12.56$ mm with external round threads after the cold rolling process, b) general and side view of a sample (rectangular plate $40 \times 20 \times 8$ mm cut out from the pipe)

parameters: $Ra = 8.07 \mu\text{m}$, $Rz = 54.7 \mu\text{m}$, $Rt = 63.63 \mu\text{m}$.

Next, on the surface of each of the pipes a series of round threads were made using the cold rolling process [22, 23]. In this case the TUD-35 lathe was equipped With a special angular rotational rolling head. The description of this head is given in [24, 25]. The thread cold rolling process was realized at a relatively low friction coefficient in the contact zone $\mu \approx 0.01$. The contact zone was intensively lubricated by the Esso Walzoel SFM 132 oil. The surfaces of the tubes after the rolling process were characterized by the following roughness parameters: $Ra = 4.04 \mu\text{m}$, $Rz = 34.1 \mu\text{m}$, $Rt = 42.7 \mu\text{m}$.

3.3 Characteristics of the 3D laser microscope LEXT OLS4000

The Japanese Olympus offers a wide range of 3D laser microscopes. The line of these products is marked as "LEXT" ("*Laser*" and "*Next Generation*") and now includes two main types of microscopes OLS3000 and OLS4000, as well as their various modified versions.

The 3D laser microscope LEXT OLS4000 [26, 27] used two modes for observation and measurement of the examined surface of the samples. In non-confocal (microscopic) mode instrument used a LED source of light (wavelength: $\lambda = 400\text{-}700$ nm, power: 30 mW). In this mode four observation techniques were available: brightfield, darkfield, simple polarization and DIC (*Differential Interference Contrast*) also known as NIC (*Nomarski Interference Contrast*). In confocal mode the instrument used was also a LED source of light, but with a wavelength: $\lambda = 405$ nm (violet), power: 120 mW.

Obtaining spatial mapping entailed its precise scanning, realized point by point on axes x - y . In this case Olympus patented a special scanner based on the MEMS, which enabled the acquisition of a resolution $0.120\ \mu\text{m}$ (axes x - y) and $0.01\ \mu\text{m}$ (axis z).

The confocal system was equipped with two (standard and high sensitivity) photomultipliers. This dual confocal system enabled proper amplification of the optical signal and allowed for analysis of the surfaces with a low reflection coefficient and large surface slope angle, up to 85 degrees. The instrument used a motorized revolving nosepiece with a set of five objective lenses (BF Plan SemiApochromat $5\times$, $10\times$ and LEXT-dedicated Plan Apochromat $20\times$, $50\times$, $100\times$), wherein the maximum magnification that could have been obtained was $17280\times$. The samples were placed on a motorized stage that allowed for precise realization of displacement along axes x - y (range: 100 mm) and axis z (range: 10 mm).

The image processing and analysis of the acquired images was carried out using the dedicated OLS4000 2.1 software, provided by the microscope producer. The general view of the OLS4000, as well as a schematic diagram presenting its principles of operation were presented in Fig. 3.

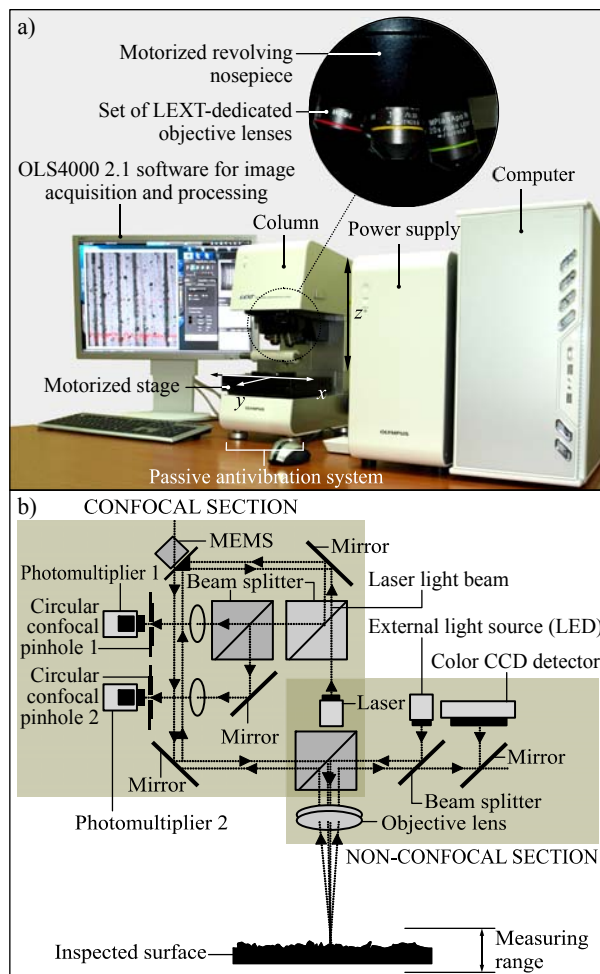


Fig. 3. The 3D laser microscope LEXT OLS4000 produced by Olympus: a) general view of the microscope, b) schematic diagram presenting the principle of operation of the instrument and its most important elements

All measurement data obtained during the experiments was acquired using a single type of LEXT-dedicated Plan Apochromat objective lens – MPLAPO N20XLEXT. Its characteristics are given in Tab.2.

Type of objective lens	Plan Apochromat
Magnification	432-3456 \times
Max. Field of view, μm	640-80
Working distance, mm	1.0
Numerical aperture, -	0.60

Table 2. Parameters of MPLAPON20XLEXT objective lens produced by Olympus

3.4 Analysis of the selected tests results

This section presents select results from the experimental tests, obtained through the use of a 3D laser microscope LEXT OLS4000 produced by Olympus, and supported by a scanning electron microscope JSM-550LV produced by JEOL (Japan).

The measurements were carried out on six sample surfaces, where several marks were located upon both the root and crest of the thread. The most interesting was sample No.5, for which a wider range of results are presented in this section.

In Fig. 4 a set of 2D real images of the surface of sample No.5, for two areas located in the root and crest of the thread respectively, are presented. Fig. 4a shows the first instance in which images of the root surface of the thread with dimensions $642\times 642\ \mu\text{m}$ were acquired using the brightfield technique. The dominant element visible in the central part of this image is a longitudinal groove with a width of 2 - $3\ \mu\text{m}$. The course of the rolling process, its particular impact on the temperature (~ 80 - $90\ ^\circ\text{C}$) and the large degree of plastic deformation, prevented the formation of a uniform surface on the rolled material, enabling what is known as an *overlapping* groove to form. A similar groove can also be observed in the upper part of Fig. 4a. As in the previous case, the reason for its creation is the impact of temperature and plastic deformation. This groove has, particular At its centre, a slightly larger width (4 - $5\ \mu\text{m}$) and is less straight, due to the cylindrical shape of the pipe and rolling rolls. The creation of such an element on the surface of the thread roots can be regarded as a defect. Some other errors produced during the rolling process were discussed in the following works [24, 28].

The real image of the surface of the thread, obtained using the same technique, is shown in Fig. 4b. This area has numerous machined marks of a longitudinal course, which are the remnants of the pretreatment turning process. Among the machined marks a groove of $20\ \mu\text{m}$ is clearly visible. The created groove is a result of the improper selection of technological parameters, in particular the pocket of the roll (tool) in the external thread rolling process is pressed into the rolled material (pipe). The result of this incorrect operation was the creation of an incomplete outline for the round thread.

This element was also previously treated as a defect. The fragments of the sample surface on which the defects described above were localized were treated to more detailed observations. For this purpose, for each of the defects, a series of measurements in the

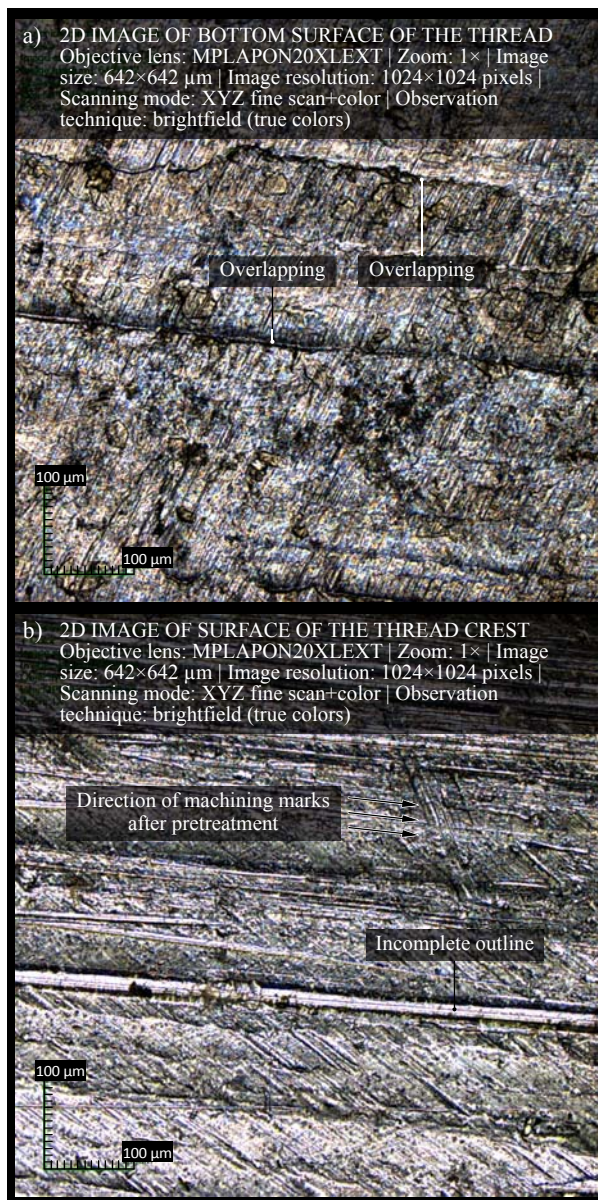


Fig. 4. 2D real image (brightfield, true colors) of the surface of sample No. 5 obtained by 3D laser microscope LEXT OLS4000 produced by Olympus: a) root surface of the thread with visible row (width 2-3 μm), b) surface of the thread crest with visible row (width 20 μm)

confocal and non-confocal modes offered by the 3D laser microscope LEXT OLS4000 produced by Olympus, were carried out.

Fig. 5 presents a collection of the results obtained for the root surface of the thread. In the column on the left are listed the 2D images and maps, while on the right are the corresponding axonometric views. Spatial representation of the test surface allows for a better understanding of the mechanisms creating these defects. It also allows for calculating the values of the parameters characterizing the analyzed surface, including the roughness parameters. The last 2D map, in the colors indexed, presents the height of elements of the analyzed surface described in relevant colors. A groove (defect) is colored yellow. A careful analysis of this map enables

the discovery of other defects (yellow) located on the surface of the sample, as well as lowered visibility on the image acquired using the brightfield technique. As can be seen, in the above case, the use of a 2D height map (in indexed colors) gives a big boost to detecting and analysing defects.

Fig. 6 presents a collection of the results obtained for the surface of the thread crest. Similarly there are, as in the previous case, the compiled 2D images and maps with the corresponding axonometric views. The different angle of the axonometric view allows for the observation of clearly visible machined marks and a defect in the form of a groove with a width of 20 μm, occurring in the central part of the image. The images and maps obtained using a 3D laser confocal microscope in confocal and non-confocal mode can be supported by the other imaging techniques such as SEM. Presenting images of the same part of the surface by using these various techniques offers many possibilities for interpreting, searching out and recognizing the invisible elements in the image, their location, size, shape, etc. It also enables these relationships to be defined, eg. between the workpiece and machined tool, as well as the mechanisms of the phenomena, the effects of which are visible in the assessed areas.

The Authors took advantage of the possibilities of using a microscope JSM-550LV produced by JEOL for the imaging of selected areas of the surface of sample No. 5. The obtained results are presented in Fig. 7. The first of the SEM images (Fig. 7a) shows a fragment of the surface with dimensions of 11.28×2.07 mm, acquired at a magnification of 35×. From the image an AOI (*Area of Interest*) was extracted (1) with dimensions of 3.75×2.71 mm and a magnification of 40×, presenting a fragment of the thread with a visible defect. The side view shows a fragment of the surface in a more spatial approach. The most interesting element here is a defect in the form of a groove, which means that the the mechanism of formation can be accurately investigated. The second SEM image (Fig. 7b) presents a vast fragment of the sample surface with dimensions of 24.68 × 2.59 mm, acquired at a magnification of × 17, with the visible area of the thread comprising its two scrolls (vertexes). An extracted AOI (2) with dimensions of 16.37 x 6.06 mm and 40 × magnification, shows a close-up of one of the zones of material deformation (darker color).

4. CONCLUSION

The experiment's results results enabled the drawing up of the following general conclusions:

- CLSM is a very useful and dynamically developing measurement technique and can be successfully used for multi-criteria assessment of various surfaces of the thread. This assessment can include, among others, analysis, examples of which were presented in this work. There was a basic analysis, as well as a more advanced study aimed at solving complex problems using OLS4000 2.1 software.
- The great potential of 3D measuring laser microscopes (high accuracy, resolution and repeatability allows for the carrying out of scientific research, as well as laboratory-industrial measurements, with varying

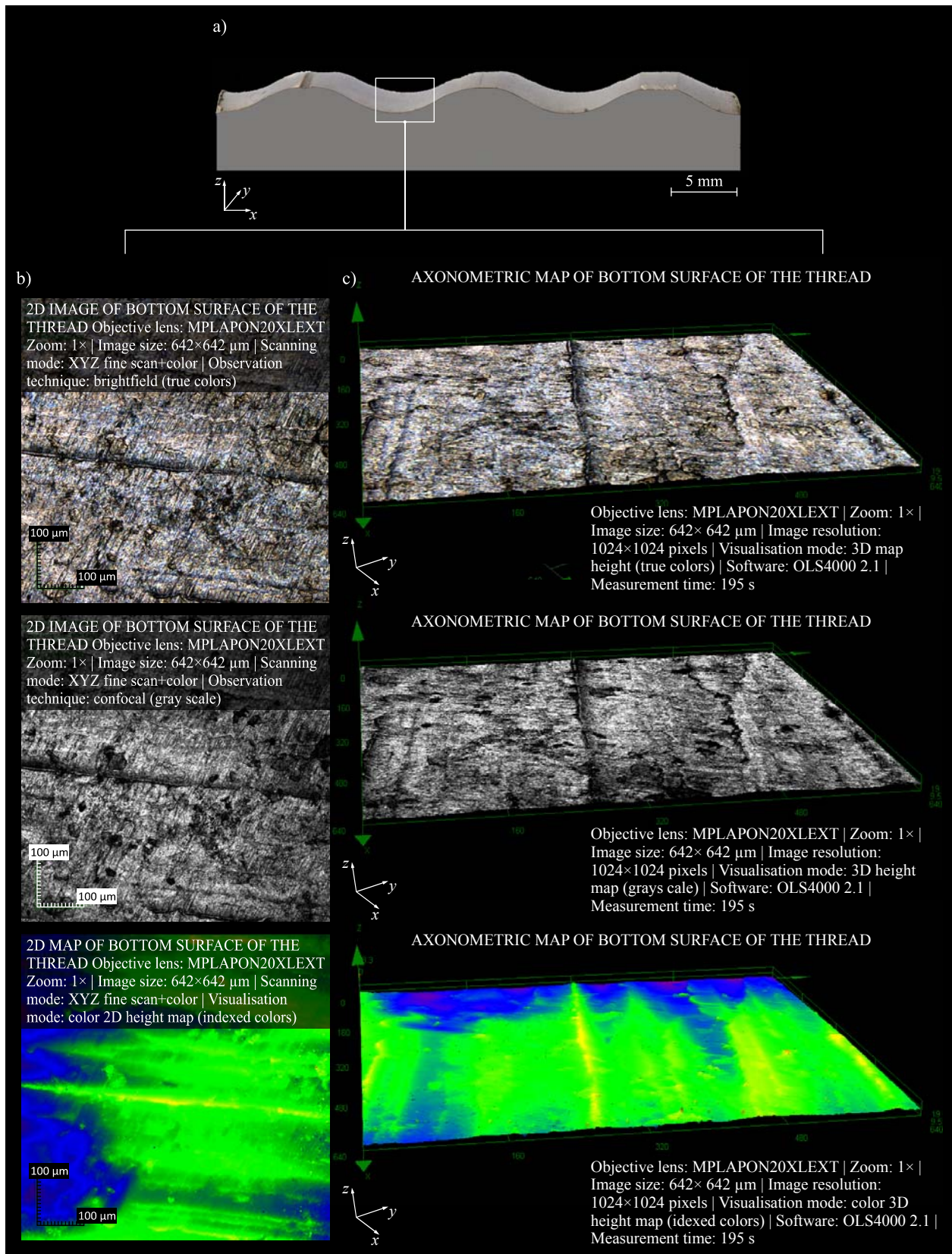


Fig. 5. Collection of selected results obtained during experimental tests carried out with a 3D laser microscope LEXT OLS4000 produced by Olympus for sample No. 5: a) side view of the sample with marked measured area 642×642 μm, b) 2D images and map of root surface of the thread obtained via different observation techniques and visualisation modes (imagea/map area 642×642 μm), c) corresponding with images/maps from Fig.5b axonometric views of root surface of the thread obtained at different visualisation modes (imagea/map area 642×642×8.3 μm)

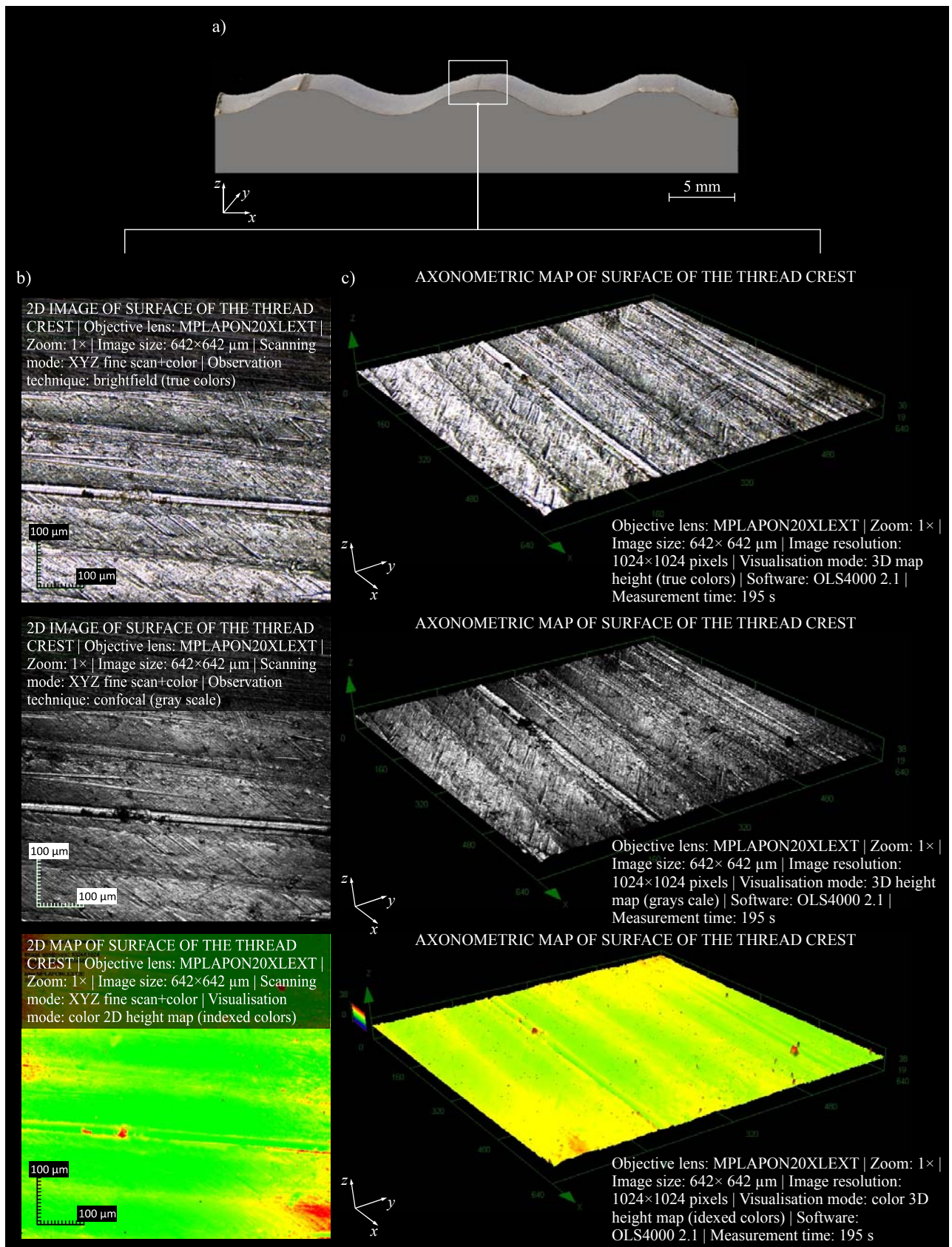


Fig. 6. Collection of selected results obtained during experimental tests carried out with a 3D laser microscope LEXT OLS4000 produced by Olympus for sample No. 5: a) side view of the sample with marked measured area $642 \times 642 \mu\text{m}$, b) 2D images and map of surface of the thread crest obtained via different observation techniques and visualisation modes (imagea/map area $642 \times 642 \mu\text{m}$), c) corresponding with images/maps from Fig. 6b axonometric views of the surface of the thread crest obtained at different visualisation modes (imagea/map area $642 \times 642 \times 8.3 \mu\text{m}$).

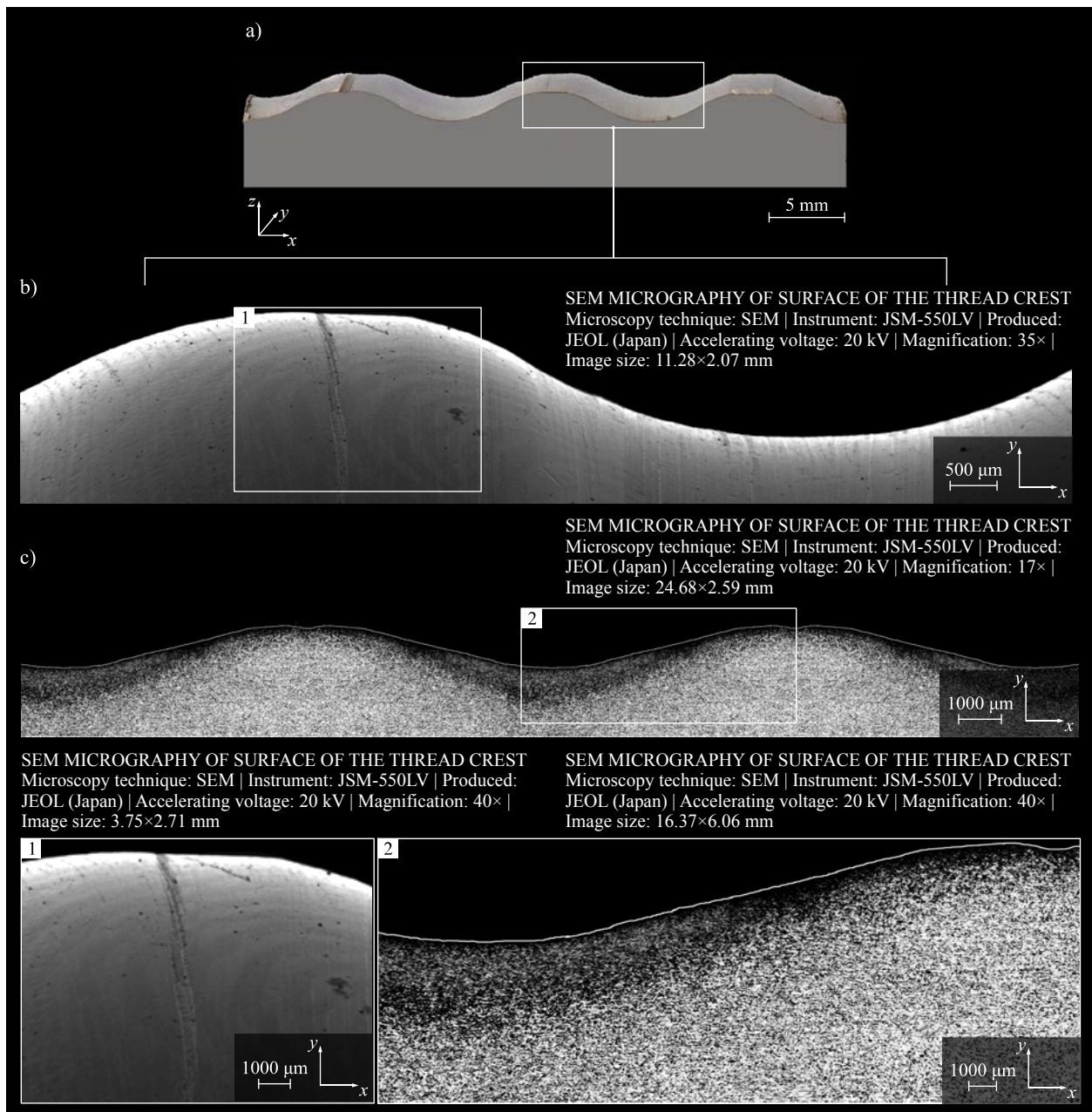


Fig. 7. Collection of selected results obtained during experimental tests carried out with a scanning electron microscope JSM-550LV produced by JEOL for sample No. 5: a) side view of the sample with marked measured area 11.28×2.07 mm, b) SEM micrograph of the surface of the thread crest (image area: 11.28×2.07 mm, mag.: 35×) and an extracted fragment (image area: 3.75×2.71 mm, mag.: 40×) presenting a centrally situated scratch (1), c) SEM micrograph of the surface profile of the thread crest (image area: 24.68×2.59 mm, mag.: 17×) and an extracted fragment (image area: 16.37×6.06 mm, mag.: 40×) presenting a microstructure of the thread crest (2)

measurements, with varying degrees of progress, depending upon the individual case.

- The measurement data obtained by a 3D measuring laser microscope can be supported by different methods, eg. SEM. The results presented show, that the measurement data acquired by SEM microscope can give interesting information pertaining to many aspects of the cold rolling process of round threads (eg. the quality of rolled surface, the state of the surface texture, the zones of deformation, and fragments of the surface which has visible defects).
- Use of the CLSM technique can be treated as a

supplement or extension of the data obtained by other methods (stylus, optical). This is very important especially in the measurement tasks, which require a number of very accurate results from the different sources. As a result of this there is an increased credibility to the scientific research carried out.

5. ACKNOWLEDGEMENTS

The Authors would like to thank Dr. Sergey Yatsunenkov Ph.D., from Olympus Poland for the 3D laser microscope measurements carried out Mr. Ryszard

Gritzman, from the Central Laboratory of the Institute of Mechatronics, Nanotechnology and Vacuum Technique at Koszalin University of Technology, for acquisition of SEM micrographs.

7. REFERENCES

- [1] Hocken, R.J., Chakraborty, N., Brown, C. *Optical Metrology of Surfaces*, CIRP Annals - Manufacturing Technology, 54(2), p.p. 169-183, 2005.
- [2] Labbé, F., *Strain-rate Measurements by Electronic Speckle-Pattern Interferometry (ESPI)*, Optics and Lasers in Engineering, 45(8), p.p. 827-833, 2007.
- [3] López-Cepero, J.M., de Arellano-López, A.R., Quispe-Cancapa, J.J., Martínez-Fernández J.: *Confocal Microscopy for Fractographical Surface Characterization of Ceramics*, Microscopy and Analysis (UK), 19(5), p.p. 13-15, 2005.
- [4] Jin, G.-C., Bao, N.-K. *Surface Detection and 3D Profilometry for Microstructure using Optical Metrology*, Optics and Lasers in Engineering, 36(1), p.p. 1-9, 2001.
- [5] Schwenke, H., Neuschaefer-Rube, U., Pfeifer, T., Kunzmann, H.: *Optical Methods for Dimensional Metrology in Production Engineering*, CIRP Annals - Manufacturing Technology, 51(2), p.p. 685-699, 2002.
- [6] Barak, M.M., Sharir, A., Shahar, R.: *Optical Metrology Methods for Mechanical Testing of Whole Bones*, The Veterinary Journal, 180(1), p.p. 7-14, 2009.
- [7] Dawson T.G., Kurfess T.R.: *Quantification of Tool Wear using White Light Interferometry and Three-Dimensional Computational Metrology*, International Journal of Machine Tools and Manufacture, 45(4-5), p.p. 591-596, 2005.
- [8] Yu T., Wang L., Zhao Y. Q., Liu Y.: *Effects of Thermal Exposure on Low Cycle Fatigue Behavior of Ti600 Titanium Alloy*, Advanced Materials Research, 118-120, p.p. 611-615, 2010.
- [9] Bračun, D, Boštjan, P. Janez, D.: *Surface Defect Detection on Power Transmission Belts Using Laser Profilometry*, Strojniški Vestnik - Journal of Mechanical Engineering, 57(3), p.p. 257-266, 2011.
- [10] Kapłonek W., Nadolny K., Hloch S.: *The Use of Opto-Digital Microscope for Analysis of the PFA-based Abrasive Tools with Surface Micro-Discontinuities*, Nigerian Journal of Technology, 33(1), p.p. 125-133, 2014.
- [11] Miller, F.P., Vandome, A.F., McBrewster, J.: *Confocal Laser Scanning Microscopy*, Alphascript Publishing, Amsterdam, 2010.
- [12] Minsky, M.: *Memoir on Inventing the Confocal Scanning Microscope*, Scanning, 10(4), p.p. 128-138, 1988.
- [13] Minsky, M.: US Patent №3013467: Microscopy Apparatus, 1957/1961.
- [14] Egger, M.D., Petráň, M.: *New Reflected-Light Microscope for Viewing Unstained Brain and Ganglion Cells*, Science, 157, p.p. 305-307, 1967.
- [15] Davidovits, P., Egger, M.D.: *Photomicrography of Corneal Endothelial Cells in vivo*, Nature, 244, p.p. 366-367, 1973.
- [16] Brakenhoff, G.J., Blom, P., Barends, P.: *Confocal Scanning Microscopy with High-Aperture Lenses*, Journal of Microscopy, 117(2), p.p. 219-232, 1979.
- [17] Carlsson, K., Danielsson, P.E., Lenz, R., Liljeborg, A., Majlöf, L., Åslund, N.: *Three-Dimensional Microscopy using a Confocal Laser Scanning Microscope*, Optics Letters, 10(2), p.p. 53-55, 1985.
- [18] Wijnandts Van Resandt, R.W., Marsman, H.J.B., Kaplan, R., Davoust, J., Stelzer, E.H.K., Stricker, R.: *Optical Fluorescence Microscopy in Three Dimensions: Microtomoscopy*, Journal of Microscopy, 138(1), 29-34, 1985.
- [19] Sheppard, C.J.R., Wilson, T.: *Effect of Spherical Aberration on the Imaging Properties of Scanning Optical Microscopes*, Applied Optics, 18(7), p.p. 1058-1063, 1979.
- [20] Müller, F.P., Vandome, A.F., McBrewster, J.: *Confocal Laser Scanning Microscopy*, Alphascript Publishing, Amsterdam, 2010.
- [21] Zajac, A., Kasprzak, J., Urbański, Ł., Gryko, Ł., Szymańska, J., Maciejewska M.: *Light in Medical Diagnostics* [in] Metrology in Medicine – Selected Issues, Military University of Technology, Warsaw, p.p. 219-298, 2011. (in Polish)
- [22] Kukielka, K. Kukielka, L., Bohdal, Ł., Kułakowska, A., Maląg, L., Patyk, R.: *3D Numerical Analysis the State of Elastic/Viscoplastic Strain in the External Round Thread Rolled on Cold*, Applied Mechanics and Materials, 474, p.p. 436-441, 2014.
- [23] Kukielka, K., Kukielka, L., Bohdal, Ł., Kułakowska, A., Maląg, L., Patyk, R.: *3D Numerical Analysis the State of Elastic/Viscoplastic Strain in the External Round Thread Rolled on Cold* [in] Novel Trends in Production Devices and Systems (Velíšek, K., Košťál P., Nad' M. Eds.), Trans Tech Publication, p.p. 436-441, 2014.
- [24] Kukielka, K.: *Modelling and Numerical Analysis of the States of Deformations and Stresses in the Surface Layer of the Trapezoidal and Round Threads Rolled on Cold*, PhD Thesis, Koszalin University of Technology, 2009. (in Polish).
- [25] Kukielka, K.: *Numerical Modelling of the Strain and Stress States in the Thread with Quick Pitch in Rolling Process on Cold*, Measurement Automation and Monitorin, 58(1), p.p. 136-139, 2012.
- [26] Nadolny, K., Kapłonek, W.: *Confocal Laser Scanning Microscopy for Characterisation of Surface Microdiscontinuities of Vitrified Bonded Abrasive Tools*, International Journal of Mechanical Engineering and Robotics Research, 1(1), p.p. 14-29, 2012.
- [27] Kapłonek, W., Nadolny, K.: *Advanced 3D Laser Microscopy for Measurements and Analysis of Vitrified Bonded Abrasive Tools*, Journal of Engineering Science & Technology, 7(6), p.p. 661-732, 2012.
- [28] LaRoux, K. G.: *Troubleshooting Manufacturing Processes: Adapted from the Tool and*

Manufacturing Engineers Handbook, Society of Manufacturing Engineers (SME), Dearborn, 1988.

Authors: Dr. Wojciech Kapłonek, Ph.D, ME,
Koszalin University of Technology, Faculty of Mechanical Engineering, Department of Production Engineering, Subject Group of Metrology and Quality, Raławicka 15-17, 75-620 Koszalin, Poland,
Phone: +48 94 3478233 , Fax: +48 94 3426753,
E-mail: wojciech.kaplonek@tu.koszalin.pl

Dr. Krzysztof Kukielka, Ph.D, ME,
Koszalin University of Technology, Faculty of Mechanical Engineering, Department of Production Engineering, Subject Group of Metrology and Quality, Raławicka 15-17, 75-620 Koszalin, Poland,
Phone: +48 94 3478478 , Fax: +48 94 3426753,
E-mail: krzysztof.kukielka@tu.koszalin.pl

Prof. Leon Kukielka, DSc, Ph.D, ME
Koszalin University of Technology, Faculty of Mechanical Engineering, Department of Technical Mechanics and Strength Materials, Raławicka 15-17, 75-620 Koszalin, Poland, Phone: +48 94 3478290 , Fax: +48 94 3426753,
E-mail: leon.kukielka@tu.koszalin.pl

Prof. Krzysztof Nadolny, DSc, Ph.D, ME
Koszalin University of Technology, Faculty of Mechanical Engineering, Department of Production Engineering, Raławicka 15-17, 75-620 Koszalin, Poland, Phone: +48 94 3478412, Fax: +48 94 3478440,
E-mail: krzysztof.nadolny@tu.koszalin.pl,

Prof. Sergej Hloch, DSc, Ph.D, ME
Technical University of Košice, Faculty of Manufacturing Technologies, Department of Manufacturing Management, Bayerova 1, 080 01 Prešov, Slovak Republic, Phone: +421 51 7722828,
E-mail: sergej.hloch@tuke.sk



Cica, Dj., Sredanovic, B., Kramar, D.

PREDICTION OF CUTTING ZONE TEMPERATURE IN HIGH-PRESSURE ASSISTED TURNING USING GA AND PSO BASED ANN

Received: 06 May 2014 / Accepted: 30 May 2014

Abstract: Control of cutting zone temperature is of great importance during machining process because it affects tool life and surface quality. The objective of this study is development of a cutting zone temperature prediction model in high pressure jet assisted turning using artificial neural networks (ANN). ANN model is coupled with two different evolutionary algorithm, namely genetic algorithm (GA) and particle swarm optimization (PSO), in order to determine properly the weights and biases in each layer of neural network. The predicted cutting zone temperature values obtained from all developed ANN models were compared with the experimental data and the results are indicated.

Key words: temperature, neural networks, evolutionary algorithms

Predikcija temperature rezanja kod obrade struganjem potpomognute mlazom SHP-a visokog pritiska korišćenjem veštačkih neuronskih mreža zasnovanim na evolucionim algoritmima. U obradnom procesu od velike je važnosti kontrola temperature rezanja, budući da ona direktno utiče na vijek trajanja alata i kvalitet obrađene površine. Cilj ovog rada je razvoj modela za predikciju temperature rezanja kod obrade struganjem potpomognute mlazom SHP-a visokog pritiska. U cilju optimalnog određivanja težinskih koeficijenata modela zasnovanog na vještačkim neuronskim mrežama koriste se dva evolucionarna algoritma: genetski algoritam i algoritam optimizacije rojem čestica. Vrijednosti temperature rezanja dobijene razvijenim modelima poredene su sa eksperimentalnim podacima i naglašeni su najvažniji rezultati.

Ključne reči: temperatura, neuronske mreže, evolucionari algoritmi

1. INTRODUCTION

Numerous attempts have been made to determinate the cutting zone temperature, with different methods including experimental, analytical and numerical analysis. However, since machining processes are non-linear and time-dependent, it is extremely difficult for classical methods to provide accurate predictive models. Recently, to address this difficulty, meta-heuristic techniques such as artificial neural networks (ANN), fuzzy logic (FL), genetic algorithms (GA), particle swarm optimisation (PSO), ant colony optimization (ACO), etc. have been used by many researchers as a very popular choice in modelling of sophisticated phenomenons. Among these, due to properties such as universal function approximation, parallel distributed processing, good generalization capability, learning and adaptive behaviour, ANN are being preferred for prediction of the machining parameters as well as for the optimization of the machining process.

Various researchers have developed ANN predictive models for tool life, surface roughness and cutting forces as a function of process parameters. A detailed review of papers related to the monitoring of tool wear was presented by Bernhard [1]. Similar a very detailed review of publications dealing with surface roughness modeling was presented by Pontes et al. [2]. However, there are only a few papers dealing with the implementation of ANN method for cutting zone temperature prediction. Adesta et al. [3] presents a ANN as an effective tool for modeling and predicting

the cutting temperature in the CNC end milling process. Tanikic et al. [4] examine the possibility of using various ANN models in metal cutting temperature modelling. Wardle et al. [5] developed an ANN based system for controlling the temperature of internally cooled tools. Choudhury and Bartaryab [6] focuses prediction of tool wear, surface finish and cutting zone temperature.

As can be seen from the literature review above, there have not been that much work on prediction of cutting zone temperature, especially in high-pressure jet assisted (HPJA) turning. In HPJA turning fluid allows a better penetration of the fluid into the chip-tool and workpiece-tool interfaces, thus providing a better cooling effect and decrease in tool wear [7]. The objective of this study is to develop an ANN model that can be used successfully for accurate prediction of cutting zone temperature while performing turning operations under high pressure cooling conditions. Furthermore, present work intends to integrate ANN with two different evolutionary algorithm, namely genetic algorithm and particle swarm optimization, in order to determine properly the weights and biases in each layer of neural network.

2. EXPERIMENTAL DESIGN AND SET-UP

The experimental work was carried out at the Laboratory for Machining, the Faculty of Mechanical Engineering in Ljubljana. The experiments were conducted in longitudinal turning process on conventional lathe, fitted with a high-pressure plunger

pump of 150 MPa pressure and 8 l/min capacity. The fluid used was the Vasco 5000 cooling lubricant from BlaserSwisslube Inc., a 5.5% emulsion without chlorine on the basis of vegetable oil mixed with water (pH 8.5-9.2). All experiments were carried out using the nickel based alloy Inconel 718 supplied as bars (145 mm diameter x 300 mm long) with hardness between 36 and 38 HRC. A PVD TiAlN-coated carbide tool (grade P25) SNMG 12 04 08-23 has been chosen.

An orthogonal array L27 has been used for design of experiments (DOE). The experiments were carried out for different combinations of following HPJA turning parameters at three levels (Table 1), while depth of cut $a_p = 2$ mm was kept constant. Cutting zone temperature (T) was measured with a thermocouple directly embedded in the insert. A 0.55 mm diameter hole was drilled in the tool using EDM in order to insert a thermocouple of 0.5 mm diameter (Fig. 1).

Turning factor	Levels		
	1	2	3
Diameter of the nozzle D_n [mm]	0.25	0.3	0.4
Distance between the impact point of the jet and the cutting edge d [mm]	0	1.5	3
Pressure of the jet p [MPa]	50	90	130
Cutting speed v_c [m/min]	46	57	74
Feed f [mm/o]	0.2	0.224	0.25

Table 1. Design factors and their levels

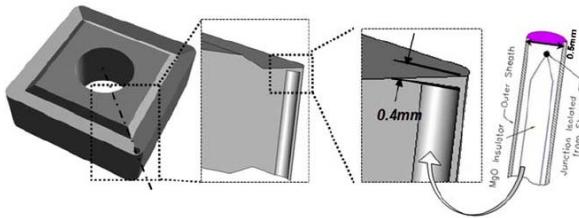


Fig. 1. Thermocouple embedded in the insert

3. DEVELOPMENT OF PREDICTIVE MODELS

3.1 ANN model

ANNs are distributed, adaptive, generally nonlinear non-linear mapping structures based on the function of the human brain. ANN are composed of a large number of highly connected neurons working in unison to solve specific problems. ANN models are specified in terms of three basic entities: models of the neurons themselves, models of synaptic interconnections and structures, and the training rules for updating the connecting weights.

The Multi-Layer Perceptrons (MLP) is the most popular arrangement of ANN which can approximate virtually any function with any desired accuracy, provided that there are enough hidden neurons in the network and that a sufficient amount of data is available. These ANN usually consists of three layers: an input layer, a hidden layer and an output layer. The number of input neurons is typically determined to correspond to the dimension of the input vector. In

these case we have five input variables: diameter of the nozzle, distance between the impact point of the jet and the cutting edge, pressure of the jet, cutting speed and feed. The number of neurons in the hidden layer can be varied based on the complexity of the problem. If this number is too small, the network is not able to learn and if it is too large, the ability of generalization ANN is lost. In this paper, number of neurons in the hidden layer was evaluated by mean absolute percent error (MAPE) and absolute fraction of variance between the experimental and the predicted values for every output nodes in respect of training the network. According to the evaluation results of various network structures, a network with 6 neurons in the hidden layer was determined as the optimal network. The number of neurons in output layer is equal to the number of functions being approximated by the model and in this case it is cutting zone temperature. The first step in developing ANN model is normalization of all the inputs and the desired outputs within the range of ± 1 . Then, the whole data are by the random method divided into two datasets: training dataset, and test data set. The training and test data sets consist of 18 and 9 data, respectively. Fig.2. shows neural network architecture used in this study.

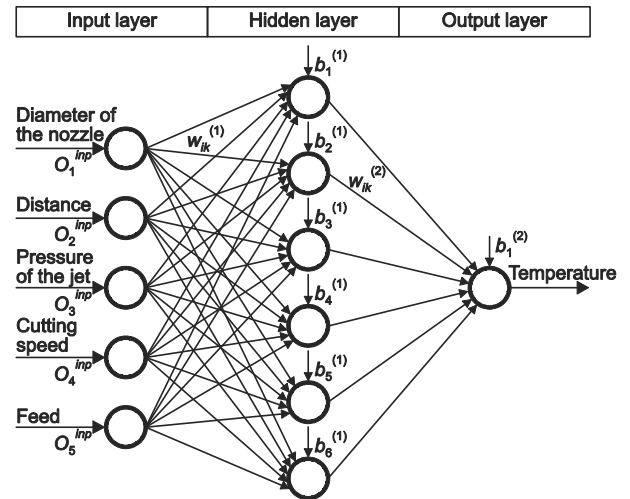


Fig. 2. Neural network architecture

Although there are numerous training algorithms depending on the type and architecture of ANN, the Back-Propagation (BP) algorithm is currently the most popular for performing supervised learning tasks. In BP algorithm the input pattern is propagated from the input to the output layer and it produces an actual output. Then the error signals resulting from any possible difference between the expected and actual outputs are back-propagated from the output to the previous layers for them to update their weights until the input layer is reached. The limitations of back-propagation neural network applied to nonlinear optimization problems is easy trapping in local optimization and also exhibit large errors when processing complicated nonlinear estimations. Instead of using gradient-based learning techniques to obtain the weights of neural network, one may apply evolutionary algorithms such as genetic algorithms and particle swarm optimization. The hybrid

neural network models are, namely, genetic algorithm-based neural network (GA-NN) model and particle swarm optimization based neural network (PSO-NN) model.

3.2 GA-ANN model

Evolutionary algorithms are quite young field of the study of computational systems based on the idea of natural evolution and adaptation. These algorithms are especially useful for complex optimization problems with a very large number of parameters and where the analytical solutions are difficult to obtain. Genetic algorithms are a particular category of evolutionary algorithms based on the mechanics of natural selection and natural genetics. The basic idea of GA is to maintain a population of chromosomes (representing candidate solutions to the concrete problem being solved) that evolves over time through a process of competition and controlled variation. GA is applied with its three genetic search operations, namely selection, crossover and mutation, to create a population of chromosomes with the purpose of improving the quality of chromosomes. Reproduction selects the copies of chromosomes proportionate to their fitness value, crossover operator is applied to the population to create better strings, while mutation is the random modification of chromosomes.

A synergism between ANN and GA, referred as evolutionary neural networks, has been recognized as a tool to increase performances of each technique. The hybrid GA-ANN is trained using genetic algorithm by adjusting its weights and biases in each layer. In this way, each string or chromosome in the population represents the weight and bias values of the ANN. The initial population is a set of N chromosome, which is generated randomly. A given set of chromosomes forms a population and at each generation every individual is evaluated according to its fitness value. The fitness function considered is the minimum of the mean squared error MSE and computed by recalling the network. After getting the fitness values of all chromosomes, they are ranked based on their fitness values and chromosomes with best fitness values in the population are selected by the reproduction operator for a second generation. In order to produce offspring parents are recombined. All offspring will be mutated with a certain probability and the fitness of the offspring is then computed. New offspring is combined with selected best population to produce a new population for the next generation. In the case that optimization criteria are not fulfilled, the creation of a another new population is created and parents are selected according to their fitness for the production of offspring. Described cycle is performed over and over again until the optimization criteria are reached or no variation of the best fitness is observed over a specified number of generations.

3.3 PSO-ANN model

Particle Swarm Optimization is a relatively new evolutionary algorithm based on the social behavior of

flocks of birds and schools of fish. PSO and GA have many similarities. Both algorithms start with a group of a randomly generated population. Furthermore, both algorithms have fitness values to evaluate and update the population. Finally, GA and PSO search for the optimum with random techniques. However, PSO does not have genetic operators like mutation and crossover. Also, PSO have significantly different information sharing mechanism. In GA chromosomes share information with each other, while in PSO only best gives out the information to others.

In PSO algorithm, each single solution is called a particle, which are initialized with a random position and search velocity. All particles have fitness values, which are evaluated by the fitness function to be optimized. These particles moving interactively through the feasible problem space by following the current optimum particles to find new solutions. The individuals best solution (global best or local best solution) is only reported for the other particles in a swarm, analogous to social interaction. In this way the global best is known to all the particles and the swarm tends to converge to the best solution quickly and efficiently. PSO algorithm terminates after a reaching the maximum iteration number or satisfaction of the minimum error condition. In this paper, hybrid PSO-ANN is trained using particle swarm optimization algorithm by adjusting its weights and biases in each layer that will minimize the error function.

4. RESULTS AND DISCUSSION

In this section, the predicted values of proposed ANN, GA-ANN and PSO-ANN models are compared with the experimental data for the validation set of experiments. To predict cutting zone temperature, all models were developed with five inputs and one hidden layer having six neurons. Then, all three models were tested with the 9 test data points which were not used for the training process. Table 2. shows comparison in prediction of cutting zone temperature obtained using ANN, GA-ANN and PSO-ANN model for test data set. The mean absolute error (MAE) of ANN model in this testing process is 7.8%, which is considered a good agreement between the simulated outputs and the experimental results. However, the optimal results obtained using the GA-NN and PSO-NN models are even more accurate. The mean absolute error of GA-ANN and PSO-ANN model for test data set were 4.3 and 4.8%, respectively. Hence, a hybrid ANN models which combines a feed forward neural network and a evolutionary algorithms, namely genetic algorithm and particle swarm optimization, was put forward to improve precision and efficiency of the model.

The comparison of the predicted and the experimental values of cutting zone temperature for the test data sets are presented in Fig. 3. From the obtained results, it can be observed that the predicted values of all three models are close and follow almost the same trend as the experimental data.

No.	Machining conditions					Exp. value of T	ANN		GA-ANN		PSO-ANN	
	D_n	d	p	v_c	f		T	Abs. error	T	Abs. error	T	Abs. error
1.	0.25	0	130	74	0.25	127	137.8	8.5	131	3.1	120.5	5.1
2.	0.25	1.5	130	74	0.224	134	130.3	2.8	127.4	4.9	133.7	0.2
3.	0.25	3	130	74	0.2	117	111.7	4.5	122.9	5	128.4	9.7
4.	0.3	0	130	46	0.25	135	125.7	6.9	131.7	2.4	142.2	5.3
5.	0.3	1.5	130	46	0.224	119	108.9	8.5	128.5	8	120.9	1.6
6.	0.3	3	130	46	0.2	129	110.9	14	124.5	3.5	117	9.3
7.	0.4	0	130	57	0.25	127	112.5	11.4	130.4	2.7	121.5	4.3
8.	0.4	1.5	130	57	0.224	130	113.8	12.5	126.8	2.5	123.4	5.1
9.	0.4	3	130	57	0.2	114	112.7	1.1	121.8	6.8	116.5	2.2

Table 2. Comparison in prediction of cutting zone temperature obtained using ANN, GA-ANN and PSO-ANN model for test data set

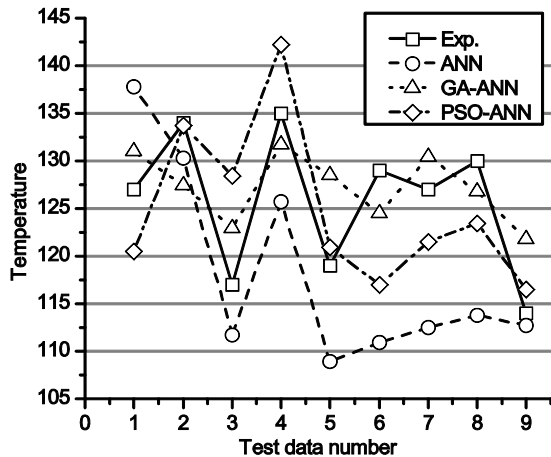


Fig. 3. Comparison of between predicted values and experimental results of cutting zone temperature

5. CONCLUSIONS

The main objective of this study has been to develop a hybrid ANN models to predict cutting zone temperature in high-pressure jet assisted turning. The inputs parameters were: diameter of the nozzle, distance between the impact point of the jet and the cutting edge, pressure of the jet, cutting speed and feed. For the selected 5-6-1 ANN structure, which uses BP algorithm an good agreement has been found between predictions and experimental data for the 9 cutting conditions used as a test data. However, due to the limitations of BP neural networks, an effort was made to apply evolutionary computational techniques for determining the network weights. Hence, a two evolutionary techniques, named genetic algorithm and particle swarm optimisation, has been used instead of a back-propagation algorithm and it is proven that the experimental results matched better with the values predicted by proposed hybrid ANN methods. Furthermore, in addition to improving precision and efficiency of the model, hybrid ANN ensures a faster algorithm for training the desired neural network.

6. REFERENCES

[1] Bernhard, S.: On line and indirect tool wear monitoring in turning with artificial neural networks: A review of more than a decade of research, *Mechanical Systems and Signal*

processing, Vol. 16, No. 4, pp. 487–546, 2002.

[2] Pontes, F.J., Ferreira, J.R., Silva, M.B., Paiva, A.P., Balestrassi, P.P.: Artificial neural networks for machining processes surface roughness modeling, *International Journal of Advanced Manufacturing Technology*, Vol. 49, No. 9-12, pp. 879-902, 2010.

[3] Adesta, T., Al Hazza, M., Suprianto, M.Y., Riza, M.: Prediction of Cutting Temperatures by Using Back Propagation Neural Network Modeling when Cutting Hardened H-13 Steel in CNC End Milling, *Advanced Materials Research*, Vol. 576, pp. 91-94, 2012.

[4] Tanikić, D., Manić, M., Devedžić, G., Čojbašić, Ž.: Modelling of the Temperature in the Chip-Forming Zone Using Artificial Intelligence Techniques, *Neural Network World*, Vol. 20, No. 2, pp. 171-187, 2010.

[5] Wardle, F., Minton, T., Ghani, S.B., Furstmann, P., Roeder, M., Richarz, S., Sammler, F.: Artificial Neural Networks for Controlling the Temperature of Internally Cooled Turning Tools, *Modern Mechanical Engineering*, Vol. 3, No. 2, pp. 1-10, 2013.

[6] Choudhury, S.K., Bartaryab, G.: Role of temperature and surface finish in predicting tool wear using neural network and design of experiments, *International Journal of Machine Tools and Manufacture*, Vol. 43, No.7, pp. 747-753, 2003.

[7] Kramar, D., Kopac, J.: High Pressure Cooling in the Machining of Hard-to-Machine Materials, *Journal of Mechanical Engineering*, Vol. 55, No. 11, pp. 685-694, 2009.

Authors: Assist. Prof Dr. Djordje Cica, MS.c Branislav Sredanovic¹, Assist. Prof Dr. Davorin Kramar.,

¹University of Banja Luka, Faculty of Mechanical Engineering, Vojvode Stepe Stepanovica 71, 78000 Banja Luka, Republika Srpska, BiH, Phone: +38751433-000

²University of Ljubljana, Faculty of Mechanical Engineering, Askerceva 6, 1000 Ljubljana, Slovenia, Phone: +38614771-200

E-mail: djordjecica@gmail.com
sredanovic@gmail.com
davorin.kramar@fs.uni-lj.si



Župerl, U., Čuš, F., Irgolič, T., Vukelić, D.

INDIRECT TOOL WEAR MEASURING TECHNIQUE COMBINED WITH OPTO-ELECTRONIC SYSTEM FOR AUTOMATED TOOL CONDITION CONTROL

Received: 19 May 2014 / Accepted: 14 June 2014

Abstract: In this paper indirect measuring technique is combined with opto-electronic system for automated tool condition monitoring. The paper presents an electro-optical vision system to quickly identify the cutting tool failure. Indirect technique employs ANFIS method to extract the features of tool wear from cutting force signals. The output of ANFIS tool wear model combined with signals of electro-optical system is applied to a decision control system which determines the control commands to the CNC controller. The decision system and error compensation module can guide control system of machine tool or provide warnings to an operator, in order to minimize tool damage.

Key words: tool condition, monitoring, tool wear, machine vision, ANFIS.

Indirektna tehnika merjenja habanja u kombinaciji sa optičko-elektronskim sistemom za automatsku kontrolu stanja reznog alata. U radu je prikazana kombinacija indirektna tehnika merjenja i optičko-elektronskog sistema za automatsko praćenje stanja reznog alata. Rad prezentuje elektronsko-optički sistem za brzu identifikaciju loma reznog alata. Indirektna tehnika koristi ANFIS metod za razdvajanje karakteristika habanja reznog alata od signala sila rezanja. Izlaz iz ANFIS modela habanja reznog alata u kombinaciji sa signalima iz elektronsko-optičkog sistema primenjuje se na kontrolni sistem odluke koji generiše kontrolne komande CNC kontrolera. Sistem koji donosi odluku i modul za kompenzaciju greške mogu da upravljaju kontrolnim sistemom mašine alatke ili da upozore operatera sa ciljem minimizovanja oštećenja reznih alata.

Ključne reči: stanje reznog alata, monitoring, habanje reznog alata, mašinska vizija, ANFIS.

1. INTRODUCTION

Many studies have been conducted on the monitoring of malfunctions and abnormal cutting states of machine tools [1]. With regard to the monitoring of cutting tool states, two main factors are tool wear and tool failure. Tool failure has become more important recently since hard tools are frequently used in the cutting process. There are two techniques for tool condition sensing: direct and indirect. Generally, direct techniques are avoided because of the difficulty with online measurements. Haber [2] has measured the flank wear of the cutting tool using computer vision. He has proved the feasibility of this technique, however he also exposed problems with the integration of such system on the machine tool. The indirect technique includes the measuring of cutting forces, torque, vibration, acoustic emission (stress wave energy), sound, temperature variation of the cutting tool, power or current consumption of spindles or feed motors, and roughness of the machined surface [3]. The recent trend in TCM is the combination of direct and indirect techniques [4]. This paper discusses the advantages of integration of machine vision into the popular indirect technique for tool condition sensing which is based on cutting force measurements.

2. MONITORING SYSTEM STRUCTURE

Fig. 1 shows the basic architecture of the proposed TCM system. The proposed system consists of four main parts. First part is ANFIS model of tool wear. It is

developed from a set of data obtained during actual machining tests performed on a Heller milling machine using a Kistler force sensor. The signal processing module analyses the machining signals for extracting features sensitive to tool wear. The trained ANFIS model of tool wear is then merged subsequently with an electro-optical vision system for assessing tool wear condition (good, broken). Tool deflection that occurs during machining and especially when flexible tools, such as end mills are used, can result in dimensional errors on workpieces. Tool deflection model (third part) is used to determine the milling dimensional error due to tool deflections. Therefore, finally the fourth part, the error compensation module is developed. This part of TCM modifies the cutting conditions, compensates for the machining errors due to tool deflection and tool wear, without degrading the production performance and the machined accuracy. The compensation strategy allows the on-line optimization of feed rates or the tool path trajectory in order to achieve a specified tolerance. The developed TCM system can guide control system or operator in tool change decisions making.

2.1 ANFIS tool wear prediction model

The relationship between the machining parameters/sensor signals and flank wear is first captured via a network and is subsequently reflected in linguistic form with the help of a fuzzy logic based algorithm. The estimation design process consists of a linguistic rule construction, the partition of fuzzy subsets and the definition of the membership function shapes. It uses training examples as input and constructs

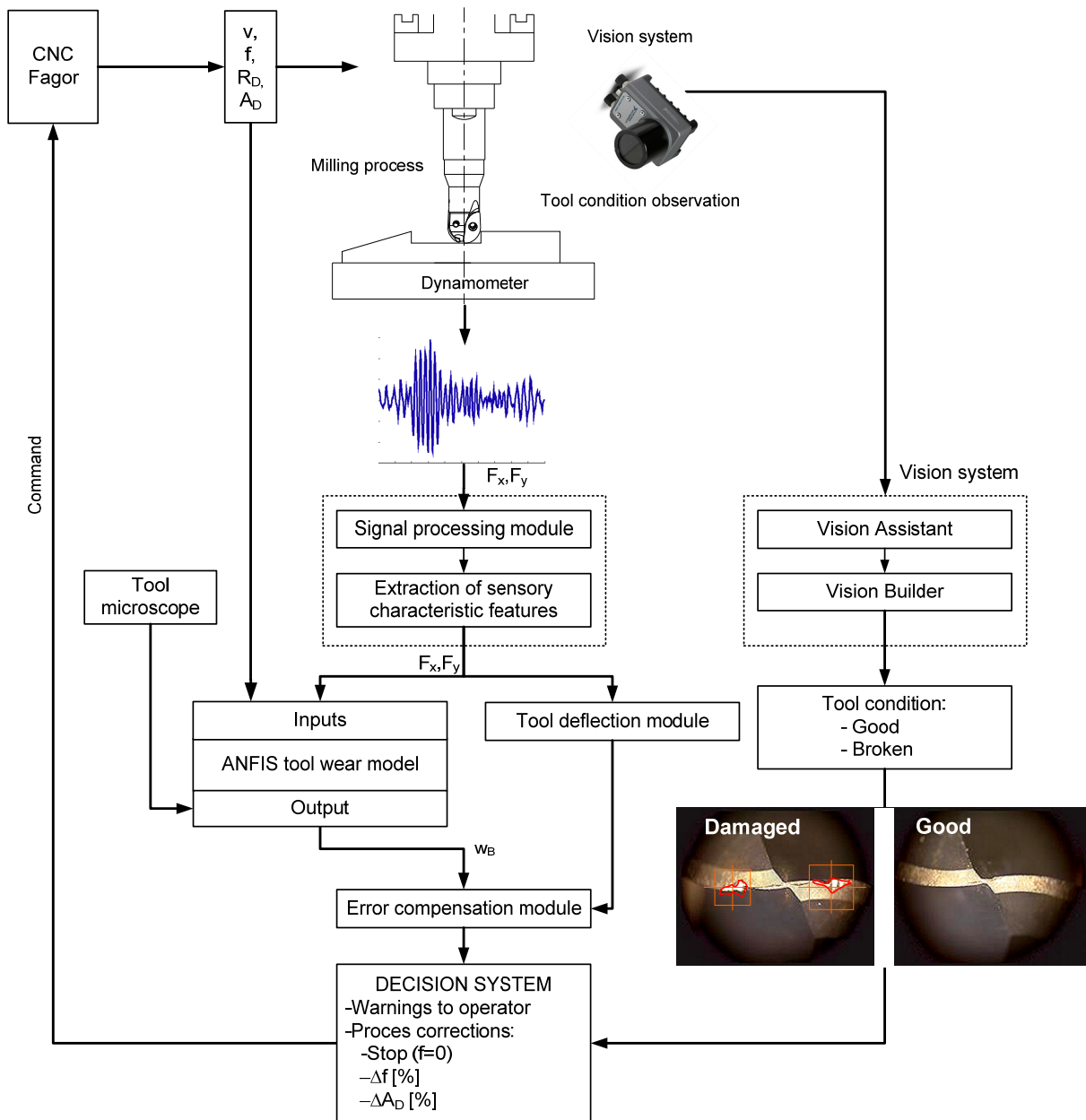


Fig.1. Architecture of tool condition monitoring system

the fuzzy if-then rules and the membership functions (MF) of the fuzzy sets involved in these rules as output. This process is called a training phase. Two different membership functions, the triangular and the trapezoidal, were adopted during the training process of ANFIS in this study in order to compare the prediction accuracy of flank wear according to the two membership functions. After training the estimator, its performance was tested under various cutting conditions. Fig. 2 shows the fuzzy rule architecture of ANFIS when the triangular membership function is adopted. The fuzzy inference system under consideration has 7 inputs and one output w_B . The process variables are force sensor readings (F_x, F_y), cutting speed (v), feed rate (f), depth of cutting (A_D/R_D), machining time and flank wear (w_B).

2.2 Electro-optical vision system

The developed vision system is adapted to end

milling and special programs were developed to monitor tool condition. The system consists of a high speed smart camera for online monitoring and special developed software. The smart camera was chosen to visually detect tool breakage. The used smart Camera 1772C is a product of National Instrument. The maximum output is 64,995 frames per second (fps). Additional Basler acA640 camera was also used. Its maximum output is 110 fps. The identified cutting tool damage explains us the adequacy of cutting conditions during a specific time in machining and which machining parameters need to be adjusted to improve the surface roughness and decrease further tool damage. Testing's are subordinated to determine the limits of the applied camera and what possibilities it offers for other applications. The programs to operate the vision system were designed in LabVIEW. In the first settings, the program was set to detect the damage of the cutting tool and a change in the proximity of the

cutting tool – chip formation.

Next the tool breakage detection is ensured. On behalf of the observation results, the user interface reports the monitoring status of the tool to the operator via network variables.

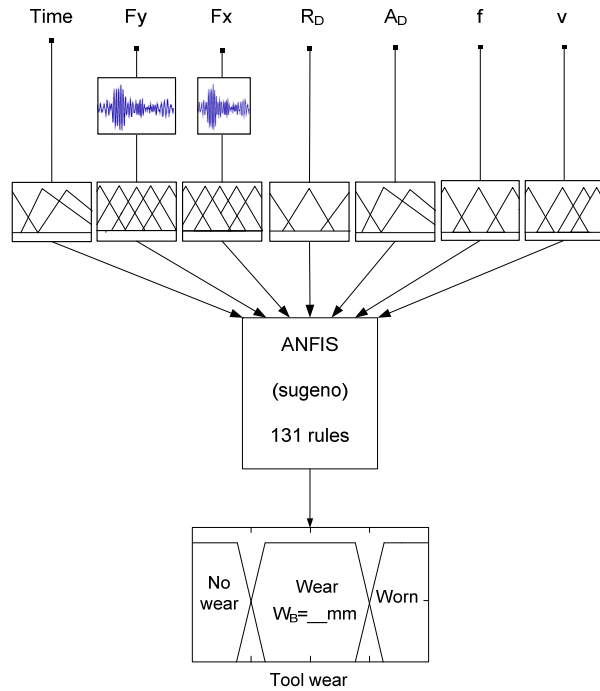


Fig. 2. Structure of ANFIS tool wear model

If the observed geometry is within predefined limits, the process runs without interruption. On the other hand, if the system detects a tool damage, a warning is issued for the operator to react.

Different options are proposed to the operator. If he does not react in a predefined time, the system automatically changes the feedrate and axial/radial depth of cutting.

The main difficulty was the connection between the vision system and the control system.

2.3 Tool deflection module

The main objective of the deflection module is to determine the deflection of end mills under milling forces.

For the deflection analysis of end mills, the tool holder is assumed to be rigid and the cantilever beam model is used. However, the holder and the clamping stiffness can also be included in the analysis if they are known. End mill deflections can be approximated by using the beam model.

The deflection of the end mill used in the model are shown in Fig. 3, where D_1 is the mill diameter, D_2 is the shank diameter, L_1 is the flute length, L_2 is the overall length, F is the point load.

Modelling can be unpractical and time consuming for each tool configuration in a virtual machining environment. Therefore, simplified equations are generated to predict deflections of tools for given geometric parameters and density.

The static characteristics of end mills can be shown

as:

$$X_m = deflection_{max} = C \frac{F}{E} \left[\frac{L_1^3}{D_1^4} + \frac{(L_2^3 - L_1^3)}{D_2^4} \right]^N \quad (1)$$

where F is the applied force and E is the modulus of elasticity (MPa) of the tool material. The constant C is 9.05, 8.30 and 7.93 and constant N is 0.950, 0.965 and 0.974 for 4-flute, 3-flute and 2-flute tools, respectively [5].

2.4 Error compensation module

The developed module (see Fig. 1) aims at facilitating the compensation of surface errors in machining caused by tool deflection and tool wear. The measured cutting forces are fed into a deflection model for the prediction of dynamic behaviour of the tool during cutting. An iterative procedure is used to determine the milling error through trial and error of the cutting force and deflection. The predicted deflected tool profile is used to identify the “real” material volume that is removed during machining. As soon as the milling error is obtained, the error compensation can be achieved by optimising the tool path or by feed rate adjustment.

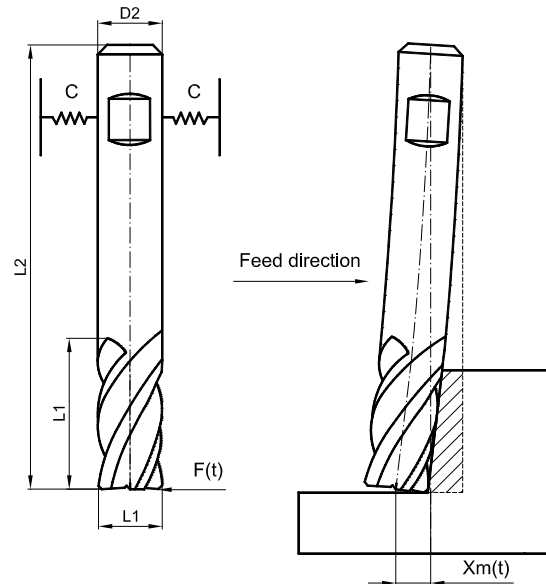


Fig. 3. Cutting force induced tool deflection

3. EXPERIMENTAL SET-UP

Experiments were performed on a CNC machining platform Heller with FAGOR CNC controller.

A vision system consisting of a high speed smart camera NI 1772C was used to detect tool breakage without dismounting the tool from the tool holder. The maximum output is 64.995 frames per second (fps). Additional Basler acA640 camera was also used. Its maximum output is 110 fps. Proper lighting condition is assured with the use of a LED ring light, which provides a adaptive illumination of the observed area. The ring light is set to adaptive mode – this provides illumination with the flashing effect of the stroboscope settings.

The Basler camera does not support such settings, furthermore it's speed requires a very capable

computer with fast processing abilities. Namely the speed of the frame acquisition is for normal computers too fast. Special adaptations are needed for the computer to save and process all the data. All the data are transferred to the PC via Giga Ethernet cable. The 1772C also possesses its own buffer and so enables to store all gathered frames without a delay in observation.

The monitoring involved in end milling process of steel parts using two end mill tools: a normal tool and a tool with a broken tooth. The cutting tools used in the machining test were solid end milling cutters (R216.24-16050 IAK32P) with two cutting edges. The tool diameter was 16 mm. Its helix angle was 10°. The corner radius of the cutter was 4 mm. The workpiece material used in the machining test was Ck 45 and Ck 45 (XM) with improved machining properties. The workpiece was mounted in a 3 component piezoelectric dynamometer (Kistler 9255) to monitor the cutting forces in the X and Y directions. It was calibrated using a 10 µm resolution.

Dynamometer was mounted on the machining table and connected to a 3-channel charge amplifier.

The signals were monitored by using a fast data acquisition card (National Instruments NI 9215 A) and software written with the National Instruments CVI programming package.

The flank wear after each cutting test was discontinuously measured with a tool microscope of 0.01 mm accuracy.

The experiments were carried out for 256 combinations of the chosen cutting parameters and tool wear. The parameters such as tool diameter, rake angle, etc. were kept constant.

4. RESULTS AND DISCUSSION

During training of the tool wear model the parameters of membership functions, the optimal rules and the output weights were determined. The best results were obtained when triangular membership functions were chosen for the neuro-fuzzy model of tool wear. By using trapezoidal membership functions higher error was reached. When the ANFIS model was trained, testing data were used for verification.

The training was very fast, and the error reached a constant value after about 30 epochs. The system was capable of detecting tool wear accurately in real time.

The accuracy of the training data was 98.1%, and the accuracy of the testing data was 94.9%.

The first results of visual system testing were used to optimize the computer program, which recognizes specific features, in our case the breakage of the tool cutting edge. The minimum capability of the system in the terms of accuracy is 7,4 µm.

Vision system compares all gathered frames of cutting tooth with a template frame (ideal tool tooth) – the differences are returned.

With the gathered data (frames) 11 different settings were tested to determine which combination of steps and settings enables the best recognition capability for a certain feature. In the end, an inspection status can be set up to determine if the frame

passed the pre-set requirements. In any case, a rule can be applied that takes actions at specified results and makes changes. If the acquired frame does not match the template, the program sends the information to decision system.

Tool condition observations were very sensitive to the lighting of the vision system.

5. CONCLUSION

The aim of this paper is to present a reliable monitoring system for cutting tools in end milling.

The vision system and cutting force sensor are used to monitor milling operations. Electro-optical visual system is used to observe the actual tool condition during the machining. The sensor signals are then sent to decision system which is trained to communicate with CNC controller. The trained adaptive neuro-inference system (ANFIS), is also used to predict tool wear from measured cutting force signals. By developed tool condition monitoring system (TCM) the machining process can be on-line monitored and stopped for tool change based on a pre-set tool-wear limit.

6. REFERENCES

- [1] Fu, P., Hope, A.D.: *Intelligent Classification of Cutting Tool Wear States*, Advances in Neural Networks, Vol. 39, 1611-3349, 2008.
- [2] Haber, R.E., Alique A.: *Intelligent process supervision for predicting tool wear in machining processes*, Mechatronics, Vol. 13, 825-849, 2013.
- [3] Achiche, S., Balazinski, M., Baron, L.: *Tool wear monitoring using genetically-generated fuzzy knowledge bases*, Engineering Applications of Artificial Intelligence, Vol. 15, 303-314, 2008.
- [4] Kuo, R.J.: *Multi-sensor integration for on-line tool wear estimation through artificial neural networks and fuzzy neural network*, Engineering Applications of Artificial Intelligence, Vol. 3, 49-261, 2011.
- [5] Mulc, T., Udiljak, T., Cus, F., Milfelner, M.: *Monitoring cutting- tool wear using signals from the control system*. Strojniški vestnik – Journal of Mechanical Engineering, Vol. 50, No. 12, 568-579, 2011.

Authors: Prof. Dr. Franc Čuš, Assist. Professor Dr. Uroš Župerl, B.Sc. Tomaž Irgolič, University of Maribor, Faculty of Mechanical Engineering, Institute of Production Engineering, Smetanova 17, 2000 Maribor, Slovenia, Phone.: +386 21 450-366, Fax: +386 2 220 7996

E-mail: franc.cus@uni-mb.si
uros.zuperl@uni-mb.si
tomaz.irgolic@um.si

Prof. Dr. Djordje Vukelić, University of Novi Sad, Faculty of Technical Sciences, Institute for Production Engineering, Trg Dositeja Obradovica 6, 21000 Novi Sad, Serbia, Phone.: 386 2 220 7500, Fax: +381 21 454-495.

E-mail: vukelic@uns.ac.rs



Mladenović,C., Kalentić, N., Zeljković,M., Tabaković, S.

THE INFLUENCE OF MILLING STRATEGIES ON ROUGHNESS OF COMPLEX SURFACES

Received: 01 June 2014 / Accepted: 15 June 2014

Abstract: *Considering the growing demands of the society, it can be concluded that the main objectives set before modern industry are the increase of accuracy and productivity, cost reduction, and savings in material and energy. Increase of productivity, as one of these goals, is particularly important in milling due to limitations in machining capabilities of complex surfaces. One of the features of milling process which has a direct impact on productivity, is the machining strategy, which represents a form of tool path motion in processing. This paper analyzes the impact of milling strategies on the roughness of the machined surface on the example of complex geometry workpiece..*

Key words: *CAD/CAM systems, Milling, Machining strategy, Roughness*

Uticaj strategija obrade glodanjem na hrapavost složenih površina. *Uzimajući u obzir rastuće zahteve društva, može se zaključiti da su osnovni ciljevi koji se postavljaju pred savremenu industriju povećanje tačnosti i proizvodnosti, smanjenje troškova, kao i uštede u materijalu i energiji. Povećanje proizvodnosti, kao jedan od pomenutih ciljeva, posebno je značajno pri obradi glodanjem zbog mogućnosti obrade složenosti površina ovim postupkom. Jedna od karakteristika obrade glodanjem na NU mašinama alatkama, koja direktno utiče na proizvodnost, je strategija obrade, a ona predstavlja oblik putanje kretanja alata pri obradi. U radu je naprimera obrade izradka složenege ometrije analiziran uticajs strategija obrade na hrapavost ravnih segmenata obradene površine.*

Ključne reči: *CAD/CAM sistemi, obrada glodanjem, strategija obrade, hrapavost*

1. INTRODUCTION

Development of products with complex geometry, as a new technological challenge originated from the automotive and aerospace industries, has greatly contributed to the development of software systems for computer aided design (CAD). As a result, modern CAD systems allow users to design very complex shapes, leading to the problems in machining of these parts in terms of time and cost of manufacturing.

Complex geometric shapes have caused the most problems in milling, especially in the machining of complex surfaces of molds for plastic injection and blow molding [1]. Therefore, a large number of studies were carried out in the field of complex surface milling and optimization of tool path [1,2,3,4], and in the field of tool path influence on the surface quality [4,5,6,7]. Certain number of the results of these studies, which are related to new and effective machining strategies have been successfully implemented in modern software systems for computer aided manufacturing (CAM).

Examination of milling strategies is especially important in cases where it is necessary to choose an adequate strategy which implies minimal surface roughness and minimal costs of manufacturing. Also, it often happens that after machining it is necessary to manually polish the machined surface so as to achieve the required surface roughness. These processing operations may be minimized or even completely eliminated by selecting an adequate finishing strategy,

whereby it is also possible to significantly reduce the time and cost of the overall process.

For the finishing milling operation of complex surfaces ball end mill is commonly used as a tool. However, if flat segments exist on the analyzed complex surface, ball mill will in these cases produce a very rough surface, which can be reduced by selecting appropriate machining strategies.

This paper analyzes, for machining of a complex shape part with ball end mill, the impact of the chosen machining strategy on roughness of flat machined surfaces. For this purpose, a complex shape part with a flat, concave and convex surface was modeled, and then, in one of the CAM software, four NC programs with different machining strategies were generated. Using the generated NC programs, four parts with complex geometry were made, and the surface roughness of each flat segment was measured, depending on the machining strategy. The impact of machining strategies on roughness of convex and concave surfaces was not analyzed in this paper.

2. MANUFACTURING STRATEGIES IN CAM SYSTEMS

The machining strategy, or tool path, is a way the tool is moving over the machined surface. [1].

Currently, there is a large number of software systems that support the various fields of production, including the area of defining the machining strategy. This software allows a variation of machining

strategies and analysis of their impact on manufacturing process. The common goal of these CAD/CAM systems is to facilitate designers and technology experts developing a new products and technology of their production.

There are certain requirements that are placed in front of a modern CAD/CAM systems, i.e. CAD/CAM system must possess [8]:

- Advanced machining strategies that will reduce the processing time to a minimum, thereby enabling the production of complex shaped parts;
- Possibility of programming 2-axis, 3-axis, 4-axis, 5-axis machine-tools, and even the manipulators, and industrial robots;
- Advanced methods of collision detection;
- User-friendly interface for fast programming of multi-axis machine tools;
- Advanced support for high speed machining, etc.

Some of today's most used CAD/CAM systems, which meet the previous requirements, are: CAM-TOOL, CATIA, EdgeCAM, ESPRIT, FeatureCAM, MasterCAM, PowerMILL, Pro/ENGINEER, ProTOOLMAKER, SurfCAM. The use of these systems makes it possible to generate NC programs for CNC machine tools in the range of 2 to 5-axis, both for rough as well as finishing machining.

The main goal of the rough milling is higher productivity, i.e. removing the largest volume of material in the shortest period of time [1], while finishing is used to remove the material remaining after rough machining, and its main goal is to achieve the desired shape, size and surface roughness of the machined part [1].

The basic strategies of rough milling, which can be found in almost any CAD/CAM systems are [2]:

- Raster milling – toolpaths are equidistant and parallel with one axis of the coordinate system of the machine tool (Figure 1a);
- Spiral milling – tool moves along a spiral path from the center of the machined surface with pre-defined tool path overlap (Figure 1b);
- Profile milling – tool path is generated based on the profile of the workpiece and the tool movement is performed at predefined steps (Figure 1c).

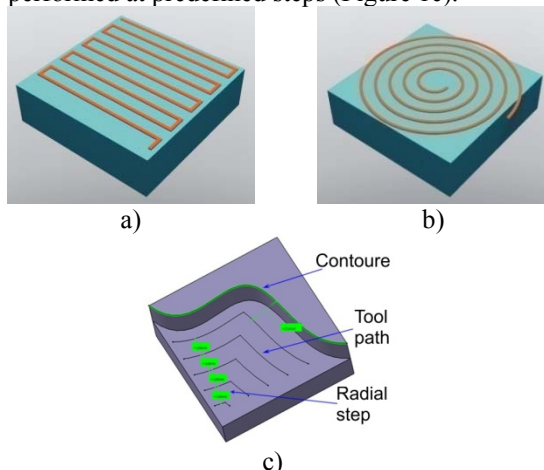


Figure 1. Examples of roughing strategies; a) Raster milling [2], b) Spiral milling [2], c) Profile milling [9]

Besides these basic machining strategy, which can be found under different names in a variety of CAD / CAM systems, there are a number of other strategies formed by combining the above mentioned.

There are more strategies for finishing in relation to the roughing. Some of the basic finish milling strategies, which can also be found under different names in the CAD/CAM systems, are [4]:

- Raster finish milling – is most commonly used for finishing of flat rectangular surfaces (Figure 2a) in which the most commonly used tool is the end mill.
- Radial milling – tool moves from a central point along a path which is mutually under defined angle (Figure 2b). This strategy is used for the machining of flat or nearly flat circular shaped surfaces, also with the end mill.
- 3D offset milling – in this strategy the tool is moving with a constant step over the defined path that follows the contour and shape of the area to be machined (Figure 2c). This strategy is usually applied for finishing of complex shape parts, and commonly used tool for this strategy is the ball end mill.
- Finish milling with constant height along the “Z” axis – tool moves following the contours of the machined workpiece, and in the direction of Z axis moves at constant pre-defined steps (Figure 2d). For obtaining the more accurate profile of machined surface, here is also commonly used ball end mill.

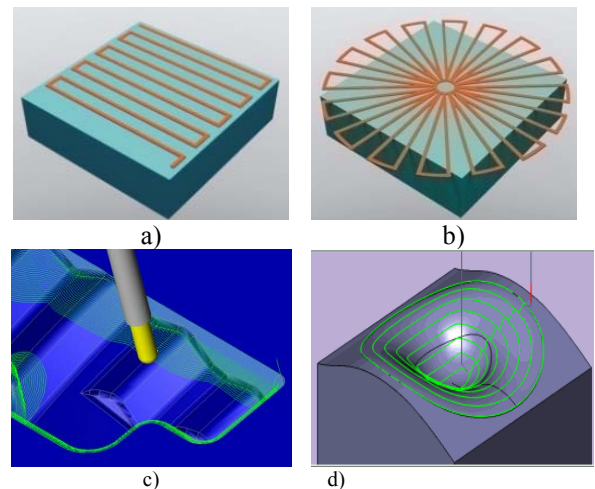


Figure 2. Examples of finishing strategies; a) Raster finish milling [2], b) Radial milling [2], c) 3D offset milling [10], d) Finish milling with constant height along the “Z” axis [9]

3. INFLUENCE OF MACHINING STRATEGIES ON THE FLAT SURFACE ROUGHNESS MACHINED WITH THE BALL END MILL

As already noted, the finish milling of a complex surface is usually performed with the ball end mill. However, due to their geometry, ball end mill often leaves roughness in the waveform on the machined surface (Figure 3) [11], which is especially expressed if on the complex surface exist a flat segment.

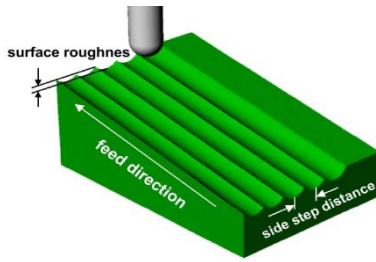


Figure 1. The maximum surface roughness in the machining with ball end mill [6]

In order to analyze the impact of the milling strategy on the roughness of the flat machined surface, four NC programs were generated in a CAM software, with different milling strategies for finishing of a complex part shown in Figure 4. This complex part was designed specifically for this purpose.

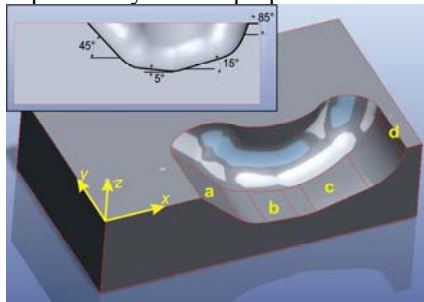


Figure 4. Complex geometry part

On the displayed complex shape part four flat segments can be noticed, marked with letters *a*, *b*, *c* and *d*, which are at a certain angle relative to the horizontal plane, i.e. at angles of 45°, 5°, 15° and 85°, respectively. In addition to these flat segments, on the complex part can also be noticed the concave and convex segments, however in this paper they will not be analyzed.

When designing a complex shape part, angles of 5° and 85°, which flat segments makes with the horizontal plane, were chosen because of technological requirements in the mold making industry. The angles 15° and 45°, that correspond to the segments *a* and *c*, were chosen as the angles which are common in the design of complex parts.

Finishing strategies that are applied in generating of NC programs are two raster strategy, *Raster 90°* and *Raster 0°*, and two offset strategy, with constant axial step and with variable axial step. These strategies have been chosen for analysis as some of the most commonly used strategies. The machining time for all of the four strategy has been set as approximately equal.

When using the strategy *Raster 90°*, the tool is moving in a straight line in the direction of the *y* axis, in the *x*-axis direction tool is moving with a constant step of $x=1,2mm$, while in the direction of the *z*-axis the tool follows the contour of the workpiece. In the case of the *Raster 0°* strategy, the only difference compared to the *Raster 90°* is the direction of linear movement, which is now in the direction of the *x*-axis.

In the *Offset* strategy with $z=const.$, the tool follows the contour of complex surface in *x-y* plane, while in *z*-axis direction tool moves with constant steps of $z=0,7mm$.

The most complicated of the four observed strategies is the *Offset* strategy with $z \neq const.$ In this case the tool also follows the contour of the complex surface

in *x-y* plane while the *z* coordinate is constantly corrected depending on the form of the complex surface. Correction of the *z* coordinates is enabled by the application of CAM software, which on the basis of the workpiece CAD model determines the necessary step in the *z*-axis direction for each tool pass.

These four parts shown in Figure 5. were made on the CNC milling machine DECKEL MAHO FP6-100. The blanks were made of AlMg4,5Mn. Cutting data used in the machining of the parts is: ball end mill $\square 16mm$, tool rpm. $n=4500 rev./min$, speed $v=500 m/min$.

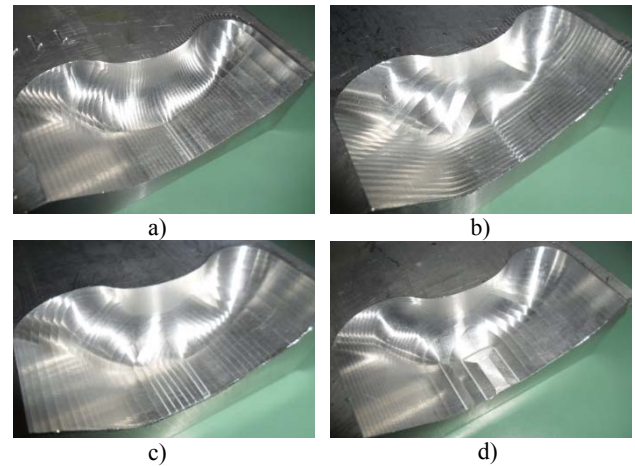


Figure 5. Parts made with appropriate machining strategies: a) *Raster 90°*; b) *Raster 0°*; c) *Offset z=const.*; d) *Offset z≠const.*

The measurements of the flat segments are conducted using the device for measuring of surface roughness Taylor – Hobson, Form Talysurf¹ (Figure 6).



Figure 6. Device for the roughness measuring Taylor–Hobson, Form Talysurf

Figure 7 shows the roughness of the flat surface "a" created with strategy *Raster 0°*, and obtained using the device for roughness measuring.

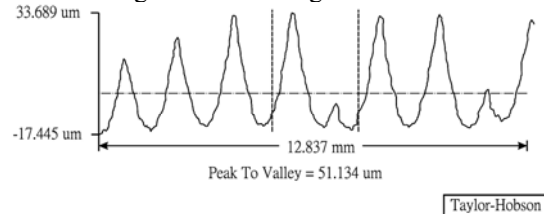


Figure 7. The scanned roughness of the flat surface "a" created with strategy *Raster 0°*

The procedure of roughness scanning of the flat surface was conducted for all four workpieces shown in Figure 5, and the maximum values of roughness for each flat surface are shown in Table 1.

¹A device for roughness measuring Taylor-Hobson, Form Talysurf is located in the measuring lab of company FKL from Temerin.

No.	Strategy	Maximum roughness of flat surface [μm]			
		<i>a</i>	<i>b</i>	<i>c</i>	<i>d</i>
1.	<i>Raster 90°</i>	48,246	53,306	50,088	38,320
2.	<i>Raster 0°</i>	51,134	51,964	45,042	23,724
3.	<i>Offset z=const</i>	38,125	22,783	25,231	24,046
4.	<i>Offset z≠const</i>	18,936	/	122,80	10,612

Table 1. The values of the maximum surface roughness of machined surfaces, depending on the finishing strategy

Analyzing the values presented in the table above it can be concluded that, depending on the different machining strategy, different values of maximum roughness are obtained for the same flat surface.

It should also be noted that, when machining the surface *b* with strategy *Offset z≠const.*, maximum roughness is very large, and its value comes out of the measuring range of the roughness measuring device, which to some extent can be noticed from the picture 5d.

4. CONCLUSION

In the machining of complex shape parts, i.e. molds for plastic injection or blow molding, it often happens that after machining it is required to manually polish the machined surface so as to achieve the required roughness. With the adequate selection of machining strategies, it is possible to minimize or even completely eliminate these subsequent finishing operations, and thereby to significantly reduce time and overall costs.

The paper analyzed the impact of the chosen machining strategy on roughness of flat surfaces machined with the ball end mill. For this purpose, a complex shape part, on which we can point out the four flat segments, was fabricated with four different machining strategy. Then, on the each sample, maximum surface roughness of flat surfaces was measured.

Since each of the machined flat surface is under some angle to the horizontal plane, it can be concluded that for relatively small values of this angle (surface *b* and *c*) the smallest roughness is obtained during application of *Offset z=const.* machining strategy, while for larger values of the angle of surface inclination (surface *a* and *d*) minimum roughness is obtained by applying strategy *Offset z≠const.* Machining strategies *Raster 90°* and *Raster 0°*, in comparison to the offset strategies, are not suitable for the machining of flat surfaces with ball end mill tool.

However in order to completely bring the conclusions on the possibilities of implementation of selected strategies in machining of complex shape parts, it is necessary to conduct an analysis of their influence on the roughness of concave and convex surfaces, which is the main direction of future research.

Acknowledgement: This paper presents a part of the research results on the project "Contemporary Approaches in the Development of Special Solutions Bearing in Mechanical Engineering and Medical Prosthetics", TR 35025, financed by the Ministry of Education and Science of the Republic of Serbia.

5. REFERENCES

1. Janák, M.: *Manufacturing Strategies In CAM Systems*, 7th International Multidisciplinary Conference, Baia Mare, Romania, May 17-18, 2007, pp. 291-295, ISSN-1224-3264
2. Novak-Marcincin, J., Janák, M., Novakova-Marcincinova, L., Fecova, V., Barna, J.: *Application Of The Computer Aided Selection Of Optimal CNC Milling Strategy*, 34th International Conference On Production Engineering, 28.-30. September, 2011, Niš, Serbia, pp. 181-184, ISBN: 978-86-6055-019-6.
3. Novák-Marcinčin, J., Janák, M.: *Software Support For Selection Of Suitable Milling Strategy*, Scientific Bulletin, Serie C, Volume XXIII, Fascicle: Mechanics, Tribology, Machine Manufacturing Technology, pp. 119-122, ISSN 1224-3264
4. Ramos, A.M., Relvas, C., Simoes, J.A.: *The influence of finishing milling strategies on texture, roughness and dimensional deviations on the machining of complex surfaces*, Journal of Materials Processing Technology 136, Elsevier, 2003, pp.209-216, ISSN: 0924-0136.
5. Liua, N., Loftusa, M., Whitten, A.: *Surface finish visualisation in high speed, ball nose milling applications*, International Journal of Machine Tools & Manufacture 45, 2005, pp.1152-1161, ISSN: 0890-6955.
6. Wang, J., Armarego, E.J.A.: *Computer-Aided Optimization Of Multiple Constraint Single Pass Face Milling Operations*, Machining Science and Technology, Vol. 5/1, 2001, pp. 77-99, ISSN: 1532-2483.
7. Zhang, C., Guo, S., Zhang, H., Zhou, L.: *Modeling and predicting for surface topography considering tool wear in milling process*, The International Journal of Advanced Manufacturing Technology, Springer-Verlag, London, 2013, ISSN:1433-3015.
8. Waurzyniak, P.: *CAD/CAM Software Drives Innovation*, Manufacturing Engineering Magazin, SME Editor, Dearborn, MI, USA, February 2010, pp. 47-55.
9. ZW3D Base: <http://help.zwsoft.com/en/zw3d/articles/article-734.html>, Accessed 26.04.2014.
10. SURFCAM 3-Axis:http://www.surfware.com/surfcam_design_3_axis_velocity.aspx, Accessed 29.04.2014.
11. Ramos, A.M.: *Surface Partitioning for 3+2-axis Machining*, Doctoral dissertation, University of Waterloo, Waterloo, Ontario, Canada, 2007.

Authors: M.Sc Cvijetin Mladenović, M.Sc Nikola Kalentić, Prof. dr Milan Zeljković, Prof. dr Slobodan Tabaković, University of Novi Sad, Faculty of Technical Sciences, Institute for Production Engineering, Trg Dositeja Obradovica 6, 21000 Novi Sad, Serbia, Phone.: +381 21 450-366, Fax: +381 21 454-495.

E-mail: mladja@uns.ac.rs, nikolakalentic@yahoo.com
milanz@uns.ac.rs, tabak@uns.ac.rs



Ješić, D., Pulić, J., Kovač, P., Savković, B., Kulundžić, N.

APPLICATION OF NODULAR CASTINGS IN THE MODERN INDUSTRY OF TRIBO- MECHANICAL SYSTEMS TODAY AND TOMORROW

Received: 16 January 2014 / Accepted: 14 February 2014

Abstract: Contemporary technology in mechanical engineering and modern industry makes use of many materials that possess specific characteristics, for example, materials that are resistant to wear and with particularly high durability properties. Such a rare combination of properties like the great durability, toughness and wear resistance is contained in the bainite- austenitic structure of the nodular casting. This enables great economizing possibilities by replacing of steel materials with isothermally upgraded nodular castings. The paper gives an example of the application of isothermally upgraded nodular castings in machine-made constructions.

Key words: nodular cast iron, bainite, austenite, wear resistance, toughness

Primena nodularnog livenja u savremenoj industriji tribomehaničkih sistema danas i sutra. Sadašnji inženjering u mašinstvu i modernoj industriji mnogo koriste materijale koji imaju specifična svojstva, na primer materijale koji su otporni na trošenje i koji sadrže naročito visoku izdržljivost. Ova retka kombinacija svojstava kao i velika izdržljivost, žilavost te velika otpornost na habanje sadržana u bainitno-austenitnoj strukturi nodularno livova. Postoje velike mogućnosti uštede pri zameni čeličnih materijala izotermički poboljšanim nodularnim livovima.

U radu je dat primer primene izotermičkog poboljšanog nodularnog liva u mašinskim konstrukcijama.

Ključne reči: nodularni liv, bainit, austenit, otpornost na habanje, čvrstoća

1. INTRODUCTION

Nodular cast iron is a new structural material that replaces carbon steel, gray and tempered cast iron, since this material is suitable for made out thin wall castings, and castings weighing up to 150,000 N as well [1].

Nodular cast iron with respect to the exploitation properties has wide application in the motor industry, agricultural machinery, ship building, power industry and rolling stock industry. It is suitable for producing loaded machine elements, e.g. crankshafts, piston rod, camshaft rod, various housing of turbines and pumps, etc...

Especially tough (modular) iron is for years used instead of cast iron and cast steel for a given range of structural elements, however, only in 1976 The General Motors Co. (USA) first announced that hypoid gear, its drive gear and its pinion differentials in some vehicles are manufactured from isothermal improved ductile iron instead of, as hitherto, cement steel (cementing and tempered). For the gear is required mechanical properties combination as following:

- high tensile strength
- good dynamic toughness
- high resistance to wear,
- good ductility and impact resistance (toughness) [2]

The Switzerland renowned manufacturers Sulzer and Georg Fischer developed each, their quality ductile iron heat treated on the bainite based structure with a relatively high proportion of retained austenite. In a joint research project of BMW Munich Institute for Research of gear of the Technical University of Munich and Switzerland Company Georg Fischer examines the application of the cast austempered ductile iron gears

and other automobile parts.

In the last ten years in the world is also a trend of expansion of austempered ductile iron in modern means of transport that can meet the demands of highly dynamic loaded elements.

In this way, performed is the substitution of forgings, rolled steel sections and steel castings - with corresponding savings in production costs and increase productivity.

2. PROPERTIES AND THE COMPARATIVE VALUE OF DIFFERENT NODULAR CAST IRONS

Properties of ductile cast iron priority depend on the structure of the metal base, as well as the quantity, size, layout and shape of nodular graphite inclusions. Side effects of graphite are explained in that the inclusions of graphite, because of its low mechanical properties, acting as many micro-notches which generate significant strain in the stress concentration and thus reduce the overall strength.

Increase of the strength and the other properties of ductile iron explains the facts, however, that graphite inclusions in the metal base form "nodules" (spherical or spheroidal shape) reduce the stress around inclusions of graphite nodules, and that this form of graphite has the lowest ratio of surface to the volume and has the graphite content at least a certain cross-section weakening.

As in, cast iron chemical composition is a very important factor that determines the properties of ductile cast iron, because the composition of the associated changes in the shape of graphite and metal base. In addition, a greater influence on the mechanical properties of nodular iron shows the structure of the metal

base and impact of the carbon inclusions is smaller than gray cast iron with lamellar shape graphite.

Due the structure, in addition to the cooling speed, is dependent on the concentration of certain chemical elements the previous test are carried out in order to determine the most appropriate amount of the individual chemical components in the nodular cast iron.

2.1 The default value

For comparative values it is important to mention standard of prescribed sizes and quantities obtained in the

tests performed and the literature data. It is necessary to analyze the structure of the metal base upon which depends properties like: strength, plasticity, but certainly shape, size and distribution of graphite nodules have a significant impact.

In Table 1 are standards values are given:

- mechanical properties are not related to the wall thickness more than 100 mm
- these values are obtained in a test specimens with a V notch at an ambient temperature ($23 \pm 5^\circ$)

Mechanical properties							
Type	Tensile strength R _m min N/m ²	Conventional tension load R _{p0.2} min	Percentage elongation after break	The minimum value of energy impact		Approximate value of hardness HB	The primary structure
				Average values of three tubes	Individually		
EN-GJS-350-17	370	230	17	13	11	do 179	ferit
EN-GJS-400-12	400	250	12	-	-	do 201	ferit
EN-GJS-500-7	500	320	7	-	-	170 do 241	ferit+perlit
EN-GJS-600-3	600	370	3	-	-	192 do 269	ferit+perlit
EN-GJS-700-2	700	420	2	-	-	229 do 302	perlit
EN-GJS-800-2	800	480	2	-	-	248 do 352	pearlite or tempered structure

Table 1. The mechanical properties of nodular cast iron obtained by testing specimens made of enough cast samples [3]

Ductile castings	Chemical composition in %							
	C	Si	Mn	Mg	P	S	Cu	N
EN-GJS-400-12	3.62	2.52		0.28	0.020	0.006		
EN-GJS-500-7	3.85	2.9	0.076	0.035	0.025	0.03		1.5
EN-GJS-600-3	3.67	3.2	0.59		0.025	0.04	1.38	
EN-GJS-700-2	3.76	2.35	0.51		0.020	0.004	1.48	

Table 2. Chemical composition of the tests specimens

Material	Tensile strength	Yield strength	Elongation after rupture	Constriction after tearing Z	Hardness HB	Impact fracture store K
EN-GJS-400-12	421 N/mm ²	286 N/mm ²	22%	19%	150	15 J
EN-GJS-500-7	485 N/mm ²	336 N/mm ²	20,6%	18,9%	186	16,6 J
EN-GJS-600-3	596 N/mm ²	378 N/mm ²	8,9%		270	12,6 J
EN-GJS-700-2	699 N/mm ²	425 N/mm ²	4,8%		320	

Table 3. Investigating the mechanical properties [4]

3. ISOTHERMAL HEAT TREATMENT OF QUENCHED AND NODULAR CAST IRON

The heat treatment is carried out isothermally so that the specimen from the austenite temperature is quenched to temperature of the isotherm which is higher than the temperature of onset of the martensite. Holding at a temperature T_i until it reaches the desired conversion, and then is cooled in air. The aim is to avoid the conversion of the austenite into merrtelzhit because it causes stress and cracking in the material.

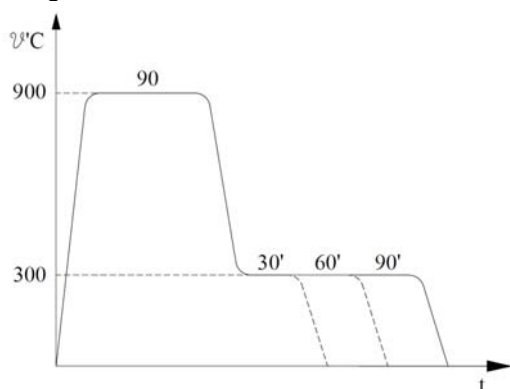


Fig. 1. Diagram of austempered specimens

Holding on the temperature T_i so-called inter bainite structure is produced. It gives the extremely good mechanical properties. Isothermal heat treatment was carried out in the Laboratory for the heat treatment of the Faculty of Mechanical Engineering and Naval Architecture in Zagreb.

3.1. The essential characteristics and comparative review of the microstructure and mechanical properties of standard quality of austempered nodular cast iron parts

The mechanical properties depend on the structure of the material. One pearlitic ductile iron EN-GJS-700-2 prior isothermal heat treatment has the microstructure whose base consists of pearlite and in it are distributed graphite nodules.

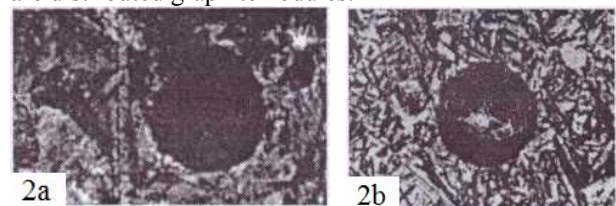


Fig. 2a. Nodular cast iron EN-GJS-700-2 with predominantly pearlite basis, Fig.2b. after isothermal improved (increased 200x)

Figure 2b shows that the amount of retained austenite is relatively high (between 20 and 40%). The austenite contributes to high toughness and ductility of austempered ductile iron. It may be, by cold forming, convert to martensite, which brings another favorable characteristic of the material, namely, it is the ability to improve on after the heat treatment in addition by the specimen surface treatment (e.g. blasting). This way it is possible to further increase the hardness of the surface and hence the wear resistance, and so created the exact tension in the surface layer, significantly increased fatigue strength.

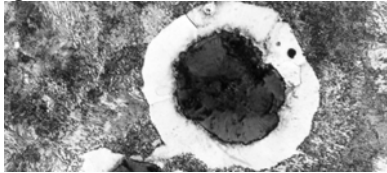


Fig. 3a. Ductile iron EN-GJS-700-2 predominantly pearlite basis (up to 500x).

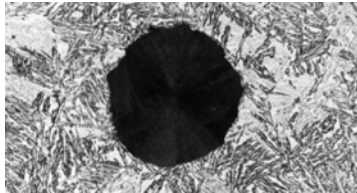


Fig. 3b. Ductile iron EN-GJS-700-2 predominantly pearlite basis upon isotherms improvement (increase 500x), (bainite-austenitic structure with a 100mm thick wall, upper bainite with 35% retained austenite, recorded by optical microscopy)

The measured yield strength $R_p 0.2 = 741 \text{ N/mm}^2$, tensile strength $R_m = 1043 \text{ N/mm}^2$, elongation after rupture

$A_5 = 9.6\%$, the hardness of 320 HB, impact fracture store at room temperature 11.2 J at $0^\circ \text{C} = 9.8 \text{ J}$ with -40°C $J = 7.7$, percentage of retained austenite 37%.

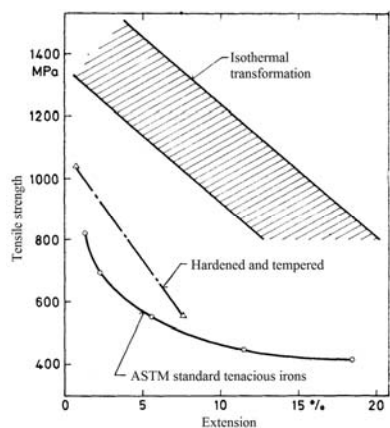


Fig. 4. Comparison of mechanical properties of standard quality nodular cast iron and austempered ductile iron castings

Figure 4 shows austempered ductile iron, which can achieve purity value of two times of the standard nodular irons, with the same ductility - in this case, extension (%). This is its important characteristics and advantages. By changing the temperature of austempering may mechanical properties vary in a rather wide area [5].

4. POSSIBLE SAVINGS IN THE USE OF AUSTEMPERED DUCTILE IRON

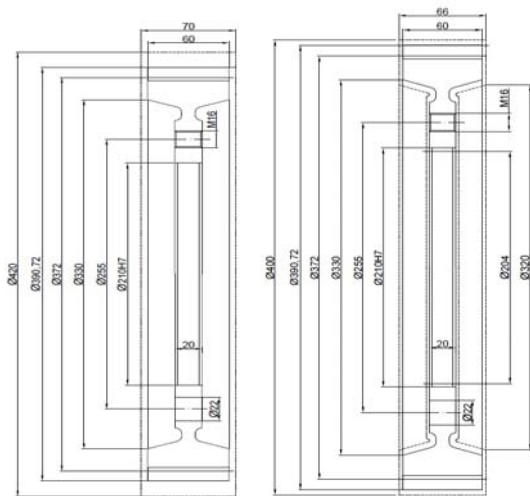
There are several views regarding the possible savings and exploitation if they are compared with isothermal steel materials with austempered ductile iron:

- Energy savings
- Savings due to casting approximately the final form
- Savings due to better workability
- Savings due to the lower density of ductile iron

4.1. Case study of use of austempered nodular cast iron in mechanical structures

Figure 4 show that the austempered ductile iron has a higher level of fracture toughness than conventional quenched and tempered ductile iron for all hardness values. At higher levels of hardness, austempered ductile iron has a fracture toughness which can be compared with fracture toughness of cast steel (quenched and tempered). Its fracture toughness is lower than the fracture toughness of steel forgings (quenched and tempered) in the longitudinal direction and is equal to or greater than the fracture toughness of steel forgings in the transverse direction for the lower and middle levels of hardness [6].

In isothermal improving obtain spheroidal graphite cast iron structure of bainitic ferrite and coarse carbon-saturated austenite (upper bainite) with a hardness of 30 to 37 HRC and the hardness (lower bainite) is in ranges from 43 to 50 HRC.



Rolled steel Steel 20MnCr4 (3 E/kg)

228.3 E/pc

Mass for ball: 76.1 kg

The mass of gears: 20.1 kg

The mass of material Roughing: 55 kg

Scabblers: 12h x 16.6 E/h 199.2 E/pc

Heat treatment (cementing): 26.8

E/items Total: material + roughing +

TO = 454.3 E/pc

Austempered ductile iron (3.9 E/kg)-1

7.4 E/pc

Mass for ball: 30.1 kg / pc

The mass of gears: 20.1 kg / pc

The mass of material Roughing: 9 kg

Hard mechanical treatment: 1.3h x

16.7E/h=21,72 E/pc

Heat treatment: 13.4 E/pc

Total: material + roughing + thermal

processing = 155.82 E/pc

Fig. 5. Compare the cost of the gear vibrating roller ($D_v = 390 \text{ mm}$, $b = 60 \text{ mm}$; module $m = 6$) made from 20MnCr4 and from austempered ductile iron

Figure 5 shows the sketch of the vibrating roller gear ($D_v = 390 \text{ mm}$ $b = 60 \text{ mm}$, module $m = 6$) and the corresponding semi-manufacture, made of low-alloy steel rods for cementing 20MnCr4, or from

austempered ductile iron and a rough comparison of the cost per piece. The total savings in this case are resulting in savings of the amount of material used, the savings in machining and saving of heat treatment [7].

4.2 There is the possibility of a wider application of nodular irons



Fig. 6. Shows the timing gears for diesel engines made from austempered ductile iron EN-GJS-700-2 initial pearlite basis

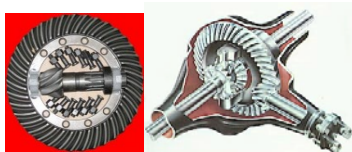


Fig. 7. Gears for drive of a passenger car axle with transverse-engine and the longitudinally-engine made of isothermal improved irons EN-GJS-700-2



Fig. 8. Teering gear of the planetary gear transmission with inner gear and made of austempered ductile iron EN-GJS-700-2

5. CONCLUSION

Previous research and application examples show that the isometric improving ductile iron can produce a structure (a mixture of bainitic ferrite and austenite is enriched with carbon), which along with high wear resistance (with high strength) has great ductility and toughness. It is, therefore, no conventional annealing, ie. martensitic transformation to get material that matches the high demands in parts of the inverted impact, fatigue and spending.

The first success prerequisite with austempered ductile iron is certainly a good and constant (standard) quality of ductile iron. The most important requirements for its structure are: to be free of inclusions and micro porosity, have a sufficient number of the uniformly distributed graphite balls (nodules), and that there is no segregation of manganese. [8]

The second a prerequisite to success is accurate and repeatable process control of isothermal heat treatment. To specifically selected composition of ductile iron, thickness of the parts and the required mechanical properties it is necessary to optimize and control the process parameters [9].

For wider application of an isometric improved ductile iron it is necessary in practice, on the one hand, a lot of data on mechanical properties for a specific

composition and the specific conditions to improve the material - which is possible to obtain its own research.

With the dear side, it is in the constructor and technologists during designing and manufacturing organizations to develop a sense of these and give them the appropriate methods and media for it. In this regard, long-term collaboration between production organizations and relevant research institutions can be of great benefit.

6. REFERENCES

- [1] Shiokawa T.: Production in Austempering of Ductile Iron Castings, Proceedings of the 1st International Conference on Austempered Ductile Iron, ASM, 1984., 107-115.
- [2] Kalevi J.: Kymenite Austempered Ductile Iron - a Material for Gears and Other Applications, Proceedings of the 1st International Conference on Austempered Ductile Iron, Chicago 2-4 April ASM, 1984, 135-148
- [3] Ješić D.: Tribološki aspekti i primjena nodularnih lijevova za izradu dijelova alatnih strojeva, Doktorska disertacija, Skopje 1995.
- [4] Golubović D., Kovač P., Ješić D., Gostimirović M., Pucovski V.: Wear Intensity of Different Heat Treated Nodular Iron, Metalurgija, 2012, Vol. 51, No 4, pp. 518-520
- [5] Golubovic D., Kovač P., Jesic D., Gostimirović M.: Tribological properties of ADI material, Journal of the Balkan Tribological Association, 2012, Vol. 18, No 2, pp. 165-173
- [6] Sukru Ergin Kisakurek, Ahmet Ozel: Unnotched Charpy Impact Energy Transition Behavior of Austempered Engineering Grade Ductile Iron Castings, Metallurgical and Materials Transactions B, 2013, DOI: 10.1007/s11663-013-9976-8, pp1-10
- [7] Cheng-Hsun Hsu, Tao-Liang Chuang: Influence of Stepped Austempering Process on the Fracture Toughness of Austempered Ductile Iron, Metallurgical and Materials Transactions A, Volume 32A, 2001, pp 2509-2514,
- [8] Voigt R.C., Loper C.R.: Austempered Ductile Iron – Process Control and Quality Assurance, Journal of Materials Engineering and Performance, Volume 22(10), 2013, pp. 291-309
- [9] Rajnovic, D., Sidjanin, L.: The ductile to brittle transition temperature of unalloyed adi material, Journal of Production Engineering, Volume 16 (1), 2013, pp 69-72

Authors: Prof. Dusan Ješić PhD¹, Josip Pulčić², Prof. Pavel Kovac PhD³, Assist. Borislav Savkovic, M.Sc.³, Kulundzic Nenad, M.Sc.³

¹Tribotehnik, Croatia, Titov trg 6/4, 51000 Rijeka

²Veleuciliste u Rijeci, Vukovarska 58, 51000 Rijeka

³University of Novi Sad, Faculty of Technical Sciences, Institute for Production Engineering, Trg Dositeja Obradovica 6, 21000 Novi Sad, Serbia, Phone.: +381 21 450-366, Fax: +381 21 454-495.

E-mail: pkovac@uns.ac.rs, savkovic@uns.ac.rs
nenadts@gmail.com

Note: This paper presents a part of researching at the CEEPUS project and Project number TR 35015.

Živković S.

PROFILING OF MANDREL FOR ROTARY FORGING

Received: 18 May 2014 / Accepted: 12 June 2014

Abstract: This article explains complete procedure of profiling and quality control on mandrel for gun barrel cold hammering. Gun barrels are produced on GFM machine by technique of Rotary Forging. The mandrel is the most significant element for final quality of gun barrels. Paper present one original developed technology method and quite different from the method used in Zastava Arms factory. Paper explains mandrel profiling on CNC grinding machine with two simultaneously controlled linear and one rotary axis. The developed method enables grinding mandrels, not only on machines specialized for that purpose.

Key words: Gun barrel, Rotary Forging, Grinding, CAD/CAM

Profiliranje trnova za rotaciono kovanje. U članku je prikazan celokupan tehnološki postupak profilisanja trnova za hladno kovanje cevi streljačkog naoružanja. Cevi streljačkog naoružanja proizvode se na GFM mašinama tehnikom rotacionog kovanja. Kovački trn je ključni element za finalni kvalitet cevi. Prikazano je originalno tehnološko rešenje koje je potpuno drugačije od onoga kojim se izrađuju trnovi u Fabrici oružja Zastava u Kragujevcu. Prikazana je izrada trna na CNC brusilici, sa dve linerane i jednom rotacionom osom, koja primarno nije specijalizovana za ovu namenu.

Ključne reči: Cevi streljačkog naoružanja, Rotaciono kovanje, Brušenje, CAD/CAM

1. INTRODUCTION

Most modern pistols, revolvers, rifles, and some shotgun barrels have what are called **rifling** in their barrels. Rifling consists of grooves cut or formed in a spiral nature, lengthwise down the barrel of a firearm.

Rifling is placed in the barrels of firearms to impart a spin on the bullets that pass through it [1]. Because bullets are oblong objects, they must spin in their flight, to be accurate.

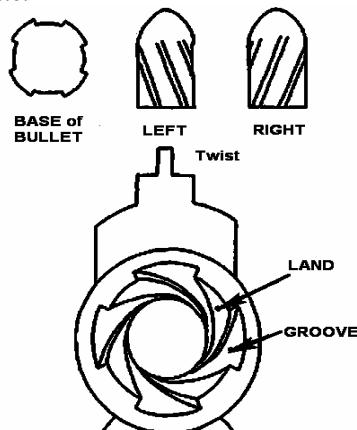


Fig. 1. Gun Barrel Rifling

Figure 1. shows a pattern of rifling containing four grooves with a right twist. In firearm examiner lingo we refer to the rifling as lands & grooves. The lands are the raised areas between two grooves [1]. A rifling pattern of six grooves with also have six lands.

2. RIFLING TECHNIQUE

There are currently three main methods by which rifling is put into the barrel.

Oldest method is the CUT RIFLING technique [1]. Cut rifling creates spiral grooves in the barrel by removing steel using some form of cutter. Up until WW2 rifling was the most time consuming operation in making a rifle.

BUTTON RIFLING is a cold forming process in which a Tungsten Carbide former, which is ground to have the rifling form in high relief upon it, is pulled through the drilled and reamed barrel blank [1]. The lands on the button engrave grooves in the barrel as it is pulled through.

The technique of ROTARY FORGING rifle barrels was developed by Germany before WW2 [2]. In this process the barrel blank is usually somewhat shorter than the finished barrel. It is drilled and honed to a diameter large enough to allow a Tungsten Carbide mandrel, which has the rifling in high relief on it, to pass down the blank. The blank is then progressively hammered around the mandrel, figure 2, by opposing hammers using a process called **rotary forging**. The hammered blank is squeezed off the mandrel like tooth paste and finishes up 30% or so longer than it started [2].

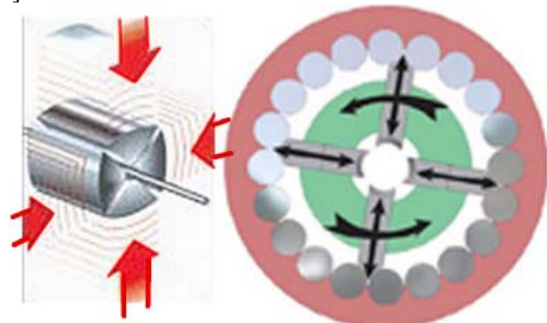


Fig. 2. Rotary forging

3. BASIC ELEMENTS OF MADREL

Mandrel for rotary forging on GFM machine (Gesellschaft Fur Fertigungstechnik und Maschinenbau – GFM - Steyr, Austria) is key element for the barrel quality. Mandrel defined a diameter (caliber) and makes grooves inside the barrel.

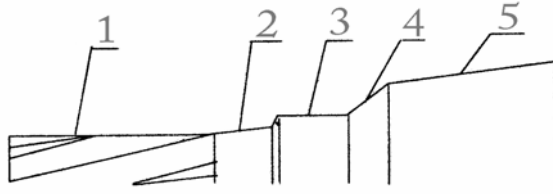


Fig. 3. Mandrel Basic Elements

Typical drawing of mandrel [3] is shown of figure 3. and consists of next elements:

1. Grooves
2. Transition cone
3. Capsule
4. Transition cone
5. Shell casing

3.1. Geometry of the groove

Figure 4. defines a radial section of mandrel. All the drawing section have same shape, but different angular position and different dimensions.

That difference defines a pitch of grooves, and lead varies from 250mm to 400mm. Mandrel have between 4 and 8 grooves, depending on caliber: for example

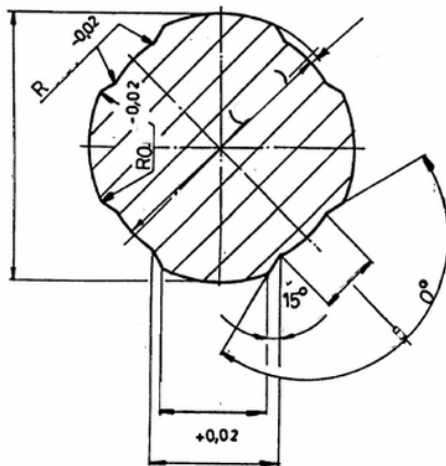


Fig. 4. Geometric Definition of the Groove

Cal. 5.56 → 4 grooves; Cal. 7.62 → 6 grooves; and Cal. 13 → 8 grooves. Depth of grooves is between 0.100mm and 0.150mm.

Differences in dimension define forging cone, and angle is approximately between 10 and 20 angular minutes. Tolerances for all section are very narrow: $\pm 2\mu\text{m}$.

Mandrel is made from two different material: Holder made from a high alloy Chrome Molybdenum steel, and forging area made from Tungsten Carbide hard metal. The connection is made by soldering process.

Grooves on mandrel are made by grinding; using profiled artificial diamond disk (fineness 0.5 – 0.8 carat) with Bakelite or metal connective.

To get spiral-shape it is necessary three simultaneous motions: two linear and one rotary. In addition, is necessary put profiled diamond disk in starting position-according slope of leading spiral curve. That angle is approximately between 4 and 5 degrees.

4. CAD DEFINITION OF THE MANDREL

All previous analyzed mandrel's drawings have a couple typical errors. Factory's internal instructions [3] have a couple remarks about these errors on the mandrels drawing. Dimensions from barrel drawing are simply copied on the mandrel drawing without taking care about production process. In the Zastava Arms Factory production engineer creates new drawings only for profiling mandrel.

Our approach in solving the manufacturing problem starts from a three-dimensional modeling on CAD/CAM system. Design of parts and components compatible with the principles of total quality management is called "design for manufacturing" [4]. The drawing is just auxiliary information for operator on the machine tool.

We analyzed more than 20 foreign and domestic different mandrel drawings. All looks same one to each other. Obviously, the draftsmen just simple copy a sample, but the wrong one.

On all drawings, sections are shown with deformity. In addition, angular position for all definition section is the same. Reason is very simple, all drawings are made on old-fashion way: using a paper and pencil, view and section explain the model.

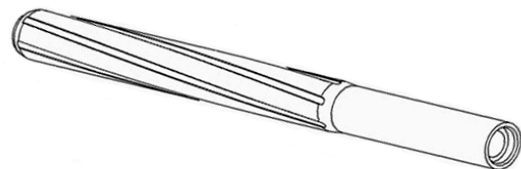


Fig. 5. Mandrel on CAD/CAM system

In the reality, view and section are result of object, not contrary. After creation of 3D model, drawing (with sections and views) is representing the object (mandrel), and some time drawing is unneeded. Modeling (CAD) process must follow production process (CAM). Except the 3D model, we have, also, and graph of creation process. The same logic we will follow during the grinding. All mandrel's drawing shows changes of definition radius of groove (bottom of the groove), by the linear law. To get that, it is necessary to change, all the time, profile of grinding diamond wheel. In the reality, it is not possible. That request is illogical.

Figure 5. displays the correct 3D model model of mandrel. One definition section from drawing "travel" along spiral curve (line wrapped around cone).

Choosing a middle section (between typical AA and BB section on mandrel's drawing) you made an error

smaller than $1\mu\text{m}$. For profiling diamond disk it is necessary to choose section perpendicular to spiral curve. That is a conic section, and profile of wheel is a part of ellipse. None of analyzed drawing not pay attention on previous remarks.

5. PREPARING GRINDING WHEEL

Two diamond disk, one for rough and another for finishing are mounted on same holder, figure 6. Cutter for this profiling is natural diamond, mounted on special holder. CNC program for profiling and sharpening is write according definition profile but in mirror position. In addition, you need very sensitive sensor for contact artificial diamond wheel and natural diamond. Temperature is very high even for small cutting depth ($1\mu\text{m}$). Holder of natural diamond needs a lot of cooling water and that's reason for cooling ON.



Fig. 6. Profiling of Grinding Wheel

Diamond disk geometry check done on coordinate measuring machine according to the CAD/CAM computer model. Figure 7. shows the measured points and theoretical profile of the grinding wheel.

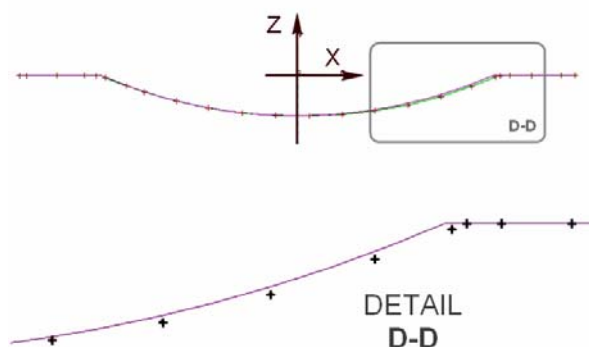


Fig. 7. Measured geometry of the wheel

Small crosses in figure 7 represents measured points are obtained using a touch trigger contact probe on the coordinate measuring machine [4]. Measured profile obtains using least square method thru measured points.

The figure 7 shows that the measured profile wheels good, but that translated aside in relation to a given axis of symmetry. It is necessary that the correction re-profiling to achieve the required accuracy of the shape

and position profile diamond grinding wheels.

The measurements were made at the CMM with MPE-E (MPE=Maximum Permissible Error, E = Volumetric Length Measuring Uncertainty) declared according to ISO10360, are given by equation (1).

$$MPE_E = \pm 2 + L / 400 \text{ } [\mu\text{m}] \quad (1)$$

L [mm] representing length of measuring. In this case diameter of the wheel is 40mm. CMM meets the required accuracy for measuring this class of problems.

6. MANDREL PROFILING

After completely very complex preparation, CNC controlled grinding machine with two linear (X & Y) and one rotary motion (B) is ready to start. Diamond wheel is incline and contact point at the same level like axis of rotation.

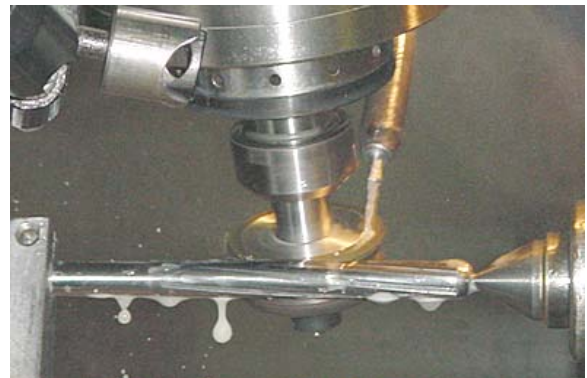


Fig. 8. Mandrel on CNC grinder

All the necessary is shown on figure 7: numerically controlled two linear and one rotary axis, cooling system and piesosensor for checking contact between wheel and mandrel.

CNC program, created on CAD/CAM system used to profiling mandrel. For caliber 5,56mm CNC program is listed below [5]:

```

N01 (Cal      5.56x45      6      grooves
Pitch=178mm)
N05 G90 T1 F800 M8 M3
N06 G78
N10 G00 X40.0 Y-30.0 B0.0
N15 G71 L100
N20 G00 B60.0
N25 G71 L100
N30 G00 B120.0
N35 G71 L100
N40 G00 B180.0
N45 G71 L100
N50 G00 B240.0
N55 G71 L100
N60 G00 B300.0
N65 G71 L100
N70 G00 B0.0
N71 G79
N75 M05
N80 M02
N100 G01 X40.000 Y-27.0
N105 G01 X42.336 Y-25.0

```

```

N110 G01 X42.380 Y-2.800 F50
N115 G41 X-0.750 Y-2.779 B:87.229
F800
N120 G01 X-20.750 Y-2.769
N125 G01 X-20.764 Y-30.000
N130 G00 G40 X38.0 Y-25.0 B:-27.229
N135 G72

```

CNC program start first with rough wheel, for each groove separately. Program repeats whole cycle between 40 and 50 times, depending of total depth.

Cutting depth is 2 - 3µm for each pass and for finishing, rest approximately 1/100 mm. Final, requested dimension, CNC program reach in 5 – 6 times up to 2µm. Next 5 – 6 times program repeat all position with same radius compensation of wheel until no sound signal from contact piesosensor.

7. MEASURING GEOMETRY AND ROUGHNESS

Inspection of geometry includes checking depth of grooves and roughness. Shape of grooves directly depends of the shape of diamond grinding wheel, which previously measured on CMM, figure 7. Depths are measured directly on grinding machine. Figure 9 shows measuring depth of the groove using instrument with 1µm accuracy.

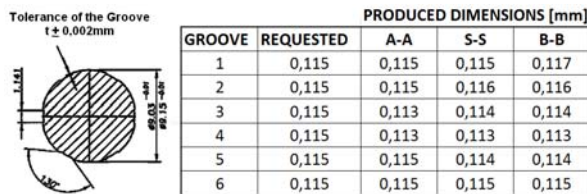


Fig. 9. Inspection report for individual mandrel



Fig. 10. Measuring depth of the groove

In figure 10. shows roughness measuring. Polish using cork disk give roughness smaller than 0.1µm.

Final report, for end user, is shown on figure 11. Final report is joining for each mandrel separately. It also includes all relevant information: dimensions, depths of groove and profile of groove, surrounding temperature, etc. Actual quality of the mandrel will copy on the whole series of barrel.

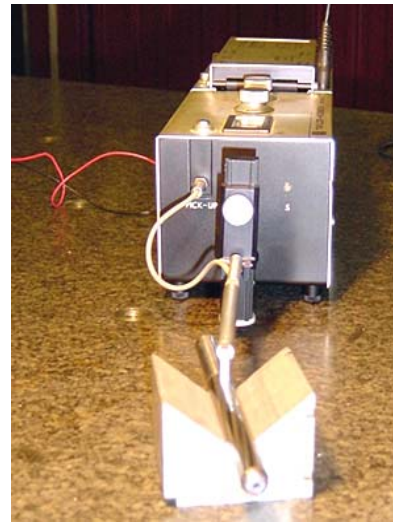


Fig. 11. Roughness measuring of the groove

8. CONCLUSION

This article on a few pages explains, actually, very complex procedure. You need also, high-skill workers, sophisticated equipment's and high-end CAD/CAM/CAE system.

All elements existed in Serbia more than twenty years, but sometime producers (factories) have lot of inertia to speed-up production process. Reasons are very different: inertia of engineers and managers due to monopoly position on market, misunderstanding new software and hardware product, ect.

The developed method enables grinding mandrels, not only on machines specialized for that purpose.

9. REFERENCES

- [1] Geoffrey Kolbe: *The Making of a Rifled Barrel*, www.FirearmsID.com Feature Article at the Month, July 2000, link: <http://www.firearmsid.com/feature%20articles/rifle%20barrelmanuf/barrelmanufacture.htm> , Accessed 20. April 2014.
- [2] Vern Briggs and James Higley: *Notes on Hammer Forged Barrels*, Precision Shooting, vol 57 No 3, Manchester UK, July 2008.
- [3] Zastava Arms, *Manufacturing technology of hard metal mandrel for GFM hammering machine, (internal instraction in Serbian)*, Kragujevac Serbia
- [4] Srđan Živković, *Optimizations of free form surfaces measuring using coordinate metrology methods*, Ph.D. thesis (in Serbian), Military Academy, Belgrade 2011.
- [5] Programming Instractions S50L-CNC311/SHZ, HAUSER GmbH, Kühlmöbel & Kältetechnik, Am Hartmayrgut 4-6, A-4040 Linz/Austria, <http://www.hauser.com/>

Author: Dr. Srdjan Živković, Head of Section, Military Technical Institute Belgrade, Ratka Resanovića 1, 11000 Belgrade, Phone: +381 66 872 14 03 Email: srdjan.vti@gmail.com, srdjan_vti@yahoo.com

Topčić, A., Cerjaković, E., Lovrić, S.

ANALYSIS OF DIMENSIONAL DEVIATION OF PARTS BASED ON CERAMIC PRODUCED BY THREE DIMENSIONAL PRINTING PROCESS

Received: 05 June 2014 / Accepted: 20 June 2014

Abstract: Thanks to numerous continuous steps forward and improvements RP processes found more and more applications in daily engineering practice. One of area that has significant potential is direct production by 3DP process of ceramic based tools for casting of nonferrous alloys, also known as a ZCast. Due to the specificity of production of objects by 3DP process there are certain smaller or larger dimensional deviations of produced parts from the original 3D CAD model. In this paper is presented an analysis of dimensional deviations of 3DP parts produced for ZCast application with the aim to determinate value of anisotropic scaling factor and post-processing parameters and achieving of adequate dimensional accuracy of produced 3DP ZCast tools.

Key words: Three Dimensional Printing (3DP), ZCast, heat treatment, dimensional deviations

Analiza dimenzione devijacije delove baziranih na keramici u trodimenzionalnom procesu štampe. Zahvaljujući brojnim kontinuiranim iskoracima i poboljšanjima, rapid prototyping procesi pronalaze više i više primena u svakodnevnoj inženjerskoj praksi. Jedna od oblasti koja ima značajan potencijal je direktna proizvodnja trodimenzionalno štampanih delova od originalnog 3D CAD modela. U ovom radu je prikazana analiza dimenzionalnih odstupanja trodimenzionalno štampanih delova proizvedenih za ZCast aplikaciju sa ciljem da se utvrdi vrednost anizotropnog faktora skaliranja i post-procesiranje parametara i postizanje adekvatne dimenzionalne tačnosti proizvedenih alata.

Ključne reči: Trodimenzionalni štampanje (3DP), ZCast, termičke obrade, dimenzionalna odstupanja

1. INTRODUCTION

Three Dimensional Printing (3DP) process is the one of Rapid Prototyping (RP) processes that due to its characteristics found many opportunities in daily applications. Essentially work of all 3DP systems is based on chemical binding by adhesive liquid medium (binder) of building material – powder, whereby the three dimensional (3D) physical objects are "printed" directly from 3D CAD environment, fig. 1. By this process is possible to create 3D parts with any geometry and form from powder composite materials on the basis of ceramics, metals and polymers.

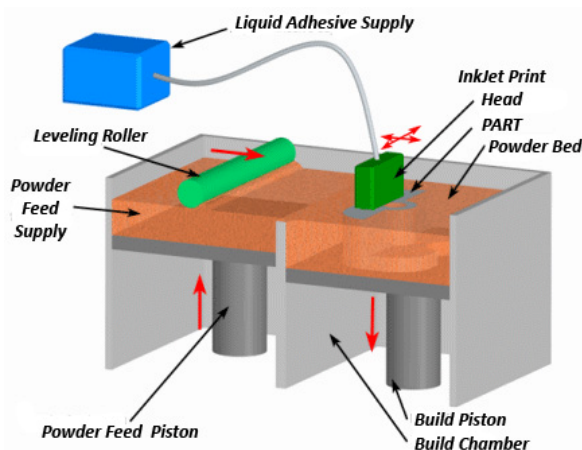


Fig. 1. Working principles of 3DP process [1]

With development of 3DP systems and spreading the range and improving of characteristics of used materials (building materials, binders, infiltrants) besides production of so called non-functional prototypes for validation of ideas and concepts, marketing purposes, or for some other aims implementation of produced 3DP parts as functional ready made parts, as well as, theirs usage as tools for different purposes is enabled. [2]

2. THEORETICAL CONSIDERATIONS

Usage of 3DP parts as tools is mainly oriented toward production of tools for casting, where application of mentioned tools is implemented on one of two ways: indirect - 3DP part (positive) is base for mold production (negative), respectively, direct - 3DP part is ready made mold (negative).

Direct implementation of produced 3DP parts as a casting tools in casting processes is known as ZCast [3] and enable direct production of molds for direct casting of aluminium and other non-ferrous alloys with melting temperature below 1100 [°C]. For production of 3DP parts which will be utilised in ZCast process the following material are in usage:

- powder building material (ZCast501) based on mix of: foundry sand, ceramics, plaster and other additives, with temperature endurance of 1200 [°C]; [4]
- adhesive (binding) material - binder (zb56).

According to the characteristics of building material post-processing treatment is based on depowdering and heat treatment of produced 3DP parts. Given to the purpose of 3DP parts produced for ZCast process it is necessary to provide their adequate geometrical characteristics i.e. dimensions which are within acceptable tolerance area in comparison with dimensions of initial 3D CAD model and casting process. Namely, because of characteristics of building process, the fact that a 3DP ZCast part in its untreated (raw) state contains about 10% moisture per unit weight [4] which during a heat treatment evaporates and because of corrections of path of printing head during the building process (different size of printing point and printer resolutions [5]) there are certain smaller or bigger deviations of dimensions of produced 3DP parts.

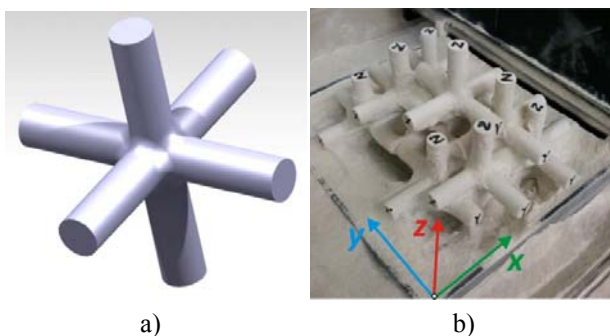


Fig. 2. a) 3D CAD geometry of 3DP test part, b) depowdering of unused building material in working chamber of 3DP machine with associated orientations and designations of test samples

Considering the above mentioned and respecting building direction and part orientation within working chamber during processing of parts it can be expected different deviations of produced parts from the dimensions defined by initial 3D CAD model. The mentioned occurrence is possible to preventive correct by adjusting the parameters of anisotropic scaling of *.st/file of CAD model during the setup of machine. Defining of values of coefficient of anisotropic scaling in direction of three axis within working chamber of 3DP machine (x – direction of movement of printing head holder, y - direction of movement of printing head, z – building direction) as well as defining of overall level of accuracy of produced 3DP ZCast parts is the goal of this paper.

3. EXPERIMENTAL RESEARCH

Analysis of influence of process parameters on dimensional deviations of produced 3DP parts for ZCast process is realised on testing samples with dimensions $100 \times 100 \times 100$ [mm], figure 2.a. presented geometry of adopted testing samples enable orientation of parts according to x , y and z axis that are significant for building process and allow measurement of corresponding dimensional deviations with acceptable production costs. Test samples are produced on machine: z310+, by building material: ZCast501 and

appropriate binder: zb56 (producer for all: Z Corp, USA), with layer thickness of building material 0,125 [mm] and with geometric orientation in direction of x , y and z axis, figure 2.b. With the aim to acquire real deviations of produced 3DP test parts from initial 3D CAD model, production process was realised without compensation and anisotropic scaling, with predefine setup by software of core andshell filler for 3DP test parts built from adopted material.

After production of 3DP parts, post-processing of produced parts in accordance with characteristics of building material (depowdering and heat treatment) was done. Parameters of heat treatment are presented on figure 3.a. Temperature (T) and time of heat processing (t) are adopted in accordance with recommendation of producer of used equipment and materials, $T=180 \div 230$ [$^{\circ}\text{C}$], $t=4 \div 8$ [h], depending on volume of part which ensuring fully drying of part until the part become medium-brown in colour, figure 3.b [3]. For the purposes of analysis 45 test samples was made, i.e. 5 pieces in each point of presented experimental plan.

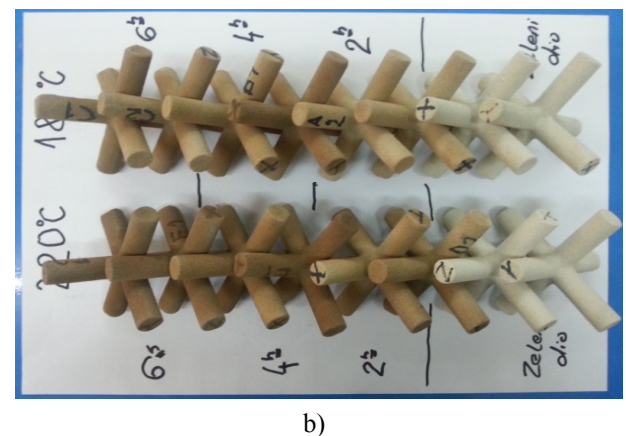
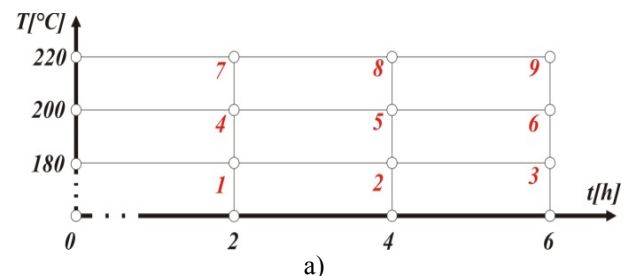


Fig.3. Scheme of experimental plan with post-processing parameters (a) and display of „green“ and heat treated test parts (b)

With the aim to analyse dimensional deviations of produced and post-processed 3DP test parts measurement in direction of x , y and z axis by 3D tactile scanner (figure 4.a) was accomplished. Each direction and each part was measured five times. Measurements of dimensional deviations are realised immediately after heat treatment and after cooling the test parts on room temperature. On the basis of measured data in direction of x , y and z axis and after their systematisation for each of analysed axes, determination of percentage deviation of 3DP test samples from CAD model, and indirect calculation of correction coefficients, which from the point of view of

production of 3DP ZCast parts presents values of anisotropic scaling factor during setup of processing parameters of 3DP machine was done, figure 5.

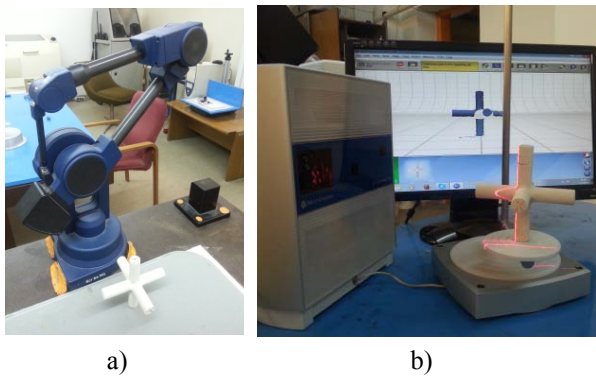


Fig. 4. Measurement of dimensional deviation of produced 3DP test samples: a) 3D tactile scanner MicroScribe MX System, producer: Imersion, USA; b) 3D laser scanner Desktop 3D Scanner HD, producer: NextEngine, USA

Previously introduced approach to analysis of dimensional deviations of produced 3DP test parts enables considerations of general indicators of geometric deviations in direction of x , y and z axis, as well as, determination of recommended values for factors of anisotropic scaling of initial 3D CAD model during the setup of machine. Unfortunately this approach does not indicate on scale of overall geometric deviations of produced parts from geometry of initial „ideal” 3D CAD model. With the aim to determine overall geometric deviations of produced parts from 3D CAD model 3D digitalisation of produced parts (figure 4.b) and CAD inspection of generated and processed cloud of points (figure 6.a) with initial 3D CAD model (figure 2.a) was carried out. By applying of CAD inspection is enabled insight in overall resulting geometric deviations of produced 3DP test parts, whose visualisation of one of analysed cases („green” part – sample 3) is presented on figure 6.b. Review of results of CAD inspection, as well as, comparative values of correction coefficient obtained by tactile scanner – Anisotropic Scaling Factor, for testing points 4, 5 and 6 are presented at figure 7.

4. CONCLUSION

On the basis of measured and systematized data it is possible to perform the following conclusions. Measurements of geometric deviations of produced 3DP test parts in direction of x , y and z axis indicates, in all analysed cases, that „green” part has higher deviations in all directions then heat treated parts. In all analysed cases largest deviation are identified in direction of z axis, while deviations in directions of x and y axis are approximately equal and for circa 50% smaller (figure 8). Furthermore, results of the study indicate that geometric deviations of test parts in direction of x and y axes are increased until the mid-range of heat treatment temperature $T=200$ [°C], i.e. until the mid-

range of time of heat treatment $t=4$ [h] and after that point deviation are decrease. Oppositely in direction of z axis geometrical deviations of test parts in direction of x and y axes are decrease until the mid-range of heat treatment temperature $T=200$ [°C], i.e. until the mid-range of time of heat treatment $t=4$ [h] and after that point deviation are increased. In accordance to that coefficients of anisotropic scaling for all three axes behave inversely (figure 5).

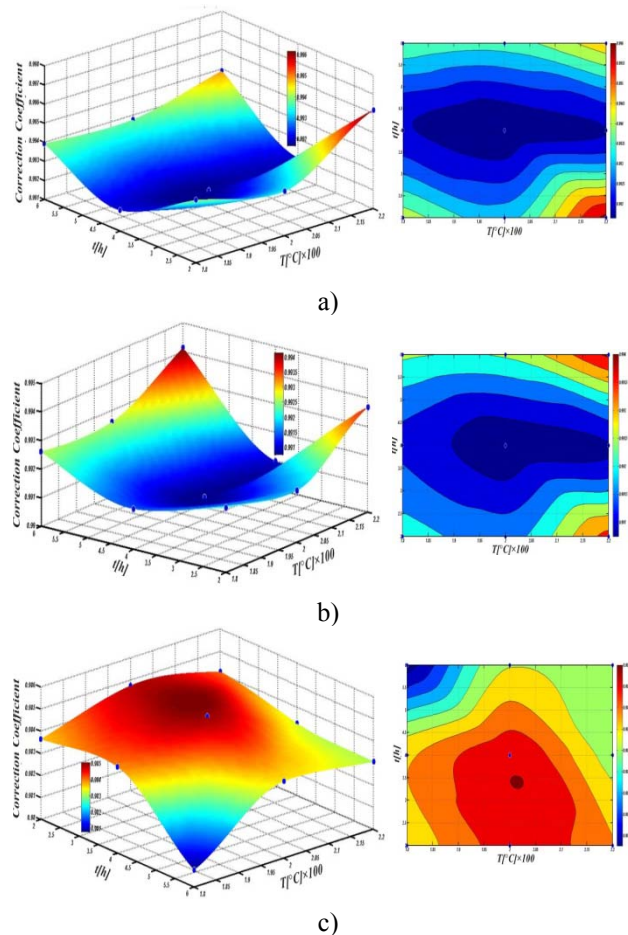


Fig. 5 Values of coefficient of anisotropic scaling for produced 3DP test parts on room temperature for: x axis (a), y axis (b) and z axis (c)

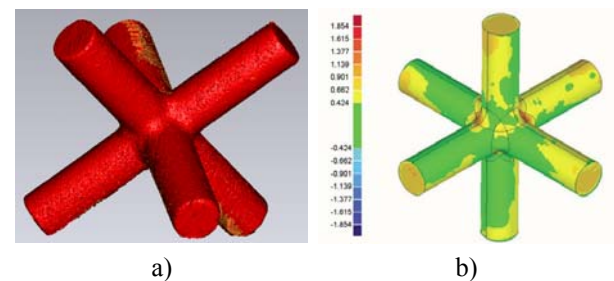


Fig. 6. Processed „cloud of points” (a) and results of CAD inspection in [mm] for „green” part – sample 3 at room temperature (b)

The identified patterns of dimensional deviations of produced 3DP test parts are valid in both cases i.e. measurements immediately after heat treatment and at room temperature. Stated indicates that in terms of dimensional deviations of produced 3DP test parts

should be taken into account the orientation of parts in the working chamber of machine, where if we want to increase the accuracy in the direction of the x and y axes then it is recommended to use the peripheral area, while in the direction of z axis it is advisable to use the area around the centre of the analysed extent of heat treatment parameters.

The obtained results of measurement indicate that minimal deviations of produced 3DP test parts, in comparison with geometric ideal 3D CAD model, corresponding to the values measured immediately after heat treatment. According to this if we want to use produced 3DP parts as ZCast tools, these parts need to be heat treated and be used for casting immediately.

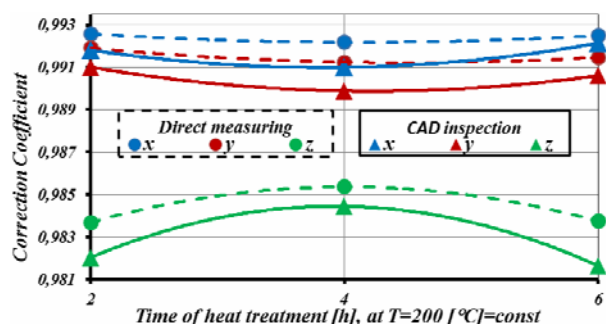


Fig. 7. Comparison of coefficients of anisotropic scaling obtained by tactile scanner and by CAD inspection for experimental points 4, 5 and 6 at room temperature

Results of CAD inspection of produced 3DP test parts completely confirm previous results, with certain smaller deviations, figure 7. Namely, maximal deviations are determinate in direction of z axis, smaller deviation in direction of x and y axis too. It is important to notice that results of geometric deviations obtained by CAD inspection (solid line, figure 7) had slightly smaller values than results obtained by measuring by tactile scanner (dashed line, figure 7). From the point of overall geometric deviations of produced 3DP test parts from initial 3D CAD model, CAD inspection indicate on satisfactory level of parts accuracy from the casting point of view (95,151% of digitalised points is within interval: $-0,376 \div 0,376$ [mm]).

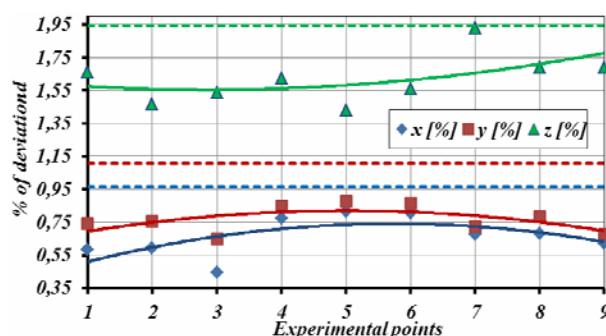


Fig. 8. Geometrical deviations of 3DP test parts for „green” part (dashed lines) and experimental points (continuous lines) measured after heat treatment

Presented results of the experiment indicate that there are certain influence of heat treatment parameters on dimensional deviations of produced 3DP test parts which has different effects in directions of x , y and z axis. Accordingly, with the aim to improve dimensional accuracy of 3DP parts for purposes of ZCast processes it is necessary to take a care about orientation of parts in working chamber of 3DP machine and perform anisotropic scaling of *.stl model with appropriate coefficient depending on heat treatment parameters, i.e summarised presented by average values: 0.993 for x axis, 0.992 for y axis and 0.984 for z axis.

5. REFERENCES

- [1] <http://www.custompartnet.com/wu/3d-printing>
- [2] Topčić, A., Cerjaković, E., Lovrić, S.: *Comparative analysis of RE/RP versus Conventional Approaches of Tool Designing in Sand Casting*, Proceedings MMA2012, p.p. 493-497, Faculty of Technical Sciences Novi Sad, Novi Sad, September 2012,
- [3] Z Corporation: ZCast® 501 Direct Metal Casting - DESIGN GUIDE
- [4] http://www.science.smith.edu/cdf/pdf_files/ZPrinter%20310%20User%20Manual.pdf
- [5] <http://congresoingraf.es/PDF/25768.pdf>

Authors: Prof. Dr. Alan Topčić, Assist. Prof. Dr. Edin Cerjaković, M.Sc. Sladjan Lovrić, University of Tuzla, Faculty of Mechanical Engineering Tuzla, Univerzitetska 4, 75000 Tuzla, Bosnia and Herzegovina, Phone.: +387 35320 920, Fax: +387 35320 921.

E-mail: alan.topcic@untz.ba
edin.cerjakovic@untz.ba
sladjan.lovrice@untz.ba

COMPARISON OF MANUFACTURING TECHNOLOGIES OF FIXED STRUCTURES IN PROSTHETIC DENTISTRY

Received: 05 June 2014 / Accepted: 20 June 2014

Abstract: Fixed structures in prosthetic dentistry are highly customized products, individually manufactured for patients that are missing teeth. When choosing the technology for fixed dental structure manufacturing, three viable options are available (precise casting, milling, selective laser melting). Fixed structure performs a holding and positioning function for a tooth prosthetics that have nutrition as well as an aesthetic function. The choice of dental structure's manufacturing technology is influenced by structures' material and economical efficiency. The choice of material is influenced by current market trends and knowledge about chemical (non-) compliance of several widely used metal alloys. Results presented in this work, show some technological as well as time-efficiency advantages of selective laser melting (SLM) technology in the field of manufacturing metal dental structures

Key words: Casting, CNC milling, Additive manufacturing, Prosthetic dentistry.

Poređenje proizvodnih tehnologija osnovnih struktura u zubnoj protetici. Fiksne strukture u zubnoj protetici su visoko prilagođeni proizvodi, svaki pojedinačno proizveden za pacijenta sa potrebama veštačkih zuba. Pri izboru tehnologije izrade fiksne stomatološke strukture, na raspolaganju su tri opcije (precizno livenje, glodanje, selektivno lasersko topljenje). Fiksna struktura obavlja funkciju držača i pozicioniranja zubne protetike koje imaju praktičnu kao i estetsku funkciju. Na izbor proizvodne tehnologije stomatoloških struktura utiče materijalna i ekonomska efikasnost strukture. Na izbor materijala utiču aktuelni trendovi tržišta i znanja o hemijskim (ne) usklađenostima nekoliko široko korišćenih metalnih legura. Rezultati prikazani u ovom radu, pokazuju neke tehnološke i vremenske prednosti tehnologije selektivnog laserskog topljenja (SLM) u oblasti proizvodnje metalnih stomatoloških struktura.

Ključne reči: Livenje, CNC glodanje, aditivna proizvodnja, protetička stomatologija.

1. INTRODUCTION

Teeth have an important role in mechanical phase of food digestion. Due to various causes (caries, illness, injuries...) losses of teeth can occur. With each missing tooth the capability of proper chewing is significantly reduced. Missing teeth can be replaced by fixed prosthetic replacements that consist of fixed (usually metal) dental structure and ceramic coating (Fig. 1).

The oldest and most common manufacturing procedure for fixed dental structures is investment casting. Due to large amounts of manual labour required in this procedure the quality of end product depends largely on skills and experience of dental technician. With development of three-dimensional scanning, computer aided design, CNC machining and additive manufacturing some manual phases of manufacturing can be replaced by dedicated computer software and computer controlled machines. The goal of this paper is to examine different possibilities of manufacturing fixed dental structures. An individual case study is also used for manufacturing time analysis.

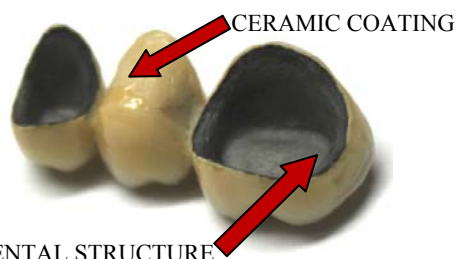


Fig. 1. Fixed prosthetic replacement

2. INVESTMENT CASTING

Manufacturing of dental structures begins by taking a negative mould of patient's jaw that is later used to produce a plaster model. In investment casting procedure, this model is used by dental technician to manually model the construction's wax pattern. Also, the casting system with channels and feeders is designed in wax (Fig. 2). This pattern is then removed from the plaster model and poured over by embedding mass to produce a mould that is later used for metal casting. Most often cobalt-chrome or gold-based dental alloys are used.

The quality of design and proper casting depend largely on complexity of individual case and experience and manual skill of dental technician. Therefore, the successful casting and proper product geometry cannot be guaranteed and if any errors occur, all work-time spend from wax pattern design to casting is lost.

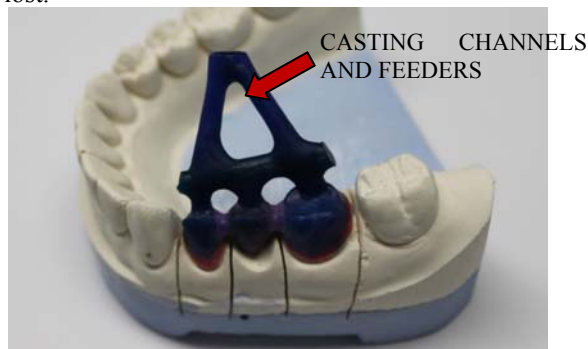


Fig. 2. Wax structure model with channels on plaster model

3. OPTICAL SCANNING

One of the main advantages of optical scanning is an ability to quickly transform complex physical geometry into accurate three-dimensional computer model [1]. In fixed dental structure production, optical scanning is used to import the geometry of plaster model into dedicated computer software. The plaster model that would otherwise be used for wax modelling can be used, but additional preparation can be required in order to achieve proper feature recognition functionality inside computer software (Fig. 3, Fig. 4, Fig. 5).



Fig. 3. Additional preparation of plaster model for optical scanning



Fig. 4. Results of additional preparation of plaster



Fig. 5. Displayed scanned plaster

Currently, there is also a lot of research into possibilities of intra-oral three-dimensional scanning. This method would make a production of plaster model unnecessary and avoid possible inaccuracies that can occur during this phase.

4. COMPUTER AIDED DESIGN AND MANUFACTURING

Regardless of what kind of scanning method is used, a three dimensional computer model of actual patient's jaw and teeth configuration is later used to model the dental construction in virtual environment of computer aided design software. This is usually dedicated dental design software, with large standard part library and automatic element and fixture creation. Because this kind of software is usually used by dental technicians some also include design functionality that is similar to manual wax modelling.

Finished dental construction CAD model is later used in manufacturing process. Two main possibilities are CNC milling or selective laser melting.

5. CNC MILLING

Milling is one of the most important manufacturing procedures by material removal. With development of CNC controlled machines complex geometry machining became possible. Writing a NC program that controls the machine is a necessary manufacturing step in CNC machining. This is usually done by computer aided manufacturing software (Fig. 6). In dedicated dental software NC programming phase is usually automatic and hidden from user. This is possible due to a significant shape similarity between customized dental constructions that can always be manufactured by the same milling strategy [2].

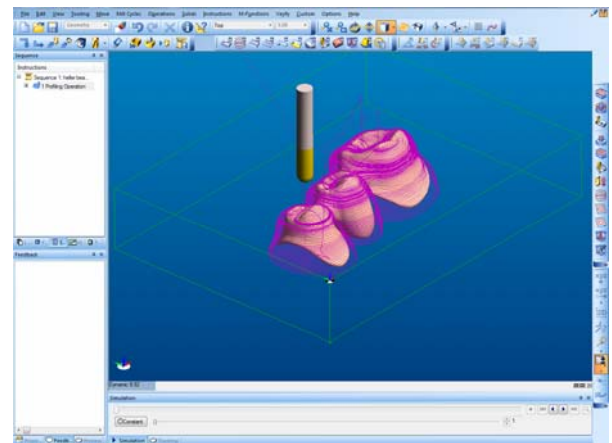


Fig. 6. Computer aided NC programming

Milling of dental structures is done by dedicated CNC milling machines. Tools used are often of smaller diameters, therefore the machine's spindle must enable higher rpm ranges. These machines are also equipped with clamping systems designed for holding standardized dental material blocks. Tool-changes during manufacturing are automatic and predefined in NC program. One of the main advantages of milling dental structures is a possibility of machining ceramic material.

6. SELECTIVE LASER MELTING

Selective laser melting is additive manufacturing technology. It is based on shaping a three-dimensional

object from powder material by laser or electronic beam. Manufacturing is done by layers of less the 0,1 mm thickness. Programming the machine is based on slicing the three-dimensional model in layers and setting the laser parameters for machining (Fig. 7).

Machining is usually done inside an inert gas atmosphere; therefore selective laser melting is very suitable for manufacturing dental constructions from titanium alloys [3].



Fig. 7. Sliced three-dimensional model in layers positioned on work tray

7. POST-PROCESSING AND CERAMIC COATING

Regardless how a fixed dental construction is manufactured, some form of post-processing before ceramic coating is necessary. When casting is used, the casting channels in feeders have to be cut away (Fig.8). When milling, finished construction has to be removed from the rest of the material blank (Fig. 9). With selective laser melting, a support structure has to be removed (Fig. 10). Also in each case, grinding of the construction surface and sandblasting is necessary [4].

Ceramic coating is usually done in three layers. After each layer a construction has to be heated up and cooled down.



Fig. 8. Casting made construction with casting channels and feeders

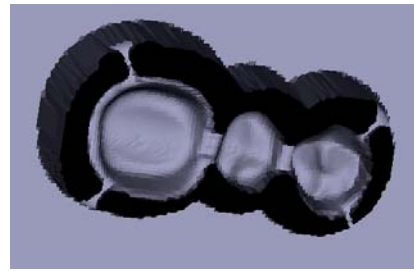


Fig. 9. Milling made construction with rest of the material blank



Fig. 10. SLM made construction with support structure

8. COMPARISON

Comparison is based on 3-part case study, already presented on previous figures. This dental construction was made with each presented methodology and time analysis and fitting test was carried out.

9. TIME ANALYSIS

Time analysis is based on measuring the time required for each individual phase of production. Some phases of production are common regardless of methodology selected.

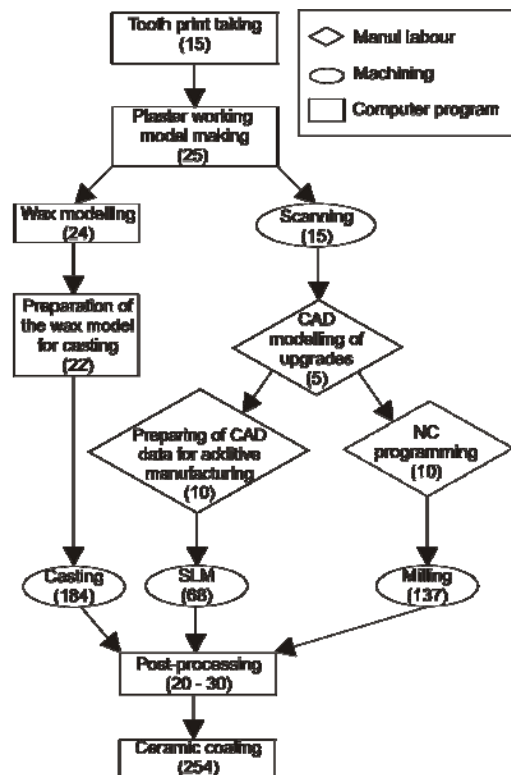


Fig. 11. The workflow of production and phases required for each methodology

The following chart (Fig. 11) presents the workflow of production and phases required for each methodology. Estimated time requirements for each phase for presented 3-part case study are also presented. Required time estimation is especially problematic for phases that include manual labour, due to be somewhat dependant on experience and skill of the technician.

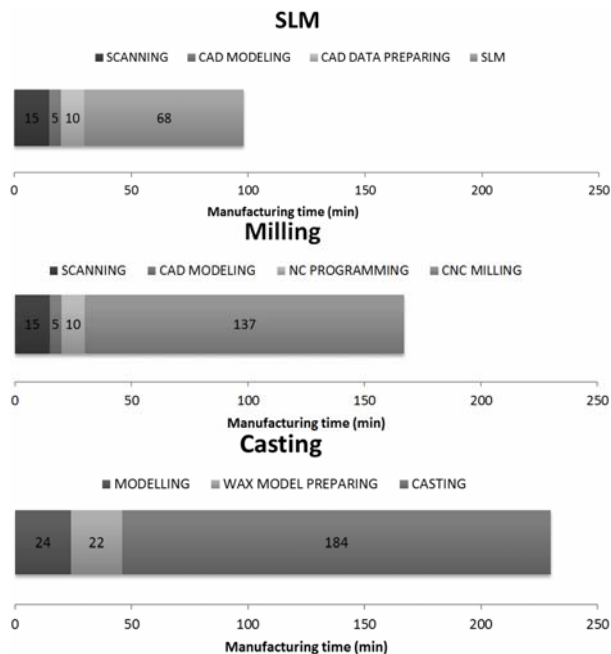


Fig. 12. Time duration for different methods

Because initial and final phases of dental replacement production are the same for each methodology, the following charts present the time requirements for intermediate phases that differ between methodologies.

Diagrams clearly show the difference between manufacturing times of each methodology. Absolute time differences are valid only for presented case study but the ratios can be generalized for optional case.

10. CONCLUSION

Investment casting is most commonly used technology despite the longer manufacturing times. This is mainly due to the long history of using casting in dentistry and consequentially a large availability of required equipment in dental laboratories.

Milling is also well established technology especially due to a possibility of producing ceramic dental constructions.

Selective laser melting is a rather new technology in the dentistry field. Research presented in this paper clearly shows the advantages of using this technology in terms of manufacturing time consumption. That is way a number of SLM machine variants specially build for dental applications is constantly increasing.

11. REFERENCES

- [1] Brajliah, T., Tasič, T., Drstvenšek, I., Valentan, B., Hadžistević, M., Pogačar, V., Balič, J., Ačko, B.:

Possibilities of using three-dimensional optical scanning in complex geometrical inspection, Journal of mechanical engineering, 57, p.p. 826-833, Nov. 2011.

- [2] Klančnik, S., Balič, J., Čuš, F.: *Intelligent prediction of milling strategy using neural networks*, Control and Cybernetics, 39, p.p. 9-22, Sept. 2010.
- [3] Zupančič, H. T., Sajko, G., Vuličević, Z. R., Anžel, I., Drstvenšek, I.: *Dodajalne tehnologije - tehnologije prihodnosti tudi v stomatologiji in medicini*, Glasilo Zdravniške zbornice Slovenije, 20, p.p. 65-67, Dec 2011.
- [4] Šafner, J., Kostevšek, U., Kadivnik, Ž., Brajliah, T., Drstvenšek, I.: *Ugotavljanje hrapavosti površin po peskanju*, Orodjarstvo 2008, p.p. 149-153, Portorož, GZS, LJ, Oct. 2008.

Authors: Prof. Dr. Igor Drstvensek, Prof. Dr. Joze Balic, Dr. Tomaz Brajliah, B.Sc. Zupančič Hartner Tjaša, M.Sc. Urska Kostevsek, B.Sc. Matej Paulic, B.Sc. Tomaz Irgolic, University of Maribor, Faculty of Mechanical Engineering, Institute for Production Engineering, Smetanova ulica 17, 2000 Maribor, Slovenia, Phone.: +386 2 220 7596, Fax: +386 2 220 7996.

E-mail: igor.drstvensek@um.si

joze.balic@um.si

tomaz.brajlih@um.si

urska.kostevsek@gmail.com

matej.paulic@um.si

tomaz.irgolic@um.si

tjasa@ortotip.com

miodrags@uns.ac.rs

Živanović, S., Glavonjić, M.

METHODOLOGY FOR IMPLEMENTATION SCENARIOS FOR APPLYING PROTOCOL STEP-NC

Received: 01 March 2014 / Accepted: 30 March 2014

Abstract: This paper describes methodology for the implementation of scenarios for applying protocol STEP-NC for programming CNC machine tools. Capabilities of the current implementation of the new programming method based on STEP-NC for the available machines, is shown, using software STEP-NC Machine and CAD/CAM system Creo. For a description of the methodology for application protocols STEP-NC were used IDEF0 diagrams. The methodology is verified in two scenarios who are shown (SC1 and SC2). The application of STEP-NC protocols is described by IDEF0 methodology experimentally verified using two examples.

Key words: STEP-NC, CAD/CAM, IDEF0

Metodologija za implmentaciju scenarija primene protokola STEP-NC. U ovom radu je opisana metodologija za sprovođenje scenarija primene protokola STEP-NC za programiranja CNC mašina alatki. Pokazane su mogućnosti trenutne primene novog metoda programiranja baziranog na STEP-NC na raspoloživim mašinama pomoću softvera STEP-NC Machine i CAD/CAM sistema Creo. Za opis metodologije primene protokola STEP-NC iskorišćeni su IDEF0 dijagrami. Metodologija je verifikovana za dva pokazana scenarija (SC1 i SC2). Primena STEP-NC protokola opisana IDEF0 metodologijom eksperimentalno je verifikovana koristeći dva primera.

Ključne reči: G code, STEP-NC, CAD/CAM, IDEF0

1. INTRODUCTION

Machine tool programming was based on the G code for more than half a century. The current machine tool programming standard is still ISO6983, also known as G-code [1]. Further developments, however, are being significantly limited by current programming language. Machine tools have evolved from simple machines with controllers that had no memory, driven by punched tape to today's highly sophisticated Computer Numerically Controlled (CNC) machine tools. Machine tool programming using G code is characterized by a low level of information content. These low level of information describes elementary actions and tools trajectories, strongly reducing possibilities at the CNC level [1]. It is necessary to prepare the tool path for each type of CNC machine tools individually using appropriate postprocessor.

Nowadays a new standard, informally known as STEP-NC (Standard for Product Model Data Exchange for Numerical Control) [3,4], is used as the basis for development of the next generation of CNC controller for new generation of machine tools. These new standards are ISO 14649 and ISO 10303 AP 238. The new programming method using standard known as STEP-NC is an open challenge in the field of machine tool programming. The development of a new method of programming is started [1-8], but not completed work.

The STEP-NC is the result of more than a decade long period of international effort to replace G code (ISO6983) with a modern associative language that connects the CAD design data used to determine the machining requirements for an operation with the CAM

process data that solve those requirements [8].

The method of programming using the STEP-NC is object-oriented view of programming in terms of manufacturing features, instead of direct coding of sequences of axis motions and tool functions as defined in ISO 6983 [5]. Classical programming is still the most commonly used way of programming and object-oriented programming has not been introduced to the full extent. However, these two methods are simultaneously used as illustrated in Figure 1.

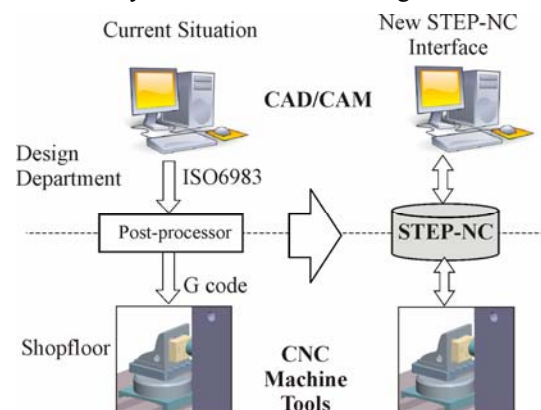


Fig. 1. Current ISO6983 and new interface ISO14649 for programming CNC machine tools [4, 5]

Figure 1 shows the comparison of current G-code programming method (ISO 6983) and new STEP-NC high level programming method (ISO 14649). The STEP-NC provides CNC controller new opportunities to support high level of information from design. It allows bi-directional flow of data between CAD/CAM and CNC Machine Tools without losing information. STEP-NC does not describe the tool trajectories for

specific CNC machine tool as G code does, but it provides a feature based data model. A STEP-NC file is not machine tool specific and can be used on various machine tool controllers [1].

The paper structured as follows. Section 2 gives an overview of the scenarios for applying STEP-NC. Section 3 gives a description of the methodology for STEP-NC machining. Section 4 describes program verification and machining experiment.

2. SCENARIOS FOR APPLYING STEP-NC

At the moment, this new method of programming based on STEP-NC can't completely be used, because the resources for its development are owned by several research centers. This paper considers two possible scenarios (SC1, SC2) for indirect application of this method of programming on existing machines and the available software, Figure 2.

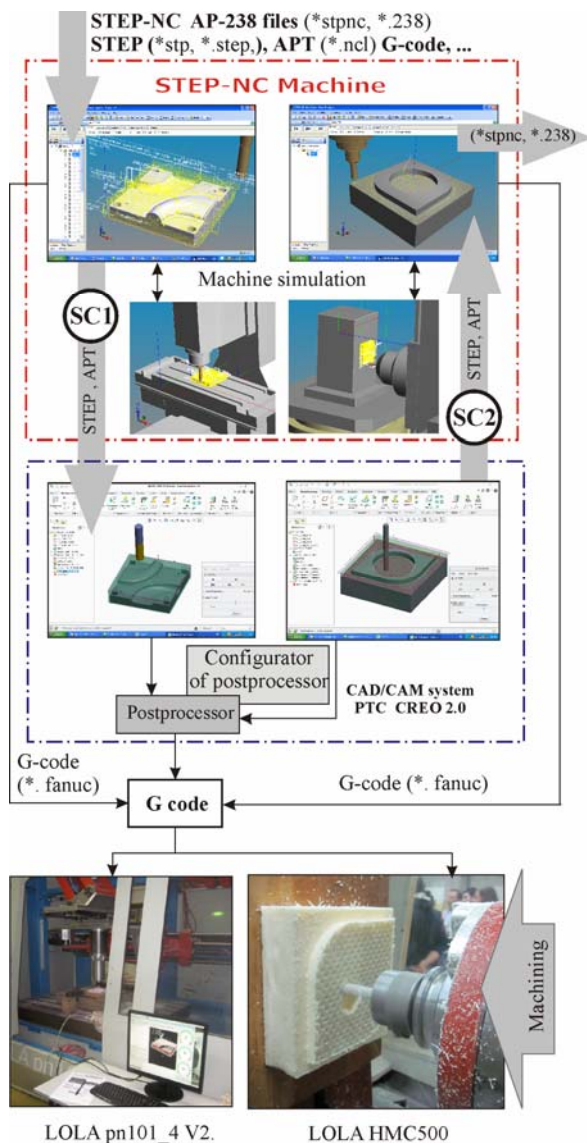


Fig. 2. Current scenarios for the application of STEP-NC programming.

These scenarios are:

- Scenario SC1 - using the original STEP-NC program, post-processing into G code and executing

on the machine tool, and

- Scenario SC2 - modeling part in the CAD/CAM system, and then exporting in the STEP format; then importing a reference model, workpiece, tools and tool path (CLF) in software STEP-NC Machine [3], where the STEP-NC program is saved in the format Part 28 (XML).

For now, the first scenario is realistic and feasible in two ways. The first way is using of CLF, which is specifically imported into the available CAD/CAM system and post-processed for the selected machine tool. CAD system takes reference model and workpiece in STEP format and CL File. Verification of material removal is done in a CAD/CAM system in the module (NC Check). CAD/CAM system uses configured postprocessor to generate G code for the available CNC machine tools. G code is executed on the available machine tools.

The second way uses an internal application to the direct export of STEP-NC program in G code from the available control units, offered by STEP-NC Machine (Fanuc, Siemens, Okuma, Haas, etc.).

Scenario SC2 involves importing geometry elements of the reference model, workpiece, tool and tool path from common CAD/CAM system into STEP-NC Machine software. The scenario SC2 is performed as follows: (i) CAD models of reference model, workpiece and tool are created in the CAD/CAM system; (ii) technology for machining (roughing and finishing) are planned and implemented; (iii) tool path CL file (*.ncl) is generated; (iv) tool path and material removal simulations (NC Check) is done; (v) the inputs for software STEP-NC Machine are prepared by exporting reference model, workpiece and tool from CAD/CAM System in STEP format; (vi) the reference model, model of the workpiece, model of tool in STEP format, and Cutter Location File (CLF - *.ncl) are loaded in software STEP-NC Machine; (vii) program is saved in the format of STEP-NC AP238 (*.stpnc, *.238); (viii) program is tested by simulations on different machines available in the software STEP-NC Machine; (ix) program for machining is directly translated into Fanuc G code using the Export option of software STEP-NC Machine; (x) workpiece is machined on available CNC machine tools.

3. METHODOLOGY FOR STEP-NC BASED MACHINING

IDEF0 is a method designed to model the decisions, actions, and activities of an organization or system. It is useful in establishing the scope of an analysis, especially for a functional analysis [2]. IDEF0 is used to produce a "function model". A function model is a structured representation of the functions, activities or processes within the modeled system or subject area.

In this paper, functions of STEP-NC based machining, are described by using the IDEF0 diagram. The special case of one box IDEF0 context diagram, containing the toplevel function being modeled with its inputs, controls, outputs and mechanisms, is shown in Figure 3.

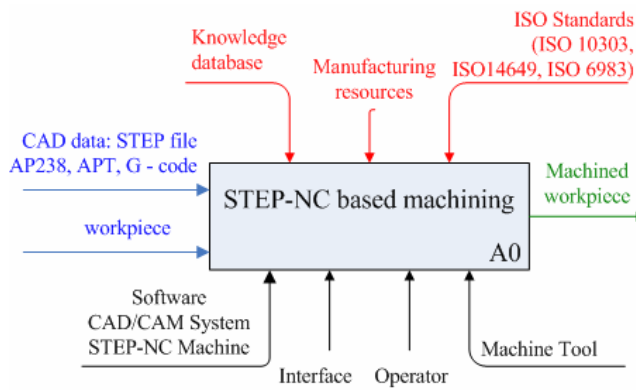


Fig. 3. Top-level IDEF0 diagram for STEP-NC based machining

The single function represented on the top-level context diagram may be decomposed into its major sub-functions by creating its child diagrams. Each child diagram contains the child boxes and arrows that provide additional detail about the parent box. The child diagram that results from the decomposition of a function covers the same scope as the parent box in details.

Top level child diagram A0 describes basic flow of activities and it is illustrated in Figure 4. According to the IDEF0 methodology, by analyzing diagram A0, we get the basic flow of activities shown in Fig. 4 The basic activities are: A1 – Generic STEP files and tool path in CAD/CAM systems, A2 - STEP-NC program generator, A3 – Post-processing programs, A4 – Machining process simulator and A5 - Machining.

The activity A1 is performed in CAD/CAM system. Input into the activity A1 can be CAD models of workpieces, tools in STEP format and programs in the APT format or G code obtained from the software STEP-NC Machine. Output from the activity A1 can be CAD model of the workpiece, tools in STEP format, APT program (CL file), G code or STEP-NC file if CAD/CAM system can generate it. These outputs are inputs for activity A2.

The activity A2 is performed in software STEP-NC Machine. Input into the activity A2 can be an original STEP-NC program in *.stpnc, *.238, *.p21, *.p28 formats. Software STEP-NC Machine implements the activity A3, that allows post-processing of STEP-NC program into G code for machining on the existing CNC machine tools.

G code obtained on this way can be directed to additional verification in the CAD/CAM system or in some of the CNC simulators (activity A4). Some of used simulators are VeriCUT and CNC Simulator. In this activity can be performed machining simulation in software STEP-NC Machine too. After verification of the program in G code, we can pass over to the activity A5 safely, where the machining is realized on CNC machine tools.

The application of this methodology is presented in Section 4. Two examples of machining are used, one for each scenario. CNC machine tools used for machining are Horizontal Machining Center (LOLA HMC500) and vertical milling machine with parallel kinematics (LOLA pn101_4 V.2).

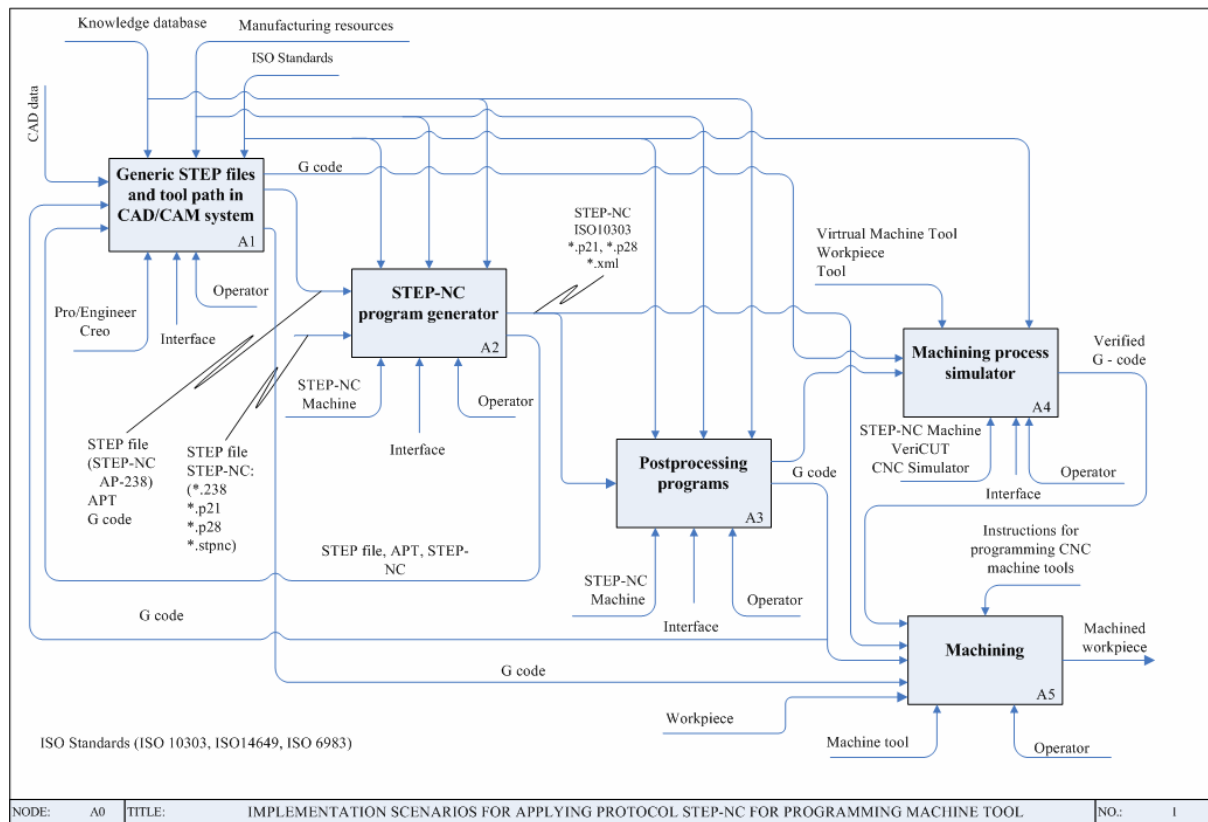


Fig.4. The basic flow of activities for STEP-NC based machining simulations

4. PROGRAM VERIFICATION AND MACHINING EXPERIMENT

The application of STEP-NC described by IDEF0 methodology is experimentally verified using two examples. For first scenario SC1 we have used the source program in STEP-NC format for a moldy workpiece [6, 7], Figure 5a,c. "Moldy" workpiece was first machined during a presentation in Renton (Washington, USA) [7]. The second example has been done for scenario SC2, Figure 5b,d.

In the first example, the format of STEP-NC program is translated into APT using the Export option of software STEP-NC Machine. Utilizing APT program, the machining technology is reconstructed in CAD/CAM system PTC Creo. Tool path is verified by simulation of material removal in module NC Check, Figure 5a. Postprocessing into G code has been carried out in the final part of the experimental verification. In the second experiment, the format of STEP-NC program for Moldy workpiece was directly translated into Fanuc G code, using the Export option of software STEP-NC Machine, the activity A3, from Figure 4. The obtained G codes were further verified in the activity A4 – Machining process simulator. Verified G codes were used for the machining on the industrial prototype of 3-axis vertical parallel kinematic milling machine LOLA pn101_4 V2 [9].

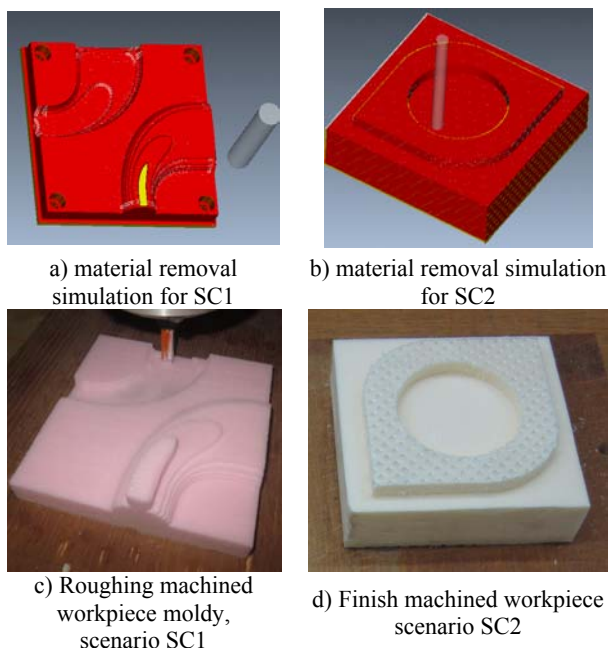


Fig. 5. Material removal simulation and machined workpieces for each scenario

Scenario SC2 involves importing geometry elements of the reference model, workpiece, tool and tool path from common CAD/CAM system into STEP-NC Machine software, where program is saved in the format Part 28 (XML). Program for machining was directly translated into Fanuc G code using the Export option of software STEP-NC Machine. The final verification is carried out, by machining on Horizontal Machining Center (LOLA HMC500).

5. CONCLUSION

The paper presents possibilities of application of the new method of programming based on ISO14649 and ISO10303 standards, known as STEP-NC. Since there is still not sufficient available CNC machines that can directly interpret the STEP-NC program, preparing for this method of programming is reduced to the translation into G code, which can be realized on the available CNC machine tools.

STEP-NC standard is almost finalized, and we can expect the first shop-floor application of STEP-NC program soon. Existing CNC machine tools will be replaced in the future by machines whose control systems can receive and execute programs in the STEP-NC format.

Our future research will be focused on the building of CNC machine tool with open architecture control system, that can download and directly execute programs in some of the STEP-NC formats.

Acknowledgment

The authors would like to thank the Ministry of Education, Science and Technological Development of Serbia for providing financial support that made this work possible.

9. REFERENCES

- [1] Rauch M., Laguionie R., Hascoet J.Y., Suh S.H.: *An advanced STEP-NC controller for intelligent machining processes*. Robotics and Computer-Integrated Manufacturing, vol. 28, p.p. 375–384, 2012.
- [2] Zhang, Y., Bai, X-L., Xu, X., Liu, Y-X.: *STEP-NC Based High-level Machining Simulations Integrated with CAD/CAPP/CAM*. International Journal of Automation and Computing, vol. 9, no.5, p.p. 506-517, 2012.
- [3] STEP NC-MACHINE, Step Tools, Inc., from <http://www.steptools.com/products/stepncmachine>
- [4] STEP-NC Newsletter, Issue 2, from <http://www.stepnc.org/data/newsletter2.pdf>
- [5] Xu X.W., He Q.: *Striving for a total integration of CAD, CAPP, CAM and CNC*. Robotics and Computer-Integrated Manufacturing, vol. 20, p.p.101–109, 2004.
- [6] STEP Tools, Inc. "Moldy" Mold Part <http://www.steptools.com/products/stepncmachine/samples/moldy/>
- [7] STEP-NC Demonstration, Renton, WA 2009 http://www.steptools.com/library/stepnc/2009_renton/
- [8] Randelović, S., Živanović, S.: *CAD-CAM Data Transfer as a Part of Product Life Cycle*. Facta Universitatis, Series: Mechanical Engineering, vol.5, no.1, p.p. 87-96, 2007.
- [9] D. Milutinovic, M. Glavonjic, V. Kvirgic, S. Zivanovic. (2005). A New 3-DOF Spatial Parallel Mechanism for Milling Machines with Long X Travel. *Annals of the CIRP*, vol. 54, no.1, p. 345-348.

Authors: Assist. Professor Dr. Saša Živanović, Prof. Dr. Miloš Glavonjić, University of Belgrade, Faculty of Mechanical Engineering, Production Engineering Department, Kraljice Marije 16, 11120 Belgrade, Serbia, Phone.: +381 11 33-02-423, Fax: +381 11 33-70-364.

E-mail: szivanovic@mas.bg.ac.rs
mglavonjic@mas.bg.ac.rs



Mishra Antaryami

INVESTIGATIONS ON WEAR CHARACTERISTICS OF TEAK WOOD DUST FILLED EPOXY COMPOSITES

Received: 31 March 2014 / Accepted: 25 April 2014

Abstract: Composites of teak wood dust particles of 300 micron size with varying weight fractions (10, 15 and 20%) have been developed by hand moulding technique. Aluminium moulds have been prepared for casting the composite pins of 8 mm diameter and 50 mm length. Sliding wear tests have been conducted on a pin on disc friction and wear monitor. From the tests it is observed that the composite with 20% weight fraction of teak wood dust exhibited lowest coefficient of friction (0.59-0.80) and is nearly equal to the value obtained for 10% dust filled composite i.e. 0.63 to 0.84. However the wear rate at varying speeds the composite with 10% weight fraction of dust showed lowest rate sliding against steel counterpart. Therefore the composite with 10% wood dust may be more suitable for frictional applications.

Keywords: Teak wood dust, Epoxy, Composites, Friction and Wear characteristics

Istraživanje karakteristika habanja epoksi kompozita punjenih sa tikovom drvenom prašinom. Kompoziti od čestica drvene tikove prašine veličine 300 mikrona sa različitim masenim frakcijama (10, 15 i 20 %) su formirani ručnim oblikovanjem. Aluminijumski kalupi su pripremljeni za oblikovanje kompozitnih pinova prečnika 8 mm a dužine 50 mm. Testovi klizanja su sprovedeni sistemom „pin na disku” i pomoću monitora habanja. Primećeno je da je kompozit sa 20 % težine frakcije tikove prašine imao najmanji koeficijent trenja (0.59-0.80) što je skoro jednako vrednosti za 10 % kompozit koji je iznosio od 0,63 do 0,84. Međutim stopa habanja pri različitim brzinama 10 % kompozita je bila najniža pri trenju o čelik. Stoga kompoziti sa 10 % prašine mogu biti pogodniji za primene koje iziskuju trenje.

Ključne reči: tikova drvena prašina , epoksi , kompoziti , karakteristike trenja i habanja

1. INTRODUCTION

Now a days natural fibre polymeric composite materials have their importance in the applications of light weight and high strength structures. Use of these materials dominate the aerospace, automotive, construction and sporting industries. However, these fibers have serious drawbacks such as non-renewability, non-recyclability, non-bio-degradability etc. These shortcomings have been highly exploited by proponents of natural fiber composites. Though mechanical properties of natural fibers are much inferior to those of other fibers, their specific properties, especially stiffness, are quite comparable to artificial fibres. The aim of this investigation is to determine the friction and wear characteristics of saw dust-epoxy composite. This study is important for manufacture of furnitures, residential deck board, rails and balusters, transportation structures, poles and cross arm, wearing surfaces and other related industrial applications. Although there are several reports in the literature which discuss the mechanical behaviour of wood/polymer composites, however, very limited work has been done on the effect of wood dust types on friction and wear characteristics of polymer composites. Against this background, the present research work has been undertaken, with an objective to explore the potential of wood dust types as reinforcing material in polymer composites and to investigate its effect on the friction and wear behaviour

of the resulting composites.

2. REVIEW OF LITERATURE

A number of investigations have been conducted on several types of natural fibres such as kenaf, hemp, flax, bamboo, and jute to study the effect of these fibres on the mechanical properties of composite materials. Fracture properties and characteristics of sisal textile reinforced epoxy composites was studied by Li et al.[1]. The study concluded that proper fibre surface treatment could improve the fracture properties of this kind of Eco-composite. Mosadeghzad et al.[2] studied the effect of surface treatment and filler loading on mechanical properties of the *acacia* saw dust unsaturated polyester resin (UPR) composite based on recycled polyethylene-terephthalate (PETP). The results showed that both tensile and flexural moduli were increased with increasing filler contents whereas the strength was decreased. This was overcome by treating the sawdust fillers with 10% sodium hydroxide (NaOH). Biswas et al. [3] worked on the effect of ceramic fillers on mechanical properties of bamboo fibre reinforced epoxy composites. In this study, a series of bamboo fibre reinforced epoxy composites were fabricated using conventional filler (aluminium oxide (Al_2O_3) and silicon carbide (SiC) and industrial wastes (red mud and copper slag) particles as filler materials. The result showed that the inclusion of fibre in neat epoxy improved the load bearing capacity

(tensile strength) and the ability to withstand bending (flexural strength) of the composites. Kranthi et al.[4] studied the wear performance of a new class of epoxy based composites filled with pine wood dust. According to the study pine wood dust possesses good filler characteristics as it improves the sliding wear resistance of polymeric resin, and filler content, sliding velocity and normal loads are the important factors which affect the specific wear rate. A study on the dry sliding wear of oil palm empty fruit bunch (OPEFB) epoxy composite was done by Kasolang et al.[5]. The result showed that the mass loss was significantly higher for smallest fibre size (100µm) examined at 30N and at other fibre sizes, the mass loss values were relatively close due to the distribution and orientation of fibres. Wang et al.[6] studied the effect of coupling agent on bonding properties of wood/polyethylene composites. The result showed that, the -OH, -C-O- and C=O functional groups were appeared on the treated surface and the surface roughness was increased after mechanical polishing treatment and coating treatment, resulting a increase in the shear bonding strength for the treated sample significantly. Hisham et al. [7] studied the flexural mechanical characteristic of sawdust and chip wood filled Epoxy Composites and found that a good quality of SW (saw wood) and CW (chip wood) fibre composite can be used for furniture utilities. Wimonsong et al.[8] worked on thermal conductivity and mechanical properties of wood sawdust/polycarbonate composites. The study showed that the Youngs moduli of composites were in general higher than the neat PC except for the one with γ -aminopropyl trimethoxy silane treatment. The tensile moduli of composites were increased as the filler loading increased and the addition of wood sawdust resulted in the tensile strength reduction of the composites, and also the thermal conductivity was reduced significantly with the increment of wood sawdust contents. Bhaskar et al.[9] worked on the evaluation of properties of polypropylene-pine wood plastic composite. Incorporation of maleated polypropylene (MAPP) coupling agent in composite formulation improved the stability.

3. SCOPE/OBJECTIVES

- Development of teak wood dust filled epoxy composites with 300 micron mesh size and different weight fractions i.e 10,15 and 20%.
- Casting of cylindrical pins of 8 mm diameter for frictional characterization by developing suitable metallic mould
- Carrying out short run and long run tests in a pin on disc friction and wear monitor to evaluate the coefficient of friction and wear characteristics of these materials sliding against mild steel plate.
- Choosing the best out of the above specimens for specific applications.

4. THERETICAL INVESTIGATIONS

The composite is usually prepared based on calculation of weight fractions or Volume fractions.

The density of the composite is found out by rule of mixtures.

Weight fraction of the reinforcement:

$$w_r = W_r / (W_r + W_m) * 100,$$

Weight fraction of the matrix:

$$w_m = W_m / (W_r + W_m) * 100$$

Where W_r = Weight of reinforcement, W_m = Weight of matrix,

Weight of the composite = $W_c = W_r + W_m$

Further as per rule of mixtures, the density of the composite is obtained by

$$\rho_c = \rho_m v_m + \rho_r v_r \quad \dots \text{(Eqn.1)}$$

where ρ_c = Density of the composite, ρ_m = Density of the matrix, ρ_r = Density of the reinforcement, v_m = Volume fraction of the matrix,

v_r = Volume fraction of the reinforcement

Further $v_m = V_m / (V_m + V_r + V_v) * 100,$

$v_r = V_r / (V_m + V_r + V_v) * 100$

Volume of the composite = $V_c = V_m + V_r + V_v$

Where V_m = Volume of the matrix, V_r = Volume of the reinforcement and V_v = Volume of voids.

Assuming modulus reinforcing efficiency as unity and as per rule of mixtures:

Modulus of elasticity of the composite

$$E_c = E_r v_r + E_m v_m \quad \dots \text{(Eqn.2)}$$

Where E_r = Modulus of elasticity of reinforcement and

E_m = Modulus of elasticity of matrix

Strength of the composite

$$\sigma_c = \sigma_r v_r + \sigma_m v_m \quad \dots \text{(Eqn.3)}$$

Where σ_r = strength of the reinforcement, σ_m = Strength of the matrix

Table .1 Properties of Teak wood dust

Properties	Value
Density (g/cc)	0.8
Youngs modulus of elasticity(GPa)	10.5
Tensile Strength(MPa)	95

Table.2 Properties of Epoxy

Properties	Value
Density (Kg/m ³)	1.2*10 ³
Youngs modulus of elasticity(GPa)	20
Tensile Strength(MPa)	75

Table. 3 Composite properties

Specimens	Density (kg/m ³)	Elastic Modulus (GPa)	Tensile strength (MPa)
Sp-1(10%)	1185.6	19.66	75.66
Sp-2(15%)	1184.96	19.64	75.64
Sp-3(20%)	1171.04	19.31	76.43

Sp-1- Composite with teak wood dust of 10%

Sp-2- Composite with teak wood dust of 15%

Sp-3- Composite with teak wood dust of 20%

5. EXPERIMENTAL INVESTIGATIONS

Materials

The teak wood dust of 300 micron mesh size (Fig.1) measured through sieve shaker were considered as reinforcing material in fabrication of the composite. Epoxy (CY 230 and Hardener- HY- 951 supplied by Hindustan Ceiba Geigy Ltd.,India) has been used as matrix material. A metallic mould has been developed in house to cast the pins for wear testing (Fig.2). After mixing epoxy and wood dust in the proposed ratio the composite was cast by pouring into the split mould and allowed to cure at room temperature for 24 hours. The pins were ejected out after solidification (Fig.3).



Fig.1 Teak wood dust of 300 micron size

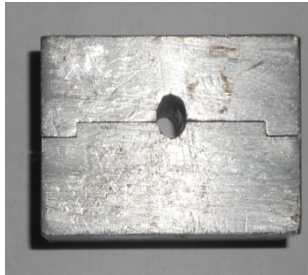


Fig. 2 Aluminium Mould (Closed)



Fig.3 Mould along with cast specimen



Fig.4.Composite pins (three types)



Fig.5. Friction and wear monitor



Fig.6. Enlarged view of disc and specimen

Experimental procedure

The tests were carried out in Pin on disc wear and friction testing machine (Fig.4 and 5) supplied by M/s Magnum Engineers, Bangalore, India, having the following specifications

Load range- Up to 100 N, Friction force measurement- Up to 100 N, Wear measurement- 2000 microns or +/- 2 mm, Sliding speed – 0.26 to 10 m/s, Disc speed – 100-2000 rpm, Diameter of track – 40-90 mm, Disc size- 100 dia and 8 mm thk, Disc material – EN-31(58-60 RC), Pin – 3-10 mm dia and length – 25 mm, Software- MAGVIEW-2011 data acquisition software. For evaluation of friction coefficient under dry sliding condition the speed and time were kept constant i.e 1000 rpm and 3 minutes with varying the load up to 5 kg. Similarly for estimating the wear , the pins were slid against mild steel disc with varying velocity and keeping load and time constant i.e.50N and 10 minutes

6. RESULTS AND DISCUSSION

The readings from the control panel of the pin on disc apparatus with respect to friction force, speed , wear and time have been taken during conduct of the wear tests. The dead weights placed on the apparatus gave direct measurement of the normal reaction. Hence the coefficient of friction could be calculated. Thus the coefficient of friction and wear in microns with varying velocities were obtained for three different specimens as mentioned below in Table.4 and 5.

Table 4 Variation of Coefficient of friction against load

Load (Kg)	Specimen-1	Specimen-2	Specimen-3
	Coefficient of friction	Coefficient of friction	Coefficient of friction
01	0.6257	0.7526	0.5870
02	0.7492	0.7668	0.6562
03	0.8561	0.7792	0.6245
04	0.8175	0.9406	0.7812
05	0.8427	0.9575	0.8035

Table 5 Variation of wear with sliding velocity

Velocity (m/s)	Specimen-1	Specimen-2	Specimen-3
	Wear in microns	Wear in microns	Wear in microns
1.675	68	30	49
2.5136	75	92	74
3.351	82	100	113
4.189	110	128	127

The results have also been plotted graphically to give a better understanding as shown in Fig.7, and 8.

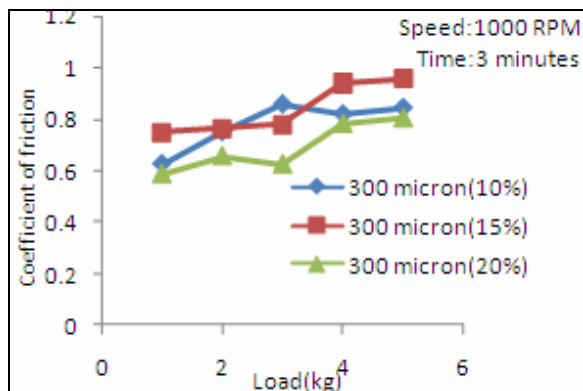


Fig.7. Variation of coefficient of friction with load

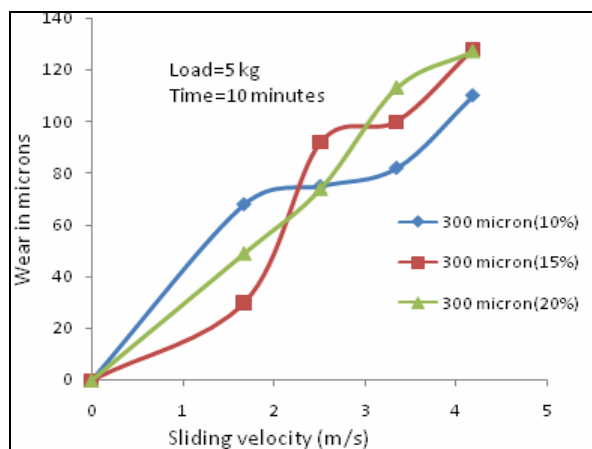


Fig. 8. Variation of wear with sliding velocities

From the above results it is observed that coefficient of friction for Sp-2 is quite high as compared to Sp-1 and Sp-3. With 20% weight fraction of wood dust it has exhibited lowest coefficient of friction (0.63-0.84). At higher loads the composite with 15% wood dust showed increase in coefficient of friction (0.96). However composite with 20% weight fraction of dust gave the lowest value of coefficient of friction (0.59-0.80) under same conditions of tests. Further during wear tests both 10 and 15 % weight fraction composites showed increase in wear and may take considerable amount of time to stabilize. The composite with 20% weight fraction of wood dust exhibited steady increase in wear and it is expected that the wear rate will stabilize and achieve steady state at a later stage. Lowest wear was observed in composite with 10% of wood dust.

7. CONCLUSIONS

Out of the results obtained it may be concluded that though the coefficient of friction for composite with 10% weight fraction of wood dust showed higher value still then the wear rate at higher speed is less. At higher loads the coefficient of friction for both 10 and 20 % dust filled composites are nearly equal. Hence the composite with 10% weight fraction may be more suitable for frictional applications.

8. REFERENCES

- [1] Li, Yan. Wing, Yiu., Ye., Mai., and Ye, Lin., "Fracture Properties and Characteristics of Sisal Textile Reinforced Epoxy Composites," *Jou. of Key Engineering Materials*, Vol. 312, pp.167-172, June, 2006,
- [2] Mosadeghzad, Z., Ahmad, I., Daik, R., Ramli, A., and Jalaludin, Z., "Preparation and properties of acacia sawdust/UPR composite based on recycled PET," *Malaysian Polymer Journal*, Vol. 4, No.1, pp.30-41, 2009.
- [3] Biswas, Sandhyarani., Satapathy, Alok., and Patnaik, Amar., "Effect of Ceramic Fillers on Mechanical Properties of Bamboo Fiber Reinforced Epoxy Composites: A comparative Study" *Journal Advanced Materials Research*, Vol. 123-125, Multi-Functional Materials and Structures III, pp.1031-1034, August, 2010,
- [4] Kranthi, Ganguluri., Nayak, Rajlakshmi., Biswas, S., and Satapathy, Alok., "Wear Performance Evaluation of Pine Wood Dust Filled Epoxy Composites," *Proceedings of the International Conference on Advancements in Polymeric Materials APM*, National Institute of Technology, Rourkela - 769008, India, 2010
- [5] Kasolang, Salmiah., Kalam, Anizah., and Ali Ahmad, Mohamad., "Dry Sliding Wear of Oil Palm Empty Fruit Bunch (OPEFB) Epoxy Composite ," *Journal of Advanced Materials Research*, Vol. 308 - 310, Advanced Design Technology: ADME 2011, pp.1535-1539, August, 2011.
- [6] Wang, Hui., Lv, Xin Ying., and Di, Ming Wei., "Effect of Coupling Agent on Bonding Properties of Wood/Polyethylene Composites," *Journal of Advanced Materials Research*, Vol. 311-313, Advanced Materials and Processes: ADME 2011, pp. 59-62, August, 2011.
- [7] Hisham, S., Faieza, A.A., Ismail, N., Sapuan, S.M., and Ibrahim, M.S., "Flexural Mechanical Characteristic of Sawdust and Chipwood Filled Epoxy Composites," *Journal of Key Engineering Materials*, Vol. 471 - 472, pp 1064-1069, 2011
- [8] Wimonsong, Wittawut. Threepopnatkul, Poosub. and Kulsethanchalee, Chanin., "Thermal Conductivity and Mechanical Properties of Wood Sawdust/Polycarbonate Composites," *Journal of Materials Science Forum*, Vol. 714, *Polymer Composite Materials: From Macro, Micro to Nanoscale*, pp.139-146, March, 2012.
- [9] Bhaskar, J., Haq, S., Pandey, A.K., and Srivastava, N., "Evaluation of properties of propylene-pine wood Plastic composites" *J. Mater. Environ. Sci.*, Vol.3(3), pp.605-612, 2012

Author: Prof. Dr. Antaryami Mishra, Professor, Mechanical Engineering and former Director, Indra Gandhi Institute of Technology, Sarang, Odisha, India, PIN- 759146. E-mail: antaryami_igit@yahoo.com

Križan, P., Svátek, M., Matúš, M., Beniak, J.

IMPACT OF PRESSING TEMPERATURE ON THE PRESSING CONDITIONS IN BRIQUETTING MACHINE PRESSING CHAMBER

Received: 05 June 2014 / Accepted: 20 June 2014

Abstract: In this paper, we will present the impact of the pressing temperature on the pressing conditions in pressing chamber during pressing of wooden briquettes. Conditions in pressing chamber can significantly impact the resulting briquettes quality. An experiment results which are showed in this paper, described the detected impact of pressing temperature on conditions in pressing chamber, especially on the friction forces between pressing chamber wall and the densified briquette. This experiment is aimed on detecting of pressing temperature effect and its role at densification in cylindrical and in conical pressing chamber. By pressing conditions setting we will be able to achieve the suitable resulting compacting pressure with respect of required final briquettes quality.

Key words: biomass, briquetting, densification, pressing temperature, briquette density

Uticaj temperature presovanja na uslove presovanja u pres komori briketirke. U ovom radu, će biti predstavljen uticaj temperature presovanja na uslove presovanja u pres komori za vreme izrade drvenih briketa. Uslovi u pres komori mogu značajno uticati na konačan kvaliteta briketa. Rezultati eksperimenta prikazani u ovom radu, opisuju detektovan uticaj temperature presovanja na uslove u pres komori, posebno na sile trenja između zida pres komore i kompresora briketa. Ovaj eksperiment je usmeren na otkrivanje uticaja temperature presovanja i njenu ulogu na kompresovanje u cilindričnoj i kupastoj pres komori. Postavljanjem uslova pritiska moći ćemo da postignemo zadovoljavajući rezultat pritiska u pogledu zahtevanog konačnog kvaliteta briketa.

Ključne reči: biomasa, briketiranje, kompresovanje, temperatura pritiska, gustina briketa

1. INTRODUCTION

For many years we are acting in area of biomass densification. This technology is a suitable option of biomass treatment prior to energy recovery. We are trying to develop a new progressive densification machines and trying to optimize a biomass treatment process before densification. For this reason we built an experimental pressing stand where we can set various monitored parameters and we try to quantify and define the relationships and influence of individual influencing parameters on the final briquettes quality. The results of this experimental research are applicable at densification machines dimensioning. On the base of our research we are able to obtain a comprehensive overview of the parameters behaviors during the densification process. In this article we would like to present experiment results and findings related an impact of pressing temperature during the densification process [1,2,3].

2. PRESSING TEMPERATURE IMPACT

The pressing temperature is one of the technological parameter of densification process. Belongs to the group of 4 significant influencing parameters next to pressing pressure „p“, moisture content „w_r“ and fraction size „L_s“ [4]. The pressing temperature (“T”) has a significant effect on the quality and strength of the briquettes. This parameter determines whether the lignin from the cellular structures is excreted [5,6]. Lignin is a very important substance in the densification process because it has a adhesive effects in the pressed material. The more lignin in the input

material, and the more we can extract in the pressing process, increases the unity and thus quality of the resulting briquette. Lignin strengthens the briquette primarily in compression. Lignin is excreted only at certain pressing temperatures, which must be accounted for in order for the densification process to be successful. Lignin plasticizing temperature and also lignin content depends on the material being pressed. From the existing dependencies between strength and temperature, we know that it is not necessary to excessively increase temperature. Higher temperatures not only evaporate water but also volatile substances. Therefore it is necessary to consider how much is necessary to increase the temperature without losing heating potential of briquette. Volatile substances are by the way very important components of a biofuel in terms of their heating potential.

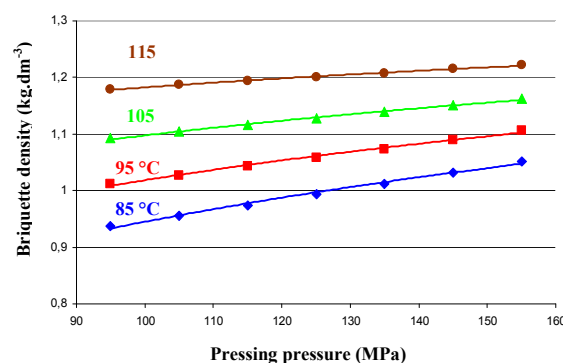


Fig. 1. Briquette density dependence with respect to pressing pressure at various pressing temperatures for pine sawdust (moisture content w_r = 10 %; fraction size L_s = 2 mm)

Lignin properties and behaviour during change of pressing temperature influences final briquettes quality, which is evaluated mainly by density. According above mentioned facts and according to research findings we can say that pressing temperature influences significantly also mutual interactions between pressing pressure, material fraction size and moisture content. On the figures 1, 2 and 3 we can see that pressing temperatures influences positively briquettes density, increases the briquettes density at all dependencies.

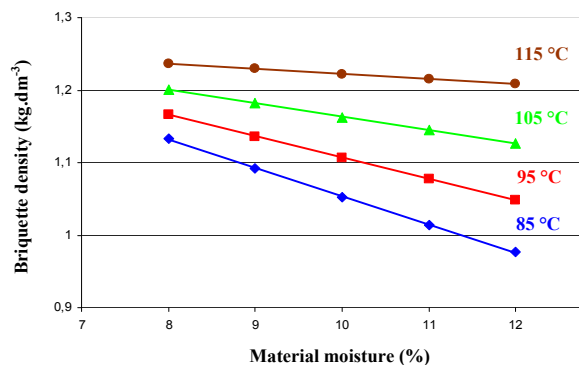


Fig. 2. Briquette density dependence with respect to material moisture at various pressing temperatures for pine sawdust (pressing pressure $p = 155$ MPa; fraction size $L_s = 2$ mm)

Pressure and temperature go „hand in hand“ in the densification process. If we increase the pressure, we can reduce the required temperature and vice versa. This is nicely shown in figure 1. Pressing at higher temperatures obtains the desired density without increasing the pressure. The same tendencies we can see also on moisture content and fraction size dependencies.

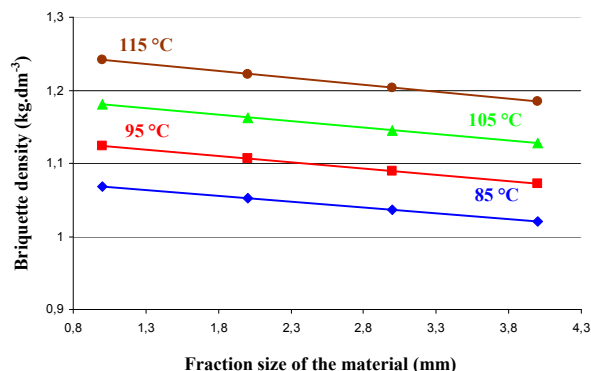


Fig. 3. Briquette density dependence with respect to fraction size at various pressing temperatures for pine sawdust (moisture content $w_r = 10$ %; pressing pressure $p = 155$ MPa)

In the previous part we presented the research findings which describe the impact of pressing temperature on final briquettes quality. According to these results we are able to find an optimal setting of 4 most important influencing parameters for different type of pressed material.

3. IMPACT OF PRESSING TEMPERATURE ON STRUCTURAL PARAMETERS OF CYLINDRICAL CHAMBER

Following research which was done on our department was investigating of pressing temperature impact of structural parameters. Can pressing temperature influence also a pressures distribution in pressing chamber during pressing? We tried to identify impact of pressing temperature in different type of pressing chambers. We designed experimental research and we used for experiment our experimental pressing stand.

In the first phase we tried to find a relationship between length of pressing chamber and briquette density and how can pressing temperature influence this dependence. Experiment was done with cylindrical shape of pressing chamber. Experiment settings were designed according to possibilities of pressing stand dimensions. On the following figure you can see the model of experimental stand where in the middle is situated the pressing chamber.

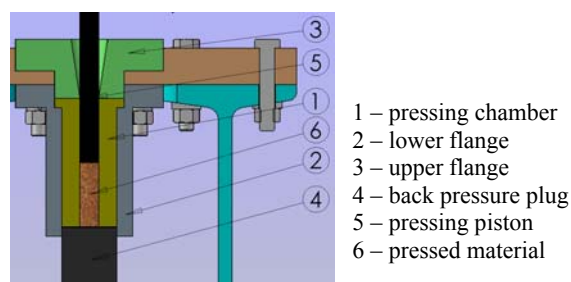


Fig. 4. Cross-section of pressing stand 3D model

We designed experiment with various pressing chambers length (80, 100, 120 and 140 mm) on the base of dimension of pressing stand. Because



Fig. 5. Cylindrical shaped pressing chambers with various length

of pressing stand have only one temperature sensor which is fitted in the middle of the length of pressing stand, pressing chamber with 80 mm length wasn't included in experiment where we increased the pressing temperature. The proof can be seen in the previous figure, where the smallest pressing chamber (80 mm length chamber) don't have the hole for sensor fixation. Technological and material parameter were constant (pine sawdust; fraction size $L_s = 1$ mm; material moisture $w_r = 8$ %). On the following figures we can see the results.

From the results presented on figures 6, 7 and 8 we can say that impact of pressing chamber length on the briquette density is not so significant as the impact of pressing temperature.

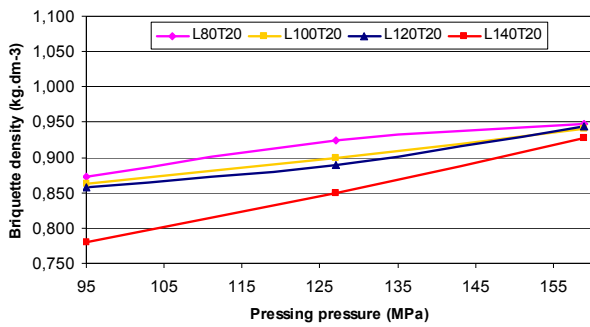


Fig. 6 Briquette density dependence with respect of pressing pressure at various pressing chambers length (at constant pressing temperature T = 20 °C)

When we pressed the briquettes without any pressing temperature (Fig. 6) we had noted that pressing chamber length impact can be most significantly described. With decreasing of pressing chamber length increases the final briquettes density. During pressing without temperature is the final briquette density value influenced mainly by pressing pressure.

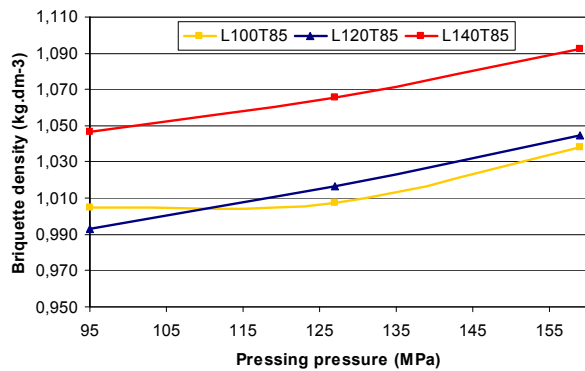


Fig. 7 Briquette density dependence with respect of pressing pressure at various pressing chambers length (at constant pressing temperature T = 85 °C)

During pressing with pressing temperature (85 °C and also at 120 °C is different situation. With increasing of pressing chamber length also increases the final briquette density. Using of higher temperatures occurs better plasticization of lignin in the cell structure of the pressed material. During pressing with some pressing temperature is the final briquette density value influenced mainly by pressing temperature.

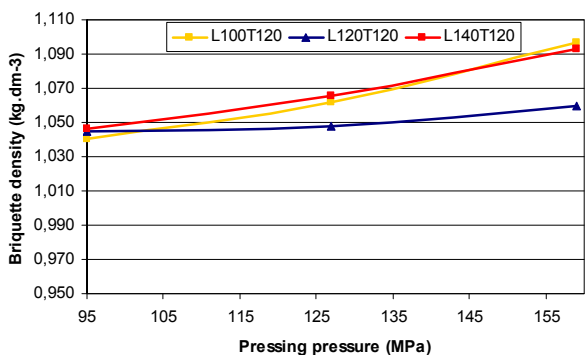


Fig. 8 Briquette density dependence with respect of pressing pressure at various pressing chambers length (at constant pressing temperature T = 120 °C)

4. IMPACT OF PRESSING TEMPERATURE ON STRUCTURAL PARAMETERS OF CYLINDRICAL CHAMBER

In the second phase we tried to identify relationship of pressing temperature, pressing chamber conicalness and briquette density. Experiment was done with conical shaped pressing chamber. Experiment settings were designed according to possibilities of pressing stand dimensions. On the following figure you can see the model of experimental stand where in the middle is situated the pressing chamber.

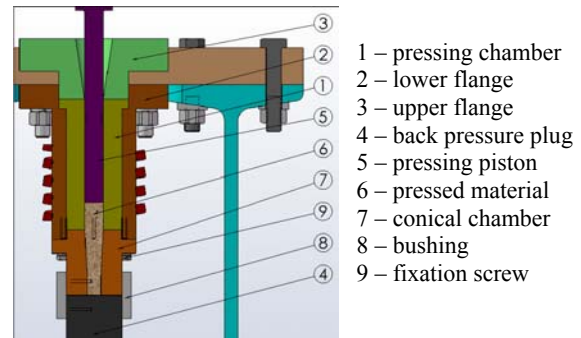


Fig. 9. Cross-section of pressing stand 3D model with conical shaped chamber

We designed experiment with various pressing chambers conical (1°, 2° and 3°) on the base of dimension of pressing stand. Technological and material parameter were constant (pine sawdust; fraction size $L_s = 1$ mm; material moisture $w_r = 8$ %). We tried to identify impact of pressing chamber conicalness on dependence of used pressing temperature (20°C, 85 °C and also at 120 °C).



Fig. 10. Negatives of internal chamber space representing different geometries

In the following table we can see the results – achieved briquettes densities. We can say that with change of cylindrical shaped chamber to conical shaped chamber increases briquettes density. This comes from the different pressures distribution along the pressing chamber during the pressing. Impact of pressing temperature is significant, with increases of pressing temperature also increases the final density. But also we have to say that without additional temperature we weren't able to produce briquettes, because of pressing stand dimensions and maximal values of hydraulic

press. The maximal value of axial pressure what we could use was 318 MPa. Also with this pressure we weren't able to press out the briquettes during pressing without temperature.

$\rho = f(\alpha)$	$T_1 = 20\text{ }^\circ\text{C}$	$T_2 = 85\text{ }^\circ\text{C}$	$T_3 = 120\text{ }^\circ\text{C}$
$\alpha = 0\text{ }^\circ$	0, 852	1, 152	1, 207
$\alpha = 1\text{ }^\circ$	-	1, 221	1, 216
$\alpha = 2\text{ }^\circ$	-	1, 236	1, 224
$\alpha = 3\text{ }^\circ$	-	-	-

Table 1. Experiment results – density of pressed briquettes, in kg/dm^3 (α represents the conicalness of the chamber)

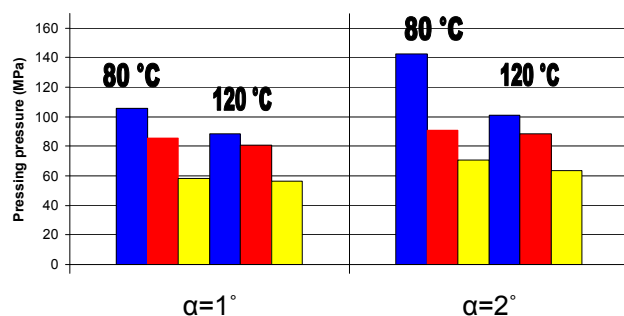


Fig. 11. Comparison of recognized pressures for pressing in conical chambers /blue columns represent the pressure needed to overcome the friction force, red columns represent pressing, and yellow columns represent the pressure needed to extrude the pressed briquette from the chamber/

These figures prove that during pressing with conical chamber acting higher pressures as with cylindrical chamber. We can state that it is possible to increase the pressures acting in the chamber by changing the degree of conicalness of the chamber. However, it can be seen that higher friction forces act in a conical chamber with a higher degree of conicalness. The friction forces can be reduced by a higher pressing temperature. As the pressing temperature increases, the pressing pressure action decreases.

5. CONCLUSION

In this paper was presented results where is identify significant impact of pressing temperature during pressing. A future study should investigate the unit production costs (energy costs and production costs).

6. ACKNOWLEDGEMENTS

The research presented in this paper is an outcome of the project No. APVV-0857-12 “Tools durability research of progressive compacting machine design and development of adaptive control for compaction process” funded by the Slovak Research and Development Agency.

7. REFERENCES

- [1] Horrihgs, W., *Determining the dimensions of extrusion presses with a parallel-wall die channel for the compaction and conveying of bulk solids*, Aufbereitungs – Technik: Magazine, Duisburg, Germany, 1985, No.12.
- [2] Križan, P.; Vukelić, Dj.: *Shape of the pressing chamber for wood biomass compacting*, International Journal for Quality Research, Vol. 2, No. 3 (2008), ART GRAFIKA d.o.o. Podgorica, Montenegro, ISSN 1800-6450, pp. 205-209
- [3] Križan, P.; Matúš, M.; Kers, J.; Vukelić, Dj.: *Change of pressing chamber conicalness at briquetting process in briquetting machine pressing chamber*. In: Acta Polytechnica. - ISSN 1210-2709. - Vol. 52, No. 3 (2012), s. 60-65
- [4] Beniák, J., Ondruška, J., Čačko, V.: *Design process of energy effective shredding machines for biomass treatment*, Acta Polytechnica, ISSN 1210-2709, Vol. 52, No. 5 (2012), pp. 133-137
- [5] Beniák, Juraj: *Zisťovanie význačnosti vybraných parametrov v procese dezintegrácie*. Energetika a životní prostředí 2007 : Sborník přednášek z mezinárodní vědecké konferenci, Ostrava, 26.-27.9. 2007. Ostrava : VŠB TU Ostrava, 2007. ISBN 978-80-248-1586-2. pp. 11-14
- [6] Beniák, Juraj - Šooš, Lubomír - Križan, Peter - Matúš, Miloš: *Influence of the area of disintegrative surface on operating load of disintegrative machine*, ERIN 2013. Proceedings of abstracts with full papers on CD, 7th international conference for young researchers and Ph.D. students. Častá-Papiernička, Slovakia, May 15-17, 2013. Bratislava : Nakladateľstvo STU, 2013. - ISBN 978-80-227-3934-4. - CD-ROM

Authors: M.Sc. Peter Križan, PhD., M.Sc. Michal Svátek, PhD., M.Sc. Miloš Matúš, M.Sc. Juraj Beniák, PhD., Slovak University of Technology in Bratislava, Faculty of Mechanical Engineering, IMSETQM, Nám. Slobody 17, 812 31 Bratislava, Slovakia, Phone.: +421 2 572 96 537, Fax: +421 2 524 97 809.

E-mail: peter.krizan@stuba.sk
svamichal@gmail.com; milos.matus@stuba.sk
juraj.beniak@stuba.sk

Senderská, K., Mareš, A., Kandra T.

TIME ANALYSIS IN THE LEAN ASSEMBLY DESIGN EXCEL APPLICATION

Received: 25 April 2014 / Accepted: 20 May 2014

Abstract: This paper presents Excel application for supporting the lean assembly and especially the part concerned to the time analysis. In the proposed methodological procedure are available three basic modules deals with time. The first is the module for direct time measurement, the second module is designed to evaluate time data using the so-called Yamazumi diagram and the last module is video analysis. In the full Excel application these modules are connected not only together but also with other modules, which are oriented to assembly operations, lay-out design and so on.

Key words: lean assembly, excel application, time analysis

Analiza vremena u excel aplikaciji za podršku projektovanja vitke (Lean) montaže. U predstavljenom radu je prezentovana excel aplikacija za podršku projektovanja vitke montaže sa posebnim osvrtom na analizu vremena. U predloženom metodološkom postupaku postoje tri osnovna modula koje se tiču vremena. Prvi modul je dizajniran za direktno merenje vremena, drugi modul za procenu vremenskih podataka pomoću Yamazumi dijagrama i poslednji modul je video analiza. U kompletnoj Excel aplikaciji ovi moduli su povezani ne samo međusobno, već i sa ostalim modulima, kao što su montažne operacije, lay-out i tako dalje.

Ključne reči: vitka (Lean) montaža, excel aplikacija, analiza vremena

1. INTRODUCTION

The concept of Lean is currently one of the major trends in improving quality and productivity, reducing costs and of course achieving and retaining competitiveness. There are a variety of approaches [1] such as Lean Manufacturing (or Lean Production), Lean Product Development, Lean Service, Lean Maintenance, Lean Logistics, Lean assembly, etc. In the framework of implementation of these concepts is used a variety of methods, techniques and tools such as: 5S method, analysis of bottlenecks, continuous flow, design for manufacturing and assembly (DFMA), settings elimination, balancing (Heijunka), intelligent automation (Jidoka), Just-In-Time, continuous improvement (Kaizen), pull systems (Kanban), the possibility of stopping the line, PDCA (Plan, Do, Check, Act), error-free production (Poka-Yoke), emergence warning in case of problem (Andon), Quality Function Deployment (QFD), shortening the time needed for adjustment (Single Minute Exchange of Die - SMED), standardized work, Cyclic time, Time Based Competition, Time observing, preventive maintenance, Total Quality Management, Visual Management and many others. Some of these tools are supported by software applications, which can be bought, but they can be also developed by their own.

2. ASSEMBLY LABORATORY

Lean Assembly laboratory (Fig. 1) is designed to solve the problems of manual assembly of the products respectively sub-assemblies of small and medium complexity with using of the lean production methods and tools. [2] For design, evaluate and testing of Lean Assembly was designed concept which consist from 16

steps, which should help to achieve optimal design of assembly workstations. The proposed concept allows to design and implement the manual assembly process from the product analysis to the assembly at the workstation respectively workstations with using a lot of methods and tools. Basically the methods and tools are designed so that it is possible:

- to connect the so-called virtual design with the assembly realization in the laboratory,
- to apply integrated and interconnected lean assembly methods,
- to apply the each method also individually,
- in the dependence of the accessible data to use variety input types,
- to compare obtained results in the virtual and experimental phase.



Fig. 1. Manual assembly workstation with Pick-to Light system

3. CONCEPT OF LEAN ASSEMBLY DESIGN

As was mentioned above, designed concept of the lean assembly design consists from 16 steps. They are arranged to three main phases:

- Analytical phase,
- Virtual phase,
- Experimental phase.

In experimental phase, there are three steps for which were developed software application (module). It is step so called Time measuring, step with name Yamazumi diagram and step called Video analysis. Software modules for these steps were developed in Microsoft Excel. Due to reason that there is intended to create complex software tool, which will be able to support all steps in the designed concept the excel application was proposed and elaborated under following conditions:

- each excel module can be used separately,
- for some modules can be selected various inputs,
- the result from one module can be an input for the next one.

3.1 Module for direct time measuring

For direct measurement of the time of assembly on any laboratory workstation or on any other workstation at any location there is available module in which it is possible to measure the duration of the operation simply by pressing start and stop button. In the module (Fig. 2) are currently available 5 forms, calculating the average time and median. In the case that for each operation is available also another time data obtained for example by calculation according to the MTM method there is possibility to calculate deviation. Automatically generated graphs make the viewing of time data more clear.

Application allows to load the assembly operations from the previous modules, namely from the MTM module - time measurement is then performed according to the classification of MTM operations, from the assembly operations analysis module, or it is possible to define own assembly operations.

It contents of the course, the total assembly time. The application also has several features that make work easier for example time deleting data across the whole table by pressing the "Clear Times"

button. Whole concept of excel application is based on 2 macros jointed with buttons - START and STOP created by record of several activities as:

- function Now (),
- cut the cell content,
- insert as value
- go to the appropriate cell

By this record must be executed the condition:

- using of relative references



By button using the cursor position must be in green cell. The moving within the cells is illustrates in the fig. 3.

cursor moving by START

cursor moving by STOP

Fig. 3. Scheme of moving by using the button START and STOP

Gained time data are shown in automatically generated graph (Fig. 4).

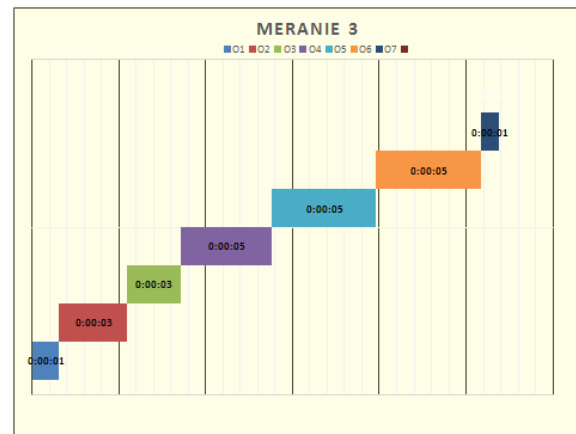


Fig. 4. Automatically generated graph – measuring results

Meranie 2			Meranie 3			M
od	do	celkový čas	od	do	celkový čas	od
			11:13:34	11:13:35	0:00:01	
			11:13:36	11:13:36	0:00:01	
			11:13:37	11:13:37	0:00:00	
			11:13:38	11:13:38	0:00:00	
			11:13:39	11:13:40	0:00:01	

CURSOR POSITION AT THE MEASUREMENT BEGIN

BUTTONS FOR BEGIN AND END OF THE ASSEMBLY OPERATION - TIME DATA

BUTTON FOR CLEARING ALL TIME DATA IN THE TABLE

Fig. 2. The screen of direct time measuring module

3.2 YAMAZUMI diagram

One of the applied methods is Yamazumi diagram. It is a Japanese method dedicated for visual display of time data of several activities identified in the analyzed process. The data are displayed in a bar graph with coloured classification of some activities based on their assignment into identified categories.

Activities marked in green are the activities that create added value; orange colour indicates a required activity such as grasping, clamping, tool gripping and so on. Marked in red are activities that can be considered as redundant – worker walking or container change. These activities would be in the process minimized. In yellow are so called optional activities respectively activities depended on for example by assembled product variant. The blue colour responds to the actions which, are performed always, but the duration may be different, for example can be depended on the assembled product variant. The method is designed either for line balancing or to identify the losses.

Inputs i.e. time data of some activities can be obtained, for example by video analysis, by direct time measuring, by calculating according to any of predefined time method or on the basis of data obtained from sensors.

The Yamazumi applications are usually created in Excel. In the first step of the analysis, it is necessary to define the operations, to assign them the time characteristics and to realize its classification. In the next procedure, based on the above mentioned data will be created the Yamazumi diagram.

On the Fig. 5 is presented the screen of the Yamazumi diagram module.

In the first phase, it is necessary to choose the data source for drawing the diagram. The application offers in the form of checkboxes selection, which cause that relevant data is retrieved directly from the analysis previously realized. Of course you can also choose your own data which will mean, entering own data – it is independent Excel module application use without any relationship or context. Other input data are task or a assembly operation assignment to workstation. The applications offer up to 4 workstations since it is an application designed for laboratory of lean assembly where are four workstations only. It is necessary to adhere sequence of operations. In case that you want to change this sequence, it is necessary to return to the previous step, respectively in mode ‘own’ rearrange the sequence of operations.

The final step in this process is the classification of each task according to the desired range to tasks, which add the value, add no value, etc. The application offers a simple selection from the drop down menu, which is also colour coded according to the usual colour classification.

The result of the application for this method is a diagram from which it is possible to determine the time balancing of the assembly workstations. Then there is also the classification of assembly operation respectively other activities and their colour marking according to the agreed meaning of each colour. At the same time exists the result of the composition i.e. percentage of the number of different types of activities in every workplace - see Fig. 6. These results should obviously be interpreted and can be proposed some measures, which can be translated into new Yamazumi diagram.

The proposed changes can have so character, that will be necessary to go into some of the earlier stages, for example to change the sequence of assembly operations and technological progress.

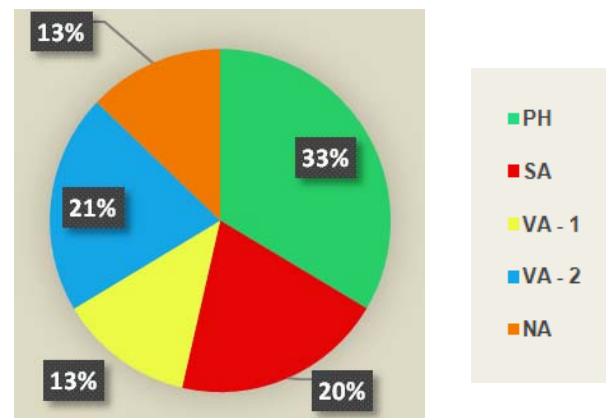


Fig. 6. Automated generated graph of activity types on the workstation 1

3.3 Module for video analysis

Video analysis is one tool for assembly process analysis support. [3] At the workstation is available own software to video analysis as a part of complex concept, which where developed in previous years. Its implementation allows assembly process analysis based on scanned video, to determine the assembly operation structure on the basis of any selected classification, to

INPUT DATA – TASKS OR ASSEMBLY OPERATIONS AND TIME			SELECTION OF THE WORKSTATION AND ACTIVITY TYPE SPECIFICATION					
Nr.	Task	Time	Workstation selection	Type of activity	Workstation 1	Workstation 2	Workstation 3	Workstation 4
1	osadiť	0:03:09	Workstation 1	PH	0:03:09			
2	lisovať	0:09:17	Workstation 2	VA - 2		0:09:17		
3	skrutkovať	0:02:39	Workstation 2	VA - 1		0:02:39		
4	položiť	0:03:12	Workstation 3	PH			0:03:12	
5	uchopiť	0:09:35	Workstation 3	VA - 2			0:09:35	
6	točiť	0:02:39	Workstation 3	NA			0:02:39	
7	zahnúť	0:03:17	Workstation 4	VA - 1				0:03:17
8	točiť	0:09:11	Workstation 4	PH				0:09:11

Fig. 5. The screen of YAMAUMI diagram template

identify the times as well as efficient or inefficient assembly operations. The video analysis output e.g. time data then will be processed in an application created in Microsoft Excel. On the Fig. 7 and 8 are print screens from excel module – data processing and generated graph.

Left hand						
P.č.	Move	symbol	from	to	Time in TMU	effectivity (e/n)
1	Reach	R	6	7,03	28,63	e
2	Grasp	G	7,03	7,11	2,22	e
3	Move	M	7,11	8,6	41,42	n
4	Place	P	8,6	12,8	115,93	e
5	Wait	W	12,77	13,8	28,08	n
6	Reach	R	13,78	14,5	18,63	e
7	Grasp	G	14,45	14,5	1,67	e
8	Reach	R	14,51	15,2	18,07	e
9	Grasp	G	15,16	15,4	7,23	e
10	Move	M	15,42	16	16,68	e
11	Reach	R	16,02	17	27,24	e
12	Grasp	G	17	17,4	11,12	e
13	Move	M	17,4	18,3	24,19	e
14	Wait	W	18,27	19,1	22,80	e
15	Screw	S	19,09	20,9	50,87	e
16	Reach	R	20,92	21,3	9,17	e

Fig. 7. Print screen of excel application

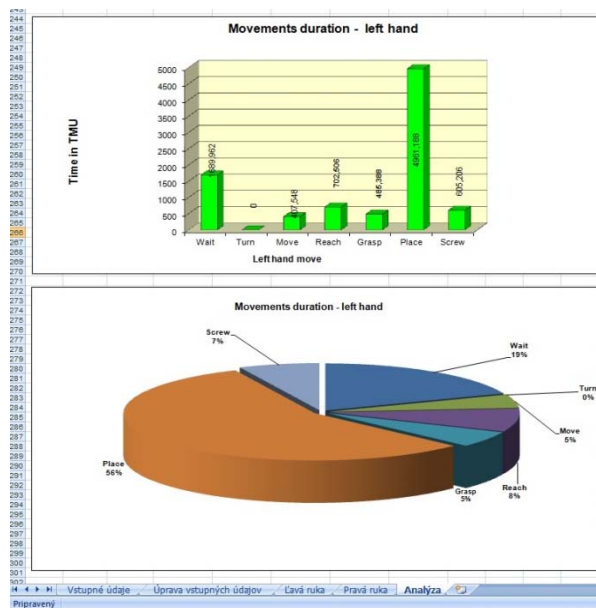


Fig. 8. Graphs generated in excel application for video analysis

4. CONCLUSION

Created and presented a software applications to support the lean assembly workstation design greatly accelerate the work and allow more efficient assembly workstation design. The advantage of such applications is their elaborating in Microsoft Excel which can be according to the needs adapted and supplemented by any additional features. Experiences with their using suggest, that this is a promising direction of the development and in the future will be elaborate also other Excel applications for other steps of the proposed procedure for creating lean assembly workstations.

ACKNOWLEDGEMENTS: This contribution is the result of the project VEGA 1/0879/13: Agile, to the market adaptable enterprise systems with high flexible organization structure.

5. REFERENCES

- [1] Rudy, V., Kováč, J.: *Innovation methods of model design of structures of production systems*. In: Oraldyn, fylým žaršycy. Vol. 15, no. 7, 2008, pp. 47-51. ISSN 1561-6908
- [2] Senderská, K., Lešková, A., Mareš, A.: *Design characteristics of manual assembly workstation system in the Lean production structures*. In: Journal of Production Engineering. Vol. 16, no. 1, 2013, pp. 87-92. ISSN 1821-4932
- [3] Mareš, A., Senderská, K.: *Experiences with the application of video analysis in the manual assembly*. In: Machines, Technologies, Materials. Vol. 6, no. 3 2012, pp. 17-19. ISSN 1313-0226

Authors: Ing. Katarína Senderská, PhD., Ing. Albert Mareš, PhD., Bc. Tomáš Kandra, Technical University of Košice, Faculty of Mechanical Engineering, Department of Technologies and Materials, Masiarska 74, 04001 Košice, Slovakia.

E-mail: katarina.senderska@tuke.sk
albert.mares@tuke.sk
tommy.kandra@gmail.com

Salokyová, Š., Gerková, J.

SCANNING AND EVALUATING VIBRATIONS ON A LABORATORY MODEL

Received: 28 May 2014 / Accepted: 20 June 2014

Abstract: Monitoring of the technical state through the means of vibrodiagnostics is the basic presumption of operation of machines and devices according to real state. The article deals with the issue of measuring and evaluating vibrations on the bearing dome of the rotating device generated through the frequency changer on the laboratory model. During the measurement of the motor rotations and load on the rotating disc we changed with weights. The basic goal of vibration observation is to provide basic information about the operation and technical state of the device in production system.

Key words: diagnostics, experiment, vibration, accelerometer, SignalExpress

Prikupljanje i vrednovanje vibracija na laboratorijskom modelu. Praćenje stanja kroz tehničku vibrodiagnostiku je bitan preduslov za rad mašina i opreme u skladu sa aktuelnom situacijom. Ovaj rad se bavi merenjem i procenom vibracija na kućištu za ležaje pomoću rotirajućeg uređaja sa pobudnim frekventnim regulatorom na laboratorijskom modelu. Tokom merenja različite brojeve obrtaja motora i opterećenja na rotirajućem točku smo dobijali sa tegovima. Osnovni cilj je da se obezbede osnovne informacije praćenjem vibracija o operativnom i tehničkom stanju opreme u proizvodnim sistemima.

Ključne reči: dijagnostika, eksperiment, vibracija, akcelerometar, SignalEkpress

1. INTRODUCTION

Vibrodiagnostics is one of the most commonly used methods of technical diagnostics used in rotation devices. The main part of these devices is the bearing, which secures the rotation movement and catches the dynamic load. Failure-free operation and general lifespan of the device depends significantly on the state of the bearing, on its lifespan. In an ideal case with quality bearings the lifespan could be unlimited; this is why it is important to come as close as possible to the ideal state. It begins with the professional installation of the bearing thanks to specialized tools with observing the required cleanliness during the installation and proper lubrication regime. If these conditions are met, then the lifespan is affected only by the dynamic forces during the operation, which are caused by other parts or their failures. The job of vibroagnostics is on one hand to find hidden defects of the parts, which have a significant influence on the quicker wear of the bearings and on the other hand to observe the state of the bearings themselves. Diagnostics thus increases the security, reliability, lifespan and last but not least, it reduces the costs for maintenance [1-6]. The article deals with the generation and observation of vibrations on the bearing with a rotating device on the laboratory model during the change of the engine rotations selected in advance with the use of asymmetrical load thanks to weights.

2. CONDITIONS OF THE EXPERIMENT

The experiments were performed in the laboratory of diagnostics of operation states of the production systems at the Department of operation of production

processes, Faculty of production technologies in Prešov. 9 sequential measurements split into 3 experiments were performed. During the measurement of the electromotor rotations changed with the help of a frequency changer (800 rpms, 1000 rpms and 3000 rpms) and the asymmetrical load with the help of weights. The structure of the experiments plan is depicted in figure 1.

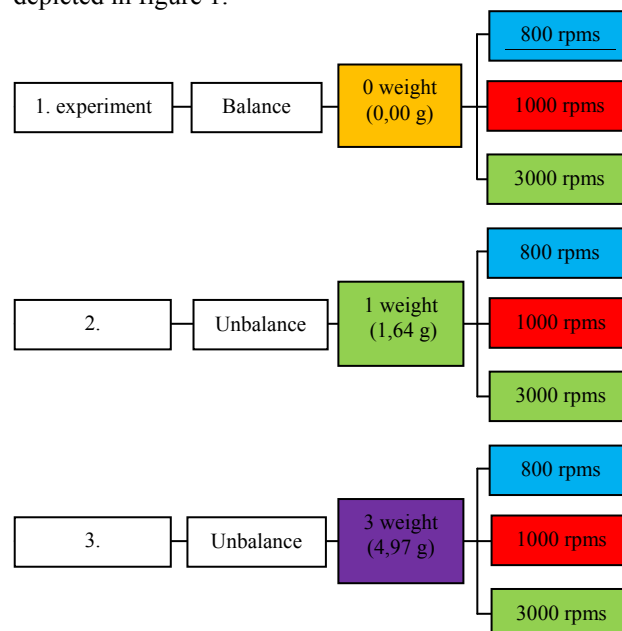


Fig. 1 Structure of the experiments plan

The vibrations were observed on the bearing dome 2 through a piezoelectric sensor attached by a quick glue (figure 2) and an example of an asymmetrical load of the monitored shaft with three weights on the inner rotating disc is depicted on figure 3.

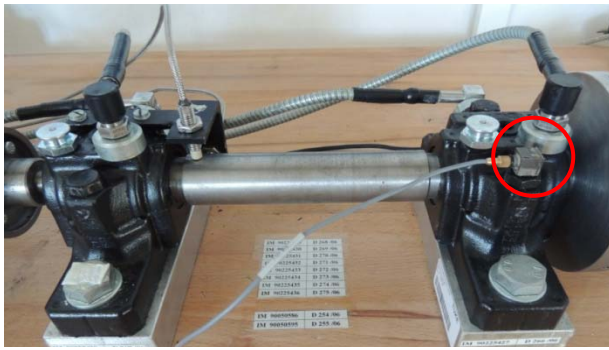


Fig. 2 Placement of sensor on the bearing dome 2

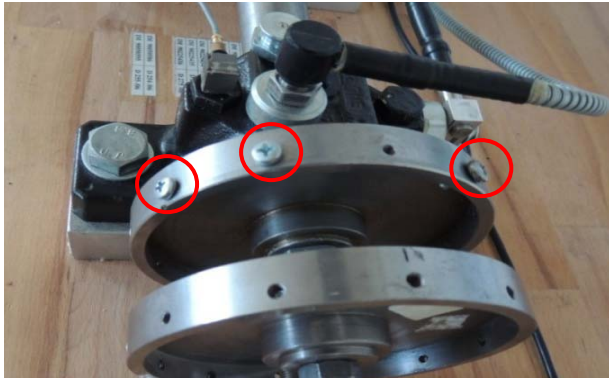


Fig. 3 Lack of balance with 3 weights

3. LABORATORY MODEL FOR GENERATION OF VIBRATIONS

The block diagram of the laboratory model for generation of vibrations is depicted on figure 4 [4].

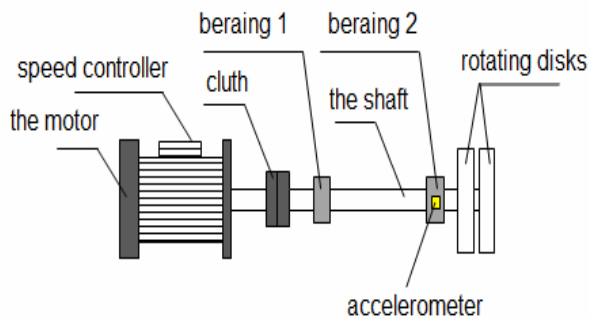


Fig. 4 Diagram of the vibrodiagnostic laboratory model

4. TECHNICAL SYSTEM FOR MEASUREMENT AND EVALUATION OF VIBRATIONS

Piezoelectric accelerometer of the Brüel & Kjær company (type: 4507-B-004, parameters: IEPE, TEDS, 1-axis, 100mV/g) was attached to the head (Pic. 2) so that its axis would be identical with the axis of the vibrations in the direction of the abrasive water current. The accelerometer was attached to the AD converter (AI $\pm 5V$ IEPE, sampling rate 25kSps) through which the created data record is stored in the PC (LENOVO) as a time record of the vibration acceleration signal [6].

The SignalExpress software was used for evaluation of the time signal, which is part of the programming and developmental environment LabVIEW of the

National Instruments company. Part of a steady course of 10 seconds was selected from the time record and from it, through Fourier transformation, a frequency spectrum of the 0 – 10 kHz range was generated. The cover of the frequency spectrum was created through the use of an algorithm filter, created with the help of the Microsoft Office Excel software [7,8].

5. MEASURED VALUES

Measured values for individual experiments and three examined rotations of the motor (800, 1000 and 3000 rpms) are depicted in the form of time courses of the vibration acceleration amplitude. An example of a time course of the vibration acceleration amplitude for motor rotations of 800 rpms without any load and with the load of one weight is depicted on the figures 5 a 6.

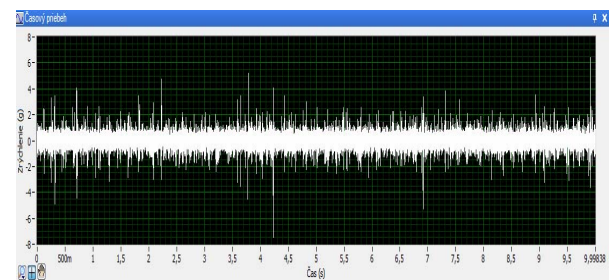


Fig. 5 Course of the vibration acceleration amplitude related to time balanced at 800 rpms of the electromotor

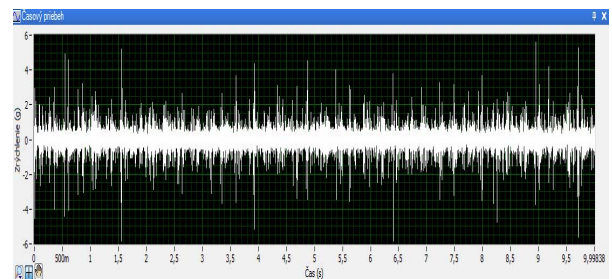


Fig. 6 Course of the vibration acceleration amplitude related to time with an unbalance of 1,64 g at 800 rpms of the electromotor

6. EVALUATION OF THE MEASURED VALUES

The evaluation consists of the creation of frequency spectrums of the vibration acceleration amplitude in the range 0 – 10 kHz. The change of the vibration acceleration amplitude's course on the frequency balanced at 800 rpms is depicted as an example on figure 7 and the cover of the frequency spectrum on figure 8. Analogous graphic dependency on the frequency at the speed of 800 rpms is depicted on figure 9. The cover of the frequency spectrum is depicted on figure 10. Analogously depicted were graphical dependencies of the acceleration amplitude, frequency vibrations and covers of the frequency spectrum with speeds of 1000 and 3000 rpms for balance and unbalance with one and three weights.

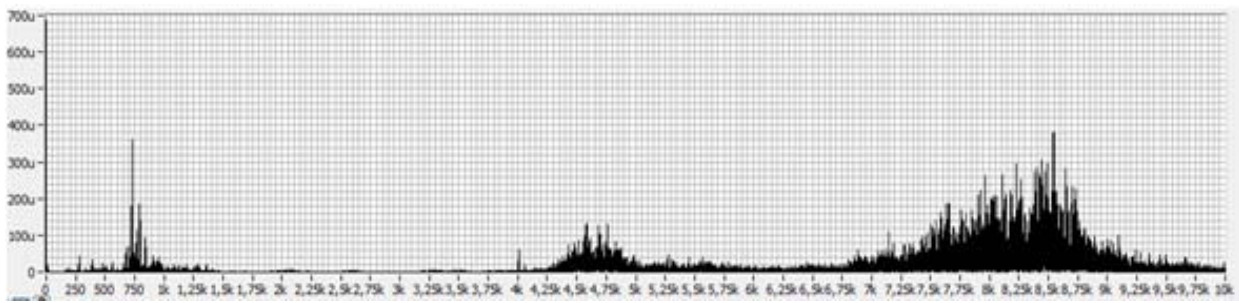


Fig. 7 Graphical dependency of the acceleration amplitude and vibration frequency balanced at 800 rpms of the electromotor

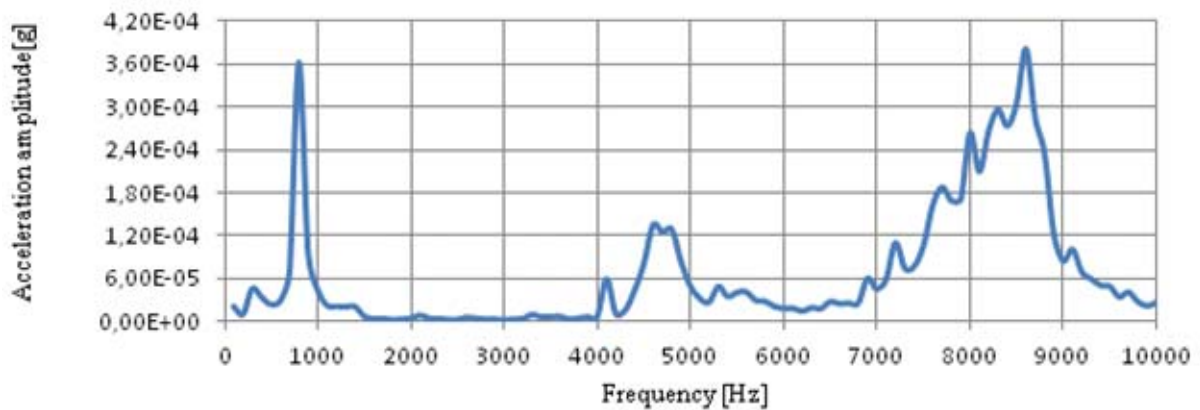


Fig. 8 Cover of the vibration frequency spectrum on the bearing dome balanced at 800 rpms of the electromotor

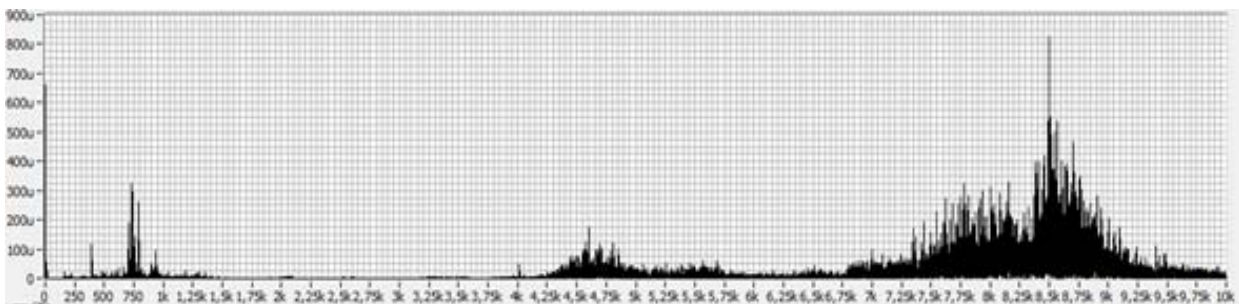


Fig. 9 Graphical dependency of the acceleration amplitude and vibration frequency with an unbalance of 1,64 g at 800 rpms of the electromotor

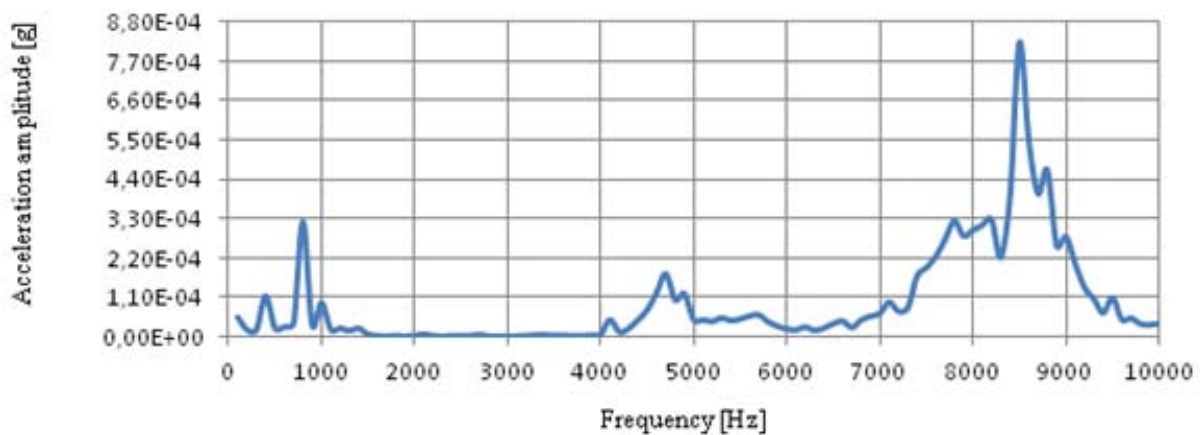


Fig. 10 Cover of the vibration frequency spectrum on the bearing dome with an unbalance of 1,64 g at 800 rpms of the electromotor

The comparison of the graphics of the covers of vibrations accelerations amplitudes and frequency spectrums individually for 3 examined experiments is depicted on the figures 11 through 13.

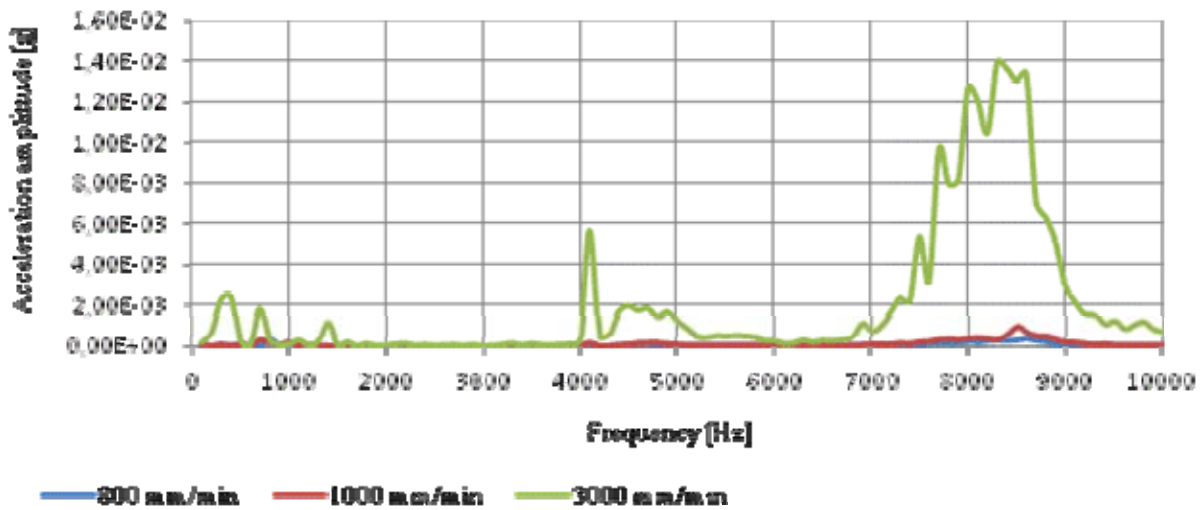


Fig. 11 Comparison diagram of the covers of the frequency spectrums on the bearing dome balanced at all three examined rpms of the motor

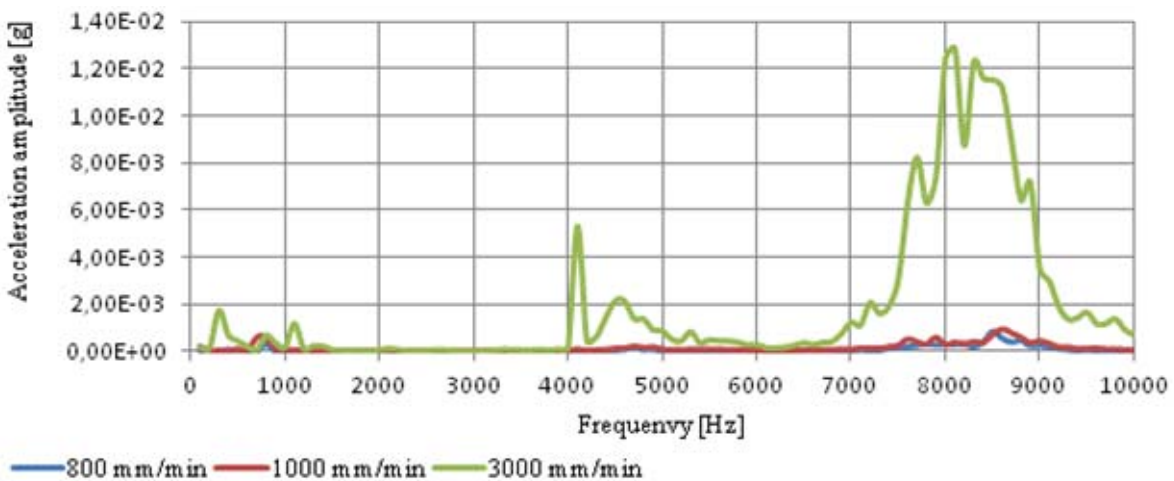


Fig. 12 Comparison diagram of the covers of the frequency spectrums on the bearing dome with an unbalance of 1,64 g at all three examined rpms of the motor

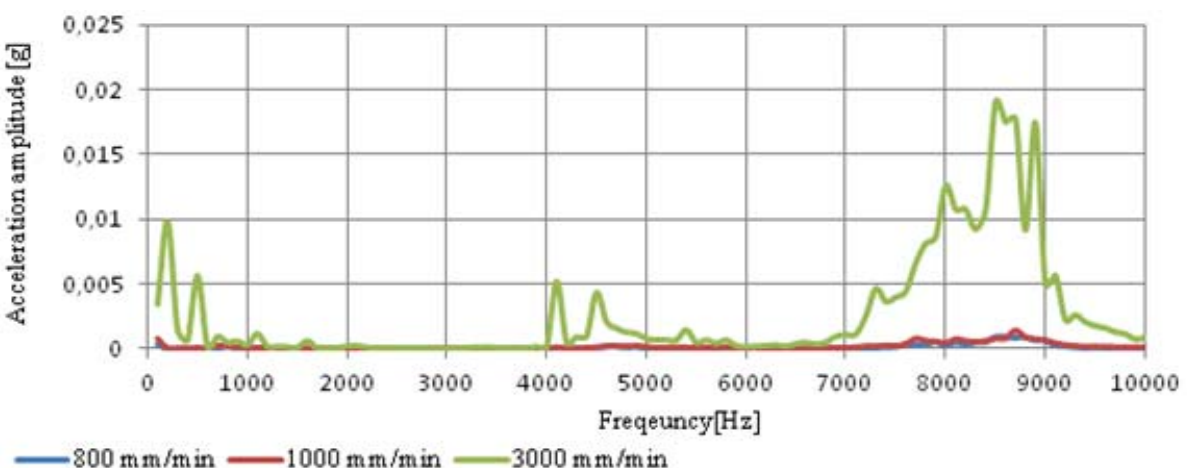


Fig. 13 Comparison diagram of the covers of the frequency spectrums on the bearing dome with an unbalance of 4,97 g at all three examined rpms of the motor

7. DISCUSSION ON THE ACHIEVED RESULTS

A set of new knowledge is formulated based on the comparison and analysis of the course of the frequency

spectrums of the vibration acceleration amplitude on the bearing dome of the monitored shaft:

- at the three observed rpms of the electromotor 800, 1000 and 3000 rpms, under balance and unbalance of the monitored shaft, the highest values of the

- vibrations of the observed range 0-10 kHz are found in the frequency spectrum 7,0 through 10,0 kHz
- the size of the vibration acceleration amplitude under balance of the monitored shaft in the examined range reaches the highest value 1,39 mg at the frequency 8,3 kHz and 3000 rpms of the motor
 - the size of the vibration acceleration amplitude with unbalance of the monitored shaft with one weight (1,64 g) in the examined range reaches the highest value 1,22 mg at the frequency 8,3 kHz and 3000 rpms of the motor
 - the size of the vibration acceleration amplitude with unbalance of the monitored shaft with three weights (4,97 g) in the examined range reaches the highest value 1,9 mg at the frequency 8,35 kHz and 3000 rpms of the motor
 - with the growing numeric value of the motor's rpms under balance in the examined range, the vibration acceleration amplitude regularly increases and compared for the 800 rpms and 3000 rpms increases 97,25 %
 - with the growing numeric value of the motor's rpms and an unbalance with the use of 1 weight of 1,64 g in the examined range, the vibration acceleration amplitude regularly increases and compared for the 800 rpms and 3000 rpms increases 93,25 %
 - with the growing numeric value of the motor's rpms and an unbalance with the use of 3 weights of 4,97 g in the examined range, the vibration acceleration amplitude regularly increases and compared for the 800 rpms and 3000 rpms increases 95,13 %

8. CONCLUSION

The goal of this article was to examine on a laboratory model the load of the monitored shaft with the help of various weighs with variable rpms of the electromotor. It can be said that the bigger the load on the rotating discs, the more the value of the vibrations regularly grows. Analysis of the graphical dependencies of the vibration acceleration amplitude on frequencies indicates, that the measured vibration values are within the bounds of the normal and there is no probability of a premature defect occurrence on the laboratory model under selected conditions.

The measurement showed, that vibrodiagnostics is an effective tool for measurement of the technical state of devices. However for a closer and more precise diagnostic of the defect, several measurements have to be performed and they have to be compared one against the other.

9. ACKNOWLEDGEMENT AND REFERENCES

The research work was supported by the Project of the SF of the EU, Operational Programme Research and Development, Measure 2.2 Transfer of knowledge and technology from research and development into practice, project: Research and development of intelligent nonconventional actuators based on artificial muscles. ITMS code: 26220220103.

9. REFERENCES

- [1] Maňková, I.: *Progresívne technológie*. Košice: Technická univerzita Košice, Strojnícka fakulta – edícia vedeckej a odbornej literatúry 2000. 275 s. ISBN 80-7099-430-4
- [2] Stejskal, T., Valenčík, Š.: *Technická diagnostika*. 1. vyd. Košice : TU, 2009. 215 s. ISBN 978-80-553-0313-0
- [3] Kreheľ, R.: *Vibračná diagnostika rotujúcich strojov*. 2007. In: MM. Průmyslové spektrum. No. 7,8 (2007), p. 29. ISSN 1212-2572
- [4] Kreheľ, R.: *Technický systém k diagnostike prevádzkového stavu strojov a zariadení*. 2008. In: Technika a trh. Vol. 16, no. 12 (2008), p. 60-61. ISSN 1210-5902
- [5] Šoltéssová, S., Baron, P., Simkulet, V., Marcinková, M.: *Konkrétne metódy technickej diagnostiky určené pre sledovanie a monitorovanie stavu výrobných strojov a zariadení*. 2013. In: Posterus. Roč. 6, č. 9 (2013), s. 1-6. - ISSN 1338-0087
- [6] Panda, A., Prislupčák, M.: *Technologické faktory pôsobiace na obrábanie*. In: Trendy a inovatívne prístupy v podnikových procesoch : 16. medzinárodná vedecká konferencia : 7. - 8.november 2013, Košice, 2013 S. 1-7. ISBN 978-80-553-1548-5
- [7] Fabian, S., Krenický, T.: *Využitie vybraných vibrodiagnostických metód v monitoringu prevádzkových charakteristík strojových zariadení*. 2010. In: Spravodaj ATD SR. Č. 1,2 (2010), s. 32-34. - ISSN 1337-8252
- [8] Fabian, S. - Salokyová, Š.: *Experimental verification of abrasive mass flow impact on the technological head acceleration amplitude and vibrations frequency in the production system with AWJ technology*. In: *Manufacturing technology*. Vol. 12, no. 12 (2012), p. 18-21. - ISSN 1213-2489

Authors: Ing. Štefánia Salokyová, Phd., Ing. Jana Gerková, Technical University of Košice, Faculty of Manufacturing Technologies, Department of Manufacturing Processes Operation, Bayerova 1, 080 01 Prešov, Slovakia
E-mail: stefania.salokyova@tuke.sk
jana.gerkova@tuke.sk



Klos, Z.

A SIMPLE TOOL FOR QUALITY IMPROVEMENT OF TECHNICAL OBJECTS AND PROCESSES

Received: 05 June 2014 / Accepted: 20 June 2014

Abstract: *The companies are forced to improve the quality of their products and services. Large organizations usually have their own R&D departments, but SMEs have problems with developing new solutions. Since 2000, at Faculty of Machines and Transport, Poznan University of Technology, the »International Summer School of Solving Technical Problems in Mechanics, Material Engineering and Transport« is organized. One of the aims of this event is to deliver the proposals of solutions for technological, design or organizational problems that industrial companies face every day. Experiences coming from the performance of this university-industry event are presented in the paper.*

Key words: *quality improvement, technical objects, processes, summer school, teaching tool*

Jednostavan alat za unapređenje kvaliteta tehničkih objekata i procesa. *Kompanije su primorane da poboljšaju kvalitet svojih proizvoda i usluga. Velike organizacije obično imaju svoje R & D odeljenja, ali mala i srednja preduzeća imaju problema sa razvojem novih rešenja. Od 2000 godine, na Fakultetu za mašine i transport, Poznanskog Tehnološkog Univerziteta, organizovana je »Međunarodna letnja škola rešavanja tehničkih problema u mehanici, materijalnom inženjerstvu i transportu«. Jedan od ciljeva ove manifestacije je da dostavi predloge rešenja tehnoloških, dizajnerskih ili organizacionih problema sa kojima se industrijske firme suočavaju svaki dan. U ovom radu su predstavljena iskustva iz učestvovanja pomenutog univerziteta na ovom događaju.*

Ključne reči: *poboljšanje kvaliteta, tehnički objekti, procesi, letnja škola, nastavno sredstvo*

1. INTRODUCTION

Institutions of higher education play a significant role in contribution to the growth of places where they act. This is the plain truth and nobody needs to be convinced. On one hand, a close relationship between the economic and on the other, business life of the city and a connection between academic and cultural spheres. However, the benefits derived from the latter are not always as immediately felt by the city as the tangible ones stemming e.g. from an expressway or a modern airport. Similar situation, but on the smaller scale in another range, can be observed when new initiatives of improvement are introduced to the education process. The attempts in this direction, with the special emphasis on project organized problem oriented activities are made at the Faculty of Machines and Transport (FMT), Poznan University of Technology (PUT). So called the POPBL aims at learning by solving problems using practical experience linked with theoretical knowledge. The teaching is based there on the project organization where the participants analyze the problems and solve them by integrating theory and practice, which are usually interdisciplinary. About one of these activities is this paper.

2. FEW WORDS ABOUT PUT AND FMT

Predecessor of Poznan University of Technology – The State Higher School of Mechanical Engineering – was founded in the year 1919. From this time the education lasted three years and since 1927 – seven

semesters. The Higher School was given the status of a university in 1945. Finally, during a number of transformations, the university received the present name in 1955. Actually about 21 000 students are studying at PUT, locating this university in second place in Poznan. Poznan, fourth academic center in Poland, with population of some 560 000 inhabitants (agglomeration – 950 000 inhabitants) attracts actually nearly 140 000 young people, who are studying in 17 university level institutions.

At the beginning Poznan University of Technology had 3 faculties: Electrical, Civil Engineering and Mechanical. Those faculties were transformed and the last one was split in 1953 and one of faculties which arisen was the Faculty of Agricultural Mechanization. The research there was dedicated to agricultural machinery. Since 1957 the education lasted five years. Within the years this faculty was changing its profile and considerably the name. In the year 1967 it was renamed as the Faculty of Machines and Vehicles and its present name – the Faculty of Machines and Transportation – was given in 2000.

Today within the faculty one can distinguish Institute of Machines and Motor Vehicles, Institute of Internal Combustion Engines and Transportation, Chair of Thermal Engineering and Chair of Basics of Machine Design. The fields of study which students can study are mechanics and mechanical engineering, and transportation. The education lasts seven semesters to reach Bachelor of Science in Engineering, next three semesters to obtain Master of Science in Engineering and four years during doctor's studies.

There is observed a growing number of students interested in studying at the FMT. At the beginning of 90's the number of them was about 600 and today there are studying around 2200 persons, despite population decline tendency in region and in Poland.

3. INTERNATIONAL SUMMER SCHOOL

3.1 Basis – quality and innovation

In societies, where basic needs are met the quality started to be most wanted category, when we consider produced products, i. e. goods and services. This rule is valid, if we analyze different economy branches and of course if we speak about other areas, e.g. education. Quality is often used to signify “excellence” of a good or service. People talk about “top quality” or using the name of one brand – “Rolls Royce quality”. In manufacturing companies the word “quality” may be used to show that a piece of material, part of machines or element of appliance, conforms to certain physical dimensional characteristics set down in the form of tight specification. If we are to define quality in the way it is useful, we have to recognize the need to include in the evaluation of quality the requirements of central figure in this issues – the customer, his/hers needs and expectations. Now, in the whole process leading to achieve top quality, the generation, exploitation and diffusion of knowledge are fundamental activities to economic growth, development and the well being of nations. Central to this is the necessity of creating and implementing the innovations. Over time, the nature and landscape of innovation has changed but the need of innovation is constantly increasing.

“The knowledge-based economy” is an expression coined to describe trends in advanced economies towards greater dependence on knowledge, information and high skill levels, and the increasing need for ready access to all of these by the business and public sectors. Knowledge and technology have become increasingly complex, raising the importance of links between companies and other organizations as a way to acquire specialized knowledge.

Innovation is central to the growth of output and productivity. However, while the understanding of innovation activities has greatly increased lately, the role of their economic impact is still deficient. For example, as the world economy evolves, so does the process of innovation. Globalization has led to dramatic increases in access to information and new markets for enterprises. It has also resulted in greater international competition and new organizational forms in order to manage global supply chains. Owing to advances in technologies and greater flows of information, knowledge and innovation is more and more viewed as a central driver of economic growth. Yet, we do not fully understand how these factors affect innovation [1]. Moreover, it is still not obvious that from innovation is the straight way to achieve the excellence in business. To meet these needs halfway the *International Summer School (ISS)* idea was risen and elaborated then into the educational project.

3.2. Organization of ISS

The project called the *International Summer School of Solving Technical Problems in Mechanics, Material Sciences and Transportation* was initiated in 2000 [2]. From that time, this annual 5-days workshop is organized usually in September. It focuses each year an attention on 30-40 students from different countries, first of from Poland, but also from Czech Republic, Slovakia, Germany, Portugal, Hungary and Slovenia.

The idea of the *International Summer School* is concentrated on cooperation between students and different companies from Poland, especially from Wielkopolska Region (Poznan is the capital of this Polands mid-west region). There are two main objectives of the project. The first one is dedicated to companies and it is concentrated on introduction of innovative solutions and in this way improving the quality in different areas of company, e.g. production line, transportation process, organizational rules. The second one puts a stress on development of students' knowledge and creativity. As future engineers, students play there a role of complex problems' solvers [3].

The companies, which take part in ISS, represent different branches of industry. Some of them such as a producer of household equipment or a producer of precise measurement devices take a part in this innovation initiative since the very beginning. The problems they present are always vivid. The most important features of those subjects are as follows:

- precisely defined problem situations,
- interdisciplinary character; most of them link different aspects, i.e. technical, economical, organizational,
- a uniqueness, which is a result of a very specific problem formulation.

Students' potential can be seen in their solutions, which are expected to be creative, innovative, including all the goals, assumptions and thresholds.

An organization of the workshop starts at the beginning of the calendar year. It is a time when an organizing committee is formed. Usually it consists of some 5 persons, mainly Ph.D. students. The inviting letters are prepared and send to companies, potentially interested in participation in this event.

Next step is highly connected with marketing. Information about a workshop is distributed to students, specially the best ones, working among others in the frame of Academic Working Group in Mechanics. The most fruitful for gaining the ISS participants are meetings with students. There are also prepared posters and leaflets, distributed in the area of PUT campus. Potential participants can visit web site with detailed information about the *International Summer School*. There is also available a registration form which can be sent to the workshop secretariat.

3.3 The International Summer School schedule

The ISS always starts on Monday by a students' registration. The participants receive a work package including a detailed schedule of the *International Summer School*, technical drawings, companies' prospects, description of the problem to solve and other information materials. After a registration the opening

ceremony begins. During this time there is delivered an invited lecture. Main subjects of these lectures focus on the different aspects of the methodology of the creative solving of engineering problems or other dilemmas. There are here invited lecturers, who deliver the most advanced and actual knowledge on these issues. Then an organizational information is also introduced. The representatives of the companies present problems to be solved. The list of selected topics is presented in Table 1.

Year	No.	Problem formulation
2002	1.	Dust elimination during fertilizer's transferring process
	2.	Optimization of internal transport system using Just-in-Time method
2003	1.	Methods of rapid bonding between glass, ceramics and metal elements
	2.	Project of transportation process of products from three packaging machines to one collection point
2004	1.	Aesthetic finish of fixing a specific element of the refrigerator
	2.	Hermetic seal of plastic packaging project using foil
2006	1.	Washing powder dose system leading to the energy and washing powder reduction
	2.	Identification of transportation development strategies on Baltic Sea Regions, including strengths and weaknesses analysis
2007	1.	A construction of universal pliers for ring installment in water meter for better access and ergonomics
	2.	An algorithm for determination of separator size based on processing data
2009	1.	Activities aimed at raising accuracy and culture of work on the production line in factory
	2.	Optimisation of bus floor service hatches construction in means of thermal and acoustic insulation
2011	1.	Protection against accidental activation of the kitchen by children
	2.	Analysis of the plywood flooring installation system, including their physical characteristics and development of a method of connecting joints in places
2012	1.	Alternative drive concept of the packaging machine dispensing the butter and margarine into cubes
	2.	Optimization of the oven burner assembly operations
2013	1.	The process of assembling and checking COAX connector for a thermocouple in a gas stove
	2.	Three concepts for pipeline and electrical assembly inside the vehicle with a selection of market assembly elements including technical and economical criteria

Table 1. List of selected problems on ISS

Students are divided into the groups of around 3-4 persons. It is badly seen establishing "national teams" and the ISS organizers' make an effort to integrate participants. As the result, it is a principle that the foreign students join the different groups. Each problem is solved by two competing teams. Groups of students can cooperate, but the proposed solutions must be different and unique. It is also possible and often met that one group is working on more than one solution of a problem, indicating on their advantages and disadvantages. Monday is also a day when in the evening a social integration trip is organized.

During this workshop students visit companies (usually on Tuesday), especially those located in Poznan or nearby, learning more about them and the problem there are to solve. Students can also consult their ideas of solutions with employees of these companies.

A very important roles have university employees, usually professors and doctors, often with industrial experience, who may play the role of advisers, very helpful in providing a methodological background to students' work.

Participants can consult their ideas from Tuesday until Thursday. Thursday is also the last day of students' creative work. Until 8 p.m. they are obliged to prepare and deliver the report to the Organizing Committee. This is a formal document, which finally goes to the companies. It is constructed on the basis of the following points:

- title of the project,
- the name of the participants (with an indication of the group's leader),
- abstract,
- introduction,
- problem presentation (with short description of the company and problem classification),
- problem solution or solutions (the method or methods of solving the problem and problem presentation),
- conclusions,
- references,
- enclosures.

Finally, in the last day of ISS, at Friday, students present the results of their work on the project. The time for each presentation is limited to 15 - 20 minutes, with 5 - 10 minutes for discussion with the jury members and other ISS participants. The number of presenters per group is not defined. Students can use supporting equipment.

Each project is judged by a jury (commission), i.e. the representatives of the university and companies, in the number of some 10 persons. One of the most important features is its objectiveness. The members of the jury are the persons not directly engaged in projects. The jury meets after all presentations and notes for each group are given. The marking scheme goes beyond simply marking a presentation. Similarly as in the case presented by [4,5] the factors, that are taken into account are as follows:

- creativeness (initiative and ideas),
- uniqueness,

- level of problem understanding,
- advancement of the project realization.

The maximum note the group can receive equals 10 points. The quality of the presentation is also marked and the notes are as follows: -1, 0 and 1. It forces students to show also their entrepreneurial skills. All those marks are collected in the form and an overall note and opinion are delivered.

The final notes are presented during the closing ceremony, which is at Friday afternoon. It is done during the nice event – the standing party. It gives the frames to direct meetings between students from the one side and representatives of companies and university from the other side. The more advanced and more interested solutions are rewarded. All students also receive a certificate of participation in ISS. This document includes information about the note they get.

One of the advantages of this workshop is a self-learning. It comes through the learning by doing and interacting with experts. This kind of experimentation is defined by El-Raghy (1999) as one of three of the most important quality engineering education skills. This is the time when learning, according to New Learning Paradigm presented by Hills and Tedford [3], is seen as an active process in which concepts are acquired, incorporated into appropriate schemes and tested in action.

Next very important feature of the workshop is a communication. The language, which is meant as the carrier of ideas during conversation or in writing, students operate is English. El-Raghy [6] indicates that it is essential for practicing engineer to know at least one foreign language and Riemer [7] emphasizes the role the English language plays for today “global” engineer.

During the workshop students can also improve their communication skills by working in groups. It is an input for a multicultural engineering workforce. Students have an opportunity to learn more about cultural differences, different points of view and to accept them.

Learning by experience, strongly recommended by McDermott, Gól and Nafalski [8], reveals among the group of students abilities of leaders, managers as well as effective team members. The effectiveness of the group strongly depends on the cooperation between its members. Trzcieniecki [9] adds to this another two aspects, i.e. communication and motivation. The last one factor is also mentioned as the most powerful in goal achieving by Hills and Tedford [3]. Motivation can have different forms. It can be considered with a perspective of a personal benefit, as a group success.

3.4. Environmental orientation of ISS solutions

In XXI century, according to the ideas of sustainable development, is a growing need for identifying economically and technically feasible and environmentally compatible solutions, which enable to manage this challenge, with the strong accent on the last one. From an earlier focus on substances and technology, modern thinking has to move towards greater attention to technical objects themselves,

including different dimensions of them. This aspect is sought-after and highly appreciated in analysis and opinion of solutions to be delivered by students to the jury.

Generally, the challenge is to combine environmental improvements and better object performance to go hand in hand and to create environmental improvements, supporting long-term industrial competitiveness. In consequence, environmental analyses should not be focused on large point sources of pollution, such industrial emissions or waste management issues. They need to be complemented by a policy that looks at the whole of an object’s life cycle. To be successful, the analysis also has to take into account several characteristics of objects and:

- 1) has to use creativity for the benefit of the environment as well as the economy,
- 2) should aim to reduce the environmental impacts of increased quantities of objects,
- 3) should ensure that well object design incorporates proper use and disposal, which minimize environmental impacts,
- 4) should contribute to improving information flows along supply-chain.

Presented factors underline the need to introduce an object dimension to consideration. It is necessary to look at the technical object in a holistic way, involving as many actors as possible and leaving to them the responsibility for the choices they make.

The frame to be applied in evaluation of proposed solutions is among others Life Cycle Management (LCM) approach, with a Life Cycle Assessment (LCA) method. The students have recommendations to use them both.

LCM concentrates on decision processes that influence system cost and usefulness. These decisions must be based particularly on full consideration of business functional requirements, economic and technical feasibility and environmental sensitivity in order to produce an effective system. The main objectives of the LCM practice comprise:

- 1) delivering quality systems which meet customer expectations, including cost estimation,
- 2) delivering systems that work effectively and efficiently within the current and planned technology infrastructure,
- 3) delivering systems that are cost-effective to enhance and maintain,
- 4) establishing a management structure with appropriate levels of authority.

LCA method is generally represented by ecobalance designation. Although the scope of the problems considered in the whole LCA is broader than in case of typical ecobalance, both methods are very often treated as equivalent to each other.

The LCA of the object (good, process or activity) is a process aimed at identifying the negative effects of it, quantifying the use of raw materials, energy consumption and emissions, evaluating the impact of these uses made of energy and materials as well as emissions into the environment, and evaluating the relevant improvements in an environmental context.

LCA is used to support decision making processes particularly in area of environmental aspects, but the true is, that LCA is also supplemented by other assessments which make it possible to take into account other factors, not usually incorporated into the LCA, for example, the economic and organizational aspects.

As we mentioned the life cycle thinking was introduced as an idea in solving the problems during our innovation project. It has to characterize all of actors who come into contact with an object. There are two areas of activities particularly important: educational, which causes raising of environmental awareness, and promotion of carefulness of environment on national and regional level. Three sets of actions are indicated as required to develop life cycle thinking:

- 1) making available information and tools (collecting and disseminating life cycle data for design and labeling purposes, promotion of methods such as LCA, which provide the best framework for assessing the potential environmental impacts of objects),
- 2) implementation and re-orientation of Environmental Management Systems (the approach which provide good framework for integrating life cycle thinking and which is re-oriented from the process dimension towards products),
- 3) technical objects design obligations (application of rules oriented on environmental requirements, which stimulate to develop greener products in form of legal base, internal market considerations, international treaty obligations).

4. CONCLUSIONS

The FMT has developed an environment for both education and training, and the ISS became a successful innovation project in this frame.

This workshop became popular within companies because of:

- the opportunity for closer contact with university,
- the chance for finding the interesting personalities among the students, participating in solving their problems,
- the opportunity to recruit fresh staff members,
- and last but not least
- finding very often many rational solutions of their problems and taking advantage of the proposals of solutions, presented by the students,

what makes many companies participate year by year in the ISS.

It is very popular within the students' community, especially the best ones. A lot of them participate at least twice in this event. There are some reasons for that:

- students find ISS as a good opportunity to familiarize with practical problems, use their knowledge and start to use their creativity by solving real problems,
- this is a competence training for them, leading to even patented solutions,
- the solved project can be an inspiration and

motivation for students to their master or even doctoral thesis,

- this is a good experience for them in finding a job, usually offered by the participating in ISS companies.

And finally, there are also the benefits for the university:

- the attractiveness of this innovation means that there is a need of such initiatives,
- such popularity within students indicates that the delivering theoretical knowledge is not enough in their education process,
- students are looking for the cooperation with companies, where both theoretical and practical aspects are highly related,
- the problems presented by the companies are characterized by the complexity, linking technical, economical, and organizational aspects, giving the university audience an opportunity to see the current real problems occurring in economy,
- quality of education improves at the FMT, by introducing such a initiative as *International Summer School*.

5. REFERENCES

- [1] Guidelines for Collecting and Interpreting Innovation Data. Oslo Manual. 3rd edition. OECD, Eurostat, Paris 2005.
- [2] from the "Głos Politechniki" (Voice of PUT) periodic magazine
- [3] Hills G., Tedford D. (2003), "*The education of engineers: the uneasy relationship between engineering, science and technology*". Global Journal of Engineering Education, Vol. 7, No. 1, pp. 17–28.
- [4] McDermott K. J., Göl Ö., Nafalski A. (2002), "*Considerations on experience-based learning*". Global Journal of Engineering Education, Vol. 6, No. 1, pp. 71–78.
- [5] Short T. D., Garside J. A., Appleton E. (2003), "*Industry and the engineering student: a marriage made in heaven*". Global Journal of Engineering Education, Vol. 7, No. 1, pp. 77–86.
- [6] El-Raghy, S. (1999), "*Quality engineering education: student skills and experiences*". Global Journal of Engineering Education, Vol. 3, No. 1, pp. 25–30.
- [7] Riemer M. J. (2002), "*English and communication skills for the global engineer*". Global Journal of Engineering Education, Vol. 6, No. 1, pp. 91–100.
- [8] McDermott K. J., Göl Ö., Nafalski A. (2002), "*Considerations on experience-based learning*". Global Journal of Engineering Education, Vol. 6, No. 1, pp. 71–78.
- [9] Trzcieniecki J. (1996), "*Project management – the flexible form of organization*" (in Polish). Organizacja i Kierowanie, Vol. 83, No. 1, pp. 31–37.

Author: Prof. Dr. Zbigniew Klos, Poznan University of Technology, Faculty of Machines and Transport, Institute of Machines and Vehicles, Piotrowo 3, 60-965 Poznan, Poland, Phone.: +48 61 665 2231, Fax: +48 61 665 2736
E-mail: zbigniew.klos@put.poznan.pl



MECHANICAL PROPERTIES OF THERMALLY STABILIZED SEDIMENT-CLAY MIXTURES

Received: 05 June 2014 / Accepted: 20 June 2014

Abstract: At present, dredged sediment (contaminated or not) in Serbia is deposited in landfills. However, landfill capacity is limited, and can cause a serious threat if it is contaminated. The advantage of immobilization by thermal treatment with silicate materials like clay lies in the possibility of utilizing the final product as a construction material. Clay-based ceramic products are potentially good incorporation materials for wastes thanks to their typically heterogeneous mineralogical composition, involving silicate phases which can dissolve considerable amounts of metals in their structures. Paper presents the mechanical properties of the sediment-clay mixtures in the view of using this mixture as a construction material.

Key words: metals, clay, waste, thermal treatment, bricks

Mehanička svojstva termički stabilizovanih sedimenta – smeša gline. Trenutno se, iskopani sedimenti (kontaminirani ili ne), u Srbiji odlažu na deponije. Međutim, kapacitet deponije je ograničen, a mogu i da izazovu ozbiljnu pretnju ako su zagađeni. Prednost imobilizacije termičkim tretmanom silikatnim materijalima kao što je glina leži u mogućnosti korišćenja krajnjeg proizvoda kao konstrukcionog materijala. Keramički proizvodi bazirani na glini su potencijalno dobri materijali za uvrščavanje u otpade zahvaljujući svom tipično heterogenom mineraloškom sastavu, uključujući i silikatne faze koje mogu da rastvaraju značajne količine metala u svojim strukturama. Ovaj rad predstavlja mehanička svojstva smeše sedimenta - gline u cilju korišćenja ove smeše kao konstrukcionog materijala.

Ključne reči: metali, glina, otpad, termička obrada, cigle

1. INTRODUCTION

Large uncontrolled metal inputs from industrial sources contribute to increased pollution in water systems. Depending on the hydrodynamics and environmental conditions, metals tend to accumulate in sediments at the bottom of the water column; if toxic levels are reached, metals can affect benthic organisms and the food chain, raising the possibility of a threat to human health for the local population. To obtain a realistic estimate of the actual environmental impact of metals in an aquatic medium, their chemical nature or potential mobility/availability must be addressed. The identification of the geochemical phases of metals in sediments, as well as their quantification by chemical speciation, is crucial to evaluate the ecological risks of these contaminants in a study area [1,2].

In some cases, due to different factors, sediments may need dredging and remediation treatments, if the dredged material is too contaminated and cannot be used directly. These sediments may contain inorganic contaminants which can end up polluting the environment. Contaminated sediments may have to be treated as a waste material. Therefore, their management has become an environmental and economical concern for a large number of countries [3]. Conventional disposal solutions for dredged sediments, such as disposal and dumping into landfills, are gradually becoming restricted in many countries to preserve the environment. Storage in confined disposal facilities requires large spaces and long term

monitoring. However, landfilling is less accepted by public opinion. Treatment processes permit a reduction in toxicity and volume of dredged material, but in comparison with open-water and upland disposal, the treatment costs are not yet competitive. This underlines the necessity to find ecological valorisation paths for the processed sediments to make these alternatives economically competitive. Thus, researchers have started to study alternative ways to incorporate large amounts of processed sediments into different aspects of construction and building materials [3,4].

At present, dredged sediment (contaminated or not) in Serbia is deposited in landfills. Clay-based ceramic products are potentially good incorporation materials for wastes thanks to their typically heterogeneous mineralogical composition, involving silicate phases which can dissolve considerable amounts of metals in their structures, and also because of the high firing temperature conditions normally used. Such heterogeneous materials can tolerate the presence of different types of wastes in considerable quantities, and hence their processing represents an interesting possibility for waste encapsulation. Thermal treatment determines the degree of final immobilization, since the major combining reactions between clay and waste particles occur upon heating, whereby sintering promotes the physical consolidation of the material by reaching a suitable microstructure. Moreover, highly (thermodynamically) stable phases tend to be formed at high temperatures. The chemical nature of the phases involved and final microstructure of the material have a

strong impact on its behaviour [3,4].

The advantage of immobilization by thermal treatment with silicate materials like clay lies in the possibility of utilizing the final product – as bricks, tiles or some other construction material. The beneficial uses of dredged sediments are becoming increasingly interesting in terms of environmental protection and sustainable development. The use of conventional bricks produced from clay has been partially restricted, for example in China due to the limitation of the clay resource [5-10]. Considering the composition of the sediments and its continuous availability, the use of dredged sediments in brick production is promising.

In view of the above, the objectives of this study were: 1) to evaluate sediment quality based on the pseudo-total metal content 2) to define metal distributions in dredged sediments and evaluate their environmental risk; 3) to assess the effectiveness of immobilization treatments with clay in order to obtain commercially applicable bricks with appropriate flexural strength and fracture toughness.

2. MATERIALS AND METHODS

Fresh sediment was sampled from the Danube-Tisa-Danube Vrbas-Bezdan canal in Vojvodina (the northern province of the Republic of Serbia). This canal is one of the most polluted sites in the country. Most of the pollution derives from industry (two sugar refineries, a tannery, a metal works, an edible oil refinery, slaughterhouses, etc.) which discharges untreated or partially treated wastewater into the canal. The total organic pollution from industry is 36.6 tCOD/day or 17.9 tBOD5/day, along with 1329 kg COD/day or 619 kg BOD5/day from municipal wastewaters. The sediment sample was taken at a point (N45°34,212' E19°39,314') on the most vulnerable section, a 6 km stretch which contains about 400 000 m³ of sediment. Sediment was taken from the middle of the riverbed at depths of 0 to 160 cm by Eijkelkamp core sampler, homogenized and placed in a sealed acid-rinsed box (15x15 cm and 20 cm deep) immediately after sampling. The organic matter content was determined as ignition loss, and was 5.31±0.1. The granular distribution was: 20.3% sand fraction, 46.1% silt and 23.9% clay.

Pseudo-total metal contents were assessed in triplicate after aqua regia digestion (ISO 11466:1995) and mean values reported. The standard deviations (% R.S.D.) obtained (n=3) were below 10%. The results of the sediment pseudo-total metal concentrations are discussed in reference to Serbian quality guidelines [11] and Canadian guidelines [12].

The microwave assisted sequential extraction procedure (MWSE) was performed as described by Jamali et al. [13], using identical operating conditions for in each individual BCR fraction. The extracting solutions were prepared from analytical grade reagents. Standard solutions of metals were prepared by diluting 1000 ppm certified standard solutions, Fluka Kamica (Buchs, Switzerland), of the corresponding metal ions. The sediment pseudo-total metal contents and the metal contents in the sequential extraction procedure steps

after aqua regia digestion were analyzed by AAS (Perkin Elmer AAnalyst™ 700) or ICP-MS (Perkin Elmer Sciex Elan 5000) according to the standard procedures.

All results are expressed with respect to sediment dry matter. Domestic clay was used as the basic immobilization agent for the S/S treatment. Clay composition was: SiO₂ (55.3%), Al₂O₃ (18.9%), Fe₂O₃ (6.12%), MgO (1.67%), CaO (1.7%), Na₂O (0.67%), K₂O (0.35%), P₂O₅ (2.31%), SO₃ (2.49%) and ignition loss 10.5 %. The CEC (meq/100 g) was 85, while the respective surface area (m² g⁻¹) was 190. The total metal concentrations (mg kg⁻¹) in clay was: Zn (13.3±1.2), Pb (38±1.1), Cr (6.5±0.5), Cu (1.9±0.1), Ni (16±0.8) and Cd (0.4 ± 0.01).

Sediment possessing an average initial moisture content of 73% was dried at 105°C to a constant mass. The raw clay was mixed with the sediment in proportion of 5:95 wt. (D5) and 10:90 wt. (D10) at optimum water content [14]. The mixtures were then homogenized on a milling machine using sieves with 3 mm pores. After homogenization, samples were shaped in vacuum. The obtained samples were dried for 24 h in air, and then at 105 °C to constant mass. The thermal treatment was carried out in an electrical furnace at a constant temperature of 1050±5°C with variations in heating rate (4.6 °C/min from 25°C to 300°C, 1.7 °C/min from 300°C to maximum T, 5h hold at max T) on the samples: D5 and D10.

Mechanical properties, that is flexural strength and fracture toughness were obtained by three point bend test at tensile machine Toyoseiki AT-L-118B, with measuring range from 0 to 1000 N. For each sample group, five specimens were tested. Flexural strength was tested with a 3-point bending device and 40 mm distance between the supports and specimen dimensions 50x10x10 mm. Fracture toughness was tested by using a SEVNB method, with specimens having the following dimensions: 50x10x10 mm. The test was performed with a 4-point test device, with 20/40 mm distance between the supports.

3. RESULTS AND DISCUSSION

The pseudo-total metal concentrations in the sediment followed this order: Zn > Pb > Cr > Cu > Ni > Cd, the corresponding values (mg kg⁻¹) being: Zn (1782±90), Pb (920±65), Cr (559±40), Cu (478±18), Ni (365±35) and Cd (25.5 ± 1.4). According to Serbian guidelines [11] the sediment samples are severely polluted with metals and belong to class 4 – they are of unacceptable quality and need highest urgency cleaning, dredging, disposal in special storage reservoirs and if possible, sediment clean-up measures. Compared with the Canadian Sediment Quality Guidelines [12] for aquatic life protection, the metal contents are above the probable effect level (PEL). Sediment concentrations above PEL values are expected to be frequently associated with adverse biological effects. Although the PEL is considered to be applicable to a variety of sediment types, it cannot define uniform values of sediment pollution as the bioavailability (and hence toxicity) of contaminants

may be different [12]. However, it is now widely accepted that the role of aquatic sediments as a sink or a source of pollutants cannot be fully assessed by measuring pseudo-total metal concentrations, as they do not give an accurate estimation of the likely environmental impact, as shown in our work. This is because the mobility of trace metals, as well as their bioavailability and related ecotoxicity to plants, critically depends upon the chemical form in which a metal is present in the sediment [15]. The distribution pattern of different metals in the sediments of the Danube-Tisa-Danube Canal Vrbas-Bezdan Metal mobilities decreased in the following order: Ni > Zn > Cr > Cd > Cu > Pb according to the results of the first phase of the sequential extraction procedure. Percentages of extracted metals in this most available, mobile, step were in the range from 28% (Cr) to 39 % (Ni), while for Cu, Cd and Pb they were much lower: 11 % (Pb) - 18% (Cd). The ranking of metals in the fractions according to their relative contents is as follows: Ni > Cd > Zn > Cr > Cu > Pb in reducible fraction, Cu > Pb > Cd > Cr > Zn > Ni in oxidizable form, and Pb > Cr > Cd > Ni > Zn > Cu in residual fraction.

The distribution of metals in the different fractions obtained by the sequential extraction procedure offers an indication of their availability, which in turn allows the assessment of the risk of their presence in the aquatic environment. Risk Assessment Code (RAC) gives an idea of the possible risk by applying a scale to the percentage of metals present in exchangeable and carbonate (i.e. labile) fractions. According to RAC, if this fraction is <1% there is no risk for the aquatic system, 1–10% exhibits low risk, 11–30% medium risk, 31–50% high risk and >75% very high risk [16].

Although the metal distributions and availability in the sediment were different, we applied the same remediation treatment because there are not enough data about the behaviour of metals differently distributed in mixtures in sediment during immobilization treatment, or about the treatment efficiency in general. The main objective of every remediation dealing with several contaminants is to carry out the treatment with the same agents, and thus achieve economic and environmental benefits.

In Table 1, flexural strength and fracture toughness results are shown, as well as corresponding standard deviations (SD). It can be seen that flexural strength and fracture toughness of the sample group designated as D5 are higher than those of sample group D10. However, in terms of flexural strength, standard deviation of specimens D10 are lower than that of D5. On the other hand, the opposite standard deviation trend is obtained when fracture strength was tested.

Sample	Savojna čvrstoća [MPa]	SD	Žilavost loma [kPam1/2]	SD
D10	5,76	0,56	236,67	33,65
D5	5,94	0,80	258,85	26,91

Table 1. flexural strength and fracture toughness results

This results are preliminary and a long way is ahead and further studies should include broad range of mechanical properties that will validate usage of sediments in commercial brick production.

4. CONCLUSION

Several hundred millions of tons of dredged sediments are annually generated around the world. Dredged sediments cannot be used as a geomaterial directly in the construction and building sector. Thus, management of dredged sediments is a critical issue of increasing concern. Conventional disposal solutions for dredged sediments, such as disposal and dumping into landfills, are gradually becoming restricted in many countries to preserve the environment. The beneficial uses of dredged sediments are becoming increasingly interesting in terms of environmental protection and sustainable development. As a major construction and building material, bricks are in great demand. The use of conventional bricks produced from clay has been partially restricted in some countries. Therefore, finding alternative raw materials in brick production is of urgent need. Considering the composition of the sediments and its continuous availability, the use of dredged sediments in brick production is promising as it was presented in the paper.

5. REFERENCES

- [1] Louriño-Cabana, B., Lesven, L., Charriau, A., Billon, G., Ouddane, B., Boughriet, A.: *Potential risks of metal toxicity in contaminated sediments of Deûle river in Northern France*. Journal of Hazardous Materials 186, 2129–2137, 2011.
- [2] Ciszewski, D., Kubsik, U., Kwaterek, U.A.: *Long-term dispersal of heavy metals in a catchment affected by historic lead and zinc mining*. Journal of Soils and Sediments, 12, 1445-1462, 2012.
- [3] Lafhaj, Z., Samara, M., Agostini, F., Boucard, L., Skoczylas, F., Depelsenaire, G.: *Polluted river sediments from the North region of France: Treatment with Novosol process and valorization in clay bricks*. Construction and Building Materials, 22, 755–762, 2008.
- [4] Chiang, K.Y., Chien, K.L., Hwang, S.W.: *Study on the characteristics of building bricks produced from reservoir sediment*. Journal of Hazardous Materials, 159(2-3):499-504, 2007.
- [5] Moon, D.H., Dermatas, D.: *An evaluation of lead leachability from stabilized/solidified soils under modified semi-dynamic leaching conditions*. Engineering Geology, 85, 67-74, 2006
- [6] Moon, D.H., Dermatas, D.: *Arsenic and lead release from fly ash stabilized/solidified soils under modified semi-dynamic leaching conditions*. Journal of Hazardous Materials 141, 388–394, 2007
- [7] Dubois, V., Abriak, N.E., Zentar, R., Ballivy, G.: *The use of marine sediments as a pavement base material*. Waste Management 29(2), 774-782, 2009.

- [8] Huang, Y., Zhu, W., Qian, X., Zhang, N., Zhou, X.: *Change of mechanical behavior between solidified and rem olded solidified dredged materials*. Engineering Geology, 119(3-4), 112-119, 2011.
- [9] Baruzzo, D., Minichelli, D., Bruckner, S., Fedrizzi, L., Bachiarrini, A., Maschio, S.: *Possible production of ceramic tiles from marine dredging spoils alone and mixed with other waste materials*. Journal of Hazardous Materials, 134 (1-3), 202-210, 2006.
- [10] China Economic Trade Committee. *Tenth five-year program of building materials industry*. China Building Materials 7, 7-10, 2001.
- [11] Ministry of Natural Resources, Mining and Spatial Planning. Regulation on limit values for pollutants in surface, ground water and sediment and deadlines for their achievement. The Official, Gazette 35/2011. (in Serbian).
- [12] CCME (Canadian Council of Ministers of the Environment). Protocol for the derivation of Canadian Sediment quality guidelines for the protection of aquatic life. CCME EPC-98E. Prepared by Environment Canada, Guideline Division, Technical Secretariat of the CCME Task Group on Water Quality Guidelines, Ottawa, 1995.
- [13] Jamali, M.K., Kazi, T.G., Arain, M.B., Afridi, H.I., Jalbani, N., Kandhro, G.A.: *Speciation of heavy metals in untreated sewage sudge by using microwave assisted sequential extraction procedure*. Journal of Hazardous Materials 163:1157-1164, 2009.
- [14] ASTM (American Society for Testing and Materials) Annual Book of ASTM Standards. Soil and Rock; Building Stones vol. 4.08. Philadelphia, PA, 1993.
- [15] Arain, M.B., Kazi, T.G., Jamali, M.K., Afridi, H.I., Jalbani, N., Sarfraz, R.A.: *Time saving modified BCR sequential extraction procedure for the fraction of Cd, Cr, Cu, Ni, Pb and Zn in sediment samples of polluted lake*. Journal of Hazardous Materials, 160, 235-239, 2008.
- [16] Jain, C. K.: *Metal fractionation study on bed sediments of River Yamuna, India*. Water Research, 38, 569-578, 2004.

ACKNOWLEDGEMENT: the authors acknowledge the financial support of the Ministry of Education and Science of the Republic of Serbia (project No. III43005).

Authors: **Assist. Prof. Dr. Dejan Krčmar, Prof. Božo Dalmacija, Assist. Prof. Dr. Jelena Tričković, Assist. Prof. Dr. Srđan Rončević, Assist. Prof. Dr. Snežana Maletić**, University of Novi Sad, Faculty of Sciences and Mathematics, Department of Chemistry, Biochemistry and Environmental Protection, Trg Dositeja Obradovica 3, 21000 Novi Sad, Serbia
Assist. Prof. Dr. Sebastian Baloš, Assist. Prof. Dr. Miljana Prica, University of Novi Sad, Faculty of Technical Science, Trg Dositeja Obradovica 6, 21000 Novi Sad, Serbia, Tel: +381 21 485 2620.



Kuruc, M., Necpal, M., Peterka, J.

MACHINING OF POLY-CRYSTALLINE CUBIC BORON NITRIDE BY LASER BEAM MACHINING IN TERMS OF SURFACE ROUGHNESS

Received: 17 May 2014 / Accepted: 10 June 2014

Abstract: Poly-crystalline cubic boron nitride (PCBN) is the hardest material beside diamonds. Generally, so hard materials could not be machined by conventional machining technologies. For this purpose, advanced machining methods have been designed. Laser beam machining (LBM) is included among them. LBM is based on ablation removing mechanism of focused and concentrated light beam. This contribution investigate quality of machined surface achieved by this advanced method during machining of PCBN.

Key words: laser beam machining, poly-crystalline cubic boron nitride, surface roughness

Obrada polikristalnog kub-bor-nitrida laserskim zrakom u odnosu na površinsku hrapavost. Polikristalni kub-bor-nitrid (PCBN) je najčvršći materijal pored dijamanta. Generalno, toliko čvrsti materijali se ne mogu obrađivati konvencionalnim tehnologijama obrade. Za tu svrhu, projektovane su napredne metode obrade. Među njima je i obrada laserskom zrakom (LBM). LBM se bazira na mehanizmu odstranjivanja materijala fokusiranim i koncentrisanim svetlosnim zrakom. Ovaj rad istražuje kvalitet obrađene površine postignut ovom naprednom metodom tokom obrade PCBN-a.

Ključne reči: obrada laserskim zrakom, polikristalni kub-bor-nitrid, površinska hrapavost

1. INTRODUCTION

PCBN is material which is usually utilized as cutting material. It is manufactured by sintering and therefore additional treatment usually is not necessary. However, there are some applications, where machining of PCBN is required. One of these application could be tools for friction stir welding (FSW). The principle of this technology consists in application of a rotating tool with specially designed shoulder pin which is impressed to the boundary of welded materials. The tool proceeds in weld line direction. Heating occurs owing to friction and plastic strain of welded metals. Mechanical power is transferred to heat during the welding process. Temperature generated in welding zone usually attains 80 to 90 % of melting point temperature of the welded metal. Advantages of FSW process include: low heat input, low residual stress allowing fabrication of precise weldments without any additional operation, then formation of fine-grained microstructure in the welded zone leading to increased mechanical properties of fabricated welds. Welding operation takes place without spatter, harmful radiation and without filler metal. Welding by FSW process guarantees a high measure of safety and is also environmentally friendly [1-5].

Welding tool used in FSW process must be sufficiently tough, robust and wear resistant at welding temperature. Other requirements include: good oxidation resistance and low coefficient of thermal conductivity to minimize the thermal losses. Shoulder profile of majority of tools is usually concave, which acts as an escape volume for the material displaced by the pin. The tool prevents material expulsion from the

side of pin shoulder and maintains the desired effect and thus the desirable material forging below the tool. These tools are characterized by different sizes depending on thickness of welded plates, and by different geometry depending on welded material. Therefore, tool for FSW of 2 mm thick steel plates has been created in experiments by LBM.

2. MACHINED MATERIAL AND MACHINING TECHNOLOGIES

2.1 Machining material

Basic As machined material, PCBN has been used. This material provides Welding Research Institute – Industrial Institute of Slovak Republic in Bratislava (VÚZ – PI SR), which also demand creation tool for FSW. They bought this material from its manufacturer– Changsha 3 Better Ultra-hard Materials Co., Ltd (3b diamonds), which is based in China. PCBN consists of grains of cubic boron nitride in alumina matrix doped by cobalt, as shown Fig. 1. Dark areas are grains of CBN, light areas are Al_2O_3 matrix. This image has been created by EDX microanalysis and it is approx. 800 times magnified. This analysis has been made in Laboratory of structural analysis in Faculty of Materials Science and Technology in Trnava, Slovak University of Technology in Bratislava (MTF STU). Beside magnified imagine of structure, EDX analysis also provides chemical composition, which is shown in Tab. 1. PCBN is characterized by very high hardness. Its value is usually in range 7000 to 8000 HV, or above (around 75 GPa). Other modifications of boron nitride

are usually softer. PCBN has high thermal stability. It is usually utilized as cutting material for machining of ferrous materials, such as hardened steels, etc [6-8].

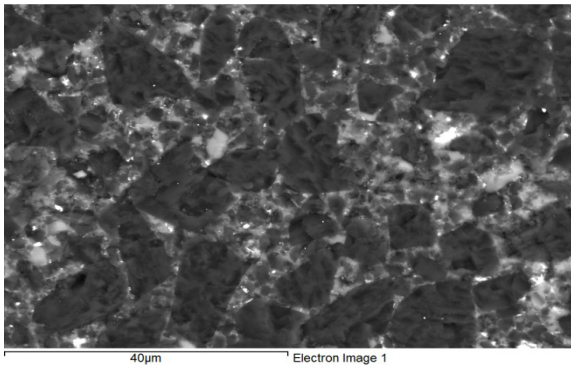


Fig. 1. Microstructure of PCBN

B	N	Al	O	Co
[wt. %]	[wt. %]	[wt. %]	[wt. %]	[wt. %]
46.99	40.58	6.26	4.68	1.49

Table 1. Chemical composition of PCBN

2.2 Machining technology

As machining technology, LBM has been used. This method is suitable for machining of hard-machinable materials. Also, it allows machining some free-form surfaces. Machine tool, which utilizes laser machining, is available in the Centre of Excellence of five-axis machining (CE5AM) in MTF STU [9].

LBM utilizes the ablation effect of concentrated and focused monochromatic and coherent light. There is no tool wear and there is no cutting force. Energy of light is so focused, that there is a very low heat-affected zone (HAZ). No cooling of the workplace is needed. Due to no cutting force, clamping of the workpiece could be performed by adhesive tape. In this experiment, a fiber laser machine LASERTEC 80 Shape, made by DMG Mori Seiki, has been used. This machine tool is shown in Fig. 2. It can continuously control five axes during machining. Its fiber is made of ytterbium and can provide a laser beam with a wavelength of 1.065 µm. It works only in pulse regime and the frequency of pulses could be controlled in the range 10 to 100 kHz. Feed rate of the laser beam could be adjusted in the range 100 to 4000 mm.s⁻¹. Maximum power of the laser generator is 100 W. Diameter of the laser beam is approx. 1 µm.



Fig. 2. Used machine tool LASERTEC 80 Shape [11]

During the experiment, the following parameters have been used: frequency 30 kHz, feed rate 1000 mm.s⁻¹, depth of cut 2 µm, laser power 12.3%. Adjusted parameters required power approx. 4 W. NC program has been generated by software Lasersoft 3D, designed by the company DMG, which is part of the machine tool [10].

3. DESCRIPTION OF THE EXPERIMENT

For the experiment, a PCBN cylinder with a diameter of 12 mm and length of 20 mm has been used. The specimen has been machined on the Lasertec 80 Shape. This specimen has been machined to the shape of the above-mentioned tool for FSW. The dimensioned longitudinal section of this tool is shown in Fig. 3. This tool has been created by LBM. Surface quality has been evaluated by roughness obtained by a confocal microscope. Machining parameters have been adjusted by recommended values based on the catalogue and experience. Depth of cut for LBM could be higher, but it should cause worse surface roughness. Therefore, the depth of cut has been suggested accordingly to reach approx. the best time-to-roughness ratio. Machining time could be shorter at the costs of higher roughness and vice versa.

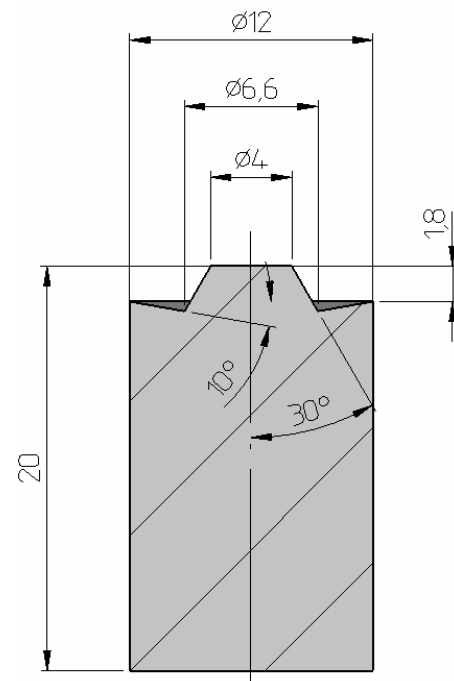


Fig. 3. Tool for friction stir welding

4. RESULT OF EXPERIMENT

Machining of FSW tool by LBM method spent approx. 4 hours at adjusted parameters. After machining, the specimen has been sent to a confocal microscope for obtaining surface topography. The resultant topography of the surface after laser machining is shown in Fig. 4. On the upper image is shown a 3D representation of the machined surface. There is also a red line of section, which is shown on the lower image. There have been measured many kinds of roughness of the machined surface after LBM. Specific values of different roughness are shown in Tab. 2 [12].

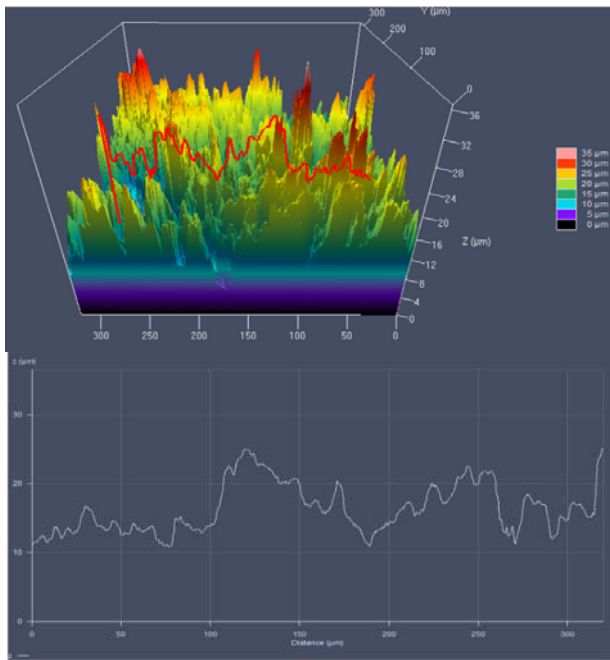


Fig. 4. Topology of machined surface after LBM

3D roughness		2D roughness	
RSc	20.925 μm	Rc	7.781 μm
RSa	3.934 μm	Ra	3.006 μm
RSq	4.977 μm	Rq	3.589 μm
RSsk	0.059	Rsk	0.588
RSku	3.051	Rku	2.325
RSp	20.087 μm	Rp	8.780 μm
RSv	16.504 μm	Rv	5.564 μm
RSt	36.591 μm	Rt	14.344 μm
RSz	27.045 μm	Rz	13.195 μm

Table 2. Surface roughness of PCBN after LBM

Where [13-15]:

Rc is mean height of the roughness profile elements (μm)

Ra is arithmetic average height (μm)

Rq is root mean square roughness (μm)

Rsk is skewness (-)

Rku is Kurtosis (-)

Rp is maximum height of peaks (μm)

Rv is maximum depth of valleys (μm)

Rt is total height of the profile (μm)

Rz is maximum height of the roughness profile (μm)

RSc (Sc) is mean height of the profile in space (μm)

RSa (Sa) is arithmetic mean height in space (μm)

RSq (Sq) is root mean squared height in space (μm)

RSsk (Ssk) is skewness in space (-)

RSku (Sku) is kurtosis in space (-)

RSp (Sp) is maximum peak height in space (μm)

RSv (Sv) is maximum valley depth in space (μm)

RSt (St) is total height of the profile in space (μm)

RSz (Sz) is maximum height in space (μm)

5. CONCLUSION

For machining of PCBN, LBM can achieve acceptable roughness ($R_a 3 \mu\text{m}$). LBM is able to create recommended shape by utilizing of only three axis (in comparison with mechanical machining methods, which required five continuously controlled axes [16]). LBM has also potential to rapidly reduce machining time. It would also cause rapidly rise of surface roughness. In that cause, roughness would be less acceptable. However, if LBM will be used only for roughing, and else method only for finishing, resultant surface will be created at relatively short time (even less than one hour), and surface could keep low roughness. For finishing could be the most suitable some mechanical machining process (such as rotary ultrasonic machining), because resultant roughness after these kind of machining methods do not so depend on previous processing – in comparison, beam machining method cannot improve surface roughness due copping of surface. Influence of surface roughness on FSW process will be objective of further research. There could be also comparison of LBM with rotary ultrasonic machining (RUM), as well as investigation of possibility to create this object by high speed cutting (HSC).

6. ACKNOWLEDGEMENTS

Authors want to thank to Ing. Marek Zvončan, PhD. for technical support, to Ing. Tomáš Kupec for ensure of cooperation with Welding Research Institute – Industrial Institute in SR, to Ing. Peter Zifčák PhD. for acquisition of material, to Ing. Kristián Šalgó for results from confocal microscope, to Ing. Martin Sahul, PhD. for EDX microanalysis, and to other people who help with this contribution.

This contribution is a part of the GA VEGA project of Ministry of Education, Science, Research and Sport of the Slovak Republic, No. 1/0477/14 “Research of influence of selected characteristics of machining process on achieved quality of machined surface and problem free assembly using high Technologies”.

This contribution is also elaborated by the support of Operational Project Research and Development of Centre of excellence of five axis machining, ITMS 26220120013, co-financed by European Funds for Regional Development.

This contribution is elaborated by support of Operational Project Research and Development of Centre of Excellence of Five Axis Machining, ITMS 26220120013, co-financed by European Funds for Regional Development.



We are supporting of research activities in Slovakia/
Project is co-financed by sources of ES

7. REFERENCES

- [1] Friction Stir Welding. Technical Handbook. ESAB 2011.
- [2] TWI – Friction Stir Welding. [online], [cit. 2014-03-01]. Available on the Internet: <http://www.twi.co.uk/technologies/welding-coating-and-material-processing/friction-stir-welding/>.
- [3] Turňa, M.: Špeciálne metódy zvrárania (Special welding methods). Bratislava: Alfa, 1989.
- [4] Friction Stir Welding. [online], [cit. 2013-11-20]. Available on the Internet: http://med.iaun.ac.ir/site/files/iaun_staff_498.pdf.
- [5] Hrivňák, I.: Zváranie a zvariteľnosť materiálov (Welding and Weldability of Materials), Bratislava 2009 ISBN 978-80-227-3167-6.
- [6] Jiaqian Qin, Norimasa Nishiyama, Hiroaki Ohfuji, Toru Shinmei, Li Lei, Duanwei He, Tetsuo Irifune. 2012. Polycrystalline γ -boron: As hard as polycrystalline cubic boron nitride. Japan, 13p. Available on Internet: <http://arxiv.org/ftp/arxiv/papers/1203/1203.1748.pdf>.
- [7] Changsha 3 Better Ultra-hard Materials Co. [online], [cit. 2013-10-23] Available on Internet: <http://3bdiamond.com/>.
- [8] Nanodiamond & Superhard Thin-films. [online], [cit. 2014-01-30]. Available on Internet: http://www.cityu.edu.hk/cosdaf/cbn_property.htm.
- [9] Baránek, I., Buranský, I. 2014. Teaching approaches to free-form surfaces design and manufacturing. In: Applied Mechanics and Materials. - . - ISSN 1660-9336. - Vol. 474. - , 2014, s. 3-8
- [10] Lasertec 80 shape. [online], [cit. 2014-02-14]. Available on Internet: <http://en.dmgmori.com/products/lasertec/lasertec-shape/lasertec-80-shape>.
- [11] Lasertec 80 Power shape. [online], [cit. 2014-02-20]. Available on Internet: <http://kr.dmgmori.com/kr,lasertec,lasertec80power-shape?opendocument>.
- [12] Čaplovič, Lubomír - Sahul, Martin: Application of the EBSD technique for the evaluation of material properties. - ITMS 26220120048. In: Vákuum a progresívne materiály. Vacuum and Advanced Materials: Škola vákuovej techniky. 8.-11.september 2011, Štrbské Pleso. - Bratislava: Slovenská vákuová spoločnosť, 2011. - ISBN 978-80-969435-9-3. - p. 10-13.
- [13] Maksound, T. M. A., Gadelmawla, E. S., Koura, M. M., Elewa, I. M., Soliman, H. H. 2002. Roughness parameters. In: Journal of Materials Processing Technology. Vol. 123, p. 133-145
- [14] Roughness (2D) parameter. [online], [cit. 2014-03-16]. Available on the Internet: http://www.olympus-ims.com/en/knowledge/metrology/roughness/2d_parameter/
- [15] Roughness (3D) parameter. [online], [cit. 2014-03-17]. Available on the Internet: http://www.olympus-ims.com/en/knowledge/metrology/roughness/3d_parameter/
- [16] Beňo M., Zvončan M., Kováč M., Peterka J.: Circular interpolation and positioning accuracy deviation measurement on five axis machine tools with different structures. In: Tehnicki Vjesnik - Technical Gazette. - ISSN 1330-3651. - Vol. 20, No. 3 (2013), p. 479-484.

Authors: Ing. Marcel Kuruc, Ing. Martin Necpal, PhD., Prof. Dr. Ing Jozef Peterka, Slovak University of Technology, Faculty of Materials Science and Technology in Trnava, Institute of Production Technologies, J. Bottu 25, 917 24, Trnava, Slovakia
E-mail: marcel.kuruc@stuba.sk
martin.necpal@stuba.sk
jozef.peterka@stuba.sk

INSTRUCTIONS FOR CONTRIBUTORS

No. of pages:	4 DIN A4 pages
Margins:	left: 2,5 cm
	right: 2 cm
	top: 2 cm
	bottom: 2 cm
Font:	Times New Roman
Title:	Bold 12, capitals
Abstract:	Italic 10
Headings:	Bold 10, capitals
Subheadings:	Bold 10, small letters
Text:	Regular 10
Columns:	Equal column width with 0,7 cm spacing
Spacing:	Single line spacing
Formulae:	Centered and numerated from 1 in ascending order. Equations must be typed in Equation Editor, with following settings: Style>Math – Times New Roman Size>Full 12pt, Subscript/Superscript 7pt, Symbol 18 pt
Figures:	High quality, numerated from 1 in ascending order (e.g.: Fig. 1, Fig. 2 etc.); Figures and tables can spread over both two columns, please avoid photographs and color prints
Tables:	Numerated from 1 in ascending order (e.g.: Tab. 1, Tab. 2, etc.)
References:	Numerated from [1] in ascending order; cited papers should be marked by the number from the reference list (e.g. [1], [2, 3] ...)
Submission:	Papers prepared in MS Word format should be e-mailed to: <u>pkovac@uns.ac.rs</u>, <u>savkovic@uns.ac.rs</u>
Notice:	Papers are to be printed in Journal of Production Engineering Sample paper with detailed instructions can be found at: <u>http://www.jpe.ftn.uns.ac.rs/</u>

FOR MORE INFORMATION, PLEASE CONTACT:

Prof. Pavel Kovač, PhD, MEng.
Borislav Savković, MSc. Assistant
FACULTY OF TECHNICAL SCIENCES
Department for Production Engineering
Trg Dositeja Obradovica 6
21000 Novi Sad
Serbia
Tel.: (+381 21) 485 23 24; 485 23 20 ; 450 366;
Fax: (+381 21) 454 495
E-mail: pkovac@uns.ac.rs, savkovic@uns.ac.rs
<http://www.jpe.ftn.uns.ac.rs/>